

The effect of prestress on concrete durability
by Michael J Gonsior

A thesis submitted to the Graduate Faculty in partial fulfillment of the requirements for the degree of
MASTER OF SCIENCE in Civil Engineering
Montana State University
© Copyright by Michael J Gonsior (1965)

Abstract:
The primary purpose of this study was to investigate the effect of prestress upon the durability of concrete. Small pretensioned concrete slabs, at stress levels of zero, 500, and 1200 psi., were fabricated from non-air-entrained concrete made with Type II cement. Half of these slabs were steam cured; the remaining slabs, were cured in a moist, room temperature environment. These slabs were subjected to a freeze-thaw environment, half with water ponded on their top surfaces and the remaining specimens with a GaCl2 solution in contact with their top surfaces. At frequent intervals the natural frequencies of transverse flexural vibration, weights, and lengths of the slabs were measured. Evaluations of the degree of surface scaling were also made.

Duplicates of these slabs were fabricated for an additional study to determine the effects of prestress, curing procedure, and type of solution upon the permeability, or absorption characteristics of concrete.

Tall glass standpipes were sealed to the surfaces of these slabs and filled with water or CaCl2 solution. Absorption rates were determined by periodically measuring the quantities of liquid necessary to maintain a constant level in the standpipes.

From statistical and qualitative interpretations of the data from these studies it was concluded that prestressing slightly improves the durability of concrete. It was also concluded that steam cured concretes are less durable, more susceptible to scaling damage, and possibly more permeable than concretes cured in a moist, room temperature environment.

The extremely deleterious surface effects of salt solutions upon concrete, in a freeze-thaw environment, were also observed; although the slabs ponded with CaGl2 solution exhibited only slightly greater durability losses than slabs ponded with water.

The only important conclusion drawn from the permeability study was that concrete absorbs CaCl2 solution at a rate which does not differ significantly from that at which it absorbs water.

THE EFFECT OF PRESTRESS ON CONCRETE DURABILITY

by

MICHAEL J. GONSIOR

A thesis submitted to the Graduate Faculty in partial fulfillment of the requirements for the degree

of

MASTER OF SCIENCE

in

Civil Engineering

Approved:

Head, Major Department

Chairman, Examining Committee

Dean, Graduate Division

MONTANA STATE COLLEGE
Bozeman, Montana

June, 1965

ACKNOWLEDGMENTS

This study was part of a project sponsored by the Montana State Highway Department, in co-operation with the U. S. Department of Commerce, Bureau of Public Roads. The author wishes to express his gratitude to Professor Martin E. Moss who, as primary investigator, provided the objectives and guidance for this work. His appreciation is also extended to Dr. E. R. Dodge and the other members of his staff, whose considerations and encouragement made this opportunity possible.

Notable among the many firms and individuals who made valuable contributions to this study are Mr. M. G. Long, president of the Long Construction Company, Mr. T. R. Murphy and the other personnel of the Mechanical Engineering Department machine shop at Montana State College, and Dr. G. R. Ingram and the members of his staff in the Montana State College Computing Center.

The terminal phase of this study was made possible through the generous financial assistance provided by the Ideal Cement Company and other funds realized through the tireless efforts of Dr. Dodge. Further, the Ideal Cement Company personnel at Trident donated the cement and provided its chemical analysis.

The author's wife, Jacqueline, is deserving of special recognition for her expert typing and proof-reading, and especially for her patience.

To the many other individuals who assisted with this research, the author is deeply indebted, and regrets that they are too numerous for personal mention.

TABLE OF CONTENTS

CHAPTER I INTRODUCTION

Concrete durability 1

Concrete protection 2

Purpose of study 4

Nature of investigation 5

CHAPTER II REVIEW OF LITERATURE

The hydration of portland cement 6

The permeability of concrete 12

Concrete deterioration 15

Causative factors 15

Protective measures 20

Freeze-thaw and related modes of destruction . . . 24

The rheology of portland cement concrete 30

Other prestressed concrete durability studies . . . 33

CHAPTER III LABORATORY INVESTIGATION

Modes of investigation 35

Description of specimens 36

Prestressing operation 37

Concrete materials 49

Concrete mix information 49

Fabrication of slabs 54

Curing of slabs 59

Normal curing 59

CHAPTER III LABORATORY INVESTIGATION

Steam curing 60

Application of mortar dikes 63

Preparation of permeability study slabs 67

Environmental conditioning 69

Durability and scaling studies 69

Permeability study 71

Tests and measurements 72

Durability and scaling studies 72

Permeability study 77

CHAPTER IV RESULTS OF INVESTIGATION

Explanatory comments 79

Durability and scaling study 80

Permeability study 115

CHAPTER V CONCLUSIONS AND SUMMARY

Conclusions 127

Effect of prestress upon durability 127

Effects of steam and normal curing upon durability 128

Effects of water and salt solution upon durability 129

Effect of prestress upon scaling resistance . . 130

Effects of steam and normal curing upon scaling resistance 130

CHAPTER V CONCLUSIONS AND SUMMARY

Effects of water and salt solution upon scaling resistance 131

Effect of prestress upon permeability 131

Effects of steam and normal curing upon permeability 131

Effects of water and salt solution upon permeability 132

Effect of permeability upon durability 132

Durability versus scaling resistance 133

Summary 133

Equipment and procedures 134

Conclusions 140

Factors affecting durability and scaling resistance 140

Factors affecting permeability 141

Additional conclusions 141

Other observations and suggestions for future research 141

APPENDIX

A DESCRIPTION OF LOAD CELLS 144

B CEMENT ANALYSIS 148

C AGGREGATE PROPERTIES 150

D CONCRETE BATCH INFORMATION 153

APPENDIX

E DURABILITY AND SCALING STUDY DATA 157

F PERMEABILITY STUDY DATA 200

LITERATURE CITED 213

LIST OF TABLES

Table		Page
I	MAJOR CONSTITUENTS OF PORTLAND CEMENT	7
II	CURING TIME REQUIRED FOR CAPILLARY DISCONTINUITY	15
III	IDENTIFICATION OF ITEMS IN FIGURE 4	39
IV	SUMMARY OF STRAND LOADING PROCEDURES	45
V	CASTING SCHEDULES	58
VI	SUMMARY AND DESCRIPTION OF TREATMENTS	79
VII	TYPICAL DURABILITY AND SCALING STUDY DATA, OBTAINED FROM SLAB NUMBER 23A10	81
VIII	NATURAL FREQUENCY INCREASES DUE TO MORTAR DIKE REPLACEMENTS AND MOIST-ROOM CURING	82
IX	COMPUTED RESULTS FOR SLAB 23A10	86
X	TREATMENT COMPARISONS CHOSEN FOR DURABILITY AND SCALING STUDY	88
XI	RESULTS OF BARTLETT TESTS OF TRANSFORMED RELATIVE DYNAMIC MODULI	99
XII	RESULTS OF BARTLETT TESTS OF ADJUSTED WEIGHT CHANGES . .	109
XIII	RESULTS OF BARTLETT TESTS OF LENGTH CHANGES	111
XIV	RESULTS OF BARTLETT TESTS OF SCALING WEIGHT LOSSES . . .	113
XV	RESULTS OF BARTLETT TESTS OF NET ABSORPTIONS	117
XVI	CEMENT CHEMICAL ANALYSIS	149
XVII	MATERIAL QUANTITIES FOR EACH 2 CU. FT. BATCH	155
XVIII	INDIVIDUAL CONCRETE BATCH PROPERTIES	155

Table Page

XIX CONCRETE CYLINDER COMPRESSIVE TEST RESULTS 156

LIST OF FIGURES

Figure		Page
1	Portland cement hydration reactions	8
2	Moisture migration in the gel pores	25
3	Pretensioned slabs	37
4	Pretensioning equipment	38
5	Pretensioning operation	41
	Pretensioning operation, continued	44
	Pretensioning operation, continued	47
6	Pretensioned casting beds	48
7	Gilson testing screen	52
8	Lancaster mixer and incidental apparatus	52
9	Vibration table with casting bed in place	55
10	Diagram of slab treatments for each concrete batch	57
11	Steam chambers and their operation	61
12	Mortar dike forms and slab with attached mortar dike	64
13	Slab prepared for permeability study	67
14	Freezer and thawing racks	70
15	Permeability study slabs	72
16	Sonometer system	75
17	Example of Bartlett and Duncan test results	90
18 - 26	Results of Duncan tests of mean transformed	

Figure		Page
	relative dynamic moduli for treatment comparisons A through I, respectively	100 ff.
27	Results of Duncan tests of mean adjusted weight changes for treatment comparison A	110
28	Results of Duncan tests of mean length changes for treatment comparison A	112
29	Results of Duncan tests of mean scaling weight losses for treatment comparison C	114
30 - 38	Results of Duncan tests of mean net absorptions for treatment comparisons A' - I', respectively	118 ff.
39	Load cell description	145
40	Bridge arrangement for load cells	146
41	Load cell calibration curves, with error limits shown	147
42	Coarse aggregate gradation	151
43	Fine aggregate gradation	152
44	Combined aggregate gradation for each concrete batch	154
45 - 56	Relative dynamic moduli of elasticity versus number of freeze-thaw cycles for individual slabs	158 ff.
57 - 68	Adjusted weight changes versus number of freeze-thaw cycles for individual slabs	170 ff.

Figure		Page
69 - 80	Length changes versus number of freeze-thaw cycles for individual slabs	182 ff.
81 - 86	Scaling weight losses versus number of freeze-thaw cycles for individual slabs	194 ff.
87 - 98	Net absorptions versus number of days for individual slabs	201 ff.

ABSTRACT

The primary purpose of this study was to investigate the effect of prestress upon the durability of concrete. Small pretensioned concrete slabs, at stress levels of zero, 500, and 1200 psi., were fabricated from non-air-entrained concrete made with Type II cement. Half of these slabs were steam cured; the remaining slabs were cured in a moist, room temperature environment. These slabs were subjected to a freeze-thaw environment, half with water ponded on their top surfaces and the remaining specimens with a $CaCl_2$ solution in contact with their top surfaces. At frequent intervals the natural frequencies of transverse flexural vibration, weights, and lengths of the slabs were measured. Evaluations of the degree of surface scaling were also made.

Duplicates of these slabs were fabricated for an additional study to determine the effects of prestress, curing procedure, and type of solution upon the permeability, or absorption characteristics of concrete. Tall glass standpipes were sealed to the surfaces of these slabs and filled with water or $CaCl_2$ solution. Absorption rates were determined by periodically measuring the quantities of liquid necessary to maintain a constant level in the standpipes.

From statistical and qualitative interpretations of the data from these studies it was concluded that prestressing slightly improves the durability of concrete. It was also concluded that steam cured concretes are less durable, more susceptible to scaling damage, and possibly more permeable than concretes cured in a moist, room temperature environment. The extremely deleterious surface effects of salt solutions upon concrete, in a freeze-thaw environment, were also observed; although the slabs ponded with $CaCl_2$ solution exhibited only slightly greater durability losses than slabs ponded with water.

The only important conclusion drawn from the permeability study was that concrete absorbs $CaCl_2$ solution at a rate which does not differ significantly from that at which it absorbs water.

CHAPTER I

INTRODUCTION

Concrete durability

The importance and versatility of portland cement concrete as a construction material is well recognized. The annual world-wide consumption of concrete is exceeded in quantity by few other materials. Yet, despite its wide usage, it is one of the least understood materials at our disposal. It has been only in the past few decades that a concentrated scientific study of this material has been attempted, and the time for reasonably accurate prediction of the behavior of concrete in all structural and environmental situations is still in the future.

Perhaps the most serious disadvantage of concrete is its lack of durability in many common environments. As with all materials, there are certain environments which are deleterious to the appearance and structural utility of concrete. Nearly everyone is aware of the damage that results when rock salt is used to remove ice from the surface of concrete. Also evident is the severe damage to concrete coastal structures caused by salt corrosion and alternate wetting and drying between the tide lines. These are just two of the many examples of conditions which cause unsightly, dangerous, and costly damage to portland cement concrete.

Of particular interest is the progressive deterioration that occurs when concrete is subjected to repeated cycles of freezing and thawing in the presence of de-icing salts. The exact mechanism of this type of

destruction is not completely understood, but it is generally conceived to be a physical mechanism.

Concrete is a relatively porous mass, with part of its porosity attributable to capillary channels, or voids. These channels, if continuous, readily allow the penetration of water into the concrete mass. When frozen, this interior water expands, thereby exerting pressure on the capillary walls. If these pressures are sufficiently great, cracking of the concrete will occur. The newly formed cracks allow further penetration of water into the concrete mass after thawing, and further freezing and thawing causes the damage to continue until the concrete is so weakened as to result in the loosening of sizeable pieces of the material. If the penetrating moisture is salt-laden, then additional pressures might be created by the growth of salt crystals in the voids.

Concrete protection

Perhaps the most effective means for improving the durability of concrete in a freeze-thaw environment is air-entrainment. Air-entrained concrete contains innumerable minute air bubbles uniformly distributed throughout the cement paste. Entrainment of air can be effected by additions interground with the portland cement during manufacture or with admixtures added during the mixing of the concrete. The entrained air reduces the destructive effects of freeze-thaw action by providing readily accessible chambers into which the liquid under pressure may escape, and thereby alleviates the pressure on the capillary walls caused by the ice and salt-crystal expansions.

Generally high strength concrete will be more durable than low strength concrete. This can be rationalized by considering the relationship between strength and the W/C (water/cement) ratio of concrete, which has been fairly well established to be that strength is inversely proportional to the W/C ratio, if all other factors remain unchanged. Since a reduction in the W/C ratio will produce a less porous concrete, hence a concrete which is probably less permeable, the general strength-durability relationship seems reasonable.

Certain admixtures such as silicone-water solutions tend to improve the durability of concrete in freeze-thaw environments. Here the effect is similar to most water-reducing admixtures, in that the desired workability of the concrete can generally be achieved with a reduced W/C ratio. It is also noteworthy that air-entrainment usually improves the workability of concrete, thereby allowing a reduction in the W/C ratio.

Surface treatments, such as certain resins and bituminous tar products, will often serve to protect concrete from the destructive effects of freeze-thaw action. These are primarily barriers to prevent ingress of liquids and do not cause basic structural alterations of the concrete.

All of these practices result in concrete which is more durable. The improved durability would seem to lend support to the concept that freeze-thaw destruction results from expansion due to ice and salt-crystal formation in the pores, since the reduced permeability resulting from these practices would decrease the effects of such a physical mechanism.

Purpose of study

Although the aforementioned practices, accompanied by stricter field inspection of concrete mixing and placement, have helped to lengthen the maintenance-free life of many concrete highway structures, the lack of durability of concrete still remains a serious weakness. The tremendous annual cost for repair of frost damage to our highway systems, as well as the discomfort to motorists, is sufficient cause for concentrated efforts to find better ways for preventing its occurrence.

That freeze-thaw destruction in the presence of de-icing salt solutions is primarily a mechanical rather than chemical action is supported by the methods employed for reducing its effects. It would appear that any practice which would reduce the permeability of concrete would improve its durability. Alternatively, any method which would increase the tensile strength, or expansion resistance, of concrete should also improve its durability.

Considering the behavior of concrete under compressive loading, and more importantly the creep of concrete under sustained load, we may hypothesize that prestressing might reduce the permeability of concrete by reducing the average capillary cross-sectional area through distortion, and thereby increase its durability. In addition, the uni-directional restraint against destructive expansion, or increased effective tensile strength, should also help to improve the durability of prestressed concrete.

Therefore, the primary purpose of this study is to determine the effect of prestressing on the durability of portland cement concrete.

Nature of investigation

Small pretensioned slabs were fabricated using carefully controlled, non-air-entrained concrete. Air-entrainment was intentionally omitted in an attempt to accelerate the destructive effects of freeze-thaw action. The levels of prestress chosen were zero, 500, and 1200 p.s.i.

In order to simulate actual field conditions, mortar dikes were attached around the peripheries of the top surfaces of the slabs to retain ponded solutions. These slabs were also used to study the effect, if any, of prestress on the scaling resistance of concrete.

The measured parameters for the durability study were the natural frequency of transverse vibration, weight, and length changes. For the scaling resistance study, the weight of material loosened from the top surface was the measured index.

Duplicate slabs were cast to determine the effect of prestress on the permeability of concrete. These slabs had standpipes sealed to their top surfaces to provide a means for the determination of rate of fluid ingress under a two-foot pressure head.

Since steam curing is the predominant practice in most prestressing operations, half of the slabs were steam cured to study this effect on the durability, permeability, and scaling resistance of prestressed and non-stressed concrete.

CHAPTER II

REVIEW OF LITERATURE

The hydration of portland cement

The chemical and physical transformations which occur when water and portland cement are combined are highly complex and not fully understood. However, basic scientific investigations in this area, with the aid of such refined techniques as X-ray diffraction analysis and electron microscopy, have greatly aided the understanding and explanation of the many complex phenomena existing in the hydration process. A thorough review and discussion of the work which has been accomplished in this area is beyond the scope of this paper; however, a brief discussion of the hydration process, as it is understood at present, seems necessary in order to better understand the porous structure of the hydrated product.

Four compounds are generally regarded to be the main constituents of portland cement. These compounds, or phases, are identified in Table I, along with their compound compositions, accepted abbreviations, and average weight percentages as calculated by the Bogue* method for a typical Type I, or standard, cement (1).**

---

* A method devised by R. H. Bogue, circa 1930, by which the amounts of the compounds in a cement can be calculated if the elements are known from a quantitative chemical analysis.

** Underlined numbers in parentheses refer to references listed in the section LITERATURE CITED, beginning on page 213.

TABLE I

MAJOR CONSTITUENTS OF PORTLAND CEMENT

Phase	Compound composition	Abbreviation	Weight content
Tricalcium silicate	$3CaO \cdot SiO_2$	C_3S	48 %
Dicalcium silicate	$2CaO \cdot SiO_2$	C_2S	27 %
Tricalcium aluminate	$3CaO \cdot Al_2O_3$	C_3A	12 %
Tetracalcium aluminoferrite	$4CaO \cdot Al_2O_3 \cdot Fe_2O_3$	C_4AF	8 %

In addition to these major phases, there exist other compounds in portland cement, such as MgO, TiO_2, Mn_2O_3, K_2O, and Na_2O, which amount to only a few per cent of the weight of the cement. $CaSO_4$, in the form of gypsum, is also added to the cement during manufacture, primarily for the purpose of preventing "flash setting" of the cement.

The manufacturing processes whereby these compounds are produced and combined in the desired proportions, are described by many authors (1, 2, 5, 14) and will not be further discussed in this paper.

The word "compound" is usually reserved for pure substances which have definite formulas. Since the four constituents listed in Table I usually contain relatively large quantities of dissolved impurities, their composition formulas are not quite correct, so most researchers prefer to call them phases. The relative amounts of these phases are dependent upon the proportioning of the raw materials from which the cement is manufactured, and portland cements have been classified into basic different types depending upon the relative amounts of these major phases and of

the other minor compounds in the cement.

When water in the correct proportions is mixed with portland cement, a plastic cohesive mass is formed composed of aqueous solution, a little powdered gypsum, and particles of cement which lie in the size range between 1/2 micron and 75 microns (3). These particles immediately begin to be transformed by reaction with the water to form new compounds approximately as shown in Figure 1 (4).

$$2(3CaO\cdot SiO_2) + 6H_2O \longrightarrow 3CaO\cdot 2SiO_2\cdot 3H_2O + 3Ca(OH)_2$$
(C_3S) (water) (tobermorite gel) (calcium hydroxide)

$$2(2CaO\cdot SiO_2) + 4H_2O \longrightarrow 3CaO\cdot 2SiO_2\cdot 3H_2O + Ca(OH)_2$$
(C_2S) (water) (tobermorite gel) (calcium hydroxide)

$$4CaO\cdot Al_2O_3\cdot Fe_2O_3 + 10H_2O + Ca(OH)_2 \longrightarrow 6CaO\cdot Al_2O_3\cdot Fe_2O_3\cdot 12H_2O$$
(C_4AF) (water) (calcium hydroxide) (calcium aluminoferrite hydrate)

$$3CaO\cdot Al_2O_3 + 12H_2O + Ca(OH)_2 \longrightarrow 3CaO\cdot Al_2O_3\cdot Ca(OH)_2\cdot 12H_2O$$
(C_3A) (water) (calcium hydroxide) (tricalcium aluminate hydrate)

$$3CaO\cdot Al_2O_3 + 10H_2O + CaSO_4\cdot 2H_2O \longrightarrow 3CaO\cdot Al_2O_3\cdot CaSO_4\cdot 12H_2O$$
(C_3A) (water) (gypsum) (calcium monosulfoaluminate)

Fig. 1. Portland cement hydration reactions (4).

It should be understood that the reactions described in Figure 1 are probably not stoichiometric equations, but serve only as a guide to visualize the transformations that occur in the hydration process. These reactions will be discussed briefly before proceeding to a discussion of the physical characteristics of their combined mass.

The reaction of tricalcium aluminate with water and calcium hydroxide is quite violent, and leads to a high heat production and rapid stiffening of the cement paste, which is called flash set. If unchecked, this reaction is very undesirable. In order to retard this reaction, gypsum is usually interground with the cement clinker during manufacture, and when water is added to the cement, the C_3A and gypsum combine to form insoluble calcium monosulfoaluminate. It has been theorized that the calcium monosulfoaluminate forms a coating over the exposed C_3A particles, and thus hinders the rapid hydration of the C_3A.

The tetracalcium aluminoferrite is a relatively unimportant phase in portland cement. It is the iron bearing phase which imparts the characteristic gray color to portland cement, and in its absence the cement will be white. However, both C_3A and C_4AF are useful in the manufacture of portland cement, since they act as a flux and therefore reduce the clinker burning temperature, facilitating the combination of lime and silica (5). It should be noted that C_4AF also may react with gypsum to form calcium sulfoferrite, which may accelerate the hydration of the two silicate phases. (One can appreciate the reasons for careful control of the gypsum content in portland cement, since it can behave as an accelerator as well as a retarder.)

The two silicate phases, C_3S and C_2S, are the most important constituents of portland cement, and the behavior of these two phases alone is reported to be similar to that of portland cement (5). Together they constitute about 75 per cent of portland cement, by weight. It is generally accepted that these two compounds form the same products when combined with

water, these being crystalline calcium hydroxide and a calcium silicate hydrate known as tobermorite gel, so called because its composition and crystal structure resemble that of the natural mineral tobermorite. In a fully hydrated cement, tobermorite gel constitutes about 50 per cent, by weight, and is the most important cementitious material in the cement. About 25 per cent, by weight, of a fully hydrated cement is composed of calcium hydroxide.

The term "cement gel" has been used in describing that part of hydrated cement which is responsible for "internal surface" and porosity (4). Powers (6) has given a figure of 650 $m.^2/cm.^3$, or 250 $m.^2/gm.$, for the specific surface of the tobermorite, and approximately 87 angstroms as the size of the gel particle, expressed as the diameter of an equivalent sphere. This diameter corresponds to about 15 "diameters" of a calcium silicate molecule. Values for specific surface and gel-particle size have been obtained from adsorption and porosity measurements. Thus the sizes of the hydrated particles are so small that hardened pastes are colloidal systems, and the term "gel" depicts a finely divided, cohesive mass.

It is known that in the hydration process, there is a doubling of the volume of solids without a significant change in the paste volume. The hydrated cement is bonded to the unhydrated cement grains, but the mechanism whereby the structure growth takes place is not certain. There are several possible explanations compatible with observed heat gain periods, X-ray diffraction evidence, differential volume measurements, and absorbed water computations. Perhaps the hydration product forms

an enclosure, or shell, around each cement grain, and the dissolving interior silicates permeate outward through the layer of hydrate to precipitate on the exterior surface. Alternatively the shells may grow from the interior by continued reaction between the remaining unhydrated grain and water which penetrates the surrounding enclosure, the shells ceasing to expand at points of contact with other shells and subsequently distorting into available voids where there are no growth restrictions. Otherwise, the process may be one in which the silicates go into solution, and are precipitated throughout the entire paste mass when the solution becomes saturated.

Regardless of the exact mechanism of formation, the terms "colloidal system" amd "gel" appear to be quite accurate in describing the cementitious hydration product. The bonding forces responsible for cementing action probably are due to physical attraction, or van der Waals' forces, between the individual gel particles, and between the gel particles and the aggregate surfaces. In addition, there may be chemical bonding, or cross-linking, between the gel surfaces. It may be noted that calcium hydroxide exerts a stronger attractive force per unit area than does the tobermorite gel, but the specific surface area of the most finely divided calcium hydroxide is only about one-tenth that of tobermorite gel (4), and thus the calcium hydroxide is a less important cementing material than is the tobermorite gel.

Finally, we arrive at a consideration of the paste structure as a whole, and patterns into which the hydrated particles become oriented. One very simple model (3) of the paste cross-section may be thought of as

the classical bubble model, with each bubble representing a gel particle. The bubbles, or spheres, are very closely packed, and the interstitial voids represent the paste voids which are called gel pores. In addition, there are large channels, or capillary voids in hardened paste, and these may be visualized in cross-section by considering that several of the bubbles in a few randomly scattered, irregularly shaped areas have burst. Considering that the specific surface of the paste proper may be about 650 $m.^2/cm.^3$, this means that the gel particles, represented by the bubble spheres, would average about 90Å in diameter (5, 6). However, the gel particles are by no means spherical; rather they are mostly fibrous and platy, so the bubble model is of little more than academic interest.

The electron microscope has been the chief tool for observing the hydration structures, and some works contain many fine illustrations of these structures (7, 8, 9). The results of such electron optical studies have been interpreted (4) to show that the gel particles tend to form in the following shapes: 1.) clusters of rod-like fibers, 2.) rolls, or tubes, made up of very thin sheets only a few molecules thick, and 3.) nearly flat, but more generally crumpled sheets -- again, very thin. The sketches in Figure 2, on page 25, better illustrate these three formations. The gel fibers, rolls, and sheets, along with the microscopic calcium hydroxide crystals, apparently form an intricate network containing other amorphous materials and void spaces.

The permeability of concrete

As mentioned previously, the fresh cement paste is a fluid mass of

aqueous solution, cement grains, and some entrapped air bubbles introduced in the mixing process. When fully hydrated, the hydration products occupy a volume which is greater than that of the original solid volume by a factor of about 2.1 (10). In actuality, a portland cement never really becomes fully hydrated, but there is still approximately a doubling of solid volume under normal hydration circumstances. Thus as the hydration process continues, that volume of the paste occupied by water is gradually reduced as the hydration products are formed. When the hydration is essentially complete, there usually will remain water-filled voids which have not been filled with hydration products. These voids are termed "capillary voids" and are the primary reason for the permeability characteristics of concrete.

Ideally, one would desire an end product of the highest possible density, with no capillary voids. This is possible, providing the hydration is continued to completion, and the W/C ratio is not in excess of about 0.35, by weight (5, 10). However, in normal concreting practice, the W/C ratio is seldom, if ever, as low as 0.4, and is usually greater than 0.5. Thus, under most circumstances, there remain capillary voids in the matrix of cured, in-service concrete.

The porosity of the gel proper is about 28 per cent, but the mean "diameter" of these gel pores is in the range of only 15Å to 25Å (5, 11). The mobility of water in such small spaces would be quite unlike that of free water, so the contribution of the gel pores to the concrete permeability is negligible. Powers (12) has given a value of 7×10^{-14} cm./sec. as the approximate permeability of the gel pores. He explains that this

is only about one-twentieth to one-hundredth of the permeability of the paste as a whole. Therefore, the permeability of concrete is generally considered to be controlled by the capillary porosity of the cement paste. The volume of capillary voids may be as low as zero per cent or as high as 40 per cent of the paste volume (5), depending primarily on the W/C ratio, and the degree of hydration.

The capillary pores form a randomly distributed system throughout the paste, and though they vary in shape of cross-section, their "diameter" has been estimated to be in the range of 0.0005 to 0.00005 inch (11). This system may or may not be continuous, again depending upon the W/C ratio and degree of hydration. In a fresh paste, the water system is continuous throughout the mass, but as hydration proceeds the system becomes segmented and gradually constricted. If the W/C ratio is low enough, and the degree of maturity sufficiently large, the capillary channels may become completely "plugged" or segmented by the gel products. Estimates for the time required for the capillary channels to become discontinuous and segmented into capillary cavities, for various water/cement ratios, have been made for an ordinary Type I cement under standard laboratory conditions (10). These estimates are given in Table II.

The permeability of any cement paste will decrease with maturity, but if the W/C ratio is too large, discontinuity of capillary pores may never be achieved. As will be discussed later, the degree of continuity or discontinuity of the capillary pores in cement paste is an important factor in the durability of concrete.

TABLE II

CURING TIME REQUIRED FOR CAPILLARY DISCONTINUITY (10)

W/C ratio by weight	Time required
0.40	3 days
0.45	7 days
0.50	14 days
0.60	6 months
0.70	1 year
> 0.70	impossible

It should be mentioned that the porosity of concrete is not due entirely to the matrix, or paste, since the aggregate is also porous. In fact, the aggregate in a concrete may often be even more permeable than the paste. However, since each aggregate particle is coated entirely with a layer of paste, the permeability of the concrete is usually considered to be dependent upon the characteristics of the paste alone.

Concrete deterioration

Causative factors

The various organic and inorganic compounds which can cause destruction of concrete by chemical attack of the cement paste are too numerous for complete discussion. The effects of chemical agents on portland cement are not of immediate interest, except in cases where the destructive effects are magnified due to penetration into the concrete through the paste capillaries. More extensive discussions of chemical attack on concrete appear in references 2, 13, and 14. Usually, the chemicals to which concrete may be exposed can be anticipated, which is fortunate since

concrete is quite easily destroyed by so many, particularly in industrial situations.

Of the more common forms of chemical attack, only the effects of leaching, sulfate solutions, sea water, alkali-aggregate reaction, and natural slightly acidic waters will be considered in this discussion, since the permeability of concrete can be an important factor in reducing or amplifying these effects. It is realized that no concrete can resist the attack of many chemicals, particularly strong acids, since such chemicals destroy the paste by compound breakdown and separation; so the density and permeability of the concrete are of no consequence under such conditions.

Leaching of compounds out of cement paste occurs when water percolates through cracks, through poorly compacted concrete, or along poorly made joints. Usually, it is the readily soluble calcium hydroxide which is dissolved and removed by the water. Ordinarily the most harmful aspect of such a process is that it mars the appearance of exposed concrete surfaces by depositing white calcium carbonate, and sometimes calcium sulfate. However, the same process conceivably can occur in reasonably "good" concrete by water migration through the capillaries, with resulting channel enlargement.

Certain ground waters are essentially sulfate solutions, and these sulfates cause destructive expansion of concrete by reacting with calcium hydroxide and with the tricalcium aluminate hydrate. The reaction products are gypsum and calcium sulfoaluminate, which have considerably greater volume than the original compounds. Of course, such reactions would occur

at any exposed concrete surfaces, but the destructive effects would be considerably more serious in the event of deep penetration of the concrete by the sulfates.

Sea water contains other salts as well as sulfates. The sulfates attack the cement compounds as described above; however, failure arising from attack by sea water is not preceded by the large expansions noted in attack of sulfate-bearing ground waters. This is presumed to be because gypsum and calcium sulfoaluminate are much more soluble in chloride solutions (14), and thus the sea water leaches out these products before expansion occurs to any degree. However, salt solutions penetrate and rise in concrete structures by capillary action, and drying at or near the tide line causes crystallization to take place. This crystallization causes expansive pressures which are deleterious to concrete, and will be discussed more thoroughly in a later section.

The active silica compounds of certain aggregates will react with the alkalis, notably Na_2O and K_2O, in cement to form an alkali-silicate gel. This results in destructive expansion in the regions of the aggregate surfaces. This gel is of the "unlimited swelling" type (6), and when it absorbs water, significant pressures are developed. This reaction does not occur in dry concrete (14), and since a continuous supply of water increases its destructive effects it is apparent that the permeability of the concrete is an important factor in this type of attack.

Naturally occurring acidic waters are obviously harmful to concrete; however, most such waters are only very slightly acidic, and the damage is not so serious as might be expected. There are indications that such

waters may corrode the surface mortar of the concrete, and then the action stops or at least subsides (13). This may be because the reaction products tend to block the pores, preventing further ingress and attack. However, the dissolved paste may be carried away by moving water, leaving additional exposed surface on which the acid can act. A highly permeable concrete would undoubtedly be more rapidly destroyed by this type of attack, since more cement surface area would be exposed to the aggressive solution.

One other type of attack which might be considered to be in the realm of chemical deterioration of concrete would be that of corrosion of reinforcing steel in the concrete. Usually portland cement concrete provides good protection of embedded reinforcing steel against corrosion. This protective value may be ascribed to its high alkalinity and relatively high electrical resistivity in atmospheric exposure (13). However if cracks should develop, or if the capillary permeability of the concrete is too large, the ingress of moisture and air can cause steel corrosion, resulting in destructive expansion due to the increase in volume of the steel oxidation products. In addition, the absorption of salts which might exist in the penetrating moisture can lead to anodic and cathodic areas in the concrete. The resulting electrolytic action can cause an accumulation of corrosion products on the steel, with a consequent rupture of the adjacent concrete, as well as a reduction of the steel cross-sectional area. Of course, cracks which extend to considerable depths into the concrete can be caused by many factors, not the least of which is the destruction promoted by an initial high capillary permeability.

It is also pertinent to note that, in the absence of cracks, a highly permeable concrete will be able to contain more water than will a more dense material. This greater water content means that the electrical resistivity of the concrete will be reduced, which can result in galvanic corrosion of the reinforcement.

Thus, we can observe many forms of concrete deterioration which we might classify as being the result of chemical attack on concrete. All of these are, to a degree, affected by the permeability of the concrete, the intensity of attack generally being increasingly dependent upon the permeability.

In the realm of physical, or mechanical destruction of concrete, we may certainly consider excessive loading, impact, and surface wear or abrasion. However, these are directly controllable by the users and can be accounted for during the design of the structure. These conditions will not be considered further in this paper.

One type of mechanical deterioration which is exceedingly important and difficult to control, however, is that of frost action against concrete. As saturated concrete is frozen, the water in the capillary pores freezes and expansion takes place. If the stresses developed by this expansion exceed the tensile strength of the concrete, damage will occur resulting in cracking and spalling. This type of destruction, as well as that occurring as a result of de-icing salts on the concrete, will be discussed later.

Protective measures

A few of the ways in which concrete can be damaged have been discussed, and now consideration will be given to some measures which can be taken to prevent, or at least hinder, these destructive mechanisms. One obvious protective measure against all of these destructive causes is complete enclosure of the concrete in an impenetrable shield. Surface treatments with bituminous or rubber products, resins, and other agents have been employed successfully, and such treatments are probably the only effective means for protecting concrete which may be exposed to harsh chemicals, such as strong acids. However, complete surface sealing can be expensive and often impossible where concrete is cast in situ.

The resistance of concrete to the attack of slightly acidic solutions can be improved by allowing the concrete to dry in air before exposure (5). The $Ca(OH)_2$ in the cement reacts with CO_2 in the air to form a surface film of $CaCO_3$, which blocks the surface pores and reduces the permeability. Air drying is usually practicable only with pre-cast concrete members. For cast-in-place structures it is best to exercise careful control of the concrete mixing and placement so that a high quality, low permeability concrete will result.

Where the concrete is to be exposed to sulfate-bearing waters, it is possible to reduce the damaging effects by using a cement which is low in C_3A content, thus providing less reactant. Also, replacement of some of the cement by pozzolanic materials is helpful, since these combine with, and effectively fix or stabilize, some of the free, or readily soluble $Ca(OH)_2$. However, the permeability of the concrete is a most impor-

tant determinant of the seriousness of sulfate attack, and the greater the permeability the more vulnerable will be the concrete.

At this point, it might be noted that steam curing of concrete is beneficial in that it increases the resistance to sulfate attack, and practically eliminates leaching and efflorescence (2). More will be said about steam curing in a later section.

In general, the best protection for concrete against sea water attack is to assure that the concrete is of low permeability and high density. Also, it is important that the reinforcement in coastal structures be covered by sufficient depth of concrete to prevent ready access of the corrosive liquids to the steel.

Control of the destructive effects of alkali-aggregate reactivity is generally achieved by limiting the alkali content of the cement, and/or by rejecting those types of aggregate which are potentially reactive with the alkalies in cement. Also, the addition of finely ground siliceous, or pozzolanic materials to the concrete can reduce the expansion by reacting initially with the alkalies, thereby reducing the quantity of alkaline materials available for reaction with the larger aggregate particles after hardening. As has been noted, however, impermeability is a highly important criterion for the resistance of concrete to this type of deterioration.

Leaching is entirely dependent upon the permeability of the concrete; and in the absence of cracks and poor compaction, the seriousness of this type of damage is primarily dependent on the capillary characteristics of the concrete. Thus, good construction practices and mix proportions are

imperative for prevention of this phenomenon.

Therefore, the importance of low permeability of concrete can not be too strongly emphasized as a factor for improvement of durability under most common natural conditions. The use of surface treatments and coatings, as well as other procedures which effectively plug the capillary pores, has already been indicated as being practical. Also, the importance of good compaction and the lowest possible W/C ratio consistent with adequate workability has been emphasized. Certain water-reducing admixtures are marketed which allow the reduction of water content in concrete without reducing the workability. Any such admixtures which allow a reduction in the W/C ratio are beneficial to the durability of concrete, providing no adverse reactions or shrinking and swelling characteristics are induced by the use of such materials.

For resistance to frost action on concrete, again low permeability is the most important single factor, in that it affects the degree of concrete saturation. In addition, the degree of aggregate saturation is important (15), since a highly saturated aggregate particle will expand upon freezing, and tend to destroy the surrounding matrix. In general, dry aggregate will result in a more frost resistant concrete.

Perhaps the most effective means for improving the freeze-thaw durability of portland cement concrete is air-entrainment. There are many compounds, notably natural resins, tallows, and sulfonated soaps or oils, which will cause billions of minute bubbles to be distributed throughout the concrete mass when added to the fresh concrete during the mixing process. Other materials interground with the cement clinker

during manufacture will accomplish the same effect. In addition, gas-forming agents, such as aluminum or zinc powder, and hydrogen peroxide, can also cause nearly the same effect.

The primary reason for the beneficial effect of air-entrainment is that the water under pressure in the capillary voids is afforded a much shorter path to other voids which can accommodate the excess moisture. This factor will be elaborated in the following section. An additional important benefit of air-entrainment is that of allowing a reduction in the W/C ratio. The tiny bubbles retain their sphericity, effectively replacing some of the fine sand particles, and thereby reducing the water demand. They are also rather like a lubricant between the solid particles of the fresh concrete, allowing the particles to glide past each other more readily, thus causing an increase in workability. The reduced W/C ratio, as has already been indicated, causes a reduced permeability in the mature paste.

Of course, any surface treatments or coatings which effect a reduction in the permeability of concrete will generally improve its frost resistance.

Thus, the effect of permeability on the ability of concrete to resist many ordinary destruction mechanisms is quite pronounced. Usually, any material or procedure whereby the ingress of moisture can be hindered or prevented will result in a concrete better able to withstand many types of chemical and/or physical attack.

Freeze-thaw and related modes of destruction

A few statements have been made concerning frost action upon concrete. As the concrete is frozen, moisture in the voids will begin to freeze and expand. Freezing will occur first at the exposed concrete surface, and then proceed slowly inward. Thus ice formed in the pores at the surface will block the pores, and the rate at which the water will be displaced by the advancing ice will depend upon the rate of freezing and the degree of saturation. The hydraulic pressure developed will depend upon the length and size of the capillary channel and the permeability of the paste between the capillary and another void that can accommodate the excess water (16). The pressures developed can be quite large, since water undergoes a volume increase of about 9 per cent when frozen.

Freezing of the water in the gel pores is quite unlikely under most natural circumstances, since these pores are so small that the formation of ice nuclei would probably not occur above about -78°C (17). However, movement of water in and out of the gel pores has been theorized as an important factor in the damaging effects of shrinking and swelling of the cement paste (4). In light of the observed physical forms of the hydrated gel products, this movement might occur as shown in the sketches of Figure 2 (4).

From entropy considerations, Powers (17) has suggested that, with a fall in the temperature of the capillary water and ice, the gel water acquires an energy potential enabling it to move into the capillary pores containing ice. Thus the ice can grow and cause further expansion.

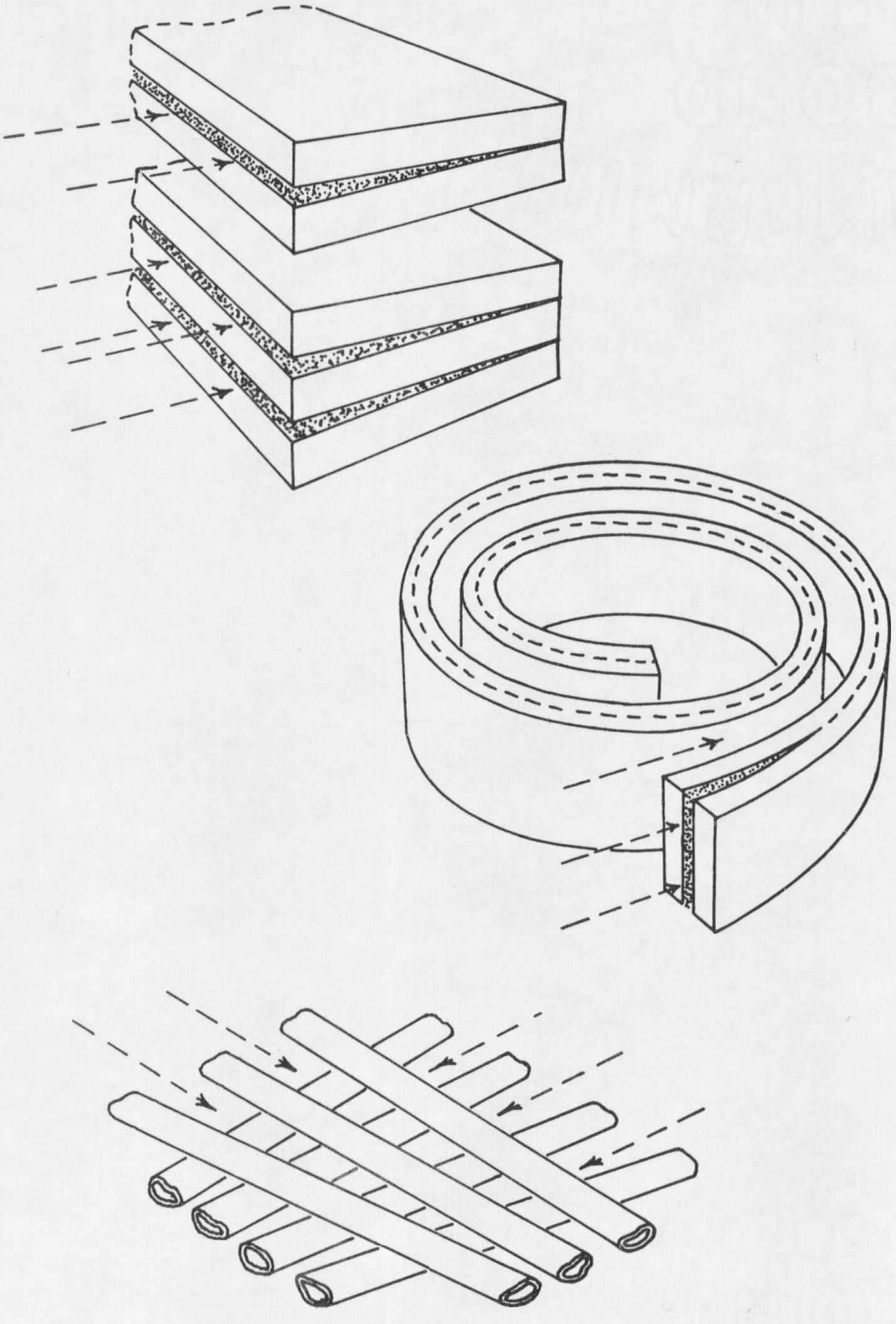


Fig. 2. Moisture migration in the gel pores (4).

Upon thawing, the moisture could be readsorbed by the gel surfaces.

Some of the expansion which occurs during freezing is non-recoverable after thawing, owing to paste disruption. Upon refreezing, further expansion occurs, and thus the effect is cumulative.

Disruptive expansion may also occur because of osmotic pressures. As "pure" water is frozen out of the otherwise impure water in the capillaries, there occur local increases in solute concentration. The cement paste can be considered as a membrane, and water will tend to flow towards the zone of freezing in order to lower the solute concentration. Osmotic pressures resulting from such flow can be quite high; and in addition, the supply of water provides opportunity for the ice crystals to grow (5). This source of pressure can be particularly important where de-icing salts are dissolved in the pore water.

Ice will form in the larger cavities or pores first, that is, in the pores where the water is least affected by adsorptive forces (18). Ice crystals existing in these larger pores will draw water molecules from the surrounding gel by a diffusion process (18) and from other water with which they are in contact but which cannot nucleate at the ambient temperature because of smaller enclosure size (19). Hansen (19) has demonstrated that such ice crystals can exert considerable pressure as they grow.

An analogous situation exists when de-icing salt solutions are contained in the capillaries, in that the salt crystals will nucleate and begin to grow in the larger pores. They will then take up solute ions from the solution with which they are in contact, but which cannot nucleate at the ambient temperature because of the size of the container (19).

Thus the increased severity of frost damage to concrete in the presence of de-icing salts can be ascribed to the osmotic pressure effect and the salt-crystal growth concept.

The chemical effect which salt solutions have on concrete has not been completely evaluated. It is believed by some researchers (20) that the salts in the water, while not reacting with the component elements of the cement, cause the cement compounds to become more soluble due to the increased ionic strength of the solution. This has the effect of intensifying and accelerating the development of the corrosion process.

As has been mentioned, reduction of the concrete permeability either by reducing the W/C ratio, or by complete or partial blocking of surface pores with surface treatments and coatings can be very effective in improving the frost resistance of the concrete. Of more interest is the effect of air-entrainment on the frost resistance of concrete.

Not only does the hydraulic pressure developed by expansion due to ice formation depend upon the permeability of the paste between the capillary void and another void which can accommodate the excess water, but also upon the "escape distance", or thickness of the paste through which the water must travel to reach the empty void. The uniform distribution of minute, closely spaced air bubbles caused by air-entraining agents accomplishes a reduction in the average escape distance, and consequently causes reduced hydraulic pressure build-ups. These bubbles, per se, have little effect upon the concrete permeability, since they are unconnected and afford no additional channels for moisture migration. However, when advantage is taken of the fact that air-entrainment generally causes a

more workable mix, the permeability will actually be reduced because of the allowed reduction in the water/cement ratio. Perhaps the only major disadvantage of air-entrainment is a slight reduction in the concrete strength, but this reduction is usually negligible, and can be accounted for in the mix design.

Most materials undergo a contraction, or volume decrease as their temperature is lowered. Such is also the case with the materials in concrete; but owing to the expansion of freezing water and growing ice crystals, a freezing, unprotected concrete will undergo a volume increase, or expansion. Air-entrained concrete, however, will continue to contract as its temperature drops below the freezing point of water. This is partly due to thermal contraction of the concrete solids and to relief of hydraulic pressures by the air voids. In addition, Nerenst (18) has drawn attention to the fact that water on the walls of the air voids may freeze on a microscopic scale and, because of the entropy effect previously described, will cause water to be drawn from the gel pores into the air voids. This would cause additional contraction of the concrete mass due to the resultant shrinking of the gel.

The essential point to be made in this discussion is that the permeability of concrete is an exceedingly important factor in the susceptibility of the concrete to damage from freezing and thawing. Although air-entrainment is a most effective means for reducing the harmful effects of ice and salt-crystal formation, it does not eliminate these formations. It would appear that any other method or treatment which would prevent the ingress of water and salt solutions would be a more direct and permanent protective

measure. Alternatively, any procedure which might effectively increase the tensile strength of concrete should also improve the durability of concrete, since the damage which occurs due to internal pressure increase is usually a result of such pressures having exceeded the tensile strength of the material.

The obvious solution is, as was mentioned, to block the cement pores with surface coatings, or other surface treatments. However, the type and location of some structures, particularly cast-in-place units, often prohibits such treatments. In addition, the usage of some structures, such as highway pavement slabs, reduces the effectiveness and life of surface treatments because of abrasive wear. It is from the two considerations of reduced permeability and increased tensile strength that prestressing might be considered as yet another alternative solution to the durability problem.

Before proceeding to the following discussion, which will be related to prestressing and its effect on concrete, a few statements concerning steam curing and its effect on the frost resistance of concrete seem pertinent. Since steam curing is such a widely used practice, mainly with precast and prestressed products, it is important to know what effects such curing might have on the durability of concrete. Neville (5) states that high pressure steam curing improves the resistance of concrete to freezing and thawing as well as to sulfate attack. In addition, such curing results in high early strength, reduced efflorescence, and reduced drying shrinkage and moisture movement. In fact, the only major disadvantages of high pressure steam curing are reduced bond strength with

reinforcement, and more brittle concrete. Troxell and Davis (2) agree with these statements. However, the effects of atmospheric pressure steam curing on the frost resistance of concrete are not so decidedly clear. Higginson (21) has reported that steam curing increases the permeability of concrete; and that steam curing up to 48 hours reduces the resistance of concrete to freezing and thawing. He also indicates that supplemental fog curing of initially steam cured concrete tends to lower the permeability and improve the frost resistance. However, Rieb (22) could detect no significant difference in the durability of steam cured and moist cured, prestressed beams in his studies. It could be that, since his beams were cast from air-entrained concrete, the change in durability may have been obscured. Other authors make no mention of the effect of atmospheric steam curing on the frost resistance of concrete (1, 2, 5).

The rheology of portland cement concrete

The mechanics of frost damage, and the factors which promote such damage, namely high permeability and low tensile strength, invite curiosity about the effects which prestress might have upon the durability of concrete. Concrete is a material which creeps, or undergoes increasing strain, when subjected to sustained stress. The creep characteristics of concrete are primarily dependent upon the behavior of the cement paste. The aggregate's contribution to creep is usually negligible, except that aggregate has been shown to restrain creep (23). If the mechanism of creep were such that a net decrease in void cross-section resulted, then the ingress of moisture should be retarded.

Although the exact mechanism of creep is not fully known, it is generally agreed that the gel response is the primary influencing factor. Glucklich and Ishai (24) state that only two theories are considered capable of explaining creep and phenomena relating to creep. These are the viscous theory and the seepage theory. The viscous theory states that the cement gel is a highly viscous liquid which flows under external loading. The seepage theory relies on the fact that cement gel is a hygroscopic solid, and that creep is due to water migration in the pores as a result of pressure differences caused by external loading. Or, stated another way, that creep is the deformation of a solid, rather than a viscous liquid, which is being damped by strong viscous resistance of absorbed water.

From tests on torsion specimens with low sand content, Glucklich (24) has shown that creep is almost non-existent in mortar deprived of nearly all of its evaporable water. These tests gave support to the seepage theory and contradicted the viscous theory, since they showed that creep is conditional on the presence of evaporable water, and not an inherent property of the gel itself.

It is reasonable to assume that the viscous theory has some applicability, however, since all solids tend to undergo some molecular rearrangement when subjected to sufficiently high stress; though perhaps the terminology "highly viscous liquid" is inappropriate for describing the gel proper.

There are many factors, which affect creep in concrete, that will not be introduced into this discussion. However, because of its pertinence to

this thesis, a few comments about steam curing are in order. A recent study at Montana State College (25) has shown that steam curing reduces creep, with longer durations of steam curing resulting in greater reductions in creep. This is in agreement with the stress/strength-creep relationship, in that steam curing hastens maturity, hence strength. From this standpoint, any durability characteristics which are affected by creep would probably be less easily influenced in steam cured concrete than in normal atmospheric moist-cured concrete.

This author has been unable to locate any information which might verify a relationship between creep and permeability. However, Neville (5) calls attention to the relationship between creep and concrete strength, suggesting that creep, like strength, is dependent upon the relative amount of unfilled gel space. A low gel/space ratio (6) is responsible for both a relatively low strength and a higher creep. Certainly, a low gel/space ratio means higher porosity, and undoubtedly higher permeability. It would seem logical, in light of the fact that the cement gel contains both pore and surface adsorbed water, that the possibility exists for relative movement between gel particles, as well as for volume decrease due to fluid migration. Such relative movement would be enhanced by moisture between the particles; and the removal of this moisture, as in the case of Glucklich's torsion tests (24), would surely hinder creep under this premise. Should particle movement occur, it would probably be in the direction of least resistance, that is, into available pore space. If such were the case, permeability might be reduced.

Thus, under the premise that creep may reduce pore size, prestressing would seem to be a possibility for reducing the permeability and improving the durability of concrete. An additional, and perhaps more significant effect of compressive prestress, is the resulting increase in the effective tensile strength of the concrete. This factor should have a decided beneficial effect on the frost resistance of concrete, since the hydraulic pore pressure build-up would apparently have to be greater in order to rupture the material.

It is possible, however, that the lateral expansion of a prestressed concrete member, due to the Poisson effect, would enhance the ingress of moisture. This expansion may even promote and add to that caused by the freezing pore water, and thereby detract from the benefits of restraint against expansion in the perpendicular direction.

Other prestressed concrete durability studies

Three investigations (22, 26, 34) of the effect of prestress on durability have been reviewed, the results of which are apparently conflicting. Rieb (22) has reported that stress levels, varying by increments of 500 psi. from zero stress up to 2000 psi. had no effect on the freeze-thaw durability of pretensioned concrete. Nor could he differentiate any effects introduced by varying the type of cement and method of curing. However, Rieb cast his specimens from concrete which was air-entrained to a level of about 4 per cent. This degree of air-entrainment may have been sufficient to so protect the concrete that any effects of prestress level might have been obscured.

Similarly, Klieger (34) was unable to detect any significant influence of a compressive prestress of 350 - 400 psi. on the resistance to freezing and thawing of either air-entrained or non-air-entrained concretes.

Gutzwiller and Musleh (26) were able to show a definite increase in freeze-thaw durability of concrete beams which were post-tensioned to 2000 psi., but they did not investigate the effect of various levels of prestress. These investigators also used air-entrained concrete, but the air content was less than 3 per cent. It is pertinent that some of the stressed beams in this study were released for testing, while the rest remained stressed during the tests. The results showed that the permanently stressed beams were significantly more durable than the intermittently stressed-released beams; and in most cases, the latter were more durable than non-stressed beams of the same mix. This would indicate that prestressing does produce a greater effective internal rupture strength; although, given enough freeze-thaw cycles, even this increased tensile strength can be exceeded. This may be a result of cumulative pressure build-up caused by rapid cycling, or it may be a fatigue phenomenon.

None of these studies was designed to evaluate the effect of prestress on the permeability and scaling resistance of concrete. Thus, in order to study the effect of prestress on these two factors, and to attempt to resolve the apparent conflict between the above mentioned studies, the following investigation was proposed.

CHAPTER III

LABORATORY INVESTIGATION

Modes of investigation

Two levels of stress other than zero stress were chosen to investigate the effect of prestress on the permeability, durability, and scaling resistance of concrete. The stresses selected were zero, 500, and 1200 psi., the maximum being dictated by the allowable strand load, specimen dimensions, and loss incurred by the method used for prestressing. The choice for the intermediate stress level, 500 psi., was arbitrary.

The following modes of investigation were followed for both steam cured and moist-room cured specimens:

(a) freeze-thaw cycling with approximately one-fourth inch depth of water ponded on the top surface of the specimen,

(b) freeze-thaw cycling with approximately one-fourth inch depth of calcium chloride solution ponded on the top surface of the specimen, with a chloride ion concentration of approximately 20,000 ppm.,

(c) two-foot head of water distributed over a circular area of the top surface of the specimen, the diameter of the circle being approximately 3-3/4 inches, and

(d) two-foot head of $CaCl_2$ solution (chloride ion concentration of approximately 20,000 ppm.) distributed as in (c) above.

The specimens of (a) and (b) were checked periodically for their natural frequencies of transverse flexural vibration, weight and length changes,

and degree of surface damage, or scaling. The rates of fluid penetration* into the specimens of (c) and (d) were measured by periodically recording the volume of fluid necessary to maintain a two-foot head on each specimen surface.

There were four replicates for each treatment. Thus for each of the four investigational modes, there were four specimens for each stress level and each curing procedure; or a total of ninety-six specimens were required for the entire study.

Description of specimens

The specimens used may more aptly be called slabs, and will hereafter be referred to as such. The nominal concrete dimensions of these slabs were: length = 10-1/2 inches, width = 4-1/2 inches, and depth = 2 inches. However, the over-all lengths of the slabs differed, depending upon the stress level. This was due to the necessity for end-bearing plates on the stressed slabs. Figure 3 is a photograph of three of these slabs, one at each stress level. Note that the slab on the left, which is non-stressed, has no bearing plates. The center slab is prestressed to 500 psi., and has 1/2 inch thick end-bearing plates, while the 1200 psi. slab on the right has 3/4 inch thick end-bearing plates.

---

* The terms "permeability" and "permeability study", which are used for describing this test procedure throughout this report, are perhaps inappropriate. Herein they are used in reference to a testing procedure which should probably be called a "moisture absorption" study, since the specimens were not saturated as in an ordinary permeability test. However, the author prefers "permeability" because the penetrating fluid was confined to a single flow direction, and was slightly forced by a relatively constant pressure head.

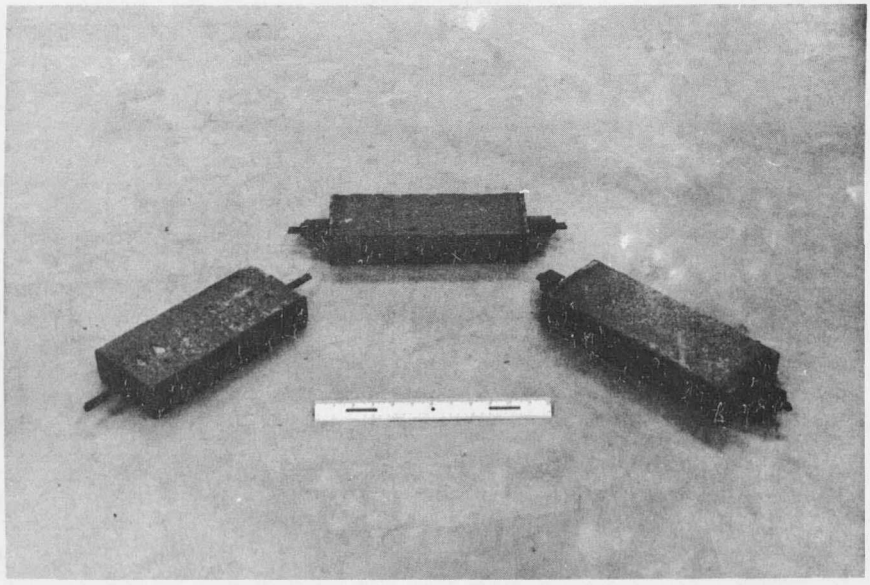


Fig. 3. Pretensioned slabs. (from left: zero, 500, and 1200 psi.)

Prestressing operation

Figure 4 is a photograph of the equipment necessary for the pretensioning operation; the items shown are described in Table III. The utilization of these items is presented in the photographs of Figure 5, and reference to the identification letters of Figure 4 and Table III will be made in the following discussion to assist the reader in understanding these procedures.

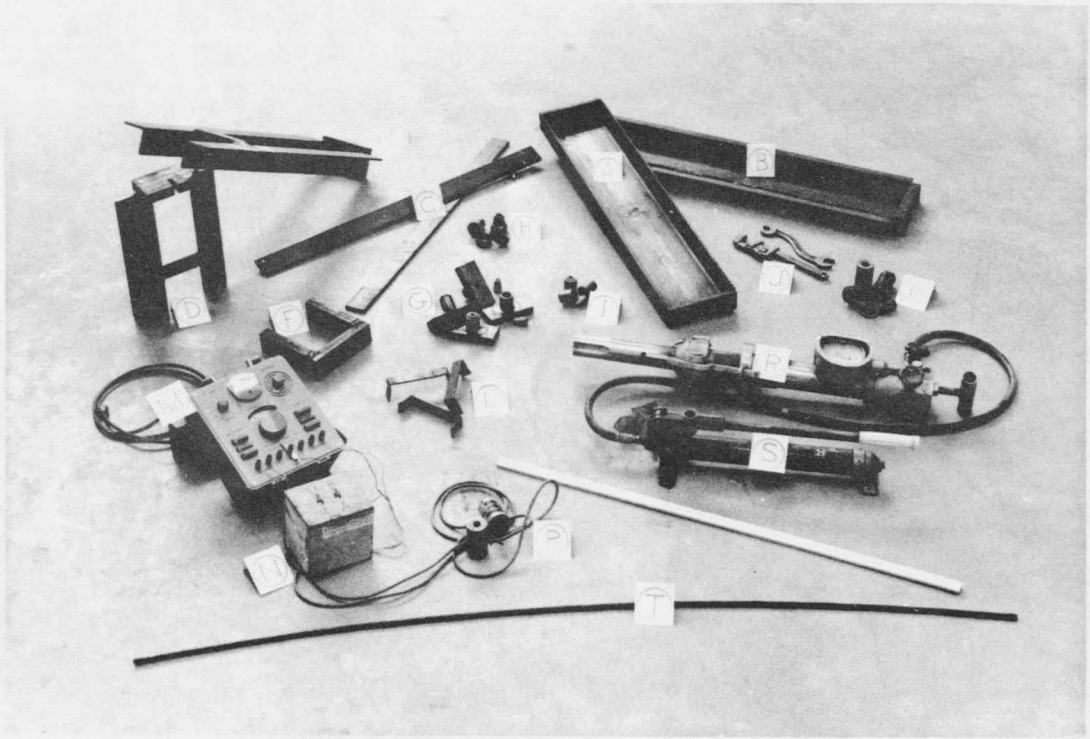


Fig. 4. Pretensioning equipment.

TABLE III

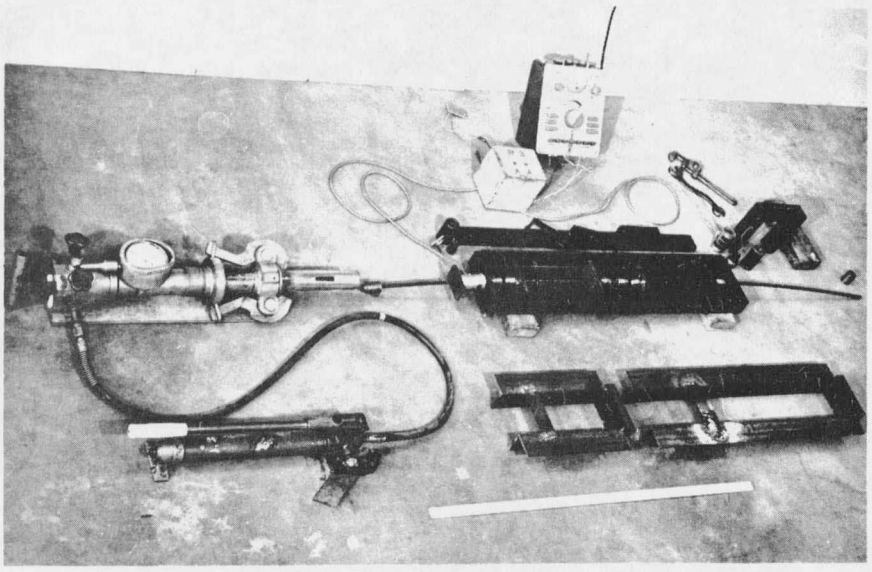
IDENTIFICATION OF ITEMS IN FIGURE 4

Identification letter	Item	Description
A	zero and 500 psi. casting bed	33½" length of 7 [9.8; 7"x2"x½" end plates, with 7/16" dia. center holes, welded to ends of channel.
B	1200 psi. casting bed	33½" length of 7 [9.8 reinforced with 1"x1"x¼" angles welded to flanges; 7"x2"x1" end plates, with 7/16" dia. center holes, welded to ends of channel.
C	slab side forms	33¼" lengths of 2"x3/8" steel bar.
D	short "seating yoke"	Two 12-3/4" lengths of 2½"x2½"x¼" angles spaced 5" apart; 5"x3"x1" steel bar, with 7/16" wide center notch, welded to one end of angles; angles braced near free end.
E	long "seating yoke"	Same as D, except that angles are 29¼" long.
F	loading "yoke"	Two 6"x2"x1" steel bars spaced 6" c. to c.; 7"x2"x1" steel bar, with 7/16" dia. center hole, welded to one end of the 6" bars.
G	end-bearing chuck-plate combinations	3/8" prestressing strand chucks welded to centers of 4½"x2"x½" steel plates for 500 psi. slabs, and to 4½"x2"x3/4" steel plates for 1200 psi. slabs; 7/16" dia. holes drilled through plates, concentric with chuck axes.
H	hollow bolt and nut	Special truck-wheel nuts (manufactured by Budd Wheel Mfg. Co.); 7/16" hole bored through each "bolt" section.
I	3/8" prestressing strand chucks	Chucks identical to those used for G (made in England, manufacturer unknown).
J	wrenches	One open-end wrench to fit "bolt" section of H, and one pipe-wrench to fit "nut" section of H.
K	3/8" prestressing strand chucks	3/8" strand chucks, No. B610, Supreme Products Corp., Chicago 16, Illinois.
L	clips for holding side forms, C	9" lengths of 1/8"x1" steel strap bent to form 5¼" wide, spring-like clips.
M	strain-gage indicator	Type N, SR-4 strain gage indicator, Baldwin-Lima-Hamilton Corp., Waltham, Mass.
N	load cell switching box	Simple 4-wire, 2-channel switching unit, made with two 2-wire, 2-channel switches.
P	load cells	Refer to Appendix A.
R	prestressing jack	Gifford-Udall Prestressing Jack, U.S.A.
S	hydraulic pump	Model P76 "Porto-Power" hydraulic hand pump, Blackhawk Mfg. Co., Milwaukee, Wis.
T	3/8" prestressing strand	Supplied by Colorado Fuel and Iron Corp., Denver, Colorado.

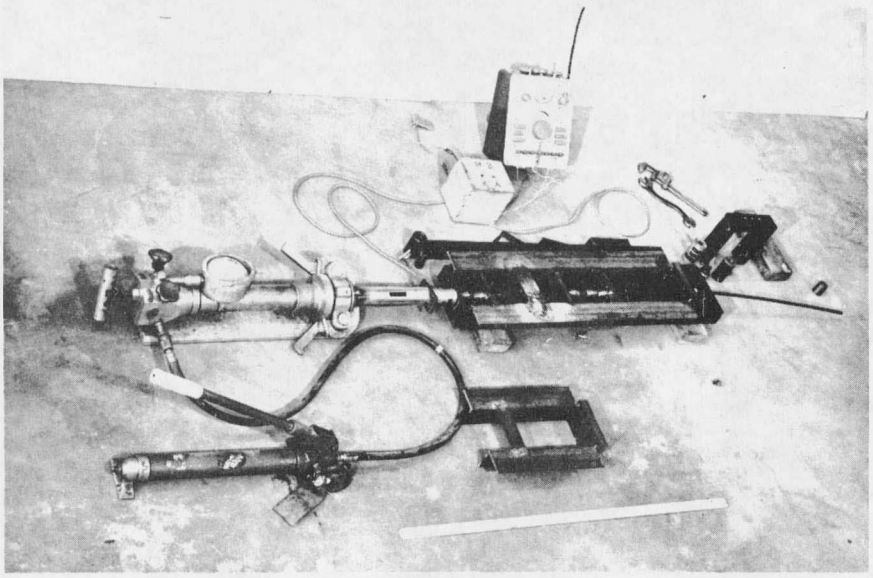
Figure 5 describes, with photographs, the procedures followed for pretensioning the strands. Each casting bed was prepared for casting two slabs of equal stress.

The shortness of the slabs made it impossible to rely upon the concrete-to-steel bond strength for stress transfer. Thus it was decided to mount end-bearing plates, backed up by strand chucks, on the prestressing strand in the casting beds. These steel plates also served as part of the slab mold. In order to prevent as much prestress loss as possible, the chuck "body", or barrel, was welded to the plate, concentric with the strand hole in the center of the plate. Further, to prevent any losses due to slippage of the chuck "jaws", or grips, on the strand and in the barrel, the chucks were pre-seated on the strand prior to pretensioning the strand. Figure 5a shows the arrangement of the strand (T) and chuck-plate combinations (G) before seating, and Figure 5b illustrates how seating was accomplished. Note that the hydraulic jacking unit (R) is located at the "left" end of the casting bed in Figure 5b. With the jack in this position, the seatings of the chuck-plate combinations at the extreme right and second from the left are effected.

In turn, each "seating yoke" (D,E) was inserted between the appropriate bearing plate and the "left" end-plate of the casting bed. In Figure 5b the long "seating yoke" (E) is shown being used to seat the chuck-plate combination (G) at the far right. Each yoke was capable of transmitting the ultimate load capacity of the prestressing strand. All chucks were seated with a load of 14,500 pounds, which exceeded the design load for the slabs, thus reasonably assuring no losses due to slippage.



a. Initial arrangement.



b. Seating of end-bearing plate.

Fig. 5. Pretensioning operations.

The load cell shown between the jack and the end plate of the casting bed, in Figure 5b indicated when the correct seating load was attained.

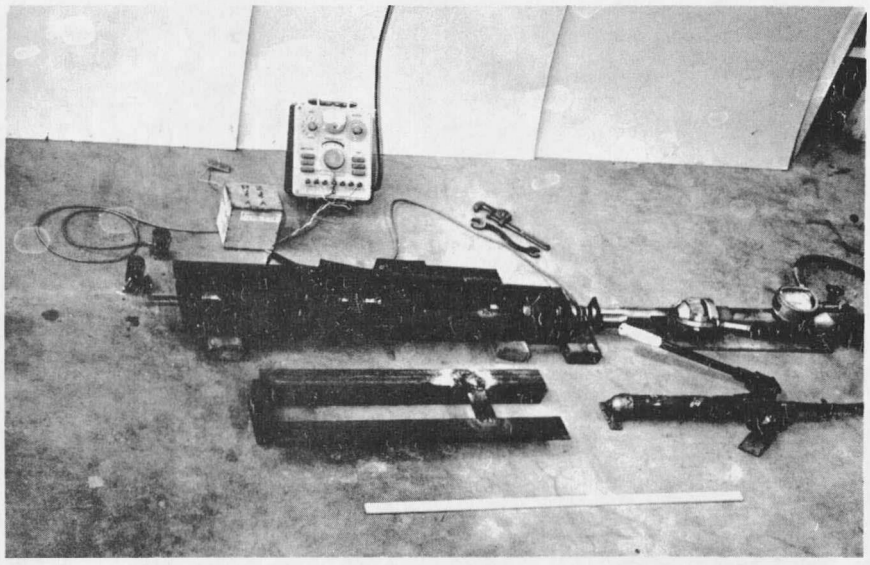
The jack was of the type that siezes a strand chuck (I) identical to those mounted with the end-bearing plates, but located on the strand exterior to the casting bed. Following the seating of the two chuck-plate combinations in Figure 5b, the jack was removed and the strand was severed about six inches from the end plate of the casting bed with an oxy-acetylene torch. This allowed removal of the load cell, and subsequent placement of another chuck (K) on the strand for final pretensioning.

The jack was then moved to the opposite, or "right" end of the casting bed. Figure 5c shows the arrangement for seating of the remaining two chuck-plate combinations, and final pretensioning of the strand. Note that the jack and load cell, in Figure 5c, do not bear directly on the end plate of the casting bed, as they did in Figure 5b. Rather, the load is transmitted to the casting bed by another yoke (F), bridging a hollow bolt and nut (H) and a larger chuck (K) mounted loosely on the strand.

With the jack located as in Figure 5c, the remaining two chuck-plate combinations (extreme left and second from right) were seated. Care was taken to space the slab end-bearing plates (G) on the strand so that, after seating, the clear distance between plates was about 10-1/2 inches. After seating each of the four chuck-plate combinations, the strand remained unstressed except for probable local stresses near the seated chucks. The steps for final tensioning of the entire strand will now be described. This discussion will be limited to 1200 psi. slab casting beds, and Table IV, on page 45, will summarize the pretensioning operation for

both the 500 and 1200 psi. slab casting beds.

A chuck (K), similar to that mounted loosely on the strand in Figure 5c, was assembled and placed on the short length of strand extending out of the "left" end of the casting bed, and mounted in contact with the end plate of the casting bed. The strand was then loaded to 14,000 pounds with the jack, the load being indicated by the load cell. With the load held at 14,000 pounds, the other chuck (K) was assembled within the loading "yoke" (F) and placed snuggly against the hollow bolt and nut combination (H), which in turn was pushed into contact with the end plate of the casting bed. With the nut held fixed against the chuck with one wrench, the bolt was turned with another wrench so that a force was exerted between the end plate of the casting bed and the chuck. The arrangement for this operation is shown in Figure 5d. The bolt was turned until the load indicated by the load cell was decreased by 2000 pounds, that is, decreased to a load of 12,000 pounds. This seating operation with the nut and bolt combination (H) assured a relatively constant slippage of the "right" end chucks (K) for all casting beds which were for 1200 psi. slabs. The jack was then released, causing a seating of the chuck (K) with a load which was determined experimentally to be about 12,000 pounds. Next, the strand was reloaded to 14,000 pounds, followed by a second seating with the bolt and nut (H) until the load indicated by the load cell dropped to 12,500 pounds. The jack was then released, leaving a load in the strand of approximately 13,500 pounds. It should be noted that this procedure was developed by numerous trials with the aid of two load cells, one located as in Figure 5d and the other located



c. Continued seating from opposite end.



d. Loading and seating of exterior chuck.

Fig. 5. Pretensioning operations, continued.

between the chuck (K) and end plate at the "left" end of the casting bed.

Table IV summarizes these strand loading procedures, as well as those followed for loading the 500 psi. slab casting beds. In this table, the "Load in load cell" refers to the load measured by the cell located in the position shown in Figure 5d. The "Load in strand" is that load determined experimentally by previous trials with another load cell located between the chuck (K) and end plate at the opposite end of the casting bed.

TABLE IV

SUMMARY OF STRAND LOADING PROCEDURES

Step	Operation	For 500 p.s.i. casting beds		For 1200 p.s.i. casting beds	
		Load in load cell (Lbs.)	Load in strand (Lbs.)	Load in load cell (Lbs.)	Load in strand (Lbs.)
1	Jack	6,100	6,100	14,000	14,000
2	Tighten bolt and nut	5,100	6,700 ± 50	12,000	15,000 ± 100
3	Release jack	0	5,000 ± 200	0	12,000 ± 300
4	Re-jack	6,100	6,100	14,000	14,000
5	Re-tighten bolt and nut	5,300	5,900 ± 50	12,500	15,000 ± 50
6	Release jack	0	5,700 ± 200	0	13,500 ± 200

It should be mentioned that the strand loads immediately after step 6 in Table IV were somewhat higher than those given in the table. However, some slight "settling", or slippage, and perhaps some steel creep occurred

for a short period after the final release of the jack. Therefore, the strand loads given in the table after step 6 represent the loads after the system had stabilized; usually these loads were obtained about one-half hour after the final release of the jack.

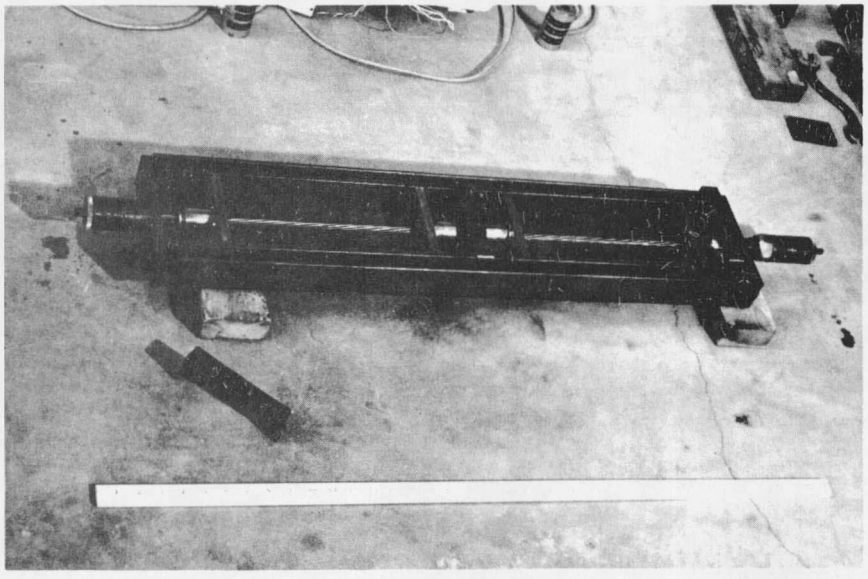
Note that the loads, 5,700 pounds and 13,500 pounds, result in somewhat higher than the desired stresses, 500 and 1200 psi., respectively, when divided by the slab cross-sectional area of nine square inches. However, based upon expected values for percentage of prestress loss given by Lin (27), a loss of about 20 per cent was anticipated. Thus, the expected final loads in the stressed slabs were 4,560 and 10,800 pounds, respectively.

After step 6 in Table IV, the jack was removed and the strand was severed with the oxy-acetylene torch, adjacent to the chuck (K) at the "right" end of the casting bed. The stressed casting bed, shortly after the strand had been severed, is shown in Figure 5e. Two long steel bars (C) were then placed in the casting bed to serve as the side forms for the slabs. These were held in place adjacent to the slab end-bearing plates by three "clips" (L), as illustrated in Figure 5f.

Figure 6a is a photograph of the casting bed after the pretensioning operation had been entirely completed. Figure 6b is a photograph of three casting beds prior to casting, one for each of the three stress levels. The casting bed at the extreme left is for non-stressed slabs and, therefore, has no chucks attached to the end-bearing plates. These plates are held in place merely by the force of the small steel clips which hold the form sides against the plates. The strands in the non-stressed casting

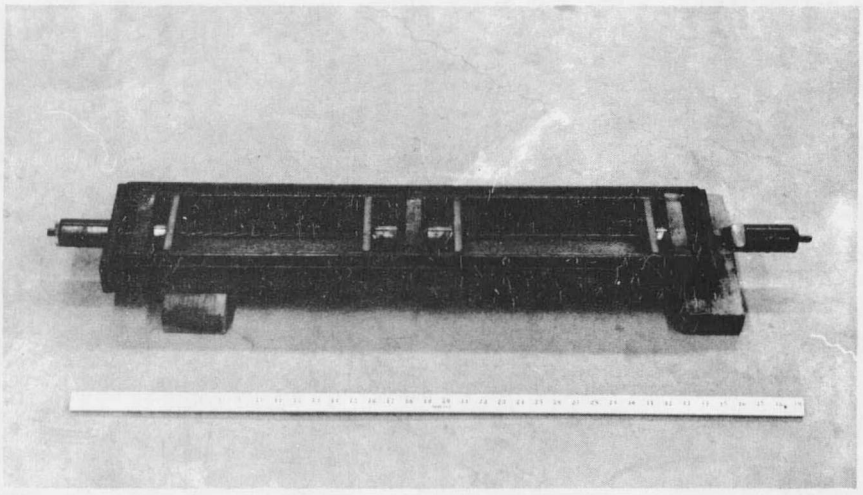


e. Jack removed and exterior strand severed.

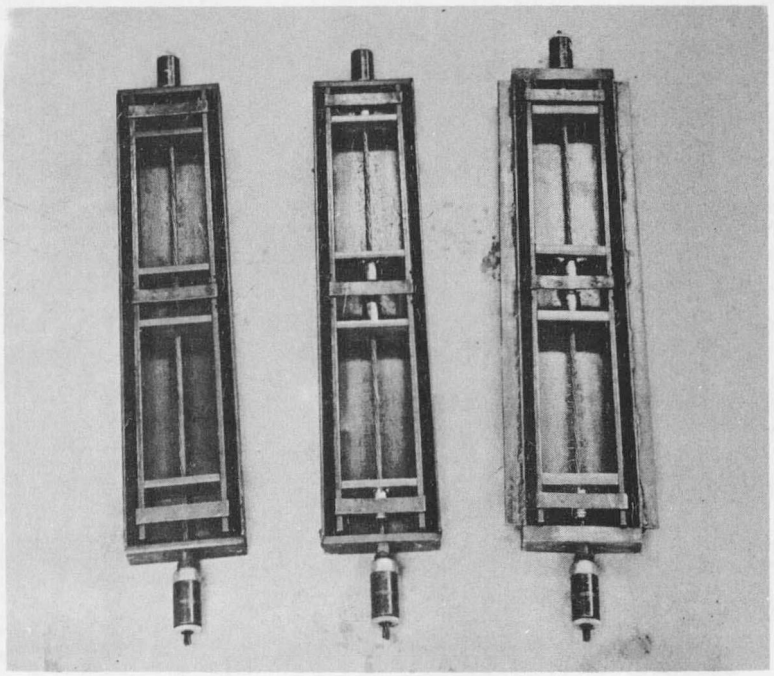


f. Side forms inserted and clipped into position.

Fig. 5. Pretensioning operations, continued.



a. Casting bed prepared in Figure 5.



b. Casting beds ready for casting. (from left: for zero, 500, and 1200 psi. slabs)

Fig. 6. Pretensioned casting beds.

beds were nominally loaded with the nut and bolt arrangement (H) merely to remove the natural strand curvature which results from being supplied on a "spool". The casting bed in the center is for 500 psi. slabs, and that on the right is for 1200 psi. slabs. Note that the higher stressed casting bed on the right is stiffened with small steel angles welded to the channel flanges. Note also that the end-bearing plates in the higher stressed casting bed are of 3/4 inch thick steel, while those in the center, or 500 psi., casting bed are of 1/2 inch thick steel.

The interior surfaces of the channel section webs served as the floors of the slab molds. All steel mold surfaces, except for the end-bearing plates, were coated with a thin oil film before casting to facilitate removal of the slabs after curing.

Concrete materials

All slabs were fabricated from concrete made with Type II cement, the supplier, and oxide and phase analyses of which appear in Appendix B. Pertinent information about the coarse and fine aggregate appears in Appendix C.

Concrete mix information

The concrete mix was designed by the method prescribed by the Portland Cement Association (28), on the basis of Type I cement, for a 28-day compressive strength of 4000 psi. The desired slump was two inches, and no air-entraining admixtures were used since it was desirable to reduce the frost resistance of the concrete as much as possible, and yet retain concrete quality commensurate with good field practice. This

mix, for 3/4 inch maximum sized aggregate, called for a sand content of about 42 per cent of the total aggregate weight.

Since control of the concrete mixes was most important, it was decided to oven dry all aggregate, separate it into standard sieve sizes, and then recombine for mixing. Thus, based upon the value of 42 per cent for the sand content, composite gradation limit curves for the combined coarse and fine aggregate were plotted according to A.S.T.M. Designation: C 33-54T, Tentative Specifications for Concrete Aggregates (28). These limits are shown in Figure 44, in Appendix D, along with the gradation curve for recombination of the aggregate described in Appendix C.

Subsequent trial mixes resulted in slight modifications of the original mix design, and the final mix is described in Appendix D. Note that the material quantities are given for a two-cubic foot mix, since this was the actual volume mixed for each batch.

All aggregate was dried for 24 hours at 110° C in a small laboratory oven*, and then separated into the sieve sizes indicated in Appendix D. Separation was accomplished with a large sieve shaker** which is pictured in Figure 7. The various sizes of aggregate were then stored in large, covered, cardboard containers, and protected from moisture.

All mixing was done in a large laboratory mixer***, pictured in

---

* Laboratory Oven, 1200 watts, American Instrument Co.

** Gilson Testing Screen, Gilson Screen Company, Malinta, Ohio.

*** Lancaster Counter Current Batch Mixer, Type SKG, Posey Iron Works, Inc., Lancaster, Pennsylvania.

Figure 8, which has a recommended capacity of about 1-1/2 cubic feet. However, trial mixing showed that two-cubic foot mixes were not excessive. It was desired to obtain one slab for each combination of treatments from each concrete batch, so that the ninety-six required slabs could be made with four concrete batches. A minimum volume of two cubic feet was required for 24 slabs plus enough excess concrete for air content tests or for fabrication of four small cylinders for compressive tests. Larger batches would have been desirable, since removal of enough material for compressive test cylinders prohibited a measurement of the air content by a pressure method. It was even necessary to return to the mixer all concrete used for slump and unit weight determinations--an inadvisable practice at best.

Therefore, compressive test cylinders were drawn from only half of the batches, while air content determinations by the pressure method were made on the remaining batches. In addition, air content measurements were made on all batches with an AE-55 Air Indicator*. This method is not considered to be as reliable as the pressure method, although Newlon (29) has reported that the average air content, as determined by the AE-55 Air Indicator, will be within 1/2 percentage point of air as compared with the pressure method. He also found that the AE-55 Air Indicator tended to give readings which were too high for mortar of low air content, and vice versa. Results from cylinder compression tests and air content tests are given in Appendix D.

---

* AE-55 Air Indicator, Model CT-158, Soiltest, Inc., Chicago 39, Illinois.



Fig. 7. Gilson testing screen.

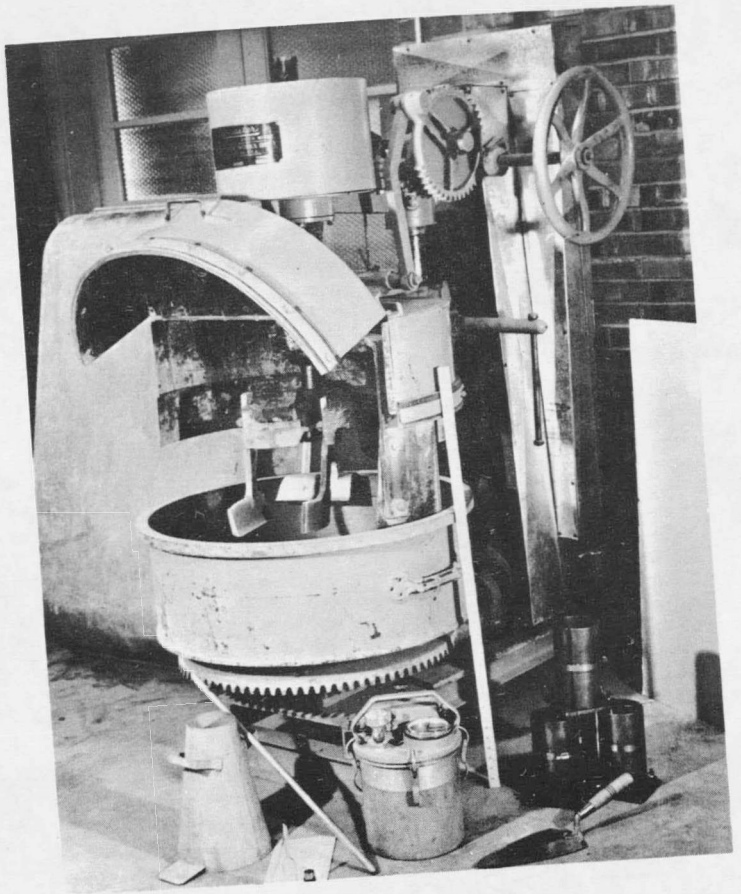


Fig. 8. Lancaster mixer and incidental apparatus.

The procedure followed for mixing each concrete batch was as follows:

1.) The appropriate weights of each size of aggregate plus the prescribed weight of cement were added to the mixer tub and dry-mixed for one minute.

2.) The proper quantity of water was added to the mixer, and mixing was continued for two minutes.

3.) Mixing was stopped and a slump test was performed according to A.S.T.M. Designation C 143-52.

4.) The slump material was returned to the mixer, and the concrete was remixed for an additional 10 seconds.

5.) Mixing was again stopped to perform the unit weight and air content tests. The unit weight was obtained by filling the 1/4 cubic foot container which was part of the pressure method air meter* used in this study. Filling of this container was in accordance with the instructions for molding concrete compression specimens, as contained in A.S.T.M. Designations C31-49 and C192-54.

Following the unit weight determination, the air content was measured either with the AE-55 Air Indicator, or with both the AE-55 Air Indicator and the pressure meter, depending upon whether compressive test cylinders were to be made. For those

---

* Techkote White Air Meter, Capacity: 0.25 cu. ft., Presstite Division, American-Marietta Co., El Segundo, California.

batches from which test cylinders were to be obtained, the material for the unit weight test was returned to the mixer, and the air content was determined by averaging the results from two tests made with the AE-55 Air Indicator. (See reference 29 for a description of the test procedure.) For those batches from which no cylinders were to be secured, the above procedure for determining the air content was also followed. In addition, a determination of the air content was made by the pressure method on the material used for the unit weight determination, according to the manufacturer's directions. This material was then discarded, since the test method necessitated an addition of water to the test sample.

6.) The concrete was then mixed for an additional 10 seconds, prior to casting of the slabs.

Pertinent information from each batch appears in Appendix D, including results of compressive tests on the cylinders. The air meters and other incidental apparatus just described appear in Figure 8, along with the concrete mixer.

Fabrication of slabs

Casting was initiated immediately after the final step of the mixing operation. The fabrication of each pair of slabs was accomplished by the following procedure:

1.) The casting bed was secured to the surface of a specially constructed vibration table, shown in Figure 9.

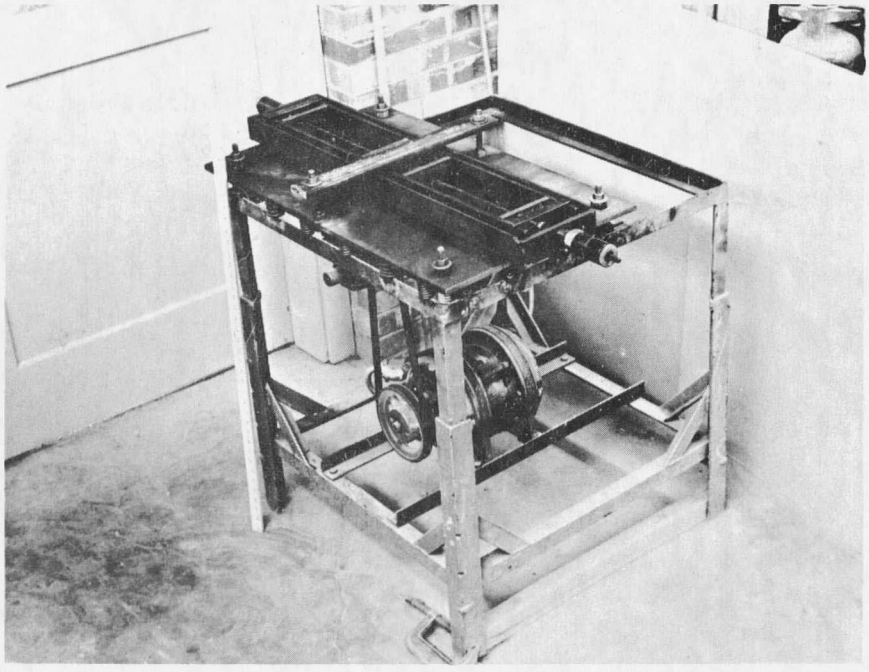


Fig. 9. Vibration table with casting bed in place.

2.) Each mold was slightly overfilled with concrete, and the concrete was gently maneuvered into the corners of the mold, and beneath the strand, with a large steel trowel.

3.) The casting bed was then vibrated for seven seconds, and the excess concrete was "struck off" with the trowel. The frequency of vibration was approximately 4200 c.p.m.

4.) The casting bed was re-vibrated for three seconds, in order to better the compaction and to close surface voids resulting from removal of the excess material in step 3.

5.) Following vibration, the surface of each slab was finished by making three passes, with slight circular motion, with a damp-surfaced wooden float, 1-1/4 inch in width.

6.) The casting bed was then released from the vibration table, and set aside in the laboratory.

7.) After casting each pair of slabs, the remaining concrete was remixed for five seconds, in an attempt to retain workability and homogeneity.

The above steps were followed for each of the twelve casting beds. For those batches from which cylinders were obtained, the procedural cycle was interrupted after half the slabs had been cast (i.e., after the sixth casting bed had been filled) in order to cast four compressive test cylinders. The methods for making, curing, and testing of these cylinders are given with the test data in Appendix D. It should also be mentioned that the concrete mixer tub remained covered at all times during the casting procedure, except for removal of concrete. This was done in order to prevent as much variation, due to moisture evaporation loss, as was possible.

Casting began about one-half hour after the addition of water to the mixer. About one hour was required to cast all 24 slabs, and approximately 20 additional minutes were required for those batches from which test

cylinders were cast. Thus, an inherent variation was realized due to the length of time required for testing of the fresh concrete properties and for casting.

As was mentioned, one slab for each combination of treatments was cast from each concrete batch. The treatments assigned to each slab from each batch are summarized in the following diagram, with the slabs numbered.

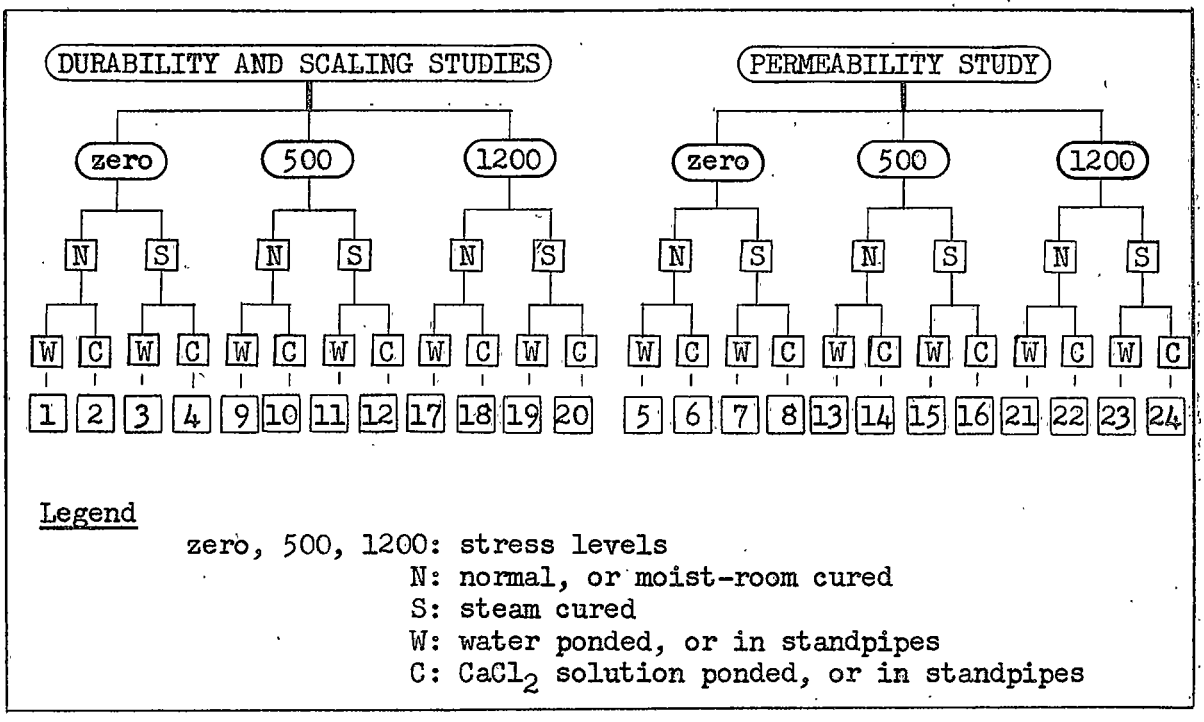


Fig. 10. Diagram of slab treatments for each concrete batch.

To remove the inherent variability due to the lengthy mixing and casting time, an attempt to randomize the rank in time of casting, for each pair of slabs, was made. Table V gives the time of casting, in minutes after addition of water to the mixer, for each pair of slabs from each batch. Thus, for example, slabs 1 and 2 from batch number 21 were cast

only one-half hour after mixing began, while the duplicate slabs, 1 and 2, from batch number 24 were cast about 1-1/2 hours after mixing was started. Hopefully this arbitrary scheduling reduced or eliminated the effect of varying fresh concrete age, at time of casting, upon the results of this study.

TABLE V

CASTING SCHEDULES

Time after mixing (minutes)	Slab numbers			
	Batch 21	Batch 22	Batch 23	Batch 24
0	add water	add water	add water	add water
30	1, 2	23, 24	21, 22	9, 10
35	15, 16	9, 10	11, 12	7, 8
40	17, 18	1, 2	5, 6	19, 20
45	5, 6	19, 20	17, 18	13, 14
50	11, 12	13, 14	15, 16	3, 4
55	21, 22	3, 4	1, 2	21, 22
60	3, 4	cast cylinders	23, 24	cast cylinders
65	13, 14	" "	9, 10	" "
70	19, 20	" "	7, 8	" "
75	7, 8	21, 22	19, 20	11, 12
80	23, 24	11, 12	13, 14	5, 6
85	9, 10	5, 6	3, 4	17, 18
90		17, 18		15, 16
95		15, 16		1, 2
100		7, 8		23, 24

After all slabs had been cast, a shallow, circular impression was made in the surface mortar of those slabs assigned to the permeability study (see Figure 10, page 57), using one of the "bottomless" milk bottles which served as standpipes. This was done so that bonding of the standpipes after curing could be accomplished more easily and accurately.

Curing of slabs

Normal curing

The casting beds containing those slabs which were to be normally cured, as identified in Figure 10, were placed into a moist-room shortly after casting had been completed. High relative humidity was maintained in this room by a nearly uniform water mist supplied by spray nozzles in the ceiling. The temperature of the water emitted by these nozzles was controlled by a thermostatic control valve, and control of the water spray temperature was the only means for regulating the room temperature. The desired curing temperature was 70°F; however, the water temperature control was inadequate and the room insufficiently insulated from the remainder of the laboratory. Consequently the rather marked laboratory temperature fluctuations, over each 24 hour period, caused considerable temperature fluctuations in the moist-room. Temperature records, obtained while the normally cured slabs from each batch were in the moist-room, showed that the temperature varied between the approximate limits of 60°F and 90°F. It is assumed, however, that all normally cured slabs were subjected to similar curing environments.

All normally cured slabs remained in the moist-room until the age of 14 days. The moist-room cure was interrupted at the age of seven days, at which time all casting beds were removed from the moist-room for stress transfer and mold disassembly. Also, shortly after stress transfer, mortar dikes were placed on the surfaces of those slabs which were assigned to the durability and scaling studies. These interruptions in moist-room cure were quite brief.

Following the 14-day moist-room cure, these slabs were placed in the laboratory to dry at room temperature for 14 days.

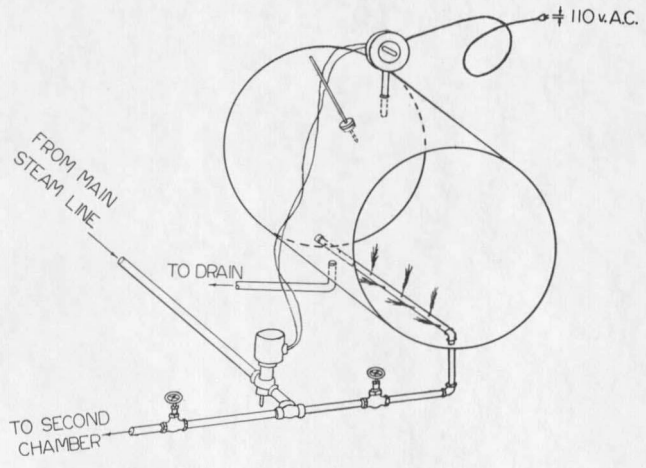
Steam curing

Approximately five hours after the initiation of mixing, the casting beds containing slabs which were to be steam cured were placed in the steam chambers, and steaming commenced. The rate of steam flow into the chambers was manually controlled such that the chamber temperature increased at a rate of about 40°F per hour. Thus, approximately two hours were required for the chambers to reach the desired curing temperature of 150°F. The temperature was maintained at approximately 150°F for a period of about 13-1/2 hours, following which the steam flow was again manually controlled in order to reduce the chamber temperature back down to the laboratory temperature at a rate of about -40°F per hour.

The steam chambers, pictured in Figure 11a, were fabricated from identical 55-gallon capacity steel "drums." The steam entered each chamber through small holes in the wall of a pipe which was located along the bottom of the chamber (see Figure 11b). These holes, spaced at three-inch intervals along the pipe length, were directed alternately at angles of approximately $\pm 30°$ to the vertical. This provided for a relatively uniform steam distribution within the chamber, and prevented the steam from striking directly on the casting beds above. To provide for a nearly uniform flow distribution along the length of the pipe, the hole diameters increased by small increments, from 1/16 inch to 1/8 inch, from the front to the back ends of the chamber. A drain, open to the atmosphere,



a. Steam chambers



b. Steam chamber operation.

Fig. 11. Steam chambers and their operation.

was located at the back end of each chamber. The chambers sloped slightly towards the back to promote drainage of the condensate.

Separate valves regulated the flow into each chamber, and these were adjusted so that the environments in the two chambers were identical throughout the curing period. These individual valves were necessary because only one chamber temperature control device was available. Before reaching these regulating valves, the steam passed through a single electromagnetic control valve* which was activated by the mercury control switch** shown on the top of the steam chamber on the right in Figure 11a. This switch was set to maintain the chamber temperature between the approximate limits of 145°F and 155°F. The chambers were not insulated, so ordinarily the rate of heat escape was rapid enough to cause the magnetic valve to open at intervals of about 10 minutes. The injection time was usually about two minutes. Thus, the air in the chamber remained moisture saturated throughout the curing period.

Following steam curing, the casting beds were transferred to the moist-room. The remainder of the 28-day curing period, for these slabs, was exactly as for the normally cured slabs.

To summarize, these slabs were cured according to the following sequence: 1.) an average air-dry set of about 4 hours, 2.) approximately 18 hours in the steam chambers, 3.) 13 days in the moist-room, and 4.) air-drying for 14 days in the laboratory.

---

* Mercoid Magnetic Valve, Type K15-3, The Mercoid Corp., Chicago, Ill.

** Mercoid Temperature Control, Type DA-36, Range: 100 - 200°F, The Mercoid Corp., Chicago.

Stress transfer

At the age of seven days, each casting bed was removed from the moist-room for stress transfer. The operation merely entailed severing of the strand with the oxy-acetylene torch, first between the two slabs, and then at the ends of the slabs between the chuck-plate combinations and the end plates of the casting bed.

The length of each slab was carefully measured before and after the cutting operation, as an additional assurance that the desired stress levels had been effected. The average decreases in slab lengths after cutting were 0.00225 inch and 0.00735 inch for all 500 psi. and 1200 psi. slabs, respectively. Thus, there was reasonable assurance that the method for pretensioning was successful. These length changes corresponded quite closely to the observed strains at 500 and 1200 psi. in a test of one cylinder from batch number 23.

After the strands were cut, and the molds disassembled, the slabs were returned to the moist-room. Mold disassembly also included removal of the end-bearing plates from the non-stressed slabs, since their only purpose was to retain the fresh concrete during the casting operation. In all, each slab was out of the moist-room for only about 15 minutes for the operations of stress transfer and form removal.

Application of mortar dikes

Usually within 24 hours after stress transfer, each of those slabs assigned to the durability and scaling resistance study was again removed from the moist-room for attachment of a mortar dike to the periphery of

its top surface. These mortar dikes were made with the aid of the forms shown in Figure 12. The sides of these forms were bevelled to facilitate their removal after the space between them had been filled with mortar.



Fig. 12. Mortar dike forms, and slab with attached mortar dike.

The interior form was fabricated from a piece of 3/4 inch thick wood, and covered with polyethylene tape to prevent its sticking to the mortar. The outer form was made from 3/4 inch by 1/8 inch steel strap. Before forming each dike, the outer steel form was coated with a film of light oil. When assembled, these forms enabled casting of a mortar dike which was 3/4 inch in height, and uniformly varying in width from

1/2 inch at its base to about 5/16 inch at its top.

The slabs were prepared, and the mortar dikes were applied, according to the following procedure:

1.) Using a small steel chisel and stiff, steel, wire-wheel brush attached to a portable electric drill, the laitance was removed from the 1/2 inch wide periphery of the top surface of each slab. After roughening, the slabs were washed thoroughly under running water, so that all dust and other loose particles were removed.

2.) Excess water was removed from the surface, and a thin layer of neat cement paste was applied to the damp concrete periphery. The paste was applied with a spatula, and worked into the surface voids.

3.) The forms for the mortar dike were then assembled in place on top of the slab and the dike formed. The mortar was placed, in small quantities, into the narrow space between the forms, and carefully worked into place with the edge of a small steel trowel so as to fill all voids. After the space was slightly overfilled, the mortar was lightly "tamped" with the end of a piece of 1/8 inch by 1 inch steel strap. Care was taken, when working the mortar, to prevent bleeding and segregation. The excess mortar was then "struck off", and the surface smoothed with the trowel.

4.) Finally, the forms were removed. The inner, or wooden, form was removed first. By carefully sliding the trowel between the mortar and the edge of the inner form at one location only, an air passage was formed to prevent suction. The form could then be lifted

carefully, accompanied by light tapping of the form with the edge of the trowel. The outer steel form was then removed by carefully lifting at one end, while lightly tapping the form with the edge of the trowel.

The neat cement paste was prepared by blending 250 grams of Type II cement, 90 ml. of water, and 5 ml. of full-strength air-entraining agent* in a tall glass container. This mixture was then "whipped" for two minutes with a small, high-speed mixer. The resulting paste contained about 5 per cent air.

The mortar mix was prepared as follows:

1.) 500 grams of well-graded sand, passing a standard #8 sieve, and 250 grams of Type II cement were dry mixed by hand in a stainless steel mixing bowl until well blended.

2.) 110 ml. of water, with 7 ml. of full-strength air-entraining agent, were slowly added and mixed with the cement and sand; and the entire mass was vigorously mixed by hand for two minutes.

The resulting fresh mortar had an air content of 16 to 20 per cent, as determined with the AE-55 Air Indicator. The mortar was stiff enough to remain practically undisturbed during removal of the dike forms. The method for making the mortar dikes proved to be quite successful, though time consuming.

The mortar mix just described provided sufficient material for two dikes, so two slabs were removed from the moist-room and prepared simul-

---

* Protex AEA.

taneously for each mortar dike application. Each pair of slabs was out of the moist-room for a period of about 45 minutes for this operation, and returned to the moist-room immediately after the dikes had been formed. The curing schedule allowed for a 6 to 7-day moist-room cure of the mortar dikes.

Preparation of permeability study slabs

At the age of 26 days (i.e., after air-drying for 12 days), the "standpipes" were attached to those slabs assigned to the permeability study. Figure 13 shows one of these slabs completely prepared for the study.

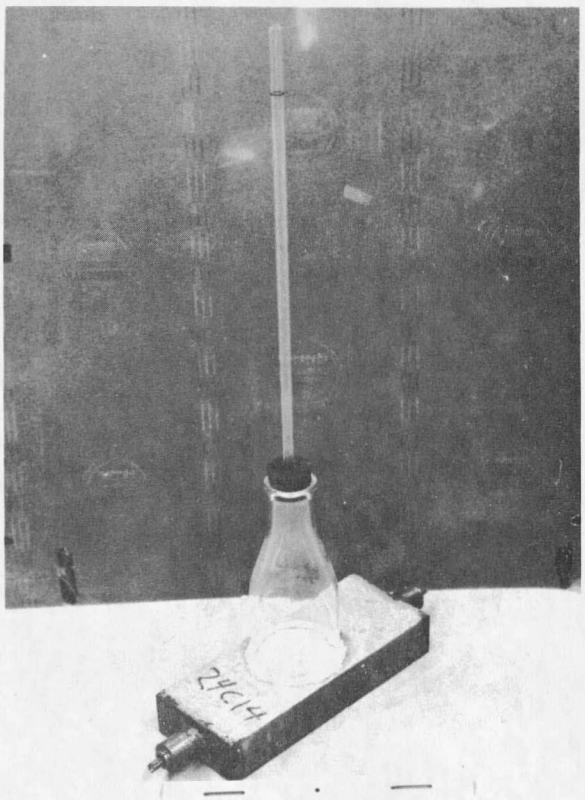


Fig. 13. Slab prepared for permeability study.

Note that the bottom portion of the standpipe is merely a standard, circular glass milk bottle, the bottom of which has been removed with a diamond saw. The upper part of the standpipe consists of a length of 12 mm. glass tubing set into a hollow rubber stopper. Note also that the glass tubing is marked at the elevation of two feet above the upper slab surface.

The procedure for bonding the bottomless milk bottles to the slabs was quite simple. The surface laitance was removed from the previously marked and slightly depressed circle with a stiff wire-wheel brush attached to a portable electric drill. After this porous surface layer had been loosened, the area was cleaned with a soft, narrow brush. Next, this narrow annular region was treated with a surface conditioner*, as was the bottom edge of the milk bottle. Finally, the bonding agent** was placed on the prepared annular surface, and the milk bottle carefully placed in the fresh sealant. A slight twisting motion was used to seat the bottle into the bonding material, and the excess material squeezed out from beneath the bottle was worked against the bottle with a narrow spatula to form a smooth fillet. About 24 hours were required for this sealant to cure and form a strong, water-tight joint.

At the age of 27 days, or after the bonding agent had cured for 24 hours, the remaining slab surfaces, except for the bottom surface and

---

* Surface Conditioner A (for use with Dow Corning 780 Building Sealant), Dow Corning Corp., Midland, Michigan.

** Dow Corning 780 Building Sealant, Dow Corning Corp.

the circular region within the milk bottle, were treated with three coats of a commercial plastic varnish*. The varnish coats were brushed on quite liberally, in order to form a completely water tight surface. This was done to prevent surface evaporation losses, since previous tests with uncoated slabs showed that the surface regions exterior to the bottles became dampened after about 24 hours under a two-foot head of water. These varnish coats, applied at intervals of four hours, were allowed to dry overnight.

Environmental conditioning

Durability and scaling studies

At the age of 28 days, all slabs from a single batch were placed into their respective test environments. Those slabs assigned to the durability and scaling resistance studies were placed into the freezing unit, shown in Figure 14, with approximately 170 ml. of water or $CaCl_2$ solution ponded on their surfaces. Thereafter, cycling consisted of removing the slabs from the freezer in the morning and placing them on a wooden rack, shown to the right of the freezer in Figure 14, for thawing--then returning them to the freezer in the evening. Generally, thawing required about eight hours, while the remaining sixteen hours of each day were used for freezing.

The freezer was equipped with fans at each of the four shelf levels, and the shelves contained the tubing through which the coolant was circu-

---

* Flecto Varathane Liquid Plastic, The Flecto Company, Inc., Berkeley, California.

lated. Twelve slabs were stacked pyramidically on each shelf, as can be seen in Figure 14. The bottom row of slabs on each shelf rested on narrow wooden slats and not directly on the shelves. The slabs were not assigned specific positions in the freezer, but rather were placed randomly into the freezer for each cycle. This was done to guard against any variations which might be caused by regions of differing temperatures within the freezing compartment. The freezer was defrosted approximately once each month in order to retain its efficiency.

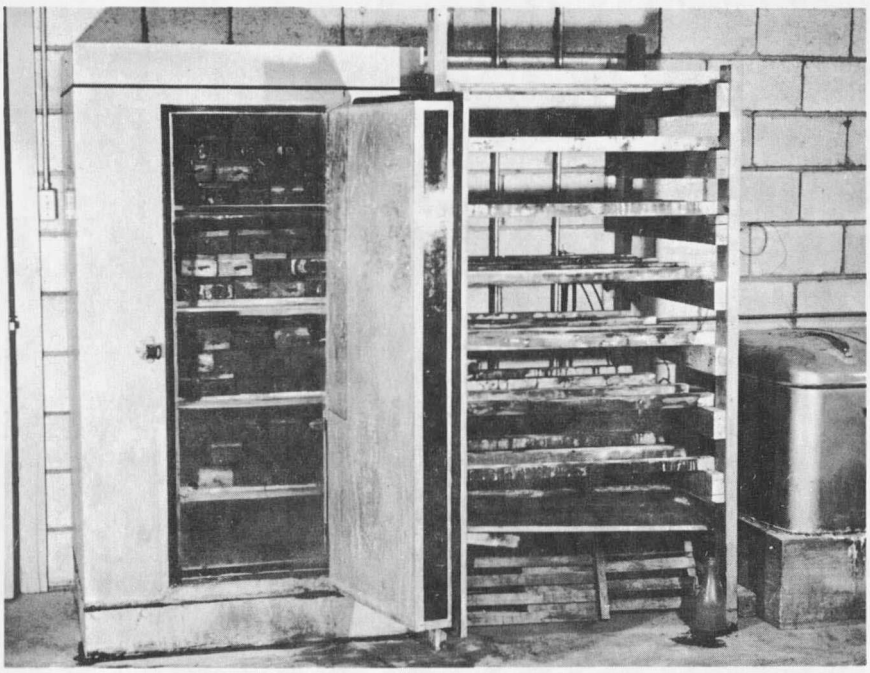


Fig. 14. Freezer and thawing racks.

The freezer temperature was maintained at approximately -5°F, and thawing occurred at ambient room temperature, which was in the region of 70°F.

At intervals of ten freeze-thaw cycles, the slabs were flushed off and tested, and then reponded with fresh water or salt solution and returned to the freezer. Periodically some slabs would develop leaks between the concrete surface and mortar dike. When this occurred, all slabs with the same ponded solution from that batch were removed from cycling, and their mortar dikes were replaced. To cure the new mortar dikes, the slabs were placed into the moist-room for a period of seven days, and then returned to the cycling procedure. (These interruptions in freeze-thaw cycling produced rather marked changes in the concrete properties which will be discussed more thoroughly in Chapter IV.

Permeability study

These slabs were supported on wooden racks, as shown in Figure 15. At the age of 28 days, after the varnish coats had dried, the milk bottles were filled with water or $CaCl_2$ solution. These fluids were at room temperature, and essentially de-aerated after having set in large containers open to the atmosphere for about two days. After filling the bottles, the hollow rubber stoppers with inserted glass tubes were placed tightly into the bottle openings, and then filled to the two-foot level with a pipette. At the same time, normal milk bottles with stoppers and glass tubes attached were filled to the same elevation. These "control" standpipes, which can be seen in Figure 15, were necessary in order to

account for evaporation losses from the fluid surfaces.

Since these were comparative studies, the room temperature and humidity were not recorded. Nor were there any means for controlling these factors.

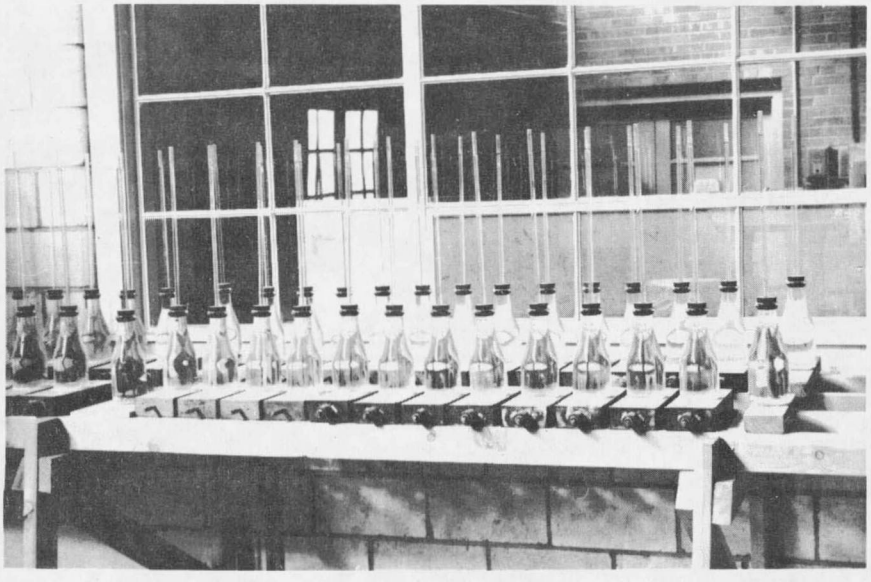


Fig. 15. Permeability study slabs.

Tests and measurements

Durability and scaling studies

At intervals of approximately ten freeze-thaw cycles these slabs were tested. Testing consisted of length, weight, and natural frequency of transverse flexural vibration measurements, plus an evaluation of the degree of surface scaling.

After thawing, and before testing, each slab was flushed under running water and then allowed to surface dry. Each slab which was ponded with salt solution was flushed over a #200 mesh sieve so that practically all the loosened surface material could be collected. This collected surface "scale" was then transferred to a paper towel, and placed in an oven to dry for 24 hours at 110°C. The dry weight of this material was used as an evaluation of the degree of scaling of each slab. This procedure was not used for those slabs which were ponded with water, since the degree of scaling on these slabs was almost negligible.

Length measurements were made with a large machinist's micrometer which measured to within 0.001 inch. The measurements were made between the end surfaces of each slab, along the central axis. For the stressed slabs, these surfaces were on the steel end-bearing plates; and for the non-stressed slabs, these surfaces were on the concrete. Thus, because of slight rusting of the steel, and because of the inherent rough nature of the concrete end surfaces of the non-stressed slabs, these measurements cannot be considered very reliable. The intent of these measurements, however, was merely to detect any sizeable length changes which might be caused by large concrete expansions. All length changes were attributed to the concrete only, under the assumption that the steel end-bearing plates underwent no change.

The surface dry weight of each slab was determined to within 0.01 pound. The weight changes of each slab consisted of (1.) an increase due to moisture absorption, and (2.) a decrease caused by scaling. Thus, by knowing the scaling weight loss, the weight of absorbed moisture could be

determined.

The natural frequency of transverse flexural vibration was measured with a Sonometer* system. The Sonometer consists of a cabinet which houses the driver and pickup amplifiers and the oscillator, a driver, and a pickup. A cathode ray oscilloscope** was also an important part of the system. This system, shown in Figure 16a, has a frequency range of 20 - 20,000 cycles per second, accurate to at least 2 per cent according to the manufacturer.

The slabs were supported at their quarter-points for testing. The supports, shown also in Figure 16a, were triangular prisms cut from pine wood and covered with foam rubber. These supports were nailed to a heavy wooden base, which in turn was supported on a mat of "horse hair." Other support systems of metal and non-covered wood were tried without success.

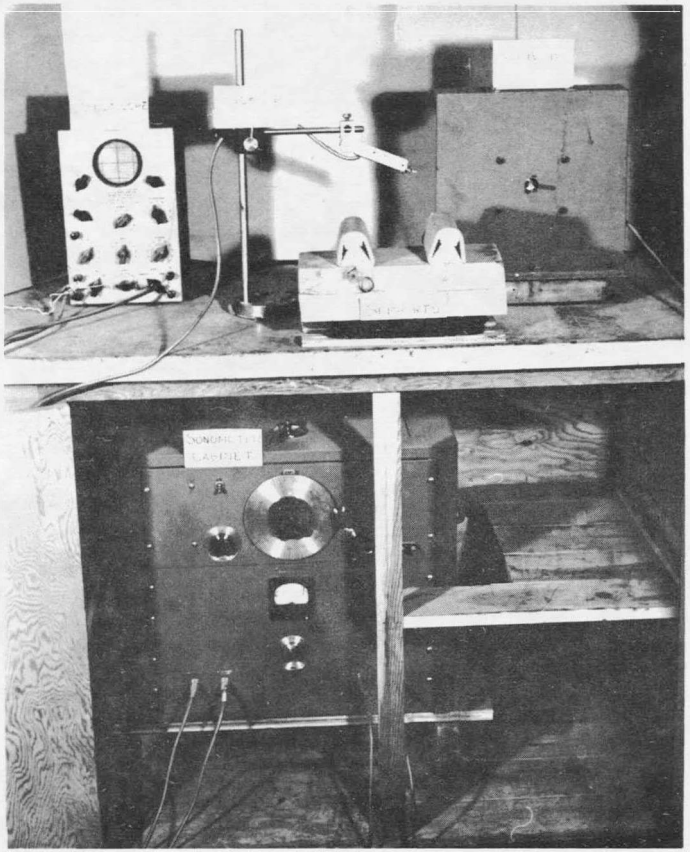
The slabs were driven at one end, and the pickup was placed in the center of the top surface to follow the response of the slab. Figure 16b shows this orientation. It should be noted that the pickup was a modification of that supplied by the manufacturer, in that the supplied pickup cartridge had been replaced with a different model***.

---

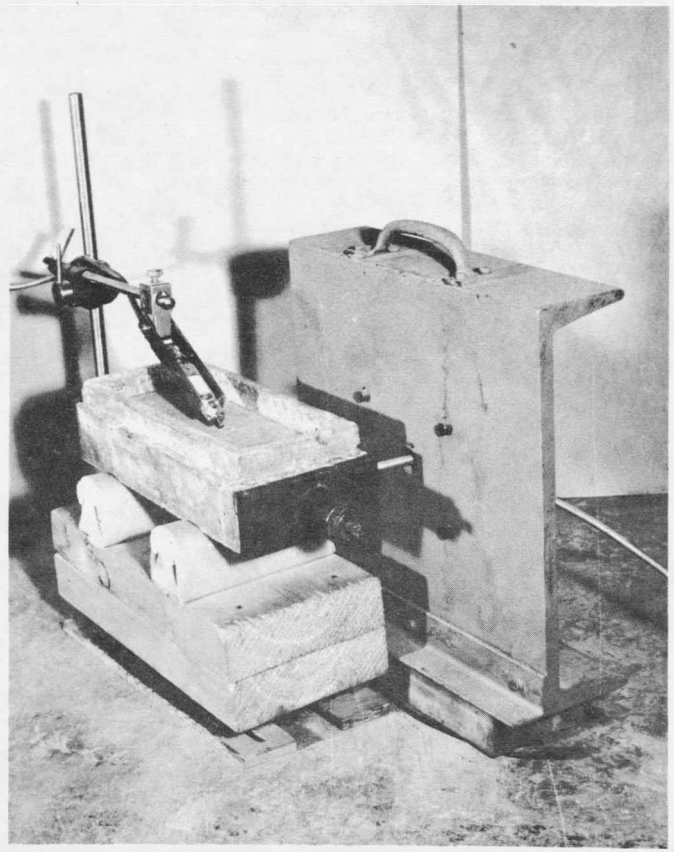
* Electro Sonometer, Model CT-360, Electro Products Laboratories, Inc., Chicago 40, Illinois.

** Type 164 Oscillograph, Allen B. DuMont Laboratories, Inc., Passaic, New Jersey.

*** Astatic 12-U, L-12-U, Astatic Corporation, Conneault, Ohio.



a. Sonometer system and slab supports.



b. Orientation of slab for frequency testing.

Fig. 16. Sonometer system.

With the slab properly supported and resting firmly against the driver, the power to the driver amplifier was raised to about one-third its capacity, and the gain of the pickup amplifier was raised to about one-half maximum. The frequency of the oscillator was then varied until the Lissajous pattern on the oscilloscope indicated that the driver frequency was very near the fundamental frequency of the slab. Then the fundamental frequency was more accurately determined by varying the oscillator, or driver frequency until a maximum response was indicated on the resonance indicator. The resonance indicator is the milliammeter attached to the Sonometer cabinet as shown in Figure 16a.

This method of test, commonly called the Sonic Method, is a widely accepted non-destructive method for the testing of concrete quality. A thorough discussion of the mathematical theories and concepts from which this method has evolved will not be presented here. However, a brief discussion of its applicability seems pertinent.

Desirable in any concrete durability testing program is the determination of strength and soundness changes in each concrete specimen. Of course, the only true determination of concrete strength arises from tests of the type which destroy the specimen. However, the general relationship that the modulus of elasticity of concrete increases approximately with the square root of strength (5) enables a non-destructive determination of concrete quality. Thus, for any single concrete specimen a variation in the elastic modulus would give an indication of the variation in the concrete strength.

The dynamic modulus of elasticity is related to the natural frequency

of vibration of the specimen by the formula $E = CWn^2$, where E is the dynamic modulus, W is the weight, and n is the natural frequency. C is a factor which depends upon the shape and size of the specimen, the mode of vibration, and Poisson's ratio. If the value for Poisson's ratio were known exactly, then an exact value for Young's modulus could be determined. For comparison studies such as this, A.S.T.M. specifications allow the assumption that C and W remain constant throughout the duration of exposure. The relative modulus of elasticity is defined by the equation, $P_c = (n_c^2/n_o^2) \times 100$, where P_c is the relative dynamic modulus, expressed as a percentage, n_c and n_o are the natural frequencies in cycles per second after "c" freeze-thaw cycles and at zero freeze-thaw cycles, respectively.

Ordinarily in a study of this type a durability factor is computed by the formula $DF = P_cN/M$, where P_c is as defined above, N is the number of cycles at which P_c reaches the specified minimum value for discontinuing the test or the number of cycles at which exposure is to be terminated, whichever is smallest, and M is the predetermined number of cycles at which exposure is to cease. However, in this study no values for M or a minimum P_c were chosen. The comparison afforded by the relative modulus, P_c, is sufficient for the purpose herein.

Permeability study

The very simple procedure for this study consisted of merely refilling each standpipe to the two-foot elevation mark at intervals of ten days. The amount of fluid added was measured to within 0.1 ml. with a

pipette. Also, the bottom of each slab was carefully examined, at the time of refilling, to determine if and when penetration through the two-inch depth occurred.

Approximately every 20 days the amount of moisture lost by evaporation from the closed-bottom standpipes was measured and recorded. These values were used to correct the penetration measurements for evaporation losses.

CHAPTER IV

RESULTS OF INVESTIGATION

Explanatory comments

To assist the reader in interpreting the results of this investigation, a summary of the treatments studied is presented in the following table. Hereafter, the presentation and discussion of the effects of

TABLE VI

SUMMARY AND DESCRIPTION OF TREATMENTS

Treatment Number	Study	Treatment Descriptions		
		Stress (psi.)	Cure	Ponded or standpipe solutions
1	Durability	0	Normal	Water
2	"	0	Normal	$CaCl_2$
3	"	0	Steam	Water
4	"	0	Steam	$CaCl_2$
9	"	500	Normal	Water
10	"	500	Normal	$CaCl_2$
11	"	500	Steam	Water
12	"	500	Steam	$CaCl_2$
17	"	1200	Normal	Water
18	"	1200	Normal	$CaCl_2$
19	"	1200	Steam	Water
20	"	1200	Steam	$CaCl_2$
5	Permability	0	Normal	Water
6	"	0	Normal	$CaCl_2$
7	"	0	Steam	Water
8	"	0	Steam	$CaCl_2$
13	"	500	Normal	Water
14	"	500	Normal	$CaCl_2$
15	"	500	Steam	Water
16	"	500	Steam	$CaCl_2$
21	"	1200	Normal	Water
22	"	1200	Normal	$CaCl_2$
23	"	1200	Steam	Water
24	"	1200	Steam	$CaCl_2$

these treatments will be referenced to the treatment numbers assigned in Table VI. Note that the treatment numbers assigned in Table VI coincide with the numbers assigned to the corresponding slabs of each concrete batch, as diagramed in Figure 10, page 57.

The investigation was separated into three main studies: 1.) durability, 2.) scaling resistance, and 3.) permeability. However, the scaling resistance study involved only those slabs assigned to treatments 2, 4, 10, 12, 18, and 20 (all stresses, both cures, ponded $CaCl_2$ solution). Since these treatments were also investigated in the durability study, the separation of the durability and scaling study will be noted only when presenting or discussing the results of the latter. (The terms "scaling study" and "scaling resistance study" are identical in meaning in this thesis.)

Durability and scaling study

Results of the tests and measurements performed on the slabs were transferred to data processing cards. Typical data obtained from the tests are given in Table VII, for slab 23A10*.

Note the repetition of data collection at 20, 50, and 80 cycles. As indicated by the remarks, the second set of measurements recorded at each of these times was actually obtained seven days after the first set,

---

* This code number refers to slab number 10 of batch number 23. The letter "A" is merely an identification label used during casting and curing to assign the slab to the durability and scaling study. Likewise, the letter "C" appears in the identification labels of those slabs assigned to the permeability study. The reader may ignore these letters.

during which time the slab was stored in the moist-room to allow for curing of the new mortar dike. Thus the slab was subjected to no additional freeze-thaw cycles during this seven-day period.

TABLE VII

TYPICAL DURABILITY AND SCALING STUDY DATA, OBTAINED FROM SLAB NUMBER 23A10

No. of F/T cycles	Length (in.)	Weight (Lbs.)	Natural frequency (cps.)	Scaling weight loss (gms.)	Remarks
0	11.697	12.64	2840	---	
5	11.697	12.80	2820	6.1	
11	11.697	12.88	2850	13.4	
20	11.697	12.78	2830	38.0	
20	11.698	12.75	2890	---	New dike
30	11.697	12.77	2890	3.5	
40	11.697	12.78	2880	6.7	
50	11.698	12.78	2880	8.6	
50	11.699	12.80	2940	---	New dike
60	11.700	12.77	2900	12.8	
70	11.702	12.77	2910	12.1	
80	11.702	12.73	2890	6.7	
80	11.703	12.74	2960	---	New dike
90	11.703	12.72	2940	3.9	
100	11.703	12.70	2950	3.6	
110	11.703	12.69	2960	5.1	
120	11.704	12.71	2950	4.8	
130	11.705	12.70	2950	6.0	

The unfortunate consequence of the aforementioned choice of mortar dikes, for retaining ponded solutions, was the marked change in the concrete slab properties observed after each of these seven-day curing periods. In particular, the almost consistent increase in natural frequency of transverse flexural vibration was quite disturbing. To determine if the natural frequency increases were due to supposed added rigidity

caused by the new mortar dikes,"healing" of the concrete slabs caused by the seven-day moist-room storage, or a combination of these two factors, the following study was performed.

Slabs numbered 2, 4, 10, 12, 18, and 20 from batches 23 and 24 were removed from the freeze-thaw cycling sequence after 50 and 40 cycles, respectively. The mortar dikes were removed from, and replaced on, the slabs of batch 24; but the mortar dikes on the slabs of batch 23 remained undisturbed. All slabs were subsequently placed in the moist-room for seven days, after which they were tested. The resultant percentage increases in natural frequency of transverse flexural vibration are presented in Table VIII.

TABLE VIII

NATURAL FREQUENCY INCREASES DUE TO MORTAR DIKE REPLACEMENTS AND MOIST-ROOM CURING

Slab numbers	Batch 23 (dikes undisturbed)	Batch 24 (dikes replaced)
2	2.54 %	1.83 %
4	4.52	2.94
10	2.08	2.08
12	2.81	2.84
18	1.12	2.95
20	1.86	3.52
Ave.	2.49 %	2.69 %

Although the average frequency increase was slightly greater for batch 24, it was concluded that the frequency increases due to mortar dike replacements were not a result of added rigidity caused by the new dikes. Rather, it appears that the dominating cause for the increases

was the "healing", or repairing effect of the moist-room environment upon the frost-damaged concrete. This effect, although interesting, introduced an unfortunate source of variation which had not been anticipated. In addition to reducing the over-all desired rapid rate of deterioration, these cycling interruptions appeared to increase the durability of the slabs, in that the rate of deterioration after each periodic moist-room curing period was generally lower than just prior to the curing period.

The necessity for these mortar dike replacements did not occur at the same number of cycles for each batch; however, the total number of dike replacements was nearly the same for each batch. Therefore, because all slabs with ponded $CaCl_2$ solution received nearly the same number of new dikes, and since no adjustment of the natural frequencies could be justified, it was decided to ignore these abrupt frequency changes.

Comparisons of effects of any of the treatments 2, 4, 10, 12, 18, or 20 (all ponded with $CaCl_2$ solution) with any or all of the others in this group should remain valid even though these abrupt frequency changes have been ignored. However, the validity of comparisons of the effects of any or all of these treatments with those of treatments 1, 3, 9, 11, 17, and 19 (all ponded with water) may be questionable, since slabs subjected to these latter treatments required no mortar dike replacements, with the exception of the slabs of batch 22, which had their dikes replaced at 40 cycles.

At least one other investigator (30) has reported the necessity for mortar dike repairs in this type of study, but he did not report any

natural frequency changes due to these repairs; nor did he describe the method of repair.

In addition to the frequency increases caused by mortar dike replacements, weight and length changes of the slabs were also observed. Because of the crude method for measuring the lengths of the slabs, the increased tendency of the end-bearing plates to rust in the moist-room environment, and the minor importance of the slab lengths to this study, no attempt was made to adjust the length measurements. However, the recorded weights were adjusted under the assumption that any weight changes observed were due to differences between the weights of the new and old mortar dikes. This assumption is not entirely valid, since slight weight increases due to moisture absorption were observed; though usually these increases were negligible. These weight adjustments were made only for comparisons of the effects of various treatments upon the weight changes of the concrete slabs. (The actual unadjusted weights were used for relative dynamic modulus of elasticity calculations, as will be discussed on page 85.)

The occurrences of mortar dike replacements are shown in the graphs of Figures 45 - 56 in Appendix E, by the abrupt discontinuities indicated with vertical dashed lines.

It may be recalled, from Chapter III, that A.S.T.M. specifications allow the assumption that C and W (weight) remain essentially constant throughout the duration of the freeze-thaw cycling period, thereby permitting the use of the equation, $P_c = (n_c^2/n_o^2) \times 100$, for determining the relative dynamic modulus of elasticity. However, because of the relatively large weight changes observed for individual slabs and, more

importantly, the significant differences between weight changes of slabs of treatments 1, 3, 9, 11, 17, and 19 (water ponded) and those of slabs of treatments 2, 4, 10, 12, 18, and 20 (ponded with $CaCl_2$ solution), it was decided to calculate the relative dynamic moduli of elasticity according to the equation

$$P_c = \frac{W_c n_c^2}{W_o n_o^2} \times 100 \quad \ldots\ldots\ldots\ldots\ldots (1),$$

where W_c is the actual unadjusted weight of the slab at n_c cycles.

Accordingly, a Fortran computer program was written which instructed the computer* to read the data, such as that in Table VII, and compute the relative dynamic moduli, adjusted weight changes, length changes, and cumulative scaling weight losses, in pounds. The scaling weight losses were converted from grams to pounds to facilitate comparisons of the total weight changes with the surface scaling weight losses. (Such comparisons will not be made in this report, but could be analyzed to determine the effects of the various treatments upon the weight changes due to absorption of the ponded solutions.) These results were punched on cards by the computer, and listed for subsequent plotting. As an example, the values computed from the data of Table VII, for slab 23A10, are presented in Table IX.

Graphs of these results for each slab assigned to the durability and scaling study appear in Figures 45 - 86 in Appendix E. It should be noted

---

* International Business Machines, Inc., Model 1620^{II} computer, Montana State College Computing Center.

that each of these figures contains the results for four replicates assigned to a specific treatment. Thus, for example, Figure 45 shows the relationship between relative dynamic modulus of elasticity and number of freeze-thaw cycles for each of slabs 21A1, 22A1, 23A1, and 24A1. Note also that these slabs are the replicates assigned to treatment number 1 in Table VI.

TABLE IX

COMPUTED RESULTS FOR SLAB 23A10

No. of F/T cycles	Relative dynamic modulus (%)	Adjusted weight change (Lbs.)	Length change (in.)	Cumulative scaling loss (Lbs.)	Comment
0	100.00	0.00	0.000	0.00	
5	99.84	0.16	0.000	0.01	
11	102.61	0.24	0.000	0.04	
20	100.39	0.14	0.000	0.12	
20	104.45	0.14	0.001	0.12	New dike
30	104.61	0.16	0.000	0.13	
40	103.97	0.17	0.000	0.14	
50	103.97	0.17	0.001	0.16	
50	108.52	0.17	0.002	0.16	New dike
60	105.34	0.14	0.003	0.19	
70	106.07	0.14	0.005	0.22	
80	104.28	0.10	0.005	0.23	
80	109.48	0.10	0.006	0.23	New dike
90	107.84	0.08	0.006	0.24	
100	108.40	0.06	0.006	0.25	
110	109.05	0.05	0.006	0.26	
120	108.49	0.07	0.007	0.27	
130	108.40	0.06	0.008	0.28	

No distinct relationship between durability, nor scaling resistance, and number of freeze-thaw cycles was desired in this study. Rather, a comparison of the effects of various treatments, after any given number of

freeze-thaw cycles, upon the characteristics of the concrete slabs was intended. Therefore, the statistical method chosen for making these comparisons was Duncan's new multiple-range test (31). This test is designed to test for the significance of differences between any number of mean values, under the assumption of homogeneity of variances (i.e., equal variances regardless of treatment).

Despite the careful control exercised throughout the progress of this study, the inherent variability between the characteristics of replicate slabs, particularly between non-stressed replicates, was appreciable. This is most evident in the graphs of Figures 45 - 52. Therefore, application of the Duncan test without regard to magnitude of variances was deemed incorrect. To test for homogeneity of variances, Bartlett's test (31) was applied.

It will be recalled that the primary purpose of this investigation was to determine the effect of prestress upon the durability of concrete. In addition, comparisons of the effects of steam curing and normal curing, and of the effects of ponded water and $CaCl_2$ solution upon durability were desired. Also intended were comparisons of the effects of prestress and of the types of curing upon the scaling resistance of concrete. Realizing that the Bartlett test would probably show non-homogeniety of variances in some of the treatment comparisons, it was decided to make nine comparisons of various treatment combinations to assure the valid application of Duncan's test. These treatment comparisons are described in Table X. (The treatment comparison identification letters, A and C, should not be confused with the letters "A" and "C" appearing in the slab labels.)

TABLE X

TREATMENT COMPARISONS CHOSEN FOR DURABILITY AND SCALING STUDY

Comparison identification	Treatments compared	Comparison description
A	1, 2, 3, 4, 9, 10, 11, 12, 17, 18, 19, 20	All treatments
B	1, 3, 9, 11, 17, 19	All stresses, both cures, ponded water
C	2, 4, 10, 12, 18, 20	All stresses, both cures, ponded $CaCl_2$ solution
D	1, 9, 17	All stresses, normal cure, ponded water
E	2, 10, 18	All stresses, normal cure, ponded $CaCl_2$ solution
F	3, 11, 19	All stresses, steam cure, ponded water
G	4, 12, 20	All stresses, steam cure, ponded $CaCl_2$ solution
H	1, 2, 9, 10, 17, 18	All stresses, normal cure, both ponded solutions
I	3, 4, 11, 12, 19, 20	All stresses, steam cure, both ponded solutions

For Bartlett's test, the 1 per cent significance level was chosen for declaration of homogeneity or non-homogeneity of variances, while the 5 per cent level was chosen for decisions regarding the significance or non-significance of differences between treatment mean values in the Duncan test.

Fortran computer programs were written which instructed the computer

to read the results for each slab, such as those listed in Table IX. The computer stored these values and then performed the nine treatment comparisons described in Table X at intervals of 10 freeze-thaw cycles for the relative modulus values, and at intervals of 20 cycles, beginning at 10 cycles, for the adjusted weight change, length change, and cumulative scaling loss values.

It will be noted, from the results presented in Appendix E, that data were not obtained at some of the freeze-thaw cycles at which these statistical tests were applied. For these instances, the computer program was designed to supply these missing values by linear interpolation between adjacent values. This procedure, though questionable, was deemed reasonable in light of the usually gradual changes observed in the measured slab characteristics with increasing number of freeze-thaw cycles.

Also, slabs 22A4 and 24A4 became so severely damaged after 70 freeze-thaw cycles that their mortar dikes could not be replaced. This necessitated their removal from the cycling and testing program. To include these slabs in the statistical tests, it was decided to assign their final values of relative dynamic moduli, adjusted weight changes, length changes, and cumulative scaling losses to the remaining cycles at which statistical tests were desired. This decision was undoubtedly the most conservative possible, but no other method for assigning these non-existent values could be reasonably justified. The omission of these replicates after 70 cycles would have made the statistical tests difficult at best, and would seriously have distorted the average effects of treatment 4.

An example of the output obtained from the computer for these programs is given in Figure 17 for treatment comparison I of the adjusted weight change values at 70 freeze-thaw cycles.

Treatment number	Mean adjusted weight change (Lbs.)	Variance (Lbs.^{2})	Standard deviation (Lbs.)
3	0.260	0.00*	0.09
4	-0.085	0.00	0.08
11	0.230	0.00	0.04
12	-0.035	0.00	0.07
19	0.222	0.00	0.05
20	-0.147	0.00	0.08

Bartlett test for homogeneity of variance:

computed χ^2	corrected χ^2	tabulated $\chi^2_{(0.05)}$	tabulated $\chi^2_{(0.01)}$
1.78	1.58	11.1	15.1

Duncan multiple-range test:

P	$SSR_{(0.05)}$	$LSR_{(0.05)}$
2	2.97	0.111
3	3.12	0.117
4	3.21	0.120
5	3.27	0.122
6	3.32	0.124

Fig. 17. Example of Bartlett and Duncan test results.

* Since the computer was instructed to truncate these values after two decimal places, these values are misleading.

In Figure 17, χ^2 (chi-squared) is the test statistic used in the Bartlett test for determining whether the variances are homogeneous or non-homogeneous. χ^2 is defined as the sum of squares of independent, normally distributed variables with zero means and unit variances. The distribution of χ^2 depends on the number of independent deviates, that is, on the degrees of freedom. Thus, there is a χ^2 distribution for each number of degrees of freedom, where the number of degrees of freedom is one less than the number of samples. Tables of these χ^2 distributions appear in many texts relating to statistics. Homogeneity or non-homogeneity of variance is declared on the basis of comparisons of computed χ^2 values with these tabulated values, at the chosen significance levels.

For the Duncan test, P refers to the number of ranked means across which a comparison is being made; and SSR is an abbreviation for "significant studentized range". SSR values are tabulated in many statistics texts for various numbers of degrees of freedom, at both the 5 per cent and 1 per cent protection levels. Presumably they are computed for means of sample characteristics which are normally distributed with unit variances. The LSR (least significant range) values are obtained by multiplying the SSR values by the "pooled" estimate of variance for all treatments.

The procedures and equations for these tests, including those for finding the "computed χ^2", "corrected χ^2", and "pooled" estimate of variance, are standard and may be found in most statistics texts; however, they will not be presented in this discussion for the sake of brevity. (See reference 31 for a complete description of these tests.)

The interpretation of the output of Figure 17 would be as presented in the following discussion:

Since the value of χ^2 is less than the appropriate tabulated values of χ^2 at both the 5 per cent and 1 per cent levels, the hypothesis that the variances are homogeneous is accepted. If χ^2 had been greater than 11.1 but less than 15.1, this hypothesis would also have been accepted. However, had χ^2 exceeded or equalled 15.1, the value of the "corrected" χ^2 would have been similarly tested. Acceptance or rejection of the hypothesis of homogeneous variances would then have been decided according to the tests of the "corrected" χ^2 value.

Since the variances have been declared homogeneous the Duncan test may be applied. To facilitate the test, the mean values are ranked.

Treatment number	Mean adjusted weight change
20	-0.147
4	-0.085
12	-0.035
19	0.222
11	0.230
3	0.260

Differences between mean values are then computed, and compared with the appropriate LSR (least significant range) values. These comparisons are presented on the following page; the treatment numbers are underlined, and in parentheses, indicating the means being compared.

Treatment mean difference calculations:

$(\underline{3} - \underline{20})$: $0.260 - (-0.147) = 0.407 > 0.124$ **
$(\underline{3} - \underline{4})$: $0.260 - (-0.085) = 0.345 > 0.122$ **
$(\underline{3} - \underline{12})$: $0.260 - (-0.035) = 0.295 > 0.120$ **
$(\underline{3} - \underline{19})$: $0.260 - 0.222 = 0.038 \leq 0.117$ n.s.

Comparison of the mean values for treatments 3 and 11 is unnecessary, since the mean values for treatments 3 and 19 are declared insignificantly different.

Conclusions thus far would be that the average adjusted weight increases of slabs subjected to treatment 3 (non-stressed, steam cured, water ponded) are greater than those of slabs subjected to treatments 20, 4, and 12 (all stresses, steam cured, ponded with $CaCl_2$ solution), but not different from those of slabs subjected to treatments 19 and 11 (1200 psi. and 500 psi., resp., steam cured, water ponded), at the 5 per cent protection level, after 70 freeze-thaw cycles.

To continue:

$(\underline{11} - \underline{20})$: $0.230 - (-0.147) = 0.377 > 0.122$ **
$(\underline{11} - \underline{4})$: $0.230 - (-0.085) = 0.315 > 0.120$ **
$(\underline{11} - \underline{12})$: $0.230 - (-0.035) = 0.265 > 0.117$ **
$(\underline{11} - \underline{19})$: declared insignificantly different above
$(\underline{19} - \underline{20})$: $0.222 - (-0.147) = 0.369 > 0.120$ **
$(\underline{19} - \underline{4})$: $0.222 - (-0.085) = 0.307 > 0.117$ **
$(\underline{19} - \underline{12})$: $0.222 - (-0.035) = 0.257 > 0.111$ **
$(\underline{12} - \underline{20})$: $-0.035 - (-0.147) = 0.112 \leq 0.117$ n.s.

Similarly, the comparison of the mean values for treatments 4 and 20 is unnecessary.

The symbols used are in keeping with common statistical notation, in that "n.s.", "*", and "**", designate test statistics which are non-significant, significant at the 1 per cent protection level, and signif-

icant at the 5 per cent protection level, respectively.

To summarize the results of this example, it is declared that the average mean adjusted weight increases of slabs subjected to treatments 3, 11, and 19 (all stresses, steam cured, water ponded) are greater than those of slabs subjected to treatments 4, 12, and 20 (all stresses, steam cured, ponded with $CaCl_2$ solution), but not different from each other at the 5 per cent protection level, after 70 freeze-thaw cycles. Nor are the average mean adjusted weight losses of slabs subjected to treatments 4, 12, and 20 different from each other after 70 freeze-thaw cycles.

The accepted method for presenting the results of the example above would be as follows,

$$\underline{20 \quad 4 \quad 12} \qquad \underline{19 \quad 11 \quad 3},$$

where the treatment identification numbers are arranged from left to right in order of ascending treatment mean values. Lines are then drawn beneath those treatment numbers which have mean values that are declared insignificantly different at the chosen protection level.

The method for presenting the statistical test results for this study is patterned after the method given above. In this case, however, the treatment mean values are plotted as functions of the number of freeze-thaw cycles, and lines have been drawn through those mean values which were declared insignificantly different at the appropriate numbers of freeze-thaw cycles where the Bartlett and Duncan tests were performed.

These results for the durability and scaling study are presented in Figures 18 - 29. The method of presentation serves a dual purpose, in that 1.) the results of the Duncan multiple-range tests are condensed for ready interpretation, and 2.) a qualitative interpretation of the relative directions and magnitudes of changes induced by the various treatments can readily be made.

As expected, the Bartlett tests did indeed show non-homogeneity of variances for many of the treatment mean comparisons. This would indicate 1.) poor laboratory control of the mixing, casting, and curing procedures, 2.) insufficient number of replications, 3.) non-reproducible testing procedures, or 4.) a combination of these factors. Nevertheless, the Duncan tests were performed and are reported in Figures 18 - 29 for every treatment comparison at each preselected number of freeze-thaw cycles. This was done to assist the reader in making qualitative interpretations of the information. Those Duncan tests which would be considered valid, according to the Bartlett tests, may be recognized by referring to Tables XI - XIV. In these tables, the symbols "n.s." and "*" indicate acceptance of the hypothesis that variances are homogeneous. The symbol "**" means non-homogeneity of variances and strictly, therefore, an invalid application of Duncan's test.

In an attempt to reduce the number of invalid applications of the Duncan test to comparisons of the mean relative dynamic moduli, an arcsin transformation of their coded values was made before applying the Bartlett and Duncan tests. The coded values were obtained by subtracting 20 per cent from each value, and then dividing by 100, to assure that all values

would be in the range: 0 to 1.0. These diminished values were further modified by extracting their square roots. Thus, the transformation used was

$$\arcsin \sqrt{\frac{P_c - 20}{100}}$$

This trigonometric transformation is recommended (31) for percentage values which lie within the range of values observed in this study, in order to stabilize the variances. Accordingly, the Bartlett test results presented in Table XI and the Duncan test results presented in Figures 18 through 26 were performed on the transformed values. However, the plotted mean values are in the original scale.

Because of the greater relative importance of the dynamic modulus of elasticity as an index of deterioration in any freeze-thaw durability study, all of the treatment comparisons described in Table X for the mean relative dynamic moduli are presented. For comparisons of mean adjusted weight changes, the conclusions to be drawn from treatment comparisons B through I are not different from those related by comparison A. Therefore, only Figure 27 is presented to summarize the results of the average adjusted weight change comparisons. The same reasoning applies to comparisons of the mean length changes, the results of which appear in Figure 28.

For the average scaling weight loss comparisons, only treatment comparisons C, E, and G are appropriate, since data for this study were not obtained from slabs assigned to treatments 1, 3, 9, 11, 17, and 19,

that is, from slabs which were ponded with water. Further, the conclusions to be drawn from comparisons E and G are not different from those to be drawn from comparison C for the scaling resistance study; nor can they be more clearly illustrated than in Figure 29, so only this figure is presented.

The reader may experience some difficulty in interpreting Figures 18 through 38. Although it is true that a graph should be entirely self-explanatory, the method of presentation chosen for these figures prohibited any further verbal elaboration in the figures. The author wishes to apologize to the reader for the inconvenience of having to refer to Tables VI and X for interpreting the treatment numbers and comparison identification letters; and he offers the following comments in the hope that the treatment numbers will become less confusing.

1.) Treatment numbers 1 - 8 refer to non-stressed slabs, numbers 9 - 16 refer to 500 psi. slabs, and numbers 17 - 24 denote 1200 psi. slabs.

2.) These three number sets are further subdivided to indicate whether the slabs are part of the durability and scaling study or part of the permeability study. Thus, numbers 1 - 4, 9 - 12, and 17 - 20 indicate slabs in the durability and scaling study, while numbers 5 - 8, 13 - 16, and 21 - 24 refer to slabs in the permeability study. (Note that Figures 18 - 29 contain information only from the durability and scaling study, while Figures 30 - 38 contain information only from the permeability study.)

3.) The first two numbers of each of these four-number subsets refer to slabs which were normally cured, while the second two numbers

refer to steam cured slabs. For example, numbers 1 and 2, 5 and 6, and 17 and 18 refer to normally cured slabs; and numbers 3 and 4, 7 and 8, and 19 and 20 denote steam cured slabs.

4.) All odd numbers denote slabs which were ponded with water, or contained water in their standpipes. All even-numbered slabs had $CaCl_2$ solution ponded on their surfaces, or contained in their standpipes.

In all of Figures 18 - 38 the treatment, for which each mean relationship is plotted, is identified only by its number. The treatment comparisons are named in the figure titles. (Tables VI and X, on pages 79 and 88, resp., fully describe the treatments and treatment comparisons.)

The following 16 pages, pages 99 - 114, contain the Bartlett and Duncan test results for data from the durability and scaling study only. Discussion of the permeability study results begins on page 115, following which Table XV and Figures 30 - 38 are presented.

TABLE XI

RESULTS OF BARTLETT TESTS OF
TRANSFORMED RELATIVE DYNAMIC MODULI

No. of F/T cycles	Comparison								
	A	B	C	D	E	F	G	H	I
10	**	n.s.	**	n.s.	n.s.	n.s.	n.s.	n.s.	**
20	**	n.s.	**	n.s.	n.s.	n.s.	*	n.s.	**
30	**	n.s.	**	n.s.	n.s.	n.s.	*	n.s.	*
40	**	n.s.	**	n.s.	n.s.	n.s.	n.s.	n.s.	**
50	**	n.s.	**	n.s.	n.s.	*	*	n.s.	**
60	**	*	**	n.s.	n.s.	*	n.s.	n.s.	**
70	**	**	**	n.s.	n.s.	**	*	n.s.	**
80	**	**	**	n.s.	n.s.	**	*	n.s.	**
90	**	**	**	n.s.	n.s.	**	*	n.s.	**
100	**	**	*	n.s.	n.s.	**	*	n.s.	**
110	**	**	*	n.s.	n.s.	**	n.s.	n.s.	**
120	**	**	n.s.	n.s.	n.s.	**	n.s.	n.s.	**
130	**	*	n.s.	n.s.	n.s.	*	n.s.	n.s.	*

Fig. 18. Results of Duncan tests of mean transformed relative dynamic moduli for treatment comparison A. (Refer to discussion, pages 97 & 98.)

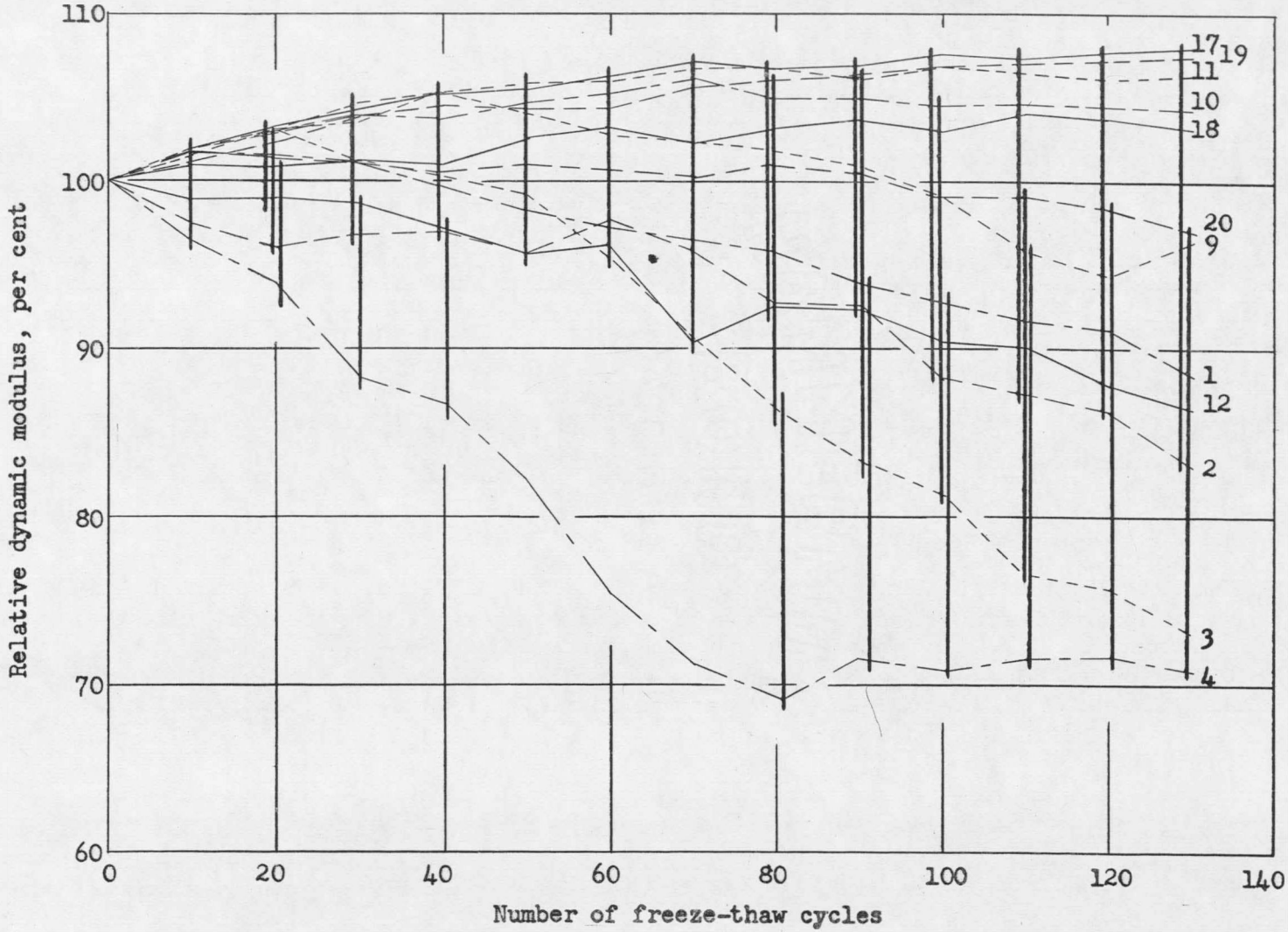


Fig. 19. Results of Duncan tests of mean transformed relative dynamic moduli for treatment comparison B. (Refer to discussion, pages 97 & 98.)

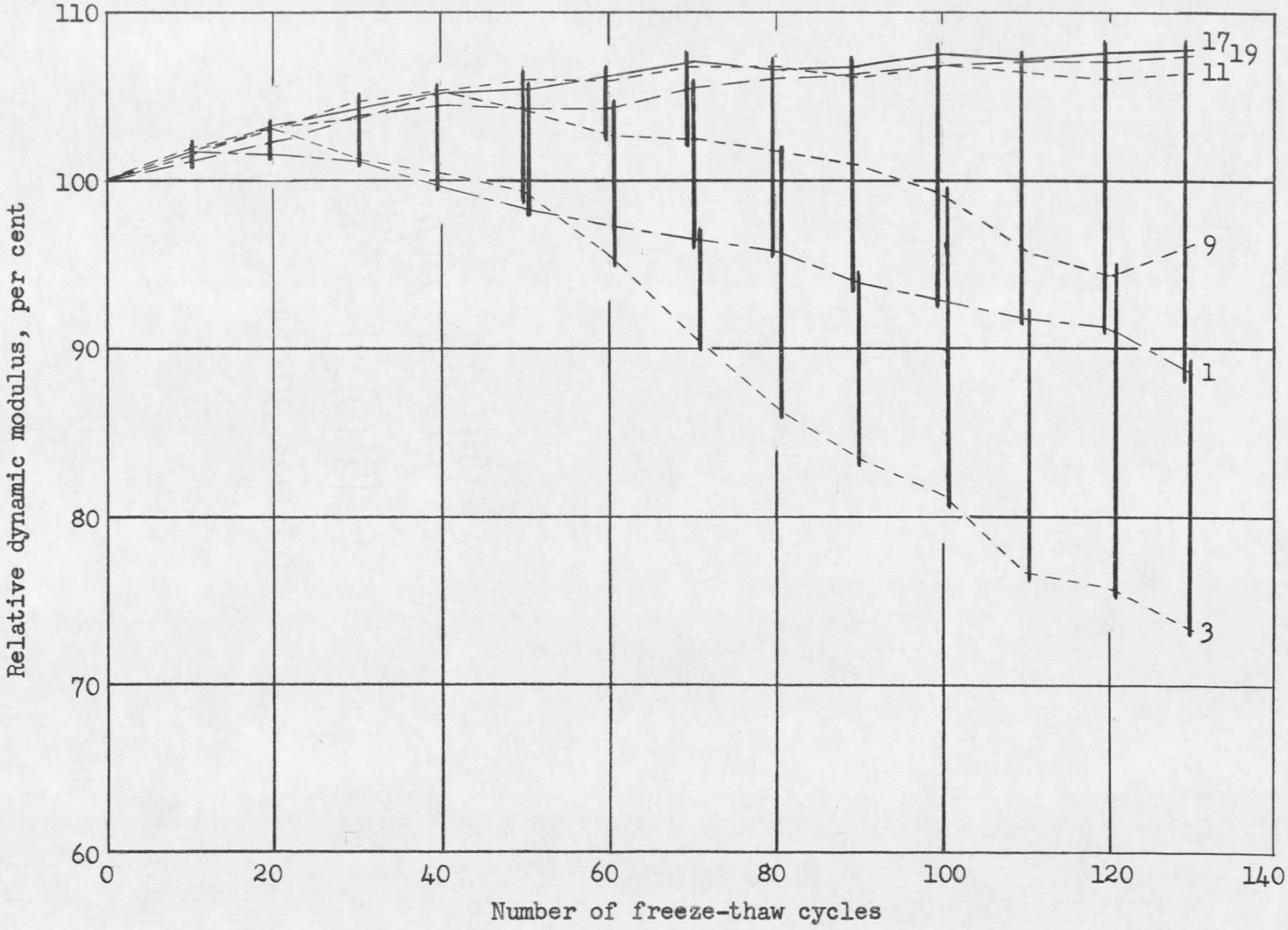


Fig. 20. Results of Duncan tests of mean transformed relative dynamic moduli for treatment comparison C. (Refer to discussion, pages 97 & 98.)

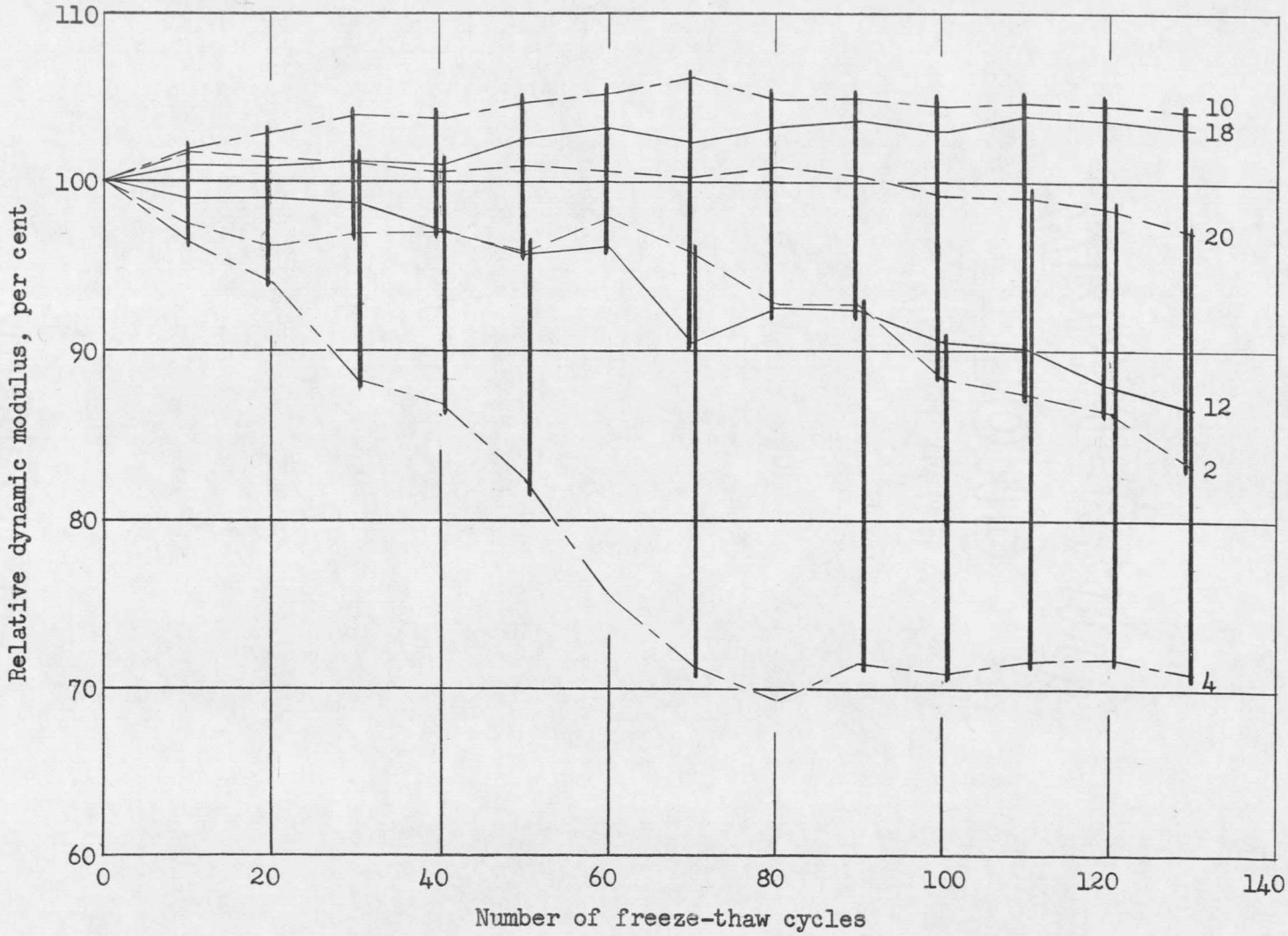


Fig. 21. Results of Duncan tests of mean transformed relative dynamic moduli for treatment comparison D. (Refer to discussion, pages 97 & 98.)

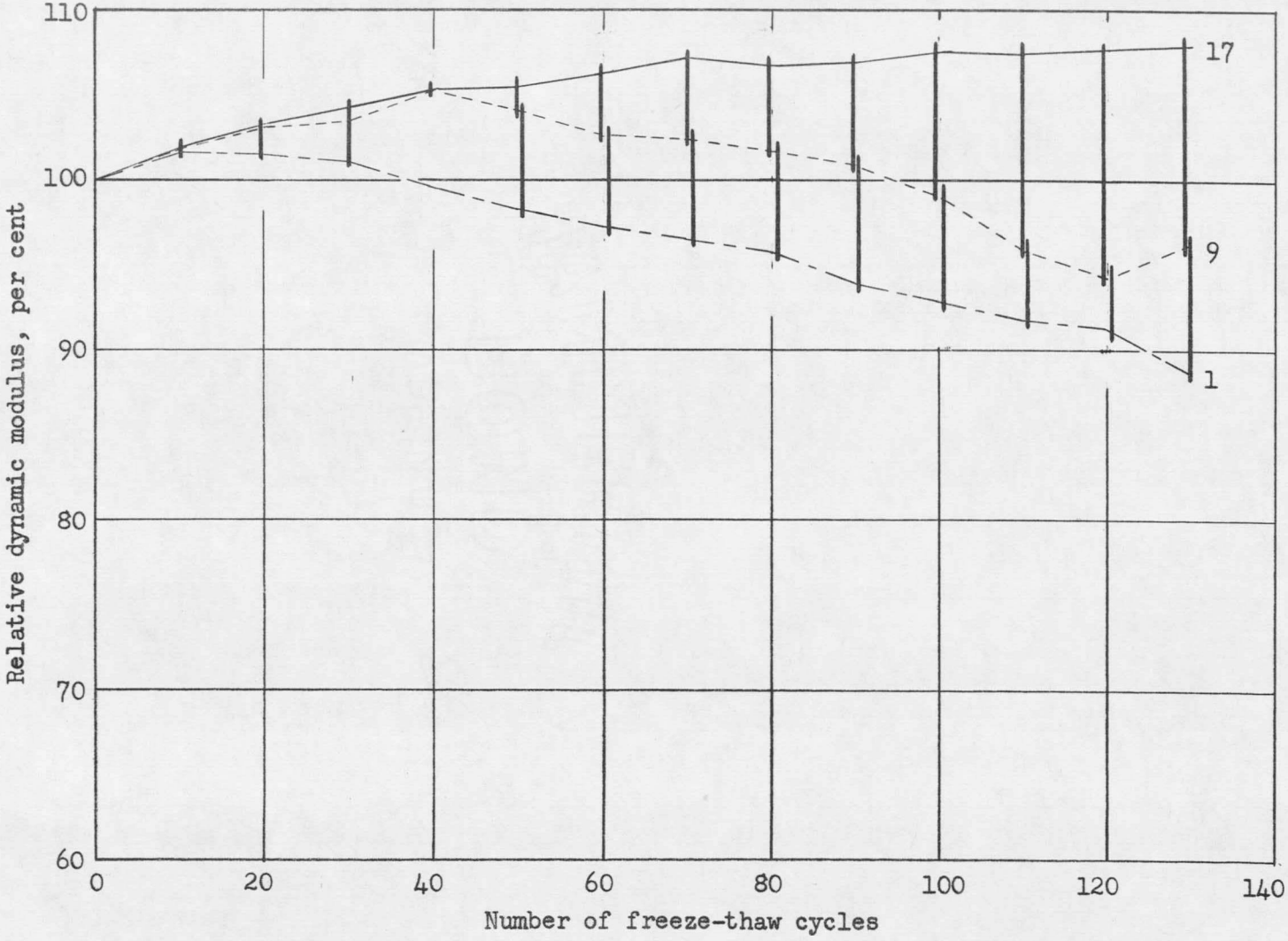


Fig. 22. Results of Duncan tests of mean transformed relative dynamic moduli for treatment comparison E. (Refer to discussion, pages 97 & 98.)

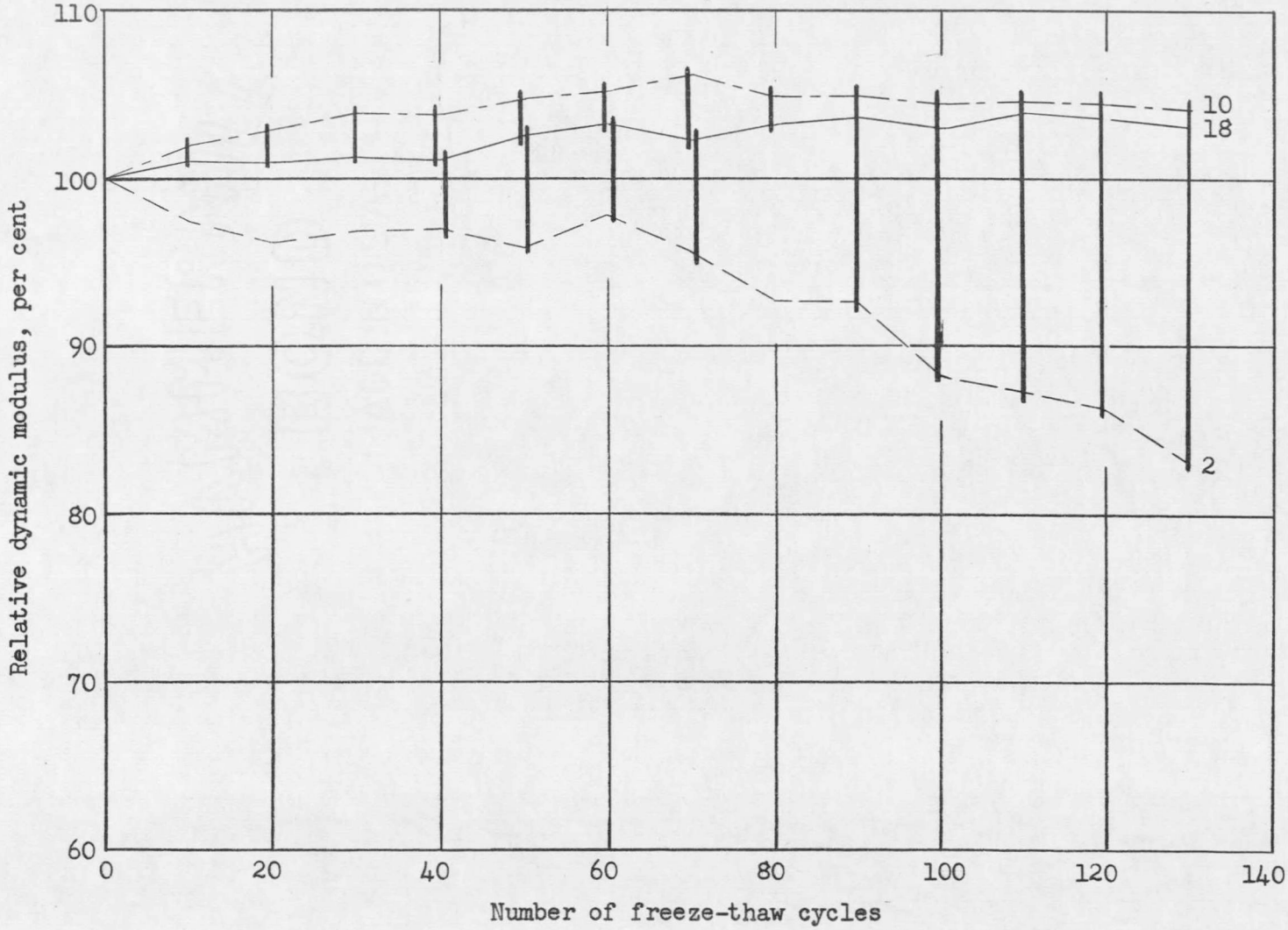


Fig. 23. Results of Duncan tests of mean transformed relative dynamic moduli for treatment comparison F. (Refer to discussion, pages 97 & 98.)

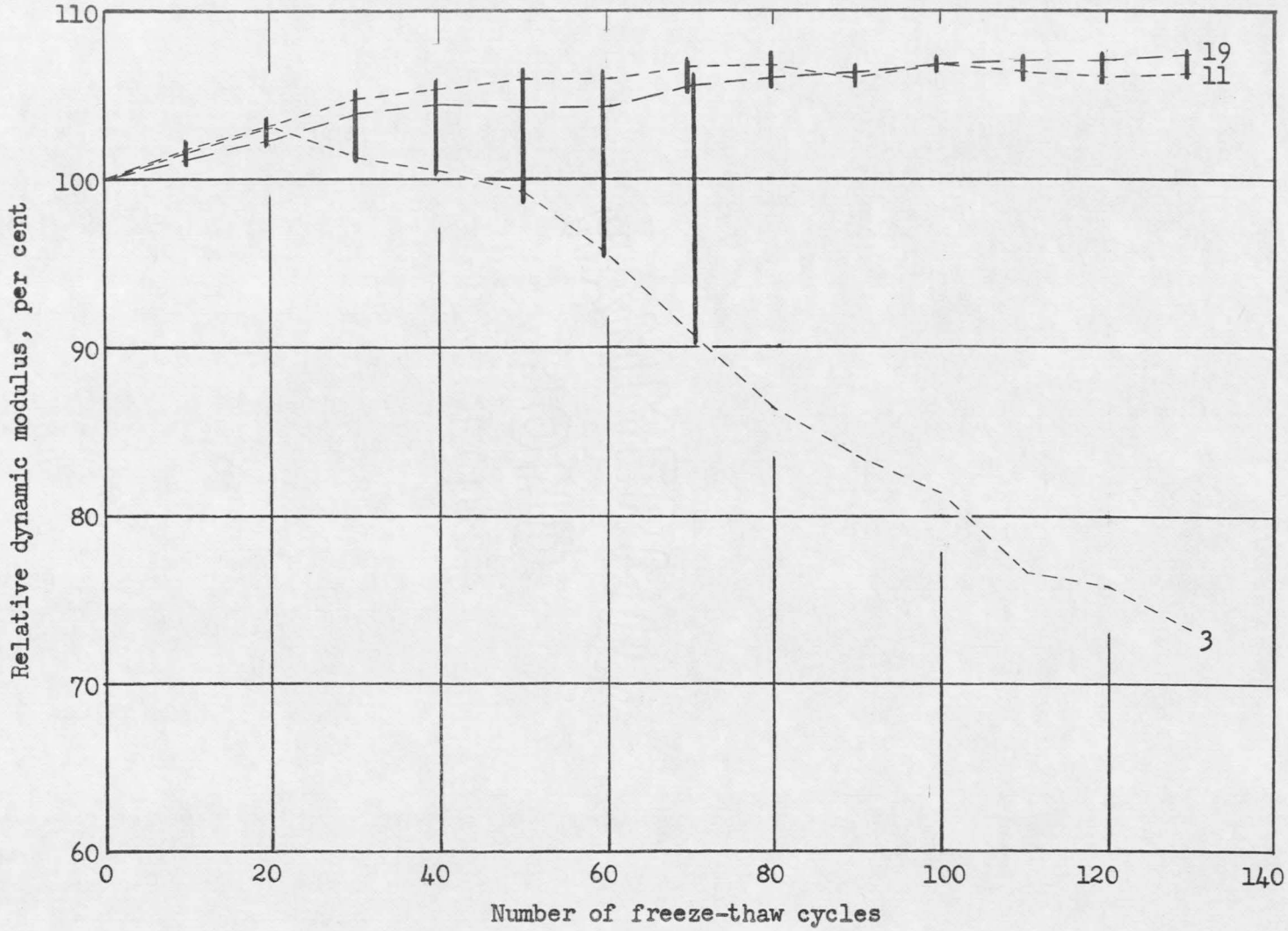


Fig. 24. Results of Duncan tests of mean transformed relative dynamic moduli for treatment comparison G. (Refer to discussion, pages 97 & 98.)

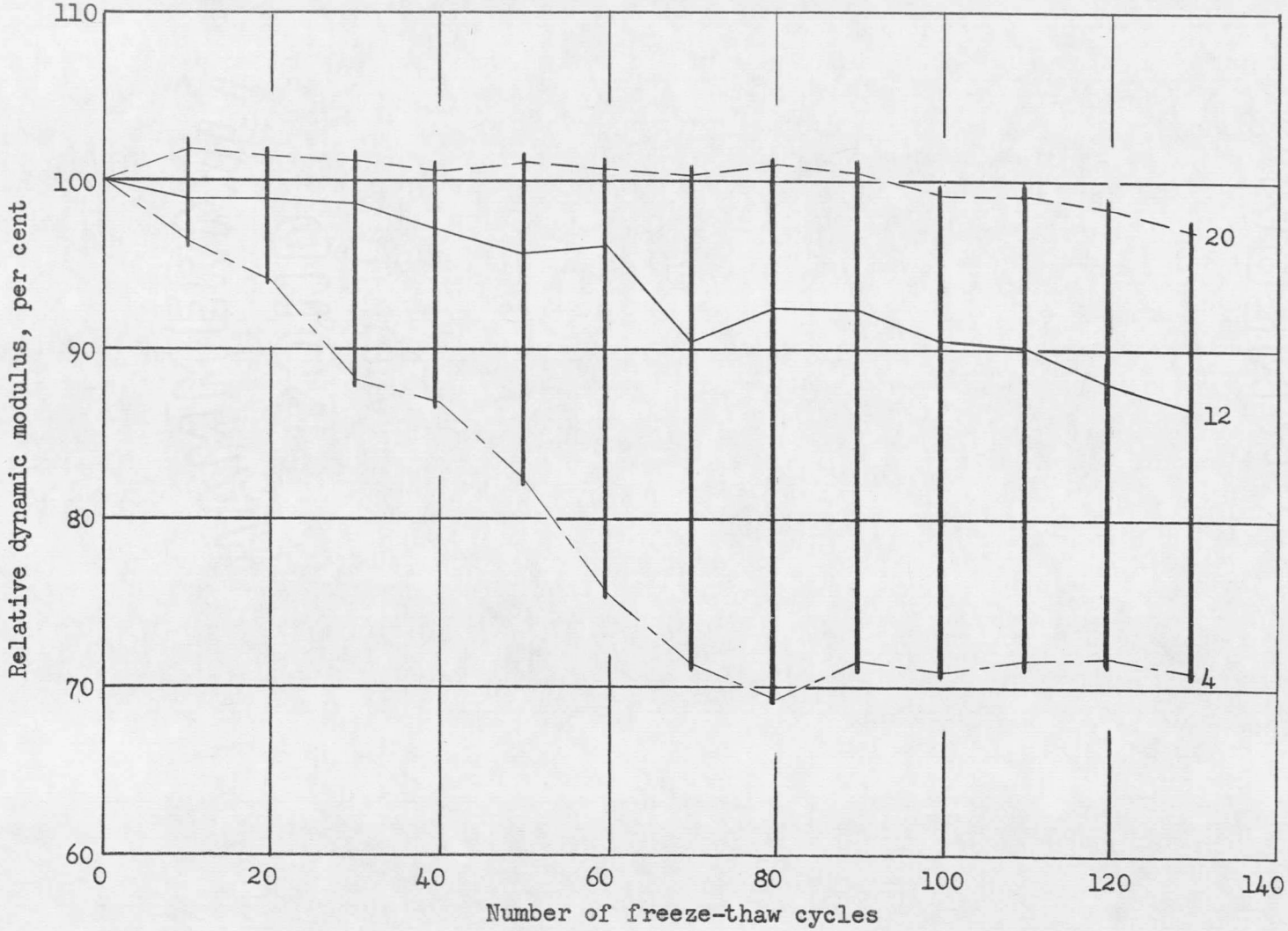


Fig. 25. Results of Duncan tests of mean transformed relative dynamic moduli for treatment comparison H. (Refer to discussion, pages 97 & 98.)

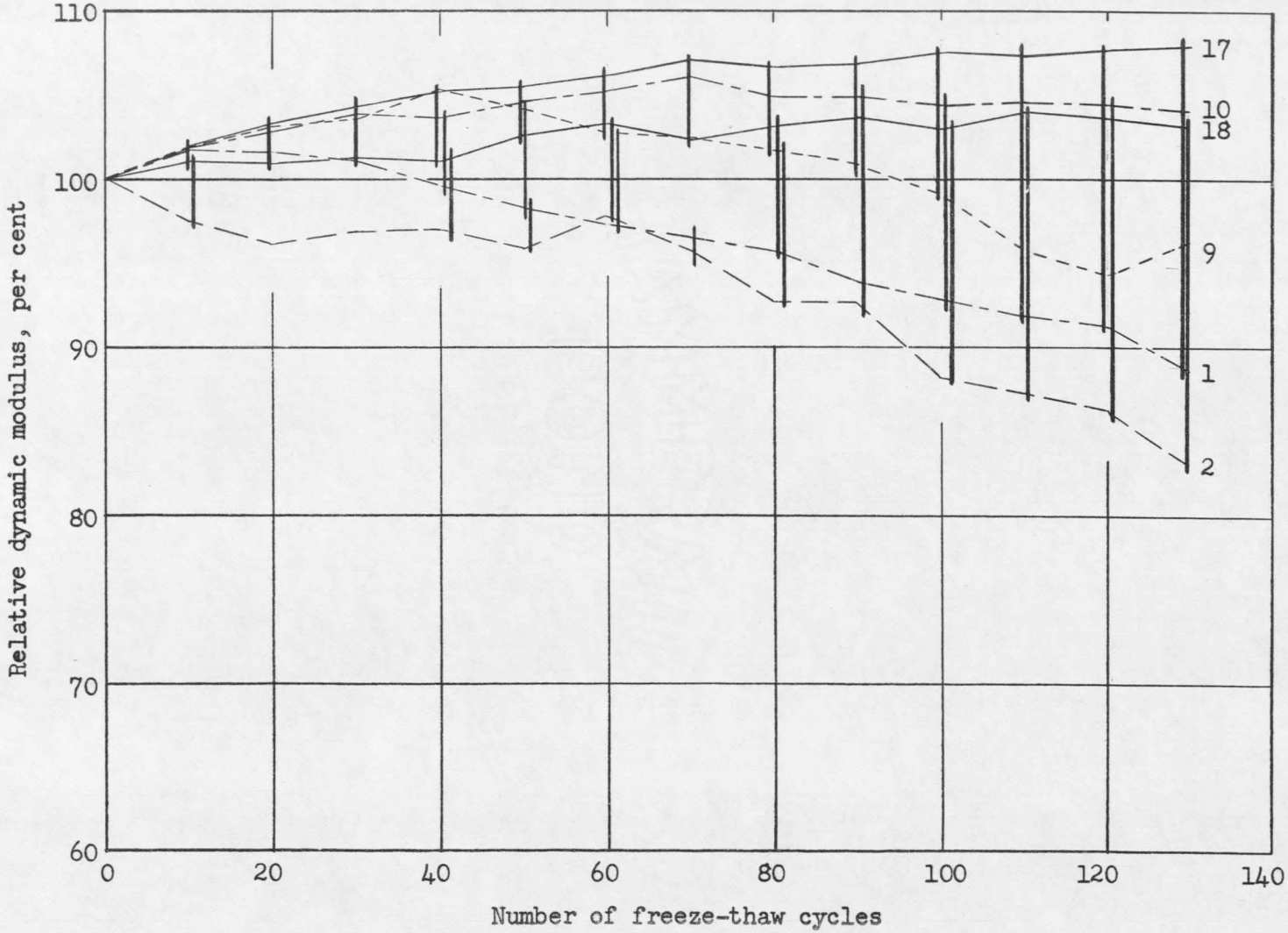


Fig. 26. Results of Duncan tests of mean transformed relative dynamic moduli for treatment comparison I. (Refer to discussion, pages 97 & 98.)

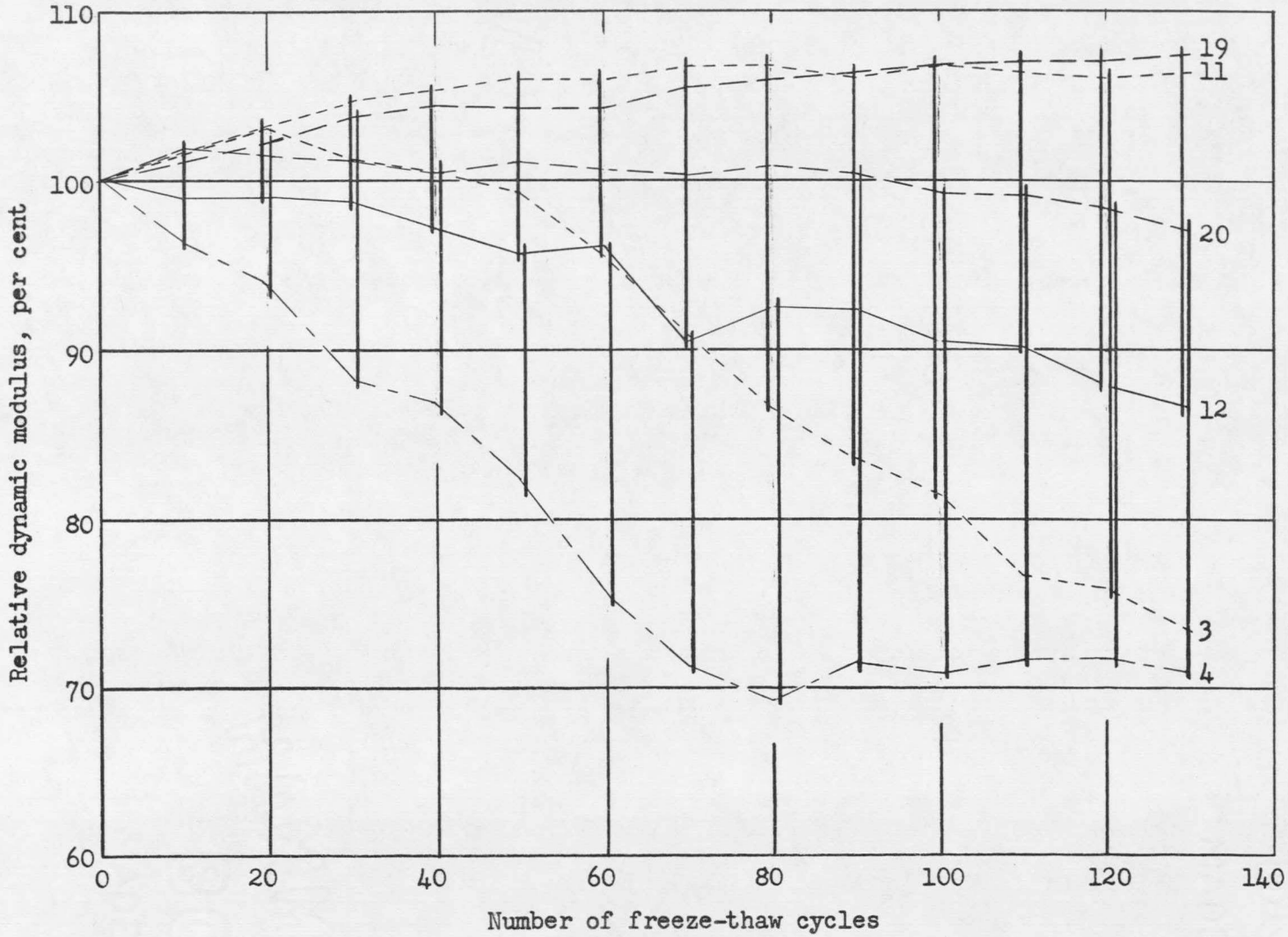


TABLE XII

RESULTS OF BARTLETT TESTS OF
ADJUSTED WEIGHT CHANGES

No. of F/T cycles	Comparison								
	A	B	C	D	E	F	G	H	I
10	n.s.	n.s.	n.s.	n.s.	n.s.	n.s.	n.s.	n.s.	n.s.
30	n.s.	n.s.	n.s.	n.s.	n.s.	n.s.	n.s.	n.s.	n.s.
50	n.s.	n.s.	n.s.	n.s.	n.s.	n.s.	n.s.	n.s.	n.s.
70	n.s.	n.s.	n.s.	n.s.	n.s.	n.s.	n.s.	n.s.	n.s.
90	n.s.	n.s.	n.s.	n.s.	n.s.	n.s.	n.s.	n.s.	n.s.
110	n.s.	n.s.	n.s.	n.s.	n.s.	n.s.	n.s.	n.s.	n.s.
130	n.s.	n.s.	n.s.	n.s.	n.s.	n.s.	n.s.	n.s.	n.s.

Fig. 27. Results of Duncan tests of mean adjusted weight changes for treatment comparison A. (Refer to discussion, pages 97 & 98.)

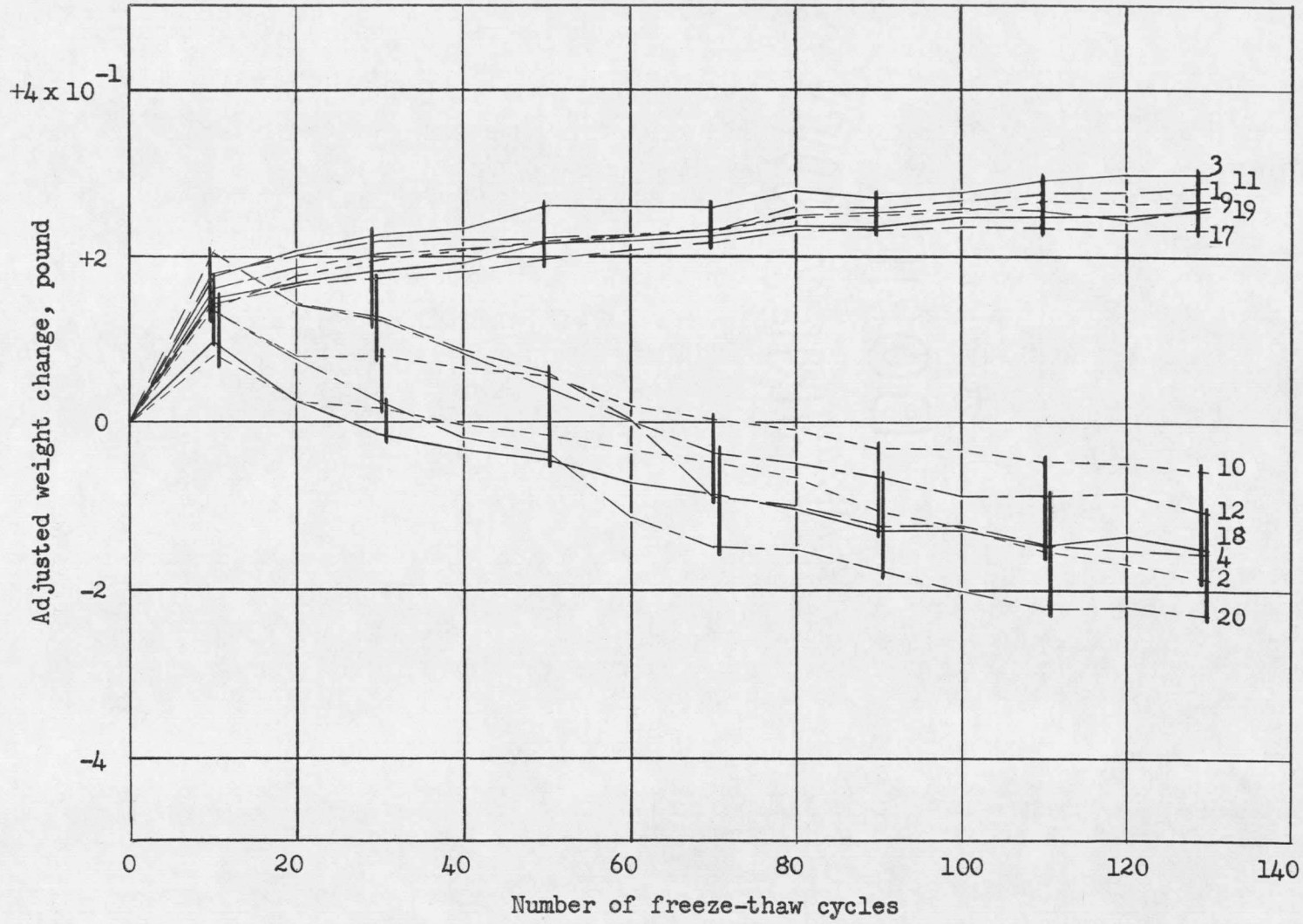


TABLE XIII

RESULTS OF BARTLETT TESTS
OF LENGTH CHANGES

No. of F/T cycles	Comparison								
	A	B	C	D	E	F	G	H	I
10	n.s.	n.s.	n.s.	n.s.	n.s.	n.s.	n.s.	n.s.	n.s.
30	**	n.s.	**	n.s.	n.s.	n.s.	**	n.s.	**
50	**	n.s.	**	n.s.	n.s.	n.s.	**	n.s.	**
70	**	*	**	*	n.s.	*	**	**	**
90	**	*	**	n.s.	*	n.s.	**	**	**
110	**	**	**	*	*	*	**	**	**
130	**	**	**	*	**	*	*	**	**

Fig. 28. Results of Duncan tests of mean length changes for treatment comparison A. (Refer to discussion, pages 97 & 98.)

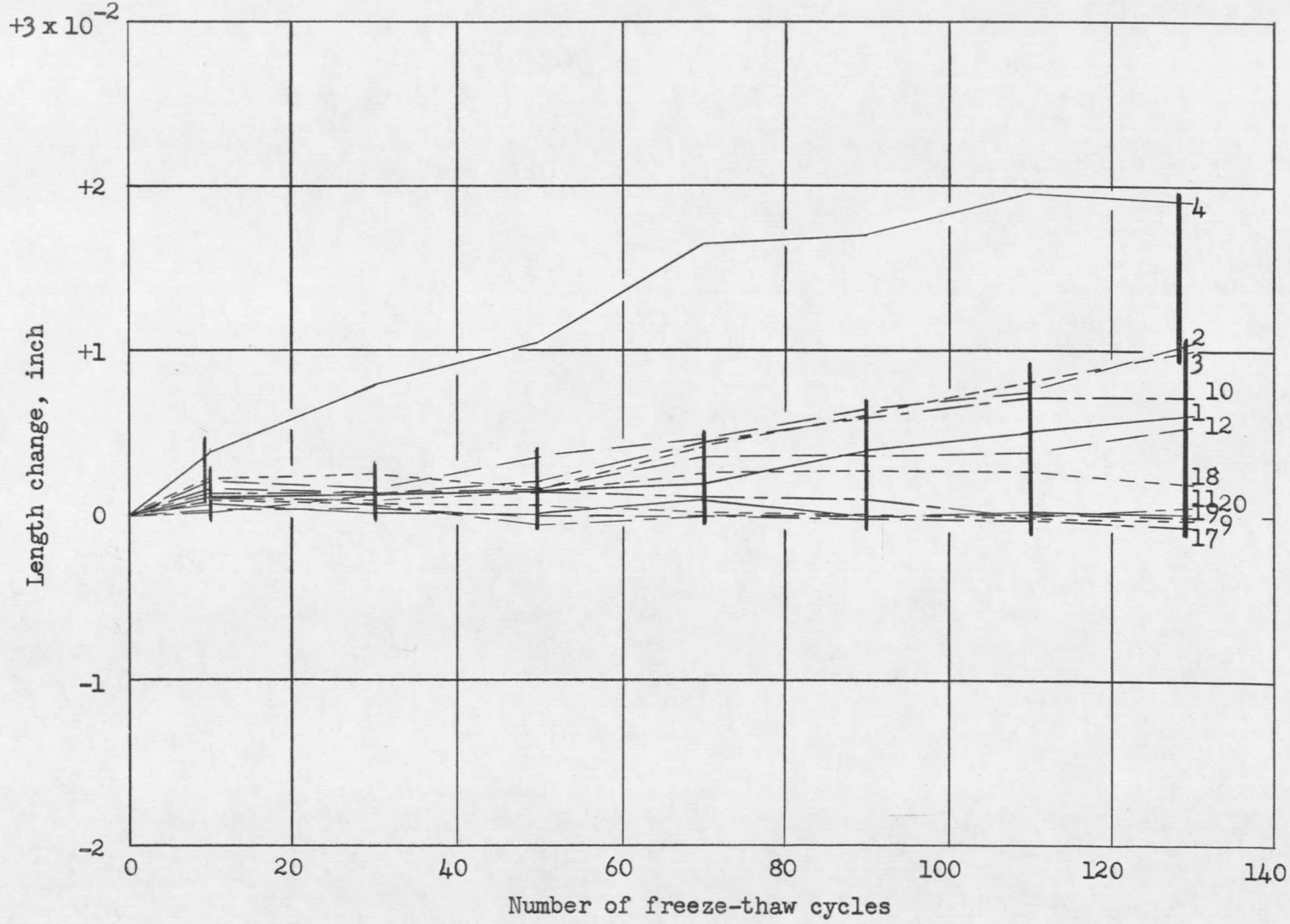
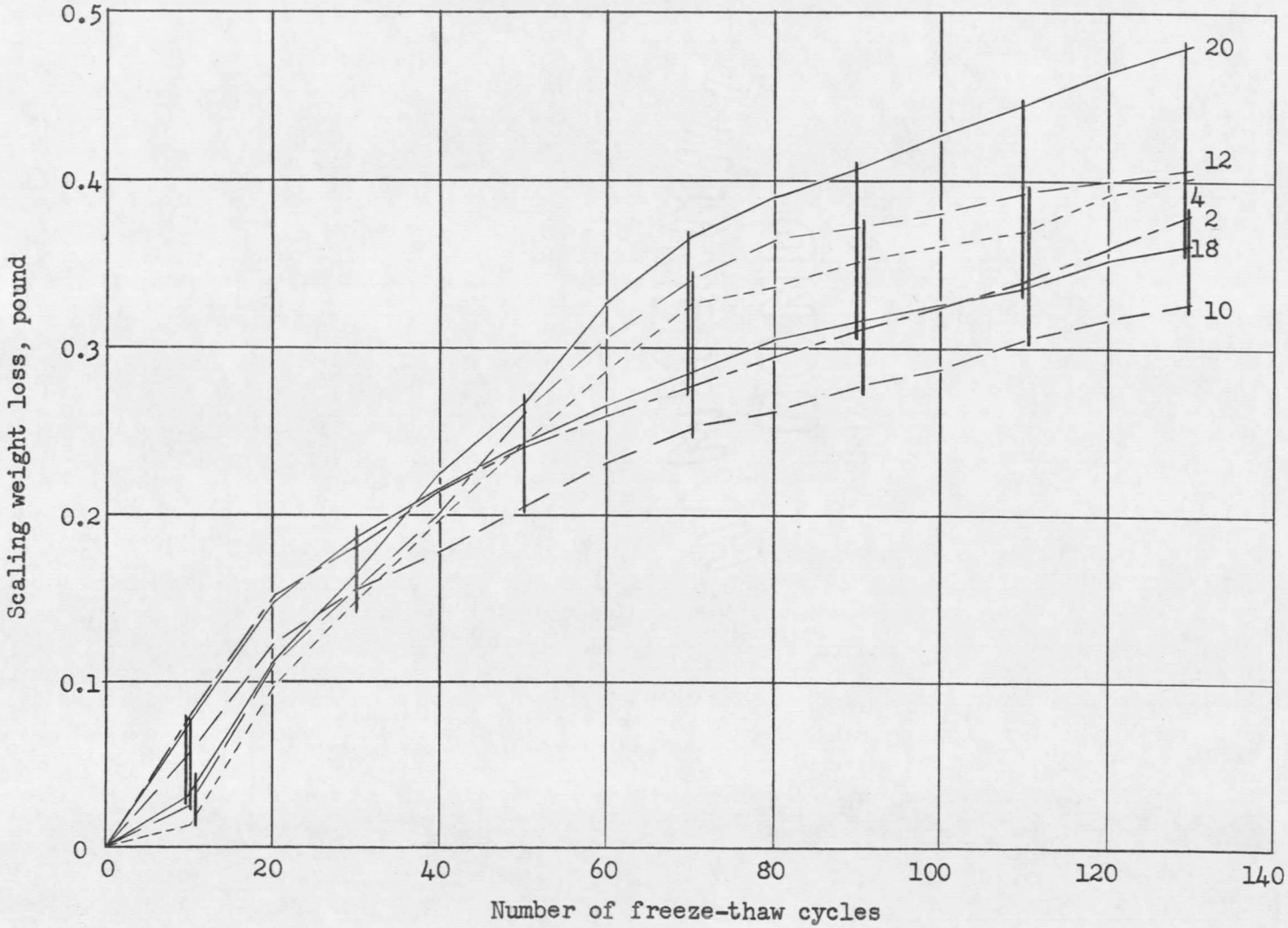


TABLE XIV

RESULTS OF BARTLETT TESTS OF SCALING WEIGHT LOSSES

No. of F/T cycles	Comparison		
	C	E	G
10	n.s.	n.s.	n.s.
30	n.s.	n.s.	n.s.
50	n.s.	n.s.	n.s.
70	n.s.	n.s.	n.s.
90	n.s.	n.s.	n.s.
110	n.s.	n.s.	n.s.
130	n.s.	n.s.	n.s.

Fig. 29. Results of Duncan tests of mean scaling weight losses for treatment comparison C. (Refer to discussion, pages 97 & 98.)



Permeability study

It will be recalled that the data obtained in this study were the periodic water quantities, in ml., added to maintain two-foot heads of water or $CaCl_2$ solution upon the slab surfaces. Also recorded were the evaporation losses, in ml., from similar standpipes located near the permeability slabs. These data were processed in a manner similar to that for the durability and scaling study. The computer was instructed to calculate the cumulative moisture additions, correct them for evaporation losses, and punch on data cards the net cumulative absorptions. These net absorptions are presented in Figures 87 - 98, in Appendix F, for the individual slabs.

The variation in total absorptions among replicates, as evidenced in the figures of Appendix F, made it apparent that absorption rates after a chosen number of days would be the most appropriate index for comparing the effects of the last twelve treatments of Table VI, on page 79. However, to assure that no effects would be overlooked by ignoring the total absorption values, Bartlett's and Duncan's tests were applied to the data of Appendix F at intervals of 40 days. (It will be noted that only three replicates were studied for treatments 5, 6, 7, 14, and 22. This was due to the fact that the standpipes of slabs 23C5 and 23C7 developed leaks shortly after their tests were begun, while slabs 24C6, 24C14, and 24C22 were reserved for another study not reported in this thesis.)

The results of the Bartlett tests are reported in Table XV to enable the reader to determine which of the subsequent Duncan tests are strictly valid. In Table XV, the primed identification letters for the treatment

comparisons correspond to the unprimed letters of Table X. This should not confuse the reader, since the twelve treatments of this study are identical with those of the durability and scaling study except for the environments to which the slabs were subjected after completion of the 28-day curing periods. By priming the comparison identification letters and adding 4 to each of the treatment numbers of Table X, the comparisons to be made in this study are fully described.

Figures 30 - 38 show the results of the Duncan tests performed in this study. (The linear portions of these graphs and those of Appendix F, after 40 days, are plots of the equations determined by linear regression analyses (31) of the data obtained after 40 days.)

Because of the apparent linearity of the absorption rates after approximately 40 days, it was decided that a test for the homogeneity of within-treatment regression coefficients (31) would be most appropriate for analyzing the effects of the various treatments upon the absorption characteristics of the slabs. However, before applying such a test it was necessary to determine if the within-replicates regression coefficients were homogeneous. Unfortunately, the replicate regression coefficients were declared non-homogeneous for every treatment except treatments 13 and 15. The differences between replicate regression coefficients for the other ten treatments were declared so highly significant that it was decided to make no treatment comparisons based upon absorption rates. (It was observed, however, that the average absorption rate for slabs subjected to treatment 15 was over twice that for slabs subjected to treatment 13. These treatments were identical except that slabs subjected to treat-

ment 15 were steam cured, whereas slabs subjected to treatment 13 were cured in the moist-room. This observation will be discussed further in Chapter V.)

Because they were meaningless in this study, the regression coefficients will not be tabulated. Their values may readily be obtained, however, from Figures 30 - 38 and Figures 87 - 98.

TABLE XV

RESULTS OF BARTLETT TESTS
OF NET ABSORPTIONS

No. of days	Comparison								
	A'	B'	C'	D'	E'	F'	G'	H'	I'
40	**	n.s.	*	*	n.s.	n.s.	n.s.	*	n.s.
80	*	n.s.	*	*	*	n.s.	n.s.	**	n.s.
120	*	n.s.	n.s.	*	*	n.s.	n.s.	**	n.s.
160	*	n.s.	n.s.	*	*	n.s.	n.s.	**	n.s.
200	*	*	n.s.	*	*	n.s.	n.s.	**	n.s.

Fig. 30. Results of Duncan tests of mean net absorptions for treatment comparison A'. (Refer to discussions, pages 97, 98, 115, & 116.)

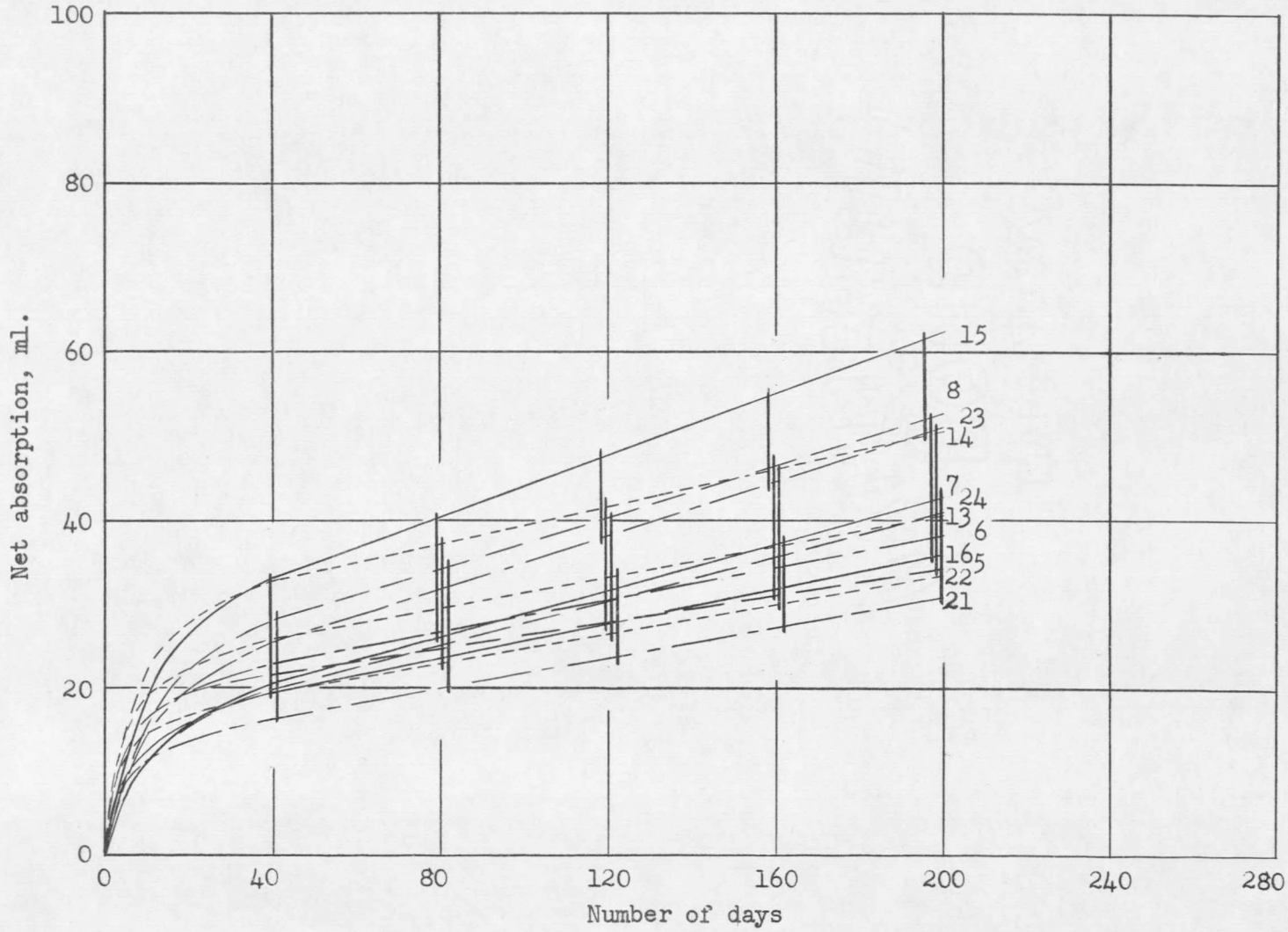


Fig. 31. Results of Duncan tests of mean net absorptions for treatment comparison B'. (Refer to discussions, pages 97, 98, 115, & 116.)

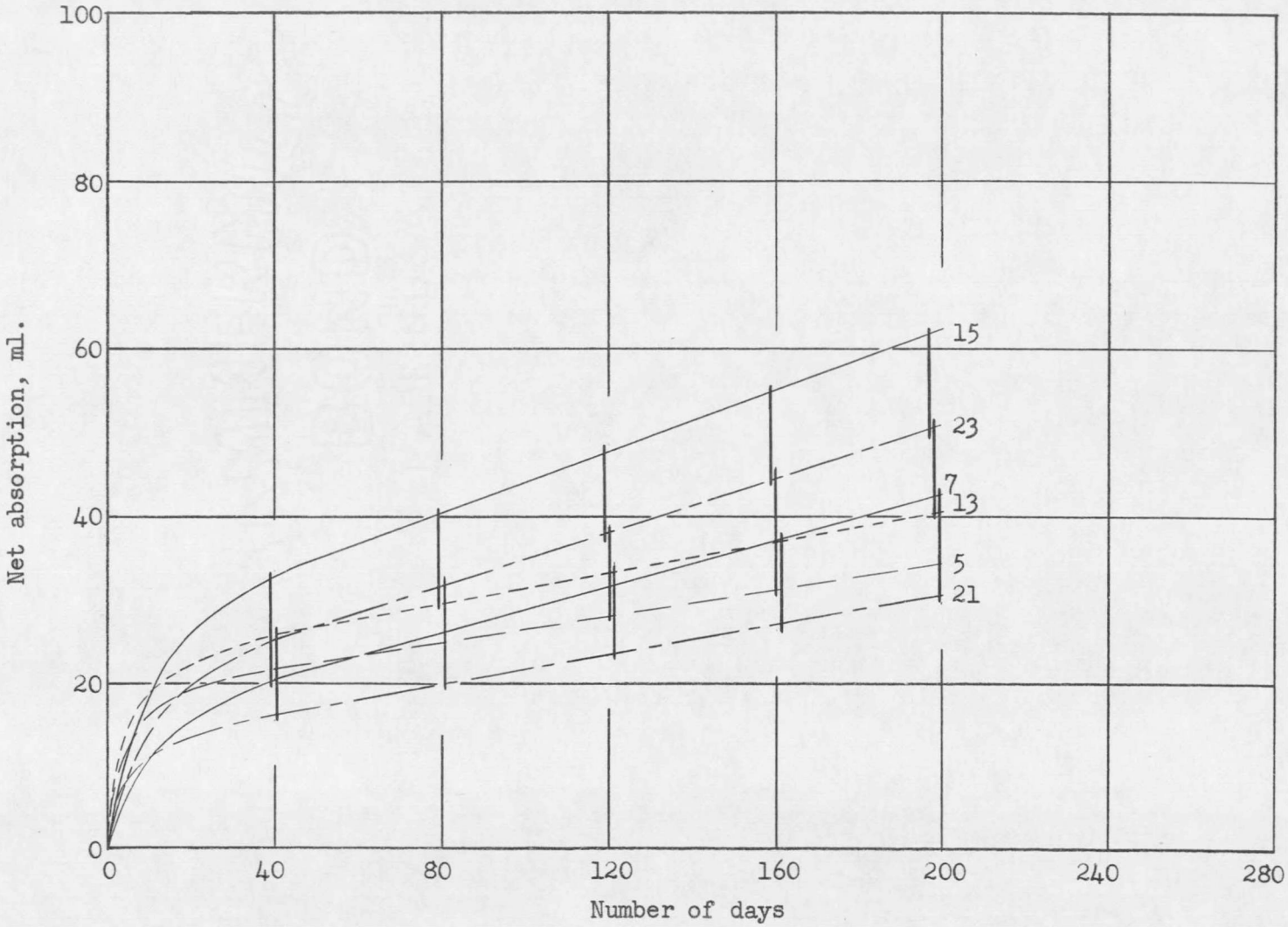


Fig. 32. Results of Duncan tests of mean net absorptions for treatment comparison C'. (Refer to discussions, pages 97, 98, 115, & 116.)

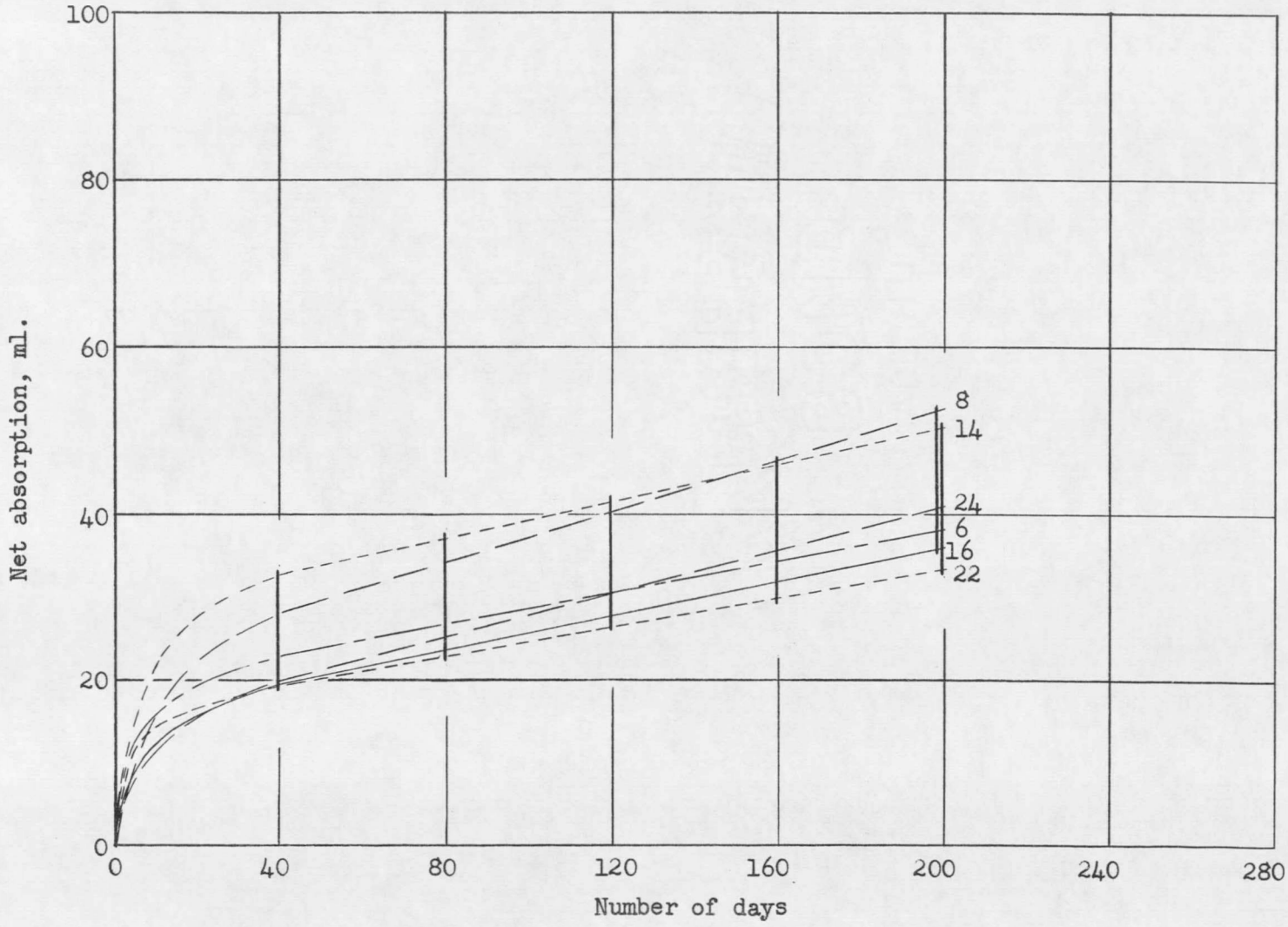


Fig. 33. Results of Duncan tests of mean net absorptions for treatment comparison D'. (Refer to discussions, pages 97, 98, 115, & 116.)

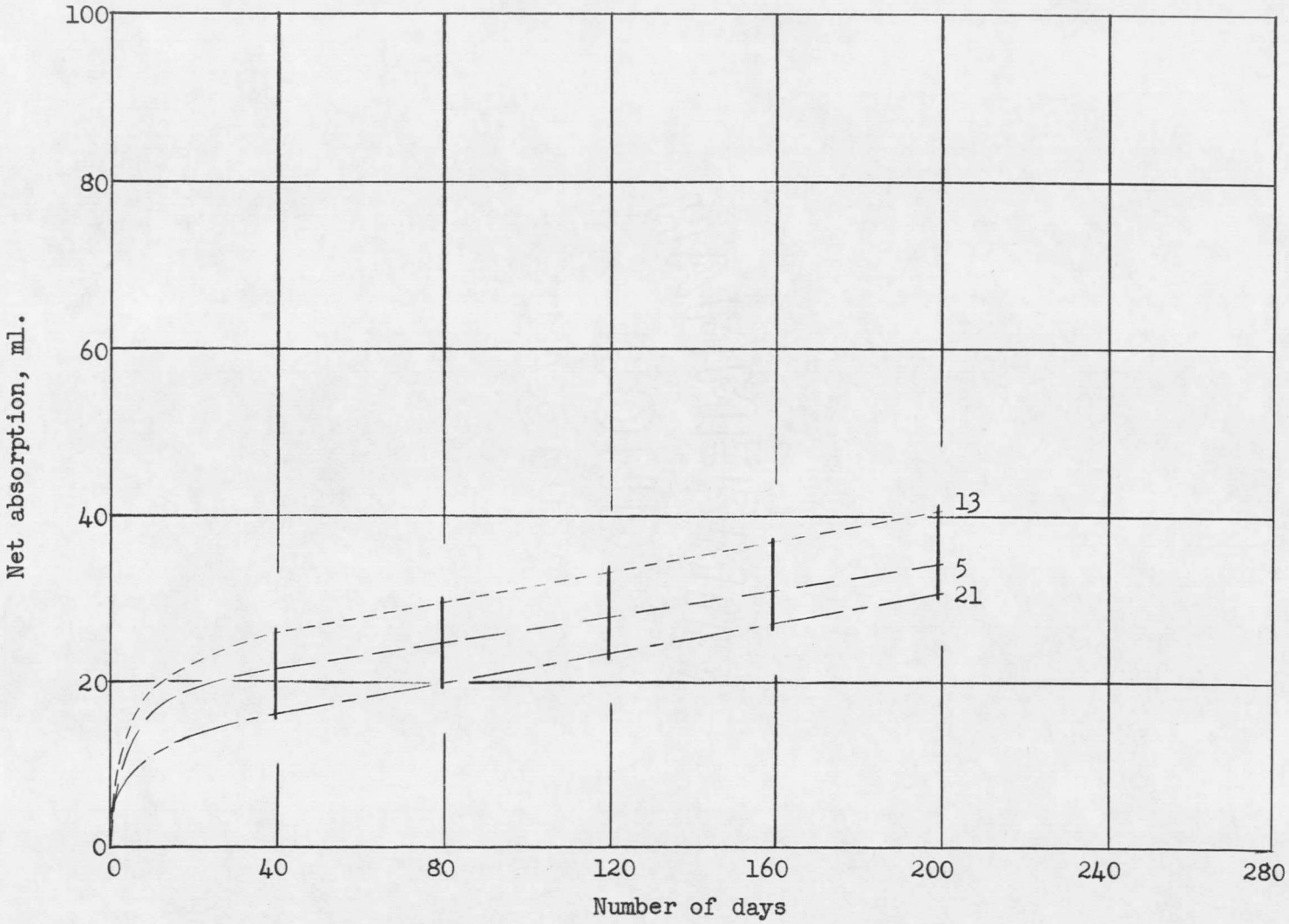


Fig. 34. Results of Duncan tests of mean net absorptions for treatment comparison E'. (Refer to discussions, pages 97, 98, 115, & 116.)

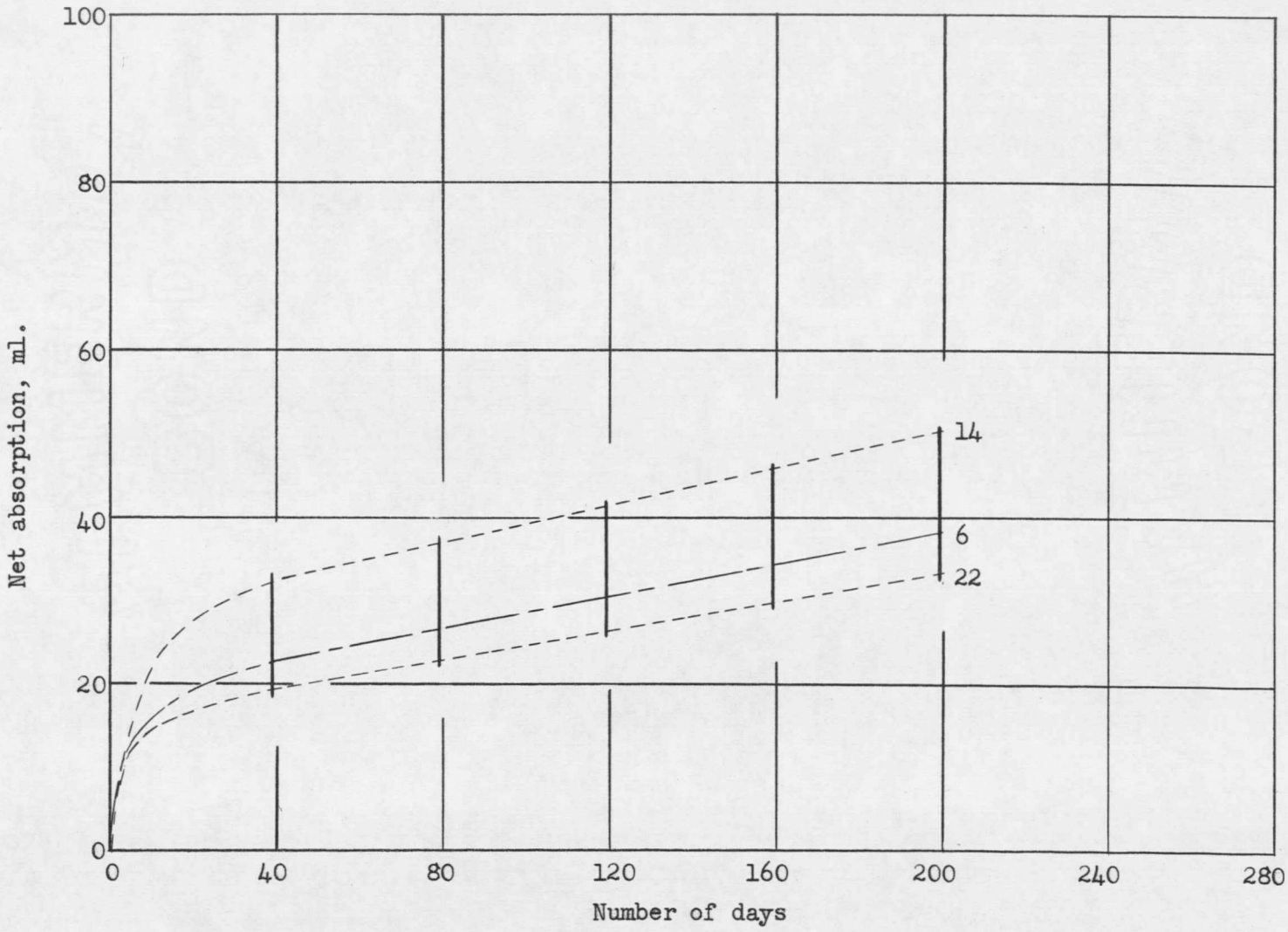


Fig. 35. Results of Duncan tests of mean net absorptions for treatment comparison F'. (Refer to discussions, pages 97, 98, 115, & 116.)

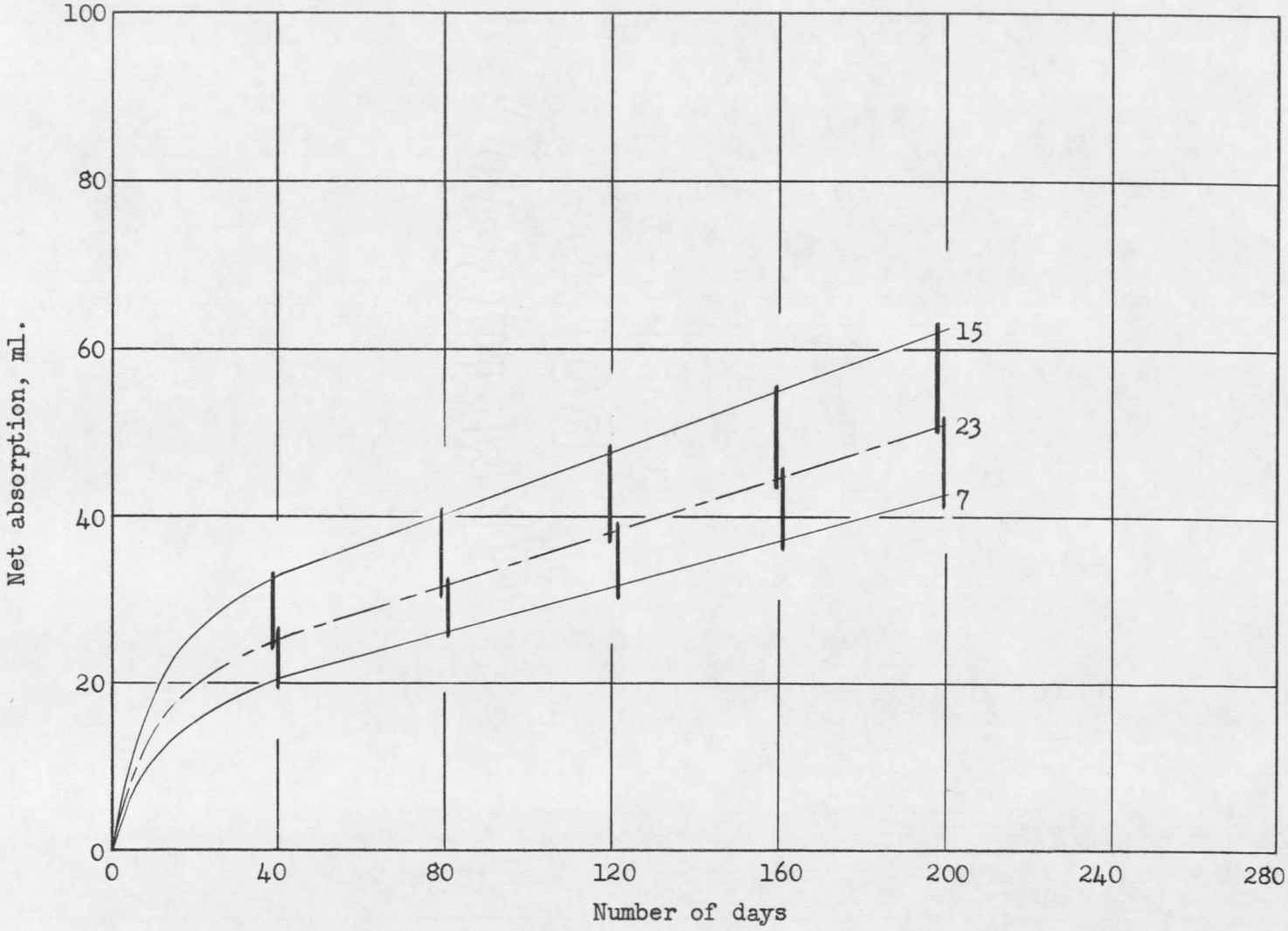


Fig. 36. Results of Duncan tests of mean net absorptions for treatment comparison G'. (Refer to discussions, pages 97, 98, 115, & 116.)

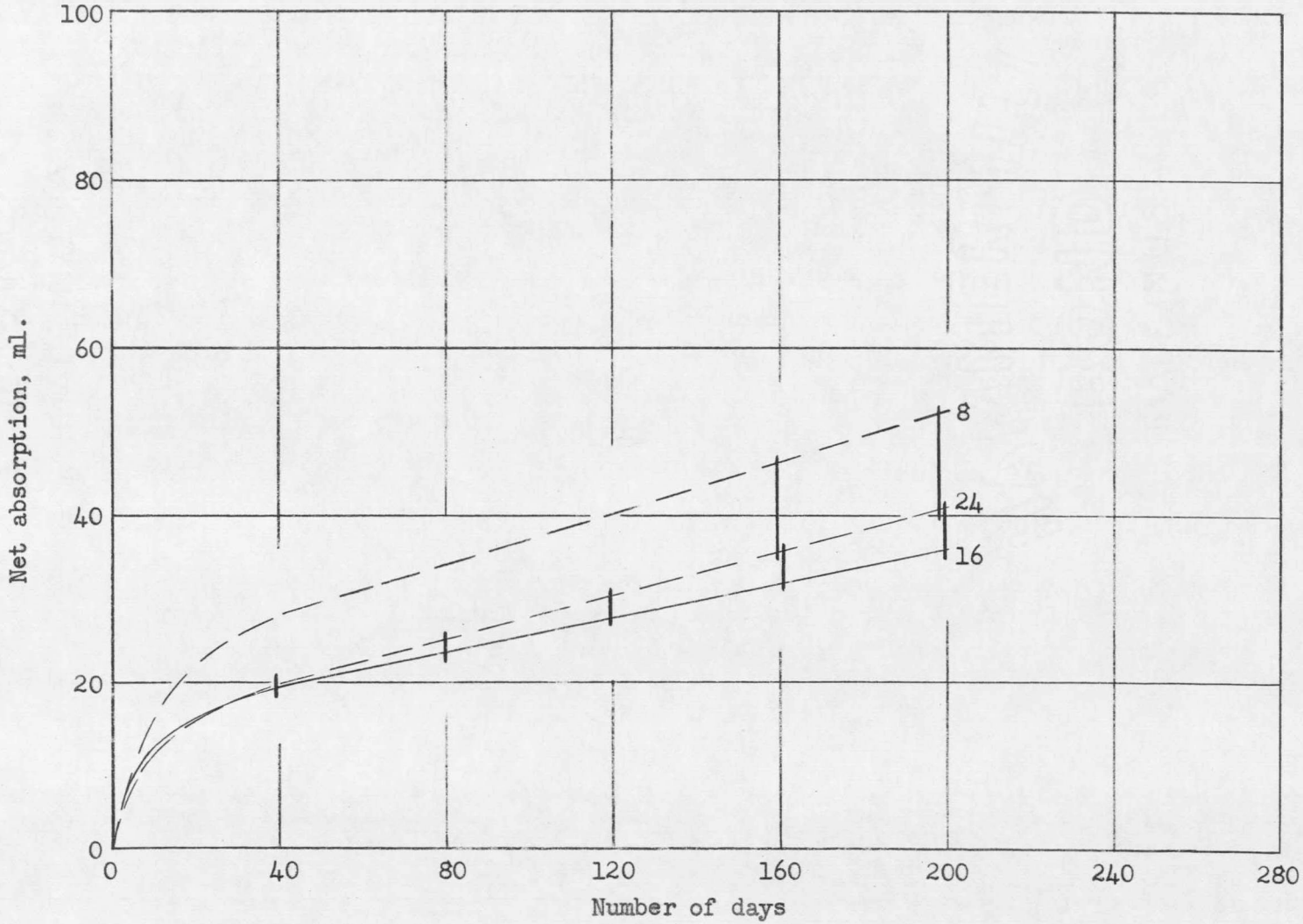


Fig. 37. Results of Duncan tests of mean net absorptions for treatment comparison H'. (Refer to discussions, pages 97, 98, 115, & 116.)

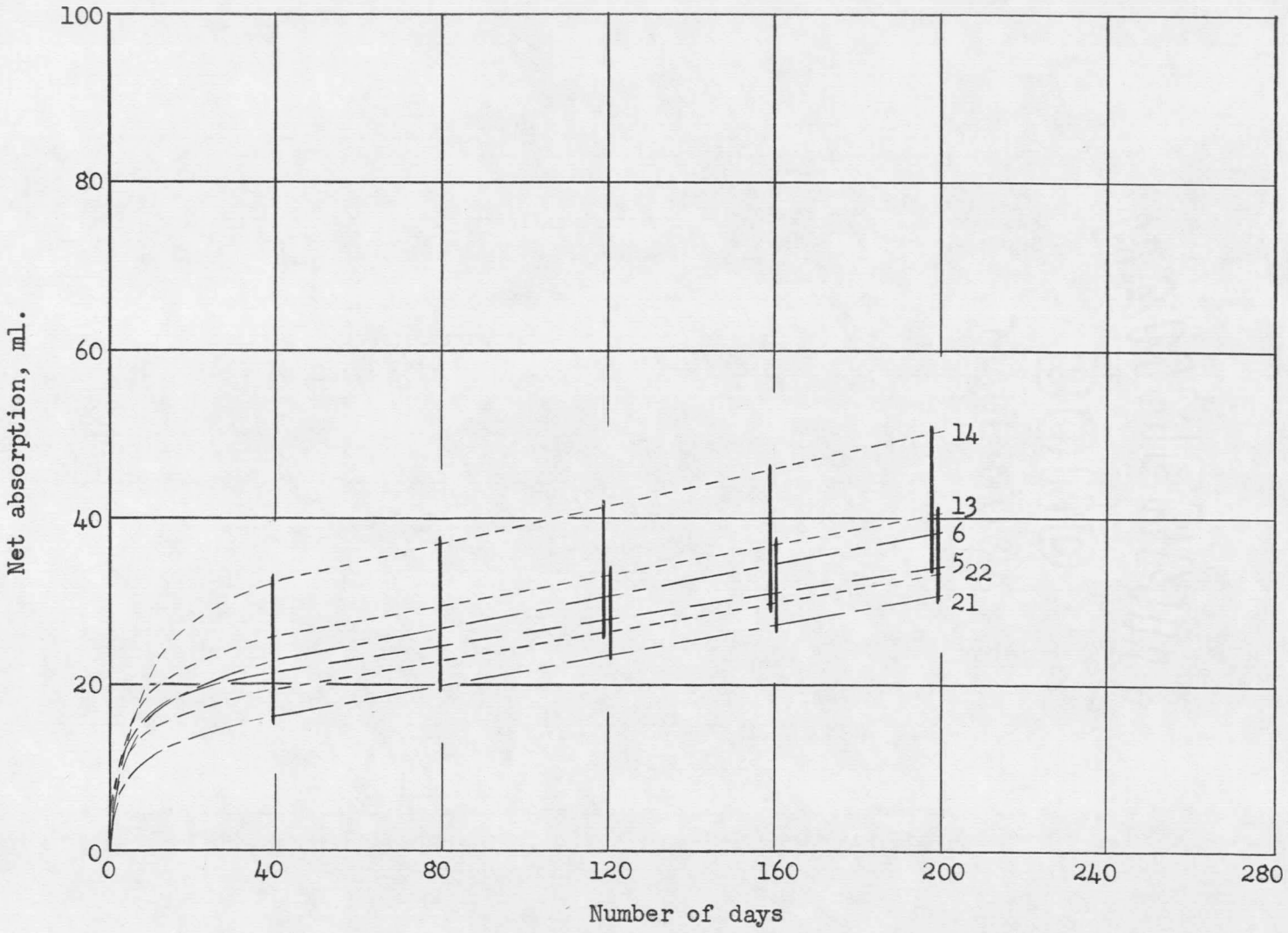
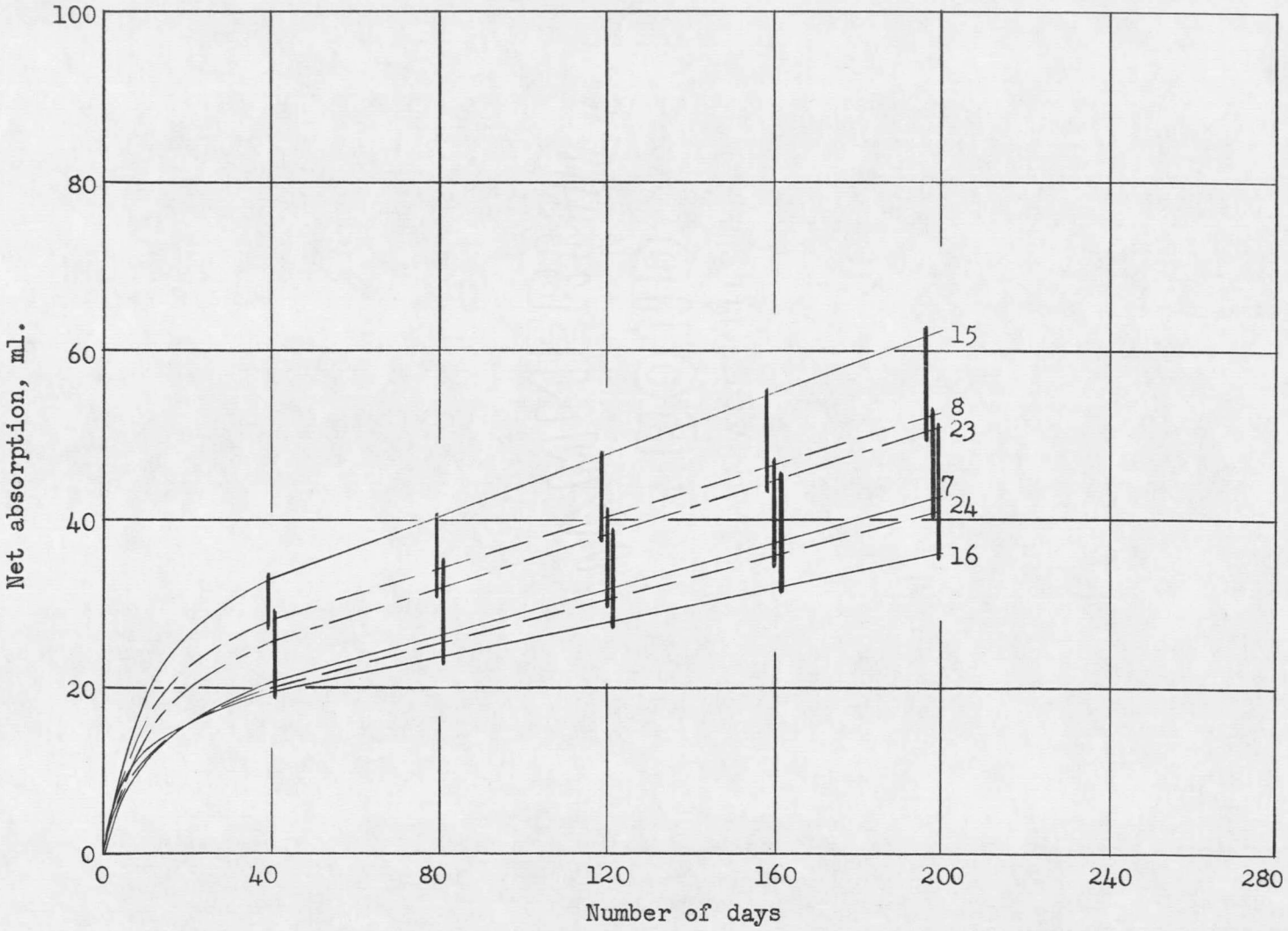


Fig. 38. Results of Duncan tests of mean net absorptions for treatment comparison I'. (Refer to discussions, pages 97, 98, 115, & 116.)



CHAPTER V

CONCLUSIONS AND SUMMARY

Conclusions

To spare the reader excessive detail, only the most general conclusions will be presented. Where particularly important points are discussed, reference to the graphs of Chapter IV will be made.

Effect of prestress upon durability

Considering the high degree of variability among replicates, no definite conclusions regarding the effect of prestress upon durability can be made based upon the statistical tests performed. A consideration of the regions of Figures 20 and 25 where the Duncan tests are valid emphasizes this point.

The best treatment comparisons on which to base a conclusion regarding the effect of prestress, and level of prestress, upon durability would be D, E, F, and G (of the mean relative dynamic moduli). Figures 21 - 24 show that durability is somewhat stress-dependent, though only from Figure 21 can such an inference validly be made from the statistical tests.

If mean adjusted weight changes are used as a basis, as in Figure 27, the stress dependency of durability is even more obscure. Nor can a valid statistically supported conclusion be drawn from Figure 28, where length changes are considered.

A qualitative interpretation of the results presented in Figures 18 through 26 leads to the conclusion that prestressed slabs are more durable than non-stressed slabs. The effect of level of prestress, however, does

not appear to be so clearly defined; although in Figures 21 - 24, where curing and solution effects are isolated, it appears that 1200 psi. slabs may be slightly more durable than 500 psi. slabs. This is contradicted in Figure 22, however.

The author feels that a continuation of these tests will tend to show a dependency of durability upon level of prestress. It is doubtful, however, that this effect will be proven of practical significance.

Effects of steam and normal curing upon durability

It is unfortunate that treatment comparisons, with stress effects isolated, were not made, as no valid statistical inferences can be drawn regarding the effects of steam curing compared with normal curing upon the durability of concrete. However, after 100 freeze-thaw cycles, Figure 18 shows that normally cured slabs tend to be more durable than steam cured slabs. This conclusion is based upon a comparison of the mean relative dynamic moduli for slabs whose treatments were otherwise identical--for example, treatments 1 and 3, 2 and 4, etc. Only for the comparison of treatments 9 and 11 is this conclusion contradicted.

It is also interesting to note the stress dependency of the differences between the mean relative dynamic moduli of steam cured and normally cured slabs. Had less conservative data values been assigned for slabs 22A4 and 24A4 after 70 cycles, or had it not been necessary to discontinue these slabs from the testing program, this stress-dependency would undoubtedly have been even more apparent in the case of treatments 2, 4, 10, 12, 18, and 20 (all ponded with $CaCl_2$ solution).

Length and adjusted weight change considerations are inconclusive regarding the effect of type of cure upon concrete durability.

Effects of water and salt solution upon durability

Perhaps the most striking contrast noted throughout this study was the difference between observable surface damage of slabs ponded with $CaCl_2$ solution and that of slabs ponded with water. So great was the damage to slabs of treatments 2, 4, 10, 12, 18, and 20 (all ponded with $CaCl_2$ solution) that the mortar dikes had to be replaced periodically, as will be recalled from Chapter IV; and in the case of slabs 22A4 and 24A4 the damage was irreparable after 70 freeze-thaw cycles. Nevertheless, a consideration of the mean relative dynamic moduli reveals a relatively moderate difference between the durability losses of slabs ponded with salt solution and those of slabs ponded with water.

From the statistical tests reported in Figures 18, 25, and 26, none of the differences between the mean relative dynamic moduli of slabs subjected to otherwise similar treatments can be declared significant. However, except for a comparison of treatments 9 and 10, it can be seen in Figure 18 that $CaCl_2$ solution is slightly more detrimental to concrete durability, in a freeze-thaw environment, than is water.

Figure 27 emphasizes the difference in severity between ponded water and ponded $CaCl_2$ solution. These large differences in weight changes were the primary reason for using Equation (1), page 85, for determining the relative dynamic moduli. If the assumption that weights remained constant had been used, as permitted by A.S.T.M., the differences noted in

Figures 18, 25, and 26 would have been even less pronounced. This is apparent since the increasing weights (W_c) of slabs subjected to treatments 1, 3, 9, 11, 17, and 19 (all ponded with water) tend to increase their relative dynamic moduli. The decreasing weights (W_c) of slabs subjected to treatments 2, 4, 10, 12, 18, and 20, after 10 freeze-thaw cycles and particularly after approximately 70 cycles, tend to decrease their relative dynamic moduli.

Therefore it is concluded that slabs ponded with water may be slightly more durable than slabs ponded with $CaCl_2$ solution (with chloride ion concentration of approximately 20,000 ppm.), in a freeze-thaw environment. Further, it is concluded that the assumption of constant weight for calculating the relative dynamic moduli, in a comparative study such as this, is highly questionable and probably incorrect.

Effect of prestress upon scaling resistance

This effect, if existent, was not detected in this study.

Effects of steam and normal curing upon scaling resistance

A definite trend, though not statistically detectable, is noted in Figure 29. Steam curing appeared to improve the initial scaling resistance of the concrete slabs. However, this improvement was effective only during the first 10 - 20 cycles, after which the scaling resistance of steam cured concrete appeared to be lower than that of normally cured concrete.

Effects of water and salt solution upon scaling resistance

The scaling weight losses of slabs ponded with water were immeasurably small. After 130 freeze-thaw cycles the most severe surface scaling observed on any of these slabs was equivalent to that observed on the slabs of treatments 2, 4, 10, 12, 18, and 20 at approximately 5 freeze-thaw cycles. Indeed, some of the slabs ponded with water have suffered no surface damage.

Of course, it is concluded that the resistance of concrete to scaling is vastly reduced when in contact with $CaCl_2$ solution, while its resistance remains relatively high when ponded with water.

Effect of prestress upon permeability

Consideration of the Duncan test results presented in Figures 30 - 38, and particularly those of Figures 32 - 35, leads to the conclusion that prestressing has no effect on the permeability of concrete, as defined in this study, which can be detected by the method of investigation used. And, as will be recalled from Chapter IV, the tests for homogeneity of regression coefficients were inconclusive.

Effects of steam and normal curing upon permeability

Except for the comparison of treatments 14 and 16, Figures 31 and 32 show a tendency for steam cured slabs to be more permeable than normally cured slabs, although the differences are statistically significant only for comparisons of treatments 13 and 15, and 21 and 23.

It will be recalled, from the discussion in Chapter IV, that the replicate regression coefficients were found to be homogeneous for treat-

ments 13 and 15 only. Also, the mean regression coefficient for treatment 15 was nearly twice that for treatment 13. Therefore, despite the crudeness of this testing method, it can be reasonably concluded that steam cured slabs are more permeable than normally cured slabs.

Effects of water and salt solutions upon permeability

A study of Figures 37 and 38 show only one treatment comparison upon which a valid statistical inference can be made, that being the comparison of treatments 15 and 16. Here the conclusion is that steam cured concrete absorbs water more rapidly than it absorbs $CaCl_2$ solution. However, this cannot be accepted as a general conclusion since in only one of the remaining five possible treatment comparisons, 23 with 24, is this tendency apparent.

The mean net absorptions of slabs subjected to treatments 5, 7, 13, and 21 were less than those of slabs subjected to treatments 6, 8, 14, and 22, respectively. Although these differences were not statistically significant, it must be concluded that concrete absorbs water at a no greater rate than it absorbs $CaCl_2$ solution, at least not at a rate difference which can be detected by this testing method.

Of course, no conclusion can be drawn from the results of the tests for homogeneity of regression coefficients.

Effect of permeability upon durability

Although the conclusion that steam cured slabs are more permeable (i.e., absorb water and $CaCl_2$ solution at a greater rate) than normally cured slabs, is rather weakly based, it would appear that permeability

does affect durability. Since it was concluded that steam cured slabs are slightly less durable than normally cured slabs, this is a confirmation of the accepted fact that high permeability adversely affects the durability of concrete.

Durability versus scaling resistance

The conclusions that steam cured slabs are both less durable and less resistant to scaling than normally cured slabs lead to an inference that observable exterior deterioration is a fair index of the soundness of the entire concrete mass. However, this conjecture has no practical significance, since the visible surface damage after 130 freeze-thaw cycles appeared no worse than at 50 cycles.

Summary

This investigation was a study of the effects of prestress, steam curing and salt solution upon the durability and scaling resistance of concrete in a freeze-thaw environment, and upon the permeability, or absorptive capacity, of concrete under a constant static head in an ordinary laboratory environment. Small pretensioned slabs were fabricated, with stresses of zero, 500, and 1200 p.s.i. Equal numbers of these slabs were steam cured and moist-room cured. In turn, half of the slabs subjected to each curing environment were placed in a freeze-thaw environment, with mortar dikes attached to their screeded surfaces for retaining continuously ponded solutions. Half of these solutions were of $CaCl_2$ and water, with a chloride ion concentration of approximately 20,000 ppm., while the remaining slabs were ponded with tap water.

The remaining slabs subjected to each curing environment were placed on racks in the laboratory, with tall glass standpipes sealed to their surfaces. Half of these standpipes were filled to, and maintained at, a level of two feet above the slab surfaces with the same $CaCl_2$ solution as described above. The remaining standpipes were filled with tap water.

Tests were performed periodically on the freeze-thaw slabs to determine their natural transverse frequencies of vibration in flexure, weight and length changes, and scaling weight losses. The standpipes on the permeability slabs were refilled periodically to the two-foot level, and the incremental fluid quantities added were recorded. These fluid additions were corrected for evaporation losses.

Equipment and procedures

Most of the equipment and procedures used for fabrication and testing of the slabs were standard, and will not be described further. Others were somewhat unique and deserving of review.

The vibration table was manufactured by undergraduate students of Mechanical Engineering, in the Mechanical Engineering Department machine shop at Montana State College. The vibrating table was mounted on several very stiff springs attached around its perimeter and to a steel frame. An eccentrically weighted wheel was mounted in bearings attached to the underside of the table, and was belt-driven by a motor resting on the frame. The compaction obtained was quite good in any small region of the table surface, but did not appear to be uniform over the entire surface. The casting beds extended over the entire length of the table, as can be seen

in Figure 9, and it appeared that those portions of the slabs near the center received a somewhat better compactive effort than did the regions near the ends of the table. Therefore, precautions were taken to assure that slabs assigned to replicate treatments were vibrated at alternate ends of the table in an attempt to randomize this possible source of variation.

This non-uniformity may have been due to variations among the stiffnesses of the springs around the table perimeter and/or insufficient flexural rigidity of the table. The table was a 7/16"-thick steel plate stiffened longitudinally by two $2\frac{1}{4}$" x $1\frac{1}{2}$" x $\frac{1}{4}$" steel angles welded to its underside; and the "forcing" wheel was mounted directly in its center. It is also possible that the casting beds were not sufficiently rigid, so that clamping them to the table only at their centers was inadequate.

It would be advisable for individuals wishing to use this type of system to pay particular attention to this non-uniformity. Perhaps the most important factor is to assure sufficient flexural stiffness of the table. Also, the use of two or more eccentrically weighted forcing wheels, evenly distributed along the length of the table and driven by a common shaft, might result in a significant improvement.

The steam chambers were very simply constructed and operated. Undoubtedly a single chamber would have been more desirable, but the convenience, low cost, and availability of the 55-gallon, open-end drums outweighed this consideration. Also, the relatively rapid rate of heat loss through the thin metal drum walls was desirable in that the resulting frequent heat demand provided for the maintenance of a constant, high

humidity. Of course, individual controls for each chamber would have been more reliable, but again cost and availability were prohibitive.

The procedure used for freezing and thawing the slabs was effective, but quite slow. The necessity for removing the slabs from the freezer for thawing, and then replacing them for freezing was very inconvenient, primarily because the thawed slabs had to be handled carefully to prevent spillage of the ponded solutions. Also, the constant handling presented the hazard of damage to the slabs and, more importantly, to the mortar dikes.

Mere opening of the freezer door and unplugging the freezer motor for thawing would have been a considerable improvement in this procedure. However, this was disallowed because of probable water damage to the wooden freezer walls. Of course, the major disadvantage of this procedure was the time required to achieve each cycle. Certainly, for any durability studies of long duration, an investment in a more rapid freeze-thaw cycling unit is advisable.

The permeability study might have been more conclusive had a controlled environment been available. The large temperature fluctuations encountered in the laboratory, both daily and seasonal, caused quite large fluid level fluctuations. In an attempt to counteract these fluctuations, liquid was added only at 10-day intervals and at approximately the same time of day. Of course, this time of day was changed with the seasonal changes in order to assure that the fluid temperatures were approximately the same at the time of every fluid addition. The "goodness of fit" of the regression lines, with the plotted data of Figures 87 - 98,

indicates fair control of this problem.

In the absence of these difficulties, however, it is doubtful that this method would have been very definitive. Therefore, it is not recommended to any researchers who might be interested in studying the permeability or absorption characteristics of concrete. The use of a silicone building sealant for obtaining a strong, water-tight bond between the glass standpipes and concrete surfaces may be of interest to researchers who wish to bond these or other seemingly incompatible materials. Also, the use of readily available household varnish was an effective method for sealing the other surfaces of these slabs.

Perhaps the most important development in this investigation was the method used for pretensioning the small slabs. There are many researchers who have reported successful methods for post-tensioning of small concrete specimens (22, 26, 33, 34). However, the problem of pretensioning short slabs, such that the interaction between the strand and concrete is similar to that in a pretensioned structure, is apparently unique. The reliability of the method described herein was reasonably established for this study, but further study of the state of stress in these slabs, particularly over long time durations after the strands are released from the casting beds, would be interesting and valuable.

No further discussion of the method will be presented here. Rather, the reader is referred to Chapter III for a complete description of the method, its advantages and disadvantages.

The author feels that the method chosen for evaluating the degree of scaling merits some discussion. Ordinarily in studies such as this, the

degree of scaling is described by a number arbitrarily assigned on the basis of the investigator's visual interpretation. Of course, the comparison of results from separate investigations is difficult since no two researchers can make identical qualitative interpretations, and usually the numerical scales of interpretations are quite variable from report to report. For example, Hussell's (30) scale rating of 5 would probably correspond to the scale rating of 10 assigned by Grieb, Werner, and Woolf (35). Likewise, the presentation of a photographic scaling description is usually unsatisfactory after the concrete surface has exposed aggregate over its entire surface, since the two-dimensional view affords little interpretation of scaling depth. Photographs are valuable, however, for describing the intial phases of surface deterioration.

Photographs were taken periodically in this study, but were not presented in this report because of the reasons given above.

Perhaps the most satisfactory method for describing scaling damage would be a measure of scaling depth. However, only the average of many depth measurements would be meaningful, since scaling depth is quite variable shortly after scaling is initiated.

The method chosen for this study was a careful collection of the loosened concrete surface material, followed by weighing of this material after it had been oven-dried to a constant weight. Since the mortar dikes were so highly air-entrained, they contributed nothing to the weight of material removed from the top surfaces. The Bartlett tests for homogeneity of variance performed on these data, results of which are given in Table XIV, are fair evidence of the reproducibility of this

procedure.

These scaling weight losses could be converted into an equivalent depth of scaling, but an accurate conversion might be difficult since the density of the surface laitance is undoubtedly different from that of the concrete at greater depths. Therefore, the author feels that the measurement of scaling weight losses is preferable to other methods used for making studies of this type.

Finally, the difficulties encountered as a result of choosing mortar dikes for retaining the ponded solutions on the freeze-thaw slabs are too numerous for much further detailed discussion. Other materials and methods were considered, such as epoxy resins, metal or wooden walls either bonded or embedded, and depression of the slab surface after screeding. All were rejected, perhaps too hastily, on the basis of cost, feasibility, or other imagined difficulties.

The leakages which developed occurred as a result of erosion of the slab surface mortar from beneath the mortar dikes, and not as a result of any deterioration or cracking of the dikes per se. Therefore, it seemed probable that any type of dike, regardless of bonding material used, would require replacement. However, in a recently reported study (36), aluminum weirs fastened around the perimeters of small concrete specimens with room-temperature vulcanizing silicone rubber were apparently satisfactory for retaining 2 per cent NaCl solution in a freeze-thaw environment.

Therefore, methods other than the application of mortar dikes should certainly be investigated before attempting this type of study.

Conclusions

The results of this investigation are reasonably well summarized in the graphs of Figures 18 - 38, and will not be discussed further. The conclusions reached from both statistical and qualitative interpretations of these results may be summarized as follows:

Factors affecting durability and scaling resistance

These conclusions are based upon results obtained during 130 freeze-thaw cycles of the small concrete slabs.

1. Prestressed concrete is more durable than non-stressed concrete, in a freeze-thaw environment, although the durability improvement is statistically significant only for concrete which is normally cured and ponded with tap water.
2. Concretes prestressed to a level of 1200 psi. tend to be slightly more durable than concretes prestressed to 500 psi. However, the stress-dependency of durability is nearly negligible, and certainly statistically insignificant.
3. Steam cured concrete is less durable than moist-room cured concrete.
4. Concretes ponded with $CaCl_2$ solution, with a chloride ion concentration of 20,000 ppm., are slightly less durable than concretes ponded with tap water.
5. Scaling resistance of concrete is not stress-dependent.
6. Steam cured concrete seems to be initially more resistant to scaling than does moist-room cured concrete. However, after

10 to 20 freeze-thaw cycles, steam cured concrete tends to be less resistant to scaling than does moist-room cured concrete.

7. $CaCl_2$ solution, in the concentration used in this study, is extremely deleterious to exposed concrete in a freeze-thaw environment, while tap water causes almost negligible scaling.

Factors affecting permeability

These conclusions are based upon results obtained during a 200-day period. However, because of the unsatisfactory nature of the testing method used, these statements are made with reservations.

1. Permeability is not influenced by prestressing -- at least below the level of 1200 psi.
2. Steam cured concretes appear to be more permeable than moist-room cured concretes.
3. There is no tendency for concrete to absorb $CaCl_2$ solution at a rate different from that at which it absorbs water.

Additional conclusions

1. Highly permeable concretes tend to be less durable than otherwise similar, but less permeable, concretes.
2. Concretes which exhibit extreme surface damage may be less durable than otherwise similar concretes which appear less severely attacked.

Other observations and suggestions for future research

Many suggestions for improvements have already been made in the

section "Equipment and procedures." However, it is doubtful that repetition of most of the work in this investigation can be justified.

The poorly controlled permeability study was practically inconclusive, and a more sophisticated approach to this problem might be warranted. For this type of study, a "true" permeability test should probably be applied, in which a measurable flow pattern would be established through the specimen, and not merely into it. Such a specimen would ideally be circular in cross-section. The method for prestressing such a specimen might be difficult, although a peripheral stress applied with a circular ring might be practicable.

Even though the permeability study was considered crude, the author doubts that any improvement of concrete durability, resulting from prestress, can be attributed to a permeability reduction. It was observed that surface cracking patterns were quite random on non-stressed slabs, while these cracks were oriented in a direction decidedly parallel to the strand on prestressed slabs. Additionally, length measurements, though considered only slightly reliable, indicated a general tendency for slabs of lesser durability to exhibit greater length increases. For these reasons, the author is reasonably sure that the durability improvement realized from prestressing is primarily due to restraint against destructive expansion. Further, the author doubts that the durability benefits realized from higher levels of prestress would be significantly greater than those realized from prestress levels commonly used in present-day highway construction. This opinion is based upon the results of this and other investigations (22, 26, 34), and upon visual examination of the

500 and 1200 psi. slabs in this study. However, this opinion is given with reservation, and may be altered upon completion of this investigation.

An incidental study, not directly related to the problem of durability, might be made to investigate the time-dependent behavior of both the concrete and strand in pretensioned concrete. The benefits of such a definitive study to designers of pretensioned structures would certainly be significant. However, it would be advisable for researchers wishing to use the pretensioning method described in this study to perform additional tests for determining the accuracy and reproducibility of the method.

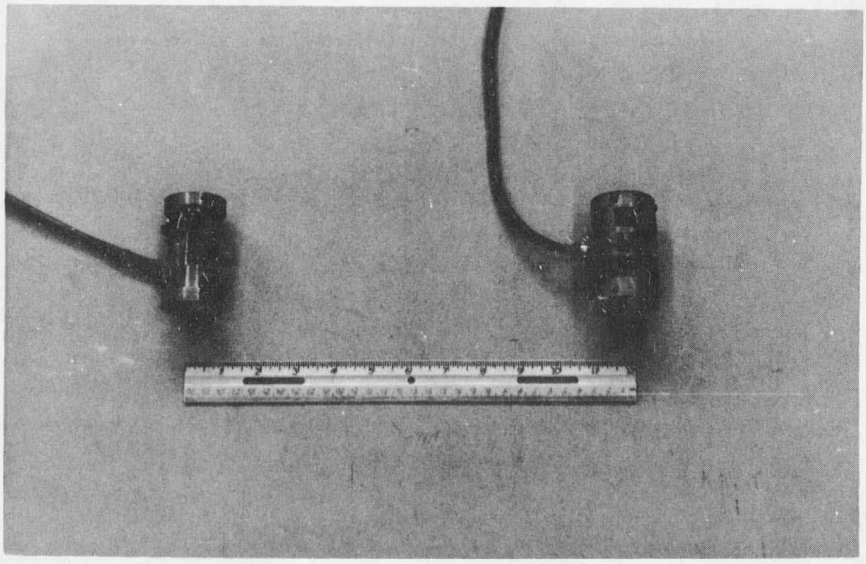
Finally, the harshness of surface attack observed on slabs ponded with $CaCl_2$ solution, in a freeze-thaw environment, raised doubts in the author's mind concerning the validity of the importance attached to the "physical destruction mechanism" concept of saline destruction of concrete. Accordingly, samples of some ponded salt solutions were subjected to a qualitative pH test* at frequent intervals, from zero to 10 days after fresh ponding. The pH values of the freshly ponded $CaCl_2$ solutions were 7, indicating neutrality. After 10 days, however, the pH value of these solutions was nearly 10, the maximum range of the indicator, denoting very high basicity. Therefore, the importance of chemical attack of salt solutions upon concrete, in a freeze-thaw environment, should not be disregarded, and is probably deserving of intensive study.

---

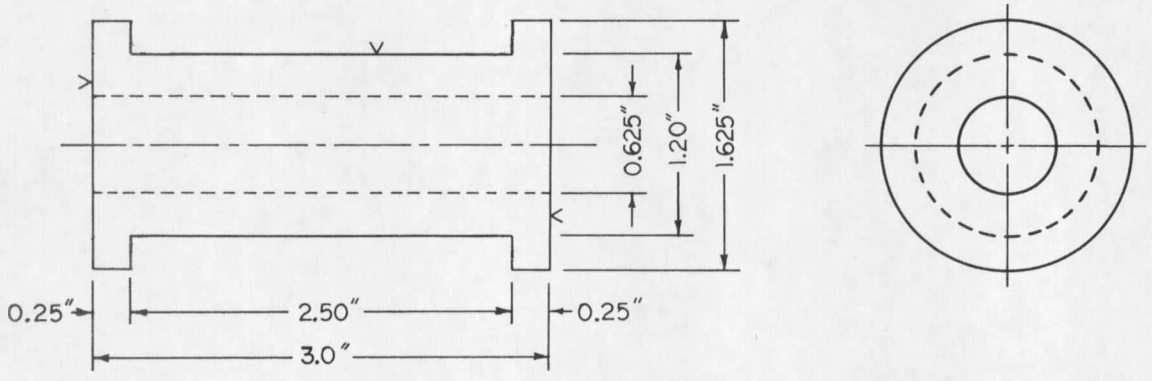
* Alkacid tester, range: pH 2 - 10, Fisher Scientific Corp.

APPENDIX A

DESCRIPTION OF LOAD CELLS



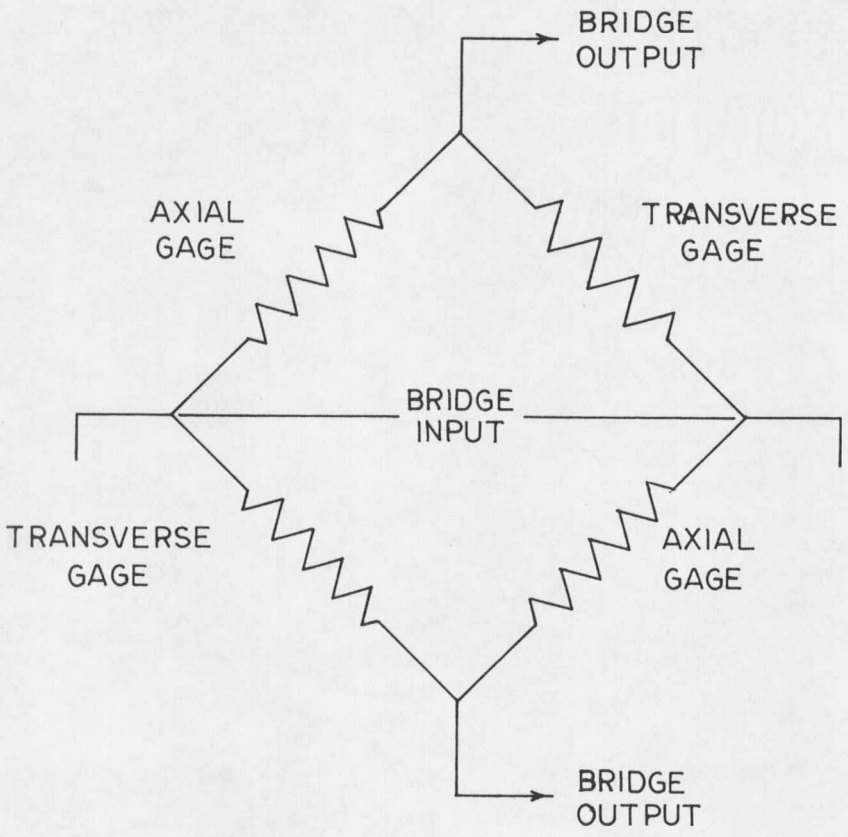
a. Load cells with and without protective shields, showing orientation of strain gages.



MAT'L.: 1020 C.R. STEEL

b. Load cell dimensions.

Fig. 39. Load cell description.



SR-4 STRAIN GAGES
TYPE: A-5
RES.: 119.2±.2 OHMS
GAGE FACTOR: 2.01±1%

Fig. 40. Bridge arrangement for load cells (32).

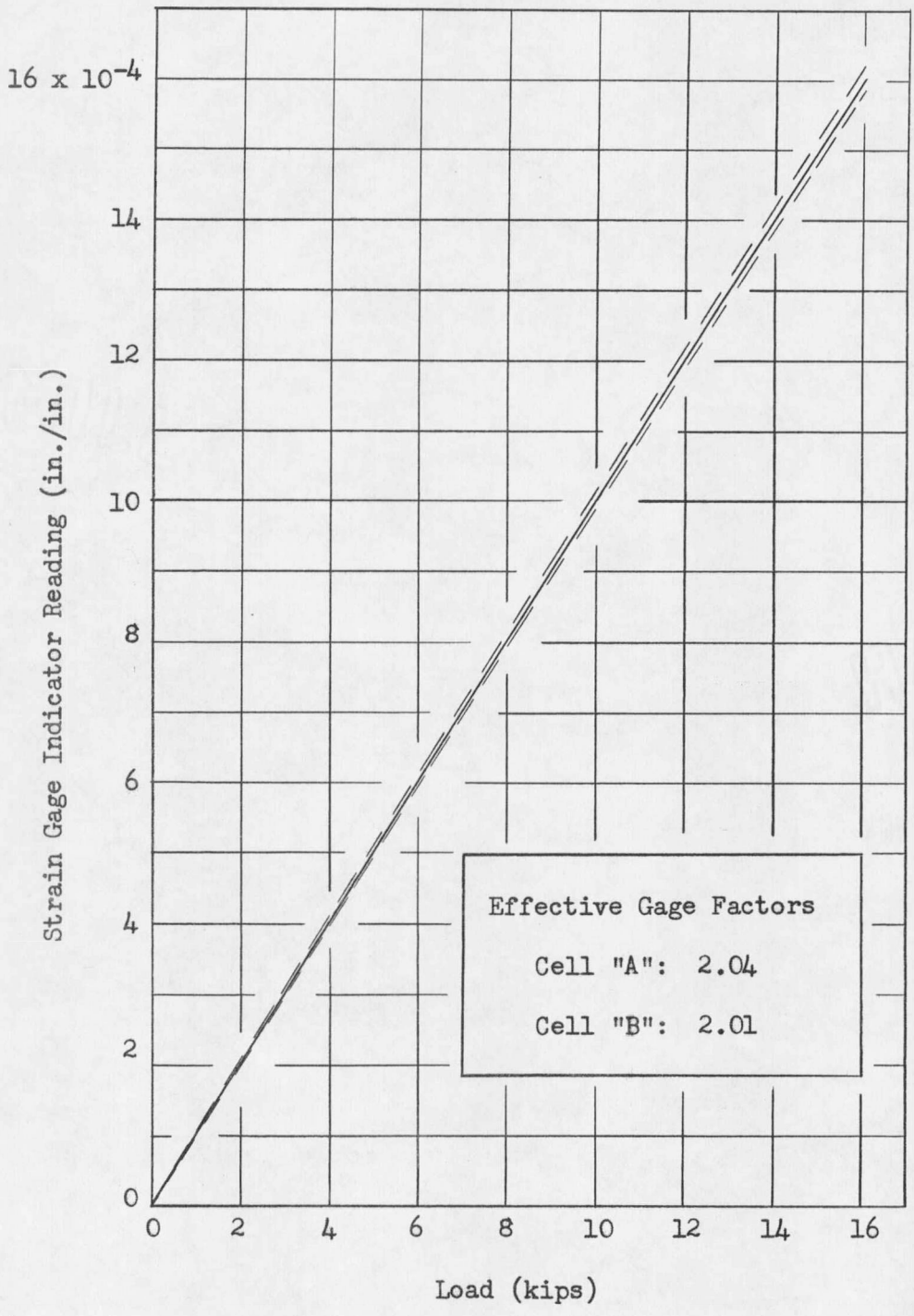


Fig. 41 Calibration curves for load cells, with error limits shown.

APPENDIX B

CEMENT ANALYSIS

TABLE XVI

CEMENT CHEMICAL ANALYSIS

Oxide	Per cent of total	Phase	Per cent of total
SiO_2	23.26	C_3S	46.3
Al_2O_3	3.97	C_2S	31.0
Fe_2O_3	4.33	C_3A	3.2
CaO	64.10	C_4AF	13.1
SO_3	1.75		
ignition loss	1.09		

Type of cement: Type II

Supplier: Ideal Cement Company
Trident, Montana

APPENDIX C

AGGREGATE PROPERTIES

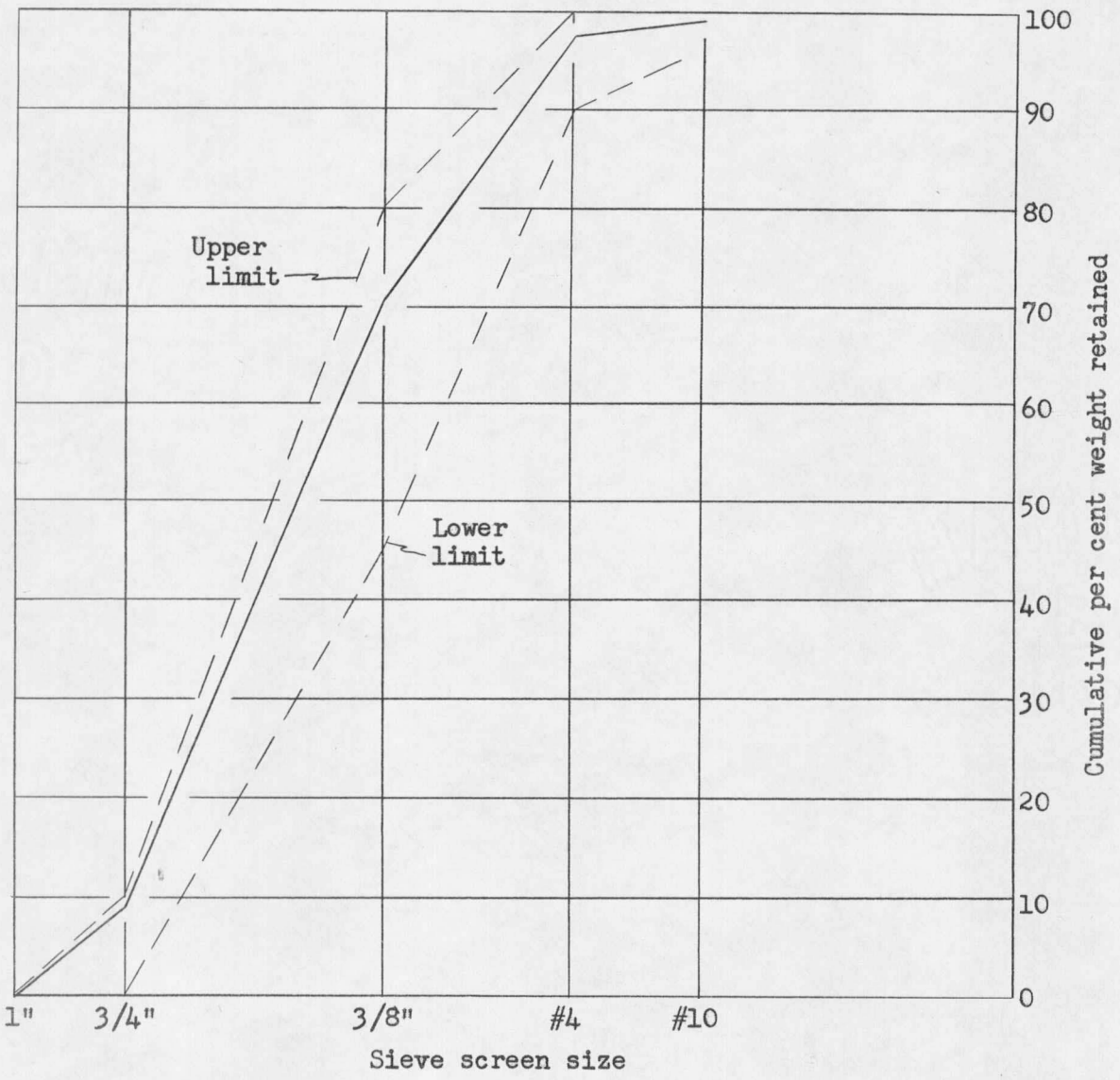


Fig. 42. Coarse aggregate gradation.

Coarse Aggregate Properties

Unit weight = 105.3 p.c.f.
Bulk specific gravity (A.S.T.M. Des. E12) = 2.60
Bulk specific gravity (saturated surface-dry) = 2.635
Apparent specific gravity (A.S.T.M. Des. E12) = 2.695
Moisture content (saturated surface-dry), by weight = 1.354%

Supplier: Pioneer Ready Mix Co.
Bozeman, Montana

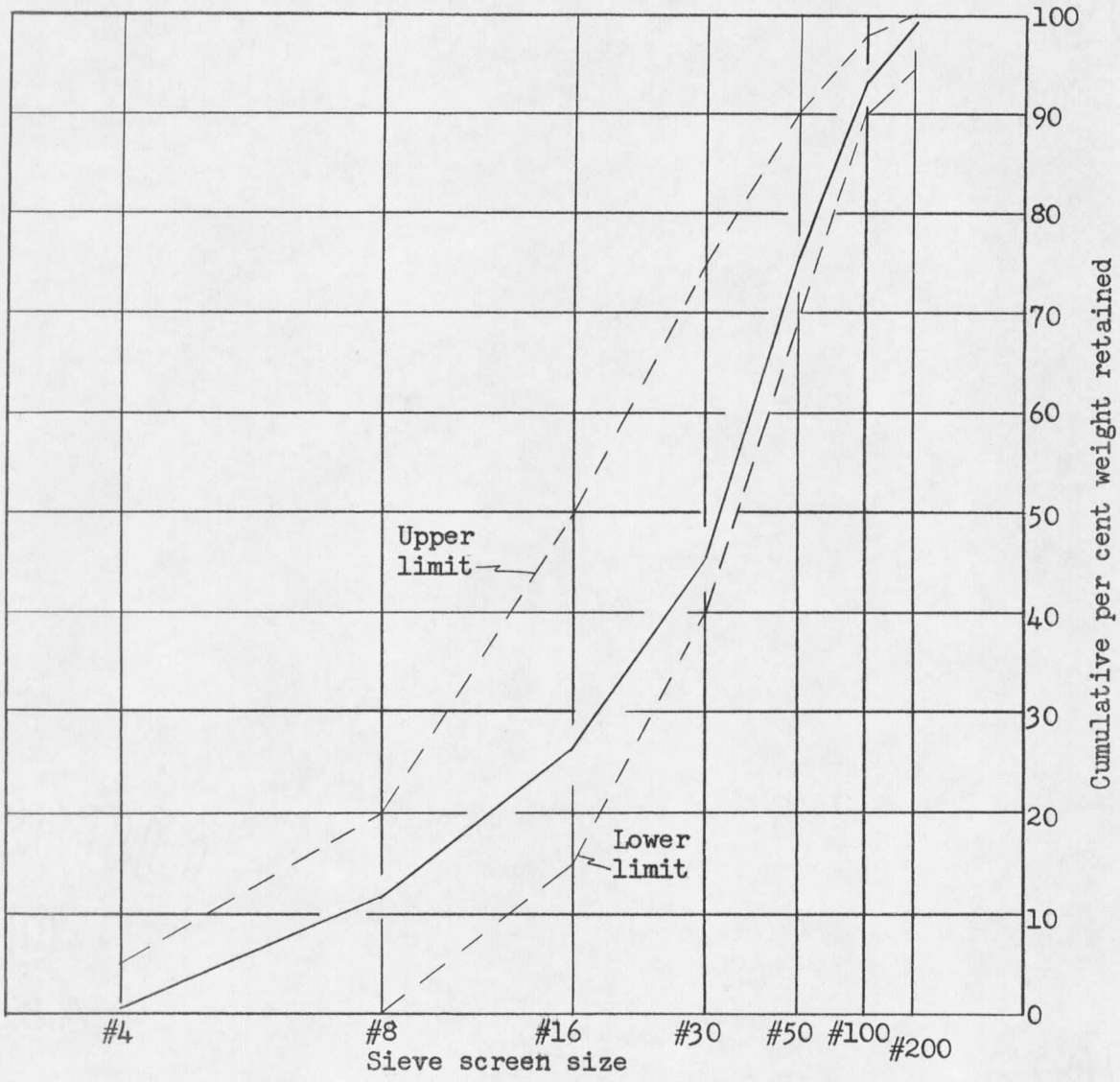


Fig. 43. Fine aggregate gradation.

Fine Aggregate Properties

Unit weight = 101.7 p.c.f.
Bulk specific gravity (A.S.T.M. Des. E12) = 2.572
Bulk specific gravity (saturated surface-dry) = 2.612
Apparent specific gravity (A.S.T.M. Des. E12) = 2.682
Moisture content (saturated surface-dry), by weight = 1.585%
Organic impurities: negligible
Fineness modulus = 2.53

Supplier: Pioneer Ready Mix Co.
Bozeman, Montana

APPENDIX D

CONCRETE BATCH INFORMATION

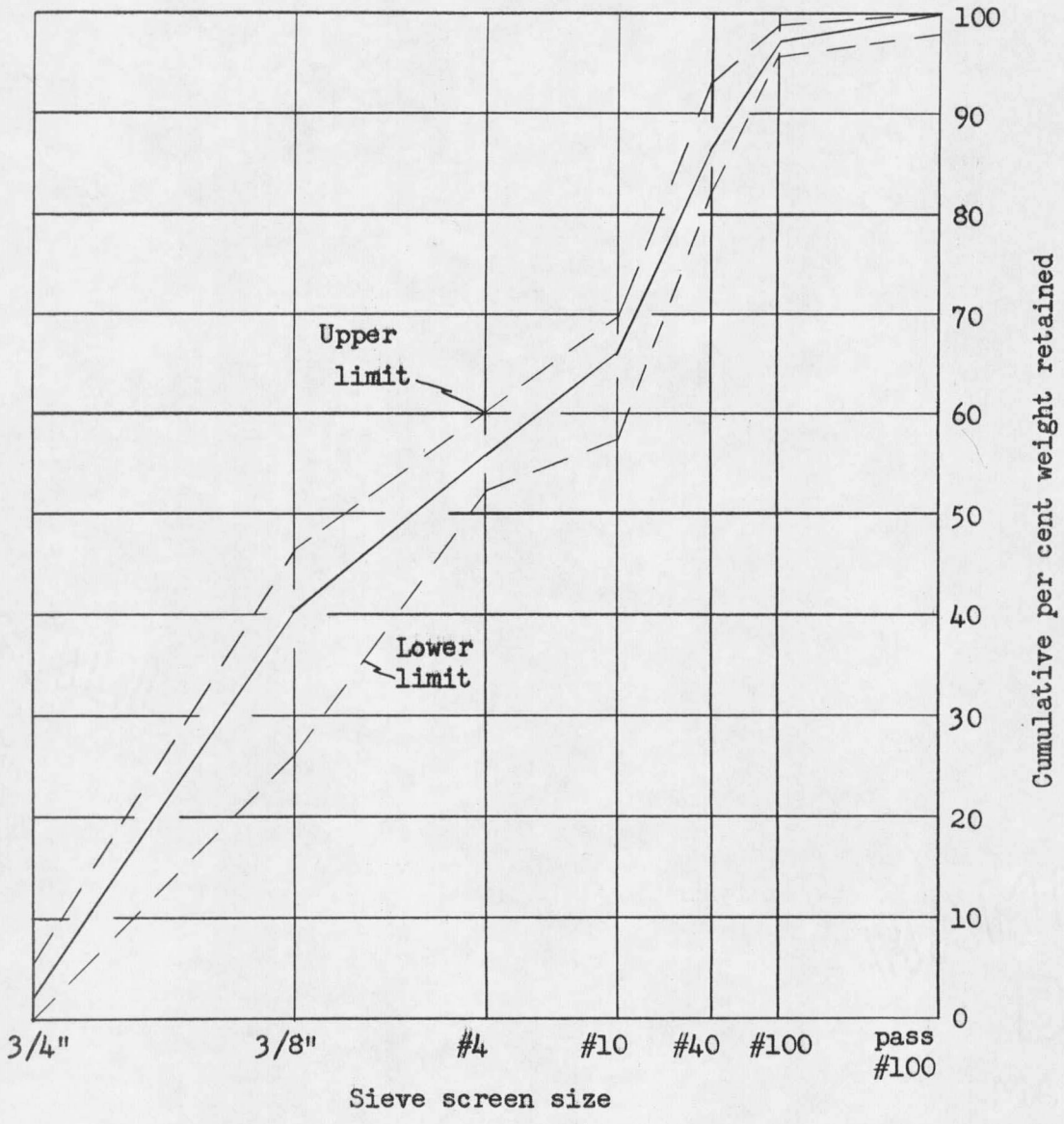


Fig. 44. Combined aggregate gradation for each concrete batch.

TABLE XVII

MATERIAL QUANTITIES FOR EACH 2 CU. FT. BATCH

Material	Description	Weight (Lbs.)
Aggregate	passing 1" sieve, but retained on 3/4" sieve	4.5
	" 3/4" " " " " 3/8" "	86.0
	" 3/8" " " " " #4 "	35.1
	" #4 " " " " #10 "	23.0
	" #10 " " " " #40 "	46.1
	" #40 " " " " #100 "	23.8
	passing #100 sieve	6.5
Cement	Type II	46.8
Water	tap water @ approx. 68°F	23.32

TABLE XVIII

INDIVIDUAL CONCRETE BATCH PROPERTIES

Batch	Slump (in.)	Unit weight (p.c.f.)	Air content (%)	
			Pressure method	AE-55 Air Indicator
21	1-1/2	147.9	2.0	3
22	1-3/4	148.0		3
23	1-3/4	148.3	1.9	3
24	2	147.7		3

Additional data common to each batch

Cement Factor = 6.73

Water/Cement (W/C) Ratio = 0.499 = 5.64 gal./sk.

TABLE XIX

CONCRETE CYLINDER COMPRESSIVE TEST RESULTS

Batch	Cylinder	Curing procedure	Age at test (days)	Strength (psi.)
22	1	continuous moist-room	7	3760
	2	18 hours steam cure, remainder in moist-room	7	4970
	3	continuous moist-room	28	4900
	4	18 hours steam cure, remainder in moist-room	28	6240
24	1	continuous moist-room	7	3385
	2	18 hours steam cure, remainder in moist-room	7	4430
	3	continuous moist-room	28	4740
	4	18 hours steam cure, remainder in moist-room	28	6045

Additional compression test information

Nominal cylinder dimensions: Batch 22, 3-1/3" x 6-2/3"
Batch 24, 3-3/4" x 7-1/2"

Casting procedure: All cylinder molds affixed to vibrating table, overfilled in a single lift, and vibrated for six seconds at approximately 4200 cpm.

Capping procedure: All cylinders capped with sulfur capping compound one day before testing.

Testing procedure: All cylinders loaded at 20,000 lbs./min. (approximately 35 psi./sec.) with a Model MCA-300 Riehle Testing Machine, American Machine and Metals, Inc., Riehle Testing Machines Division, East Moline, Illinois.

APPENDIX E

DURABILITY AND SCALING STUDY DATA

Fig. 45. Relative dynamic moduli of elasticity versus number of freeze-thaw cycles for non-stressed, normally cured, water ponded slabs.

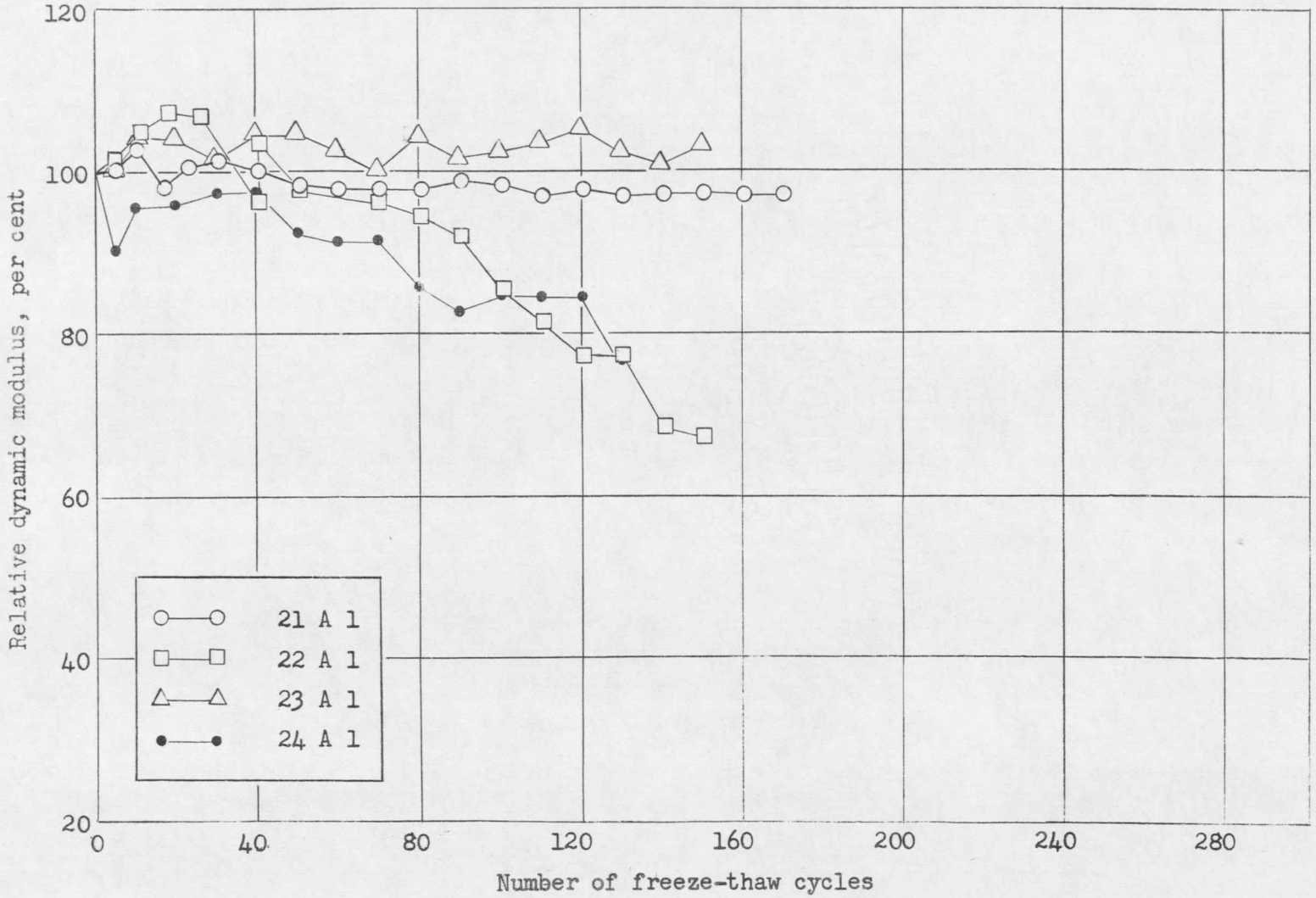


Fig. 46. Relative dynamic moduli of elasticity versus number of freeze-thaw cycles for non-stressed, normally cured, $CaCl_2$ solution ponded slabs.

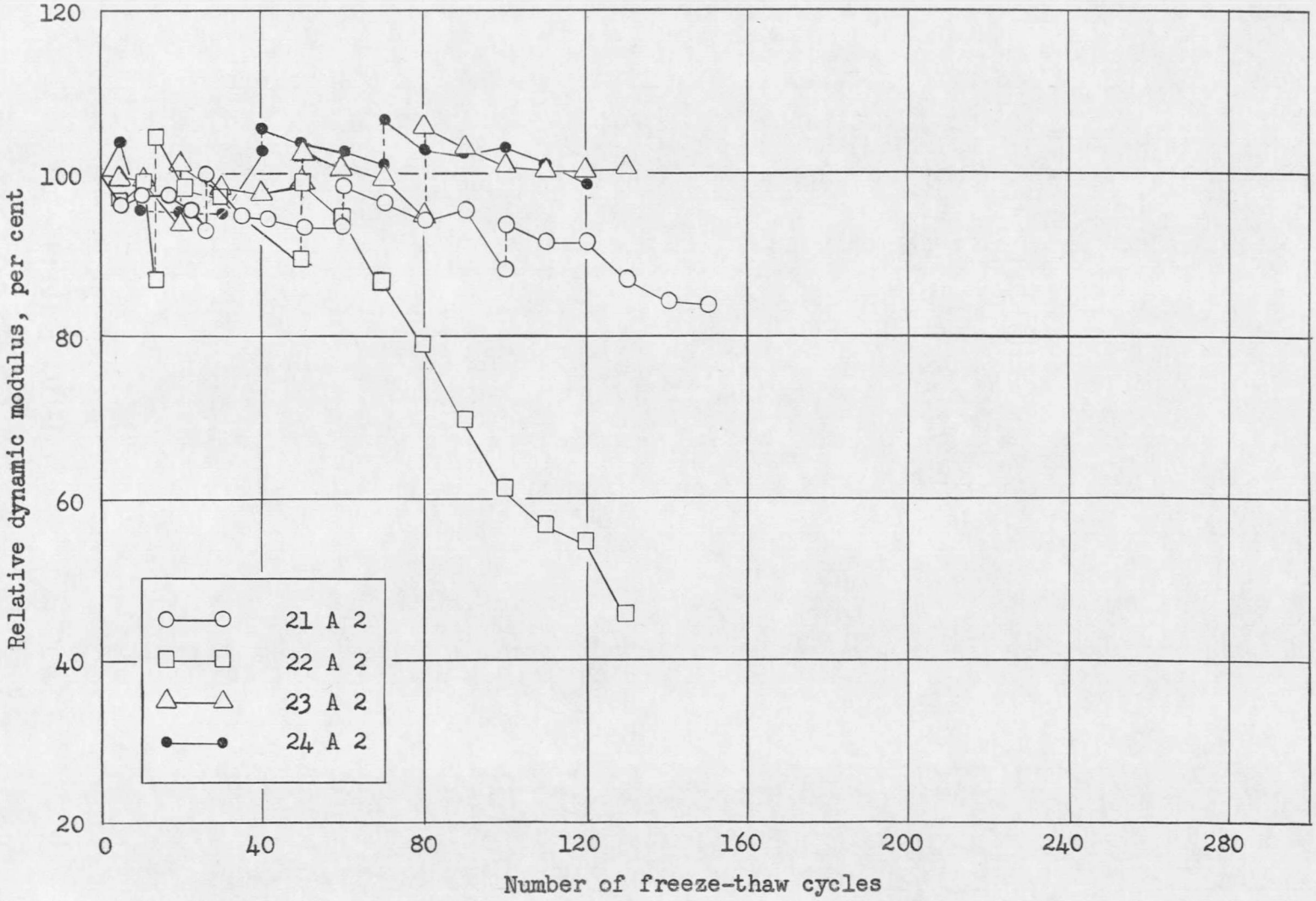


Fig. 47. Relative dynamic moduli of elasticity versus number of freeze-thaw cycles for non-stressed, steam cured, water ponded slabs.

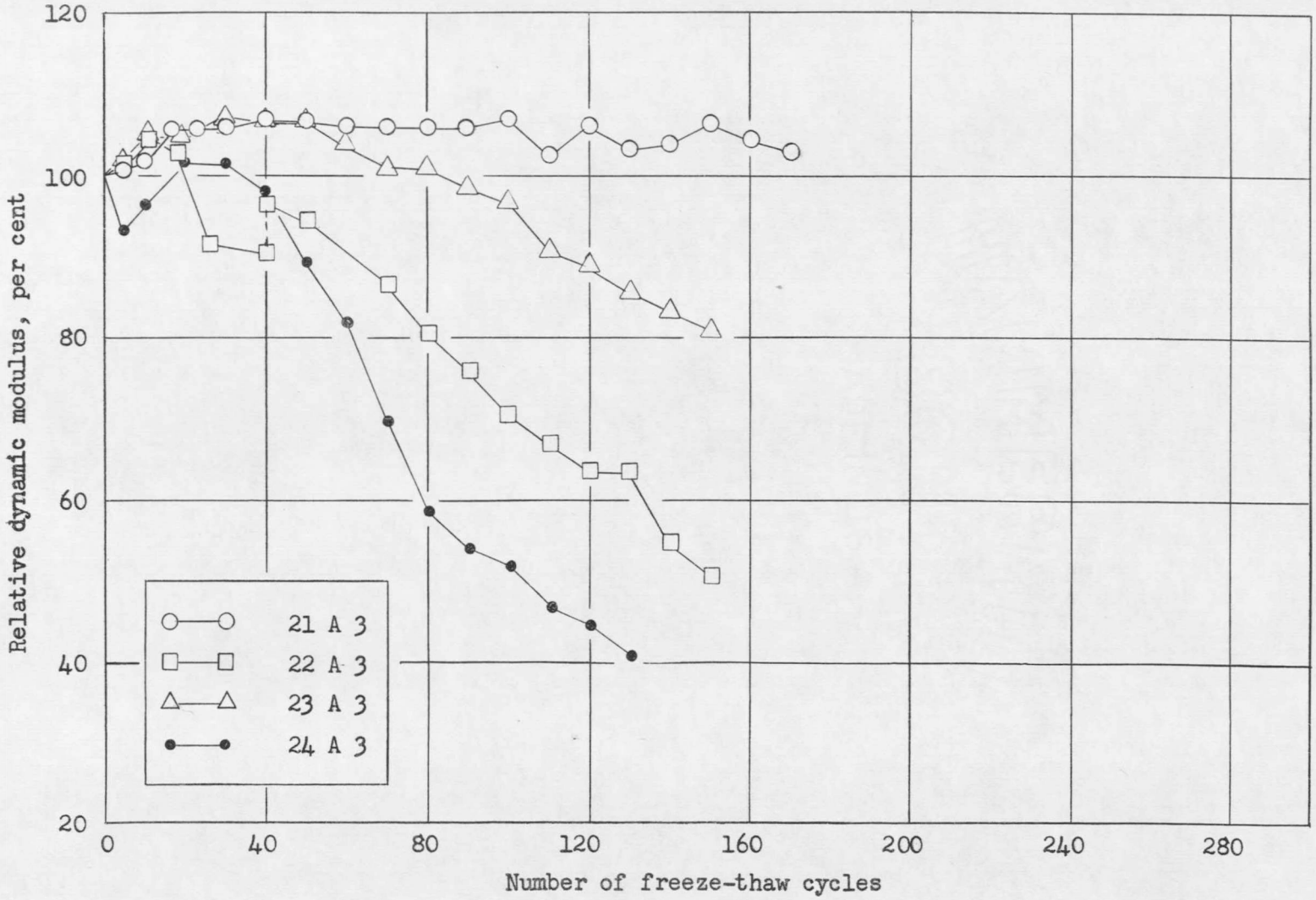


Fig. 48. Relative dynamic moduli of elasticity versus number of freeze-thaw cycles for non-stressed, steam cured, $CaCl_2$ solution ponded slabs.

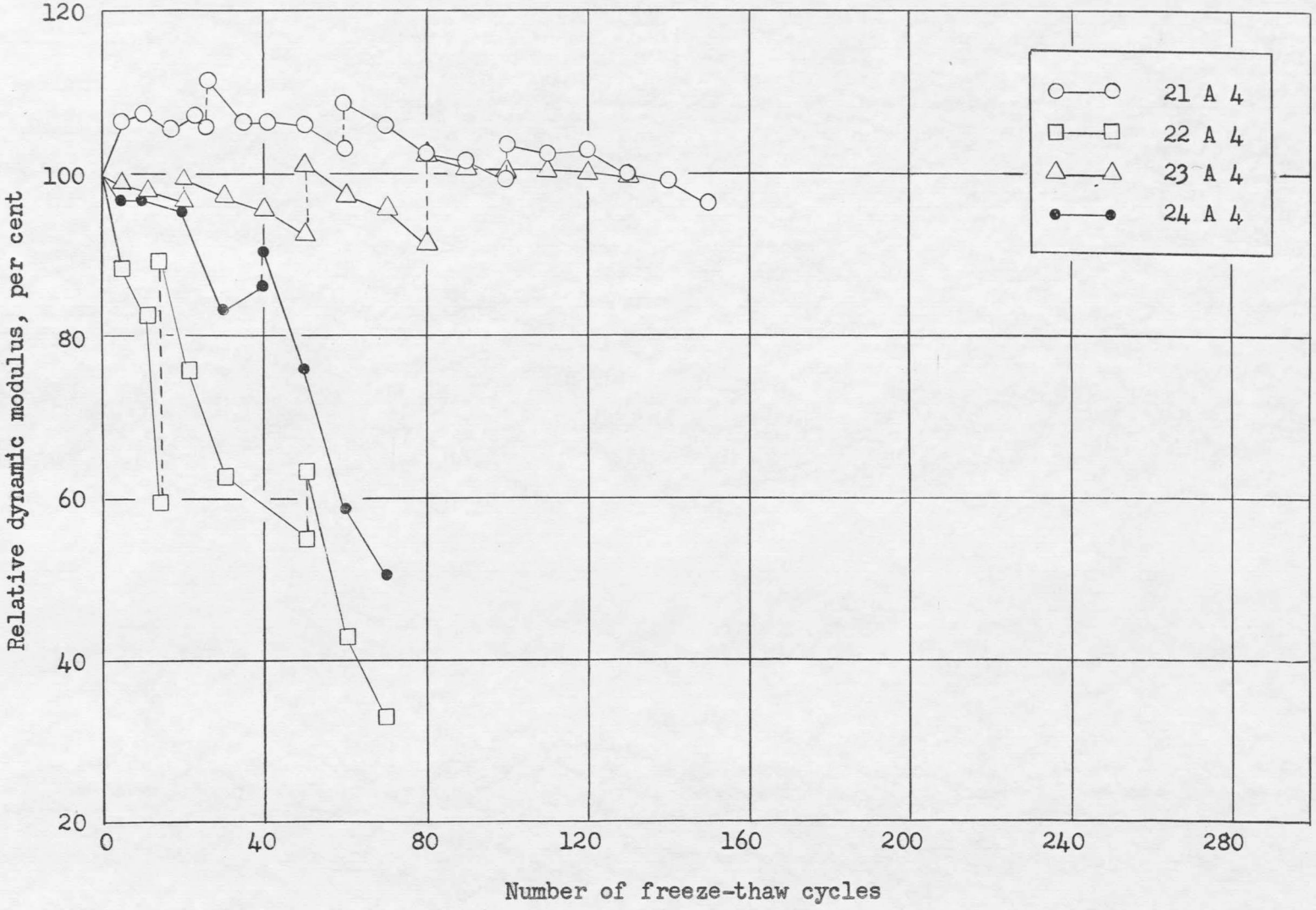


Fig. 49. Relative dynamic moduli of elasticity versus number of freeze-thaw cycles for 500 psi., normally cured, water ponded slabs.

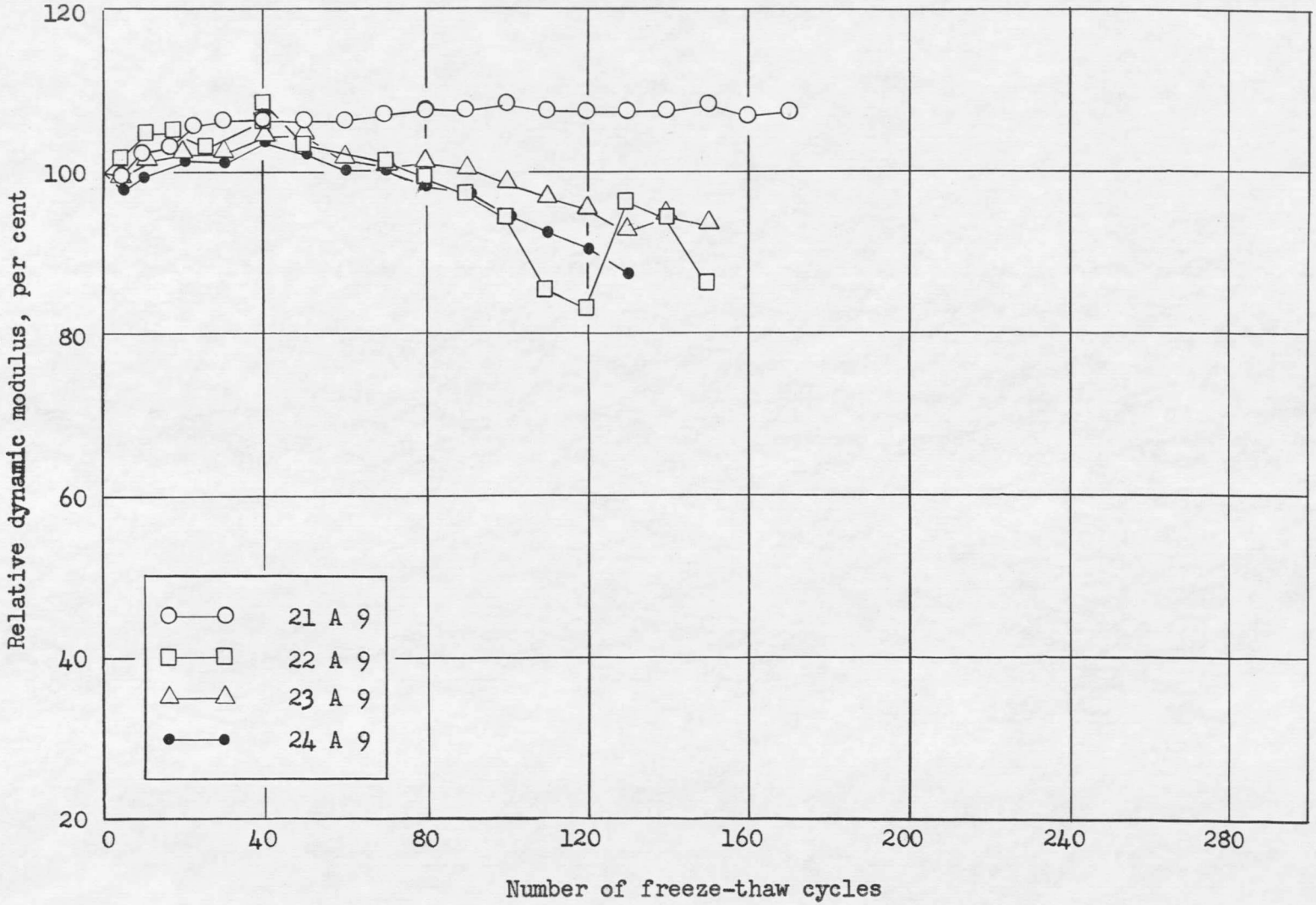


Fig. 50. Relative dynamic moduli of elasticity versus number of freeze-thaw cycles for 500 psi., normally cured, $CaCl_2$ solution ponded slabs.

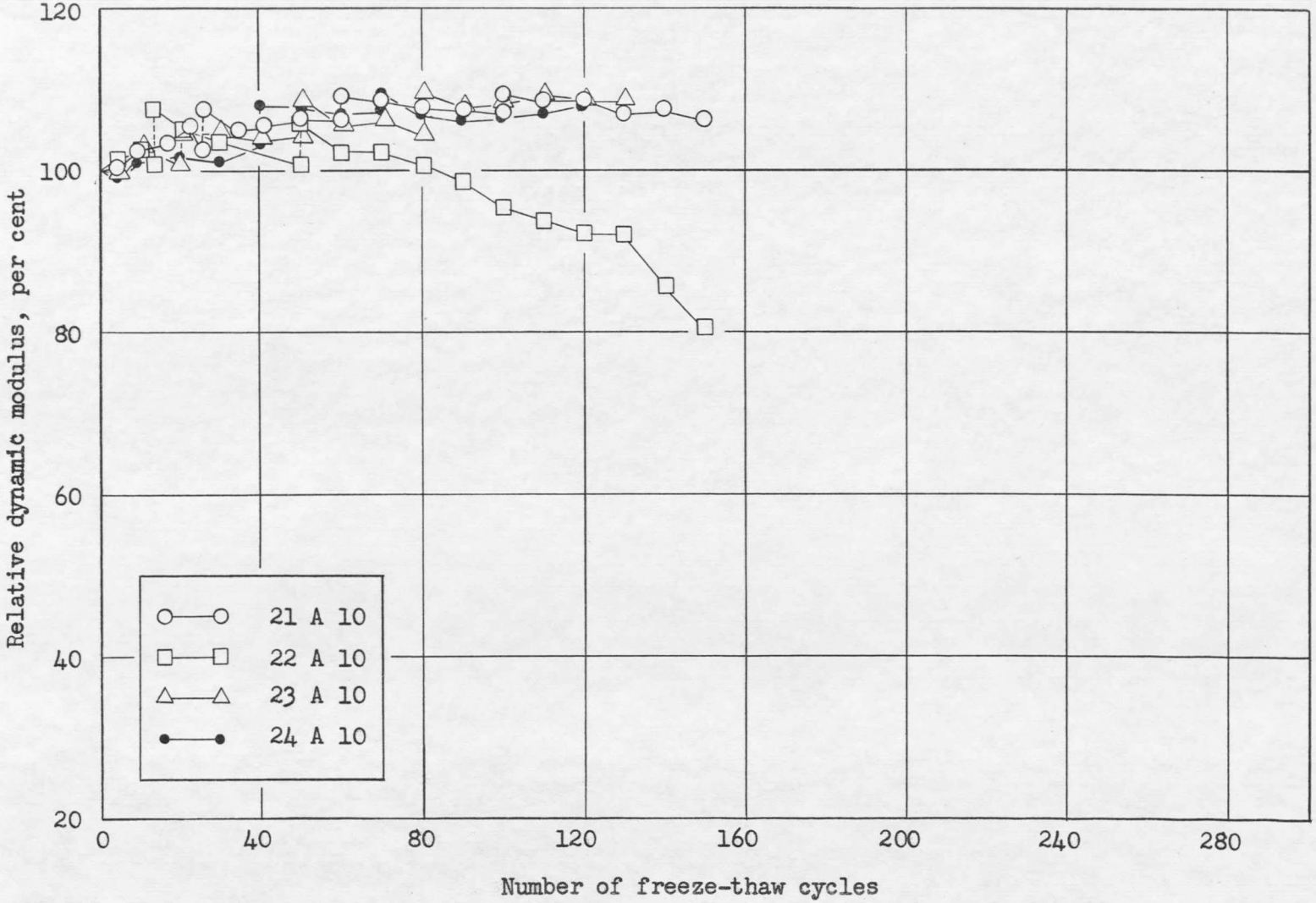


Fig. 51. Relative dynamic moduli of elasticity versus number of freeze-thaw cycles for 500 psi., steam cured, water ponded slabs.

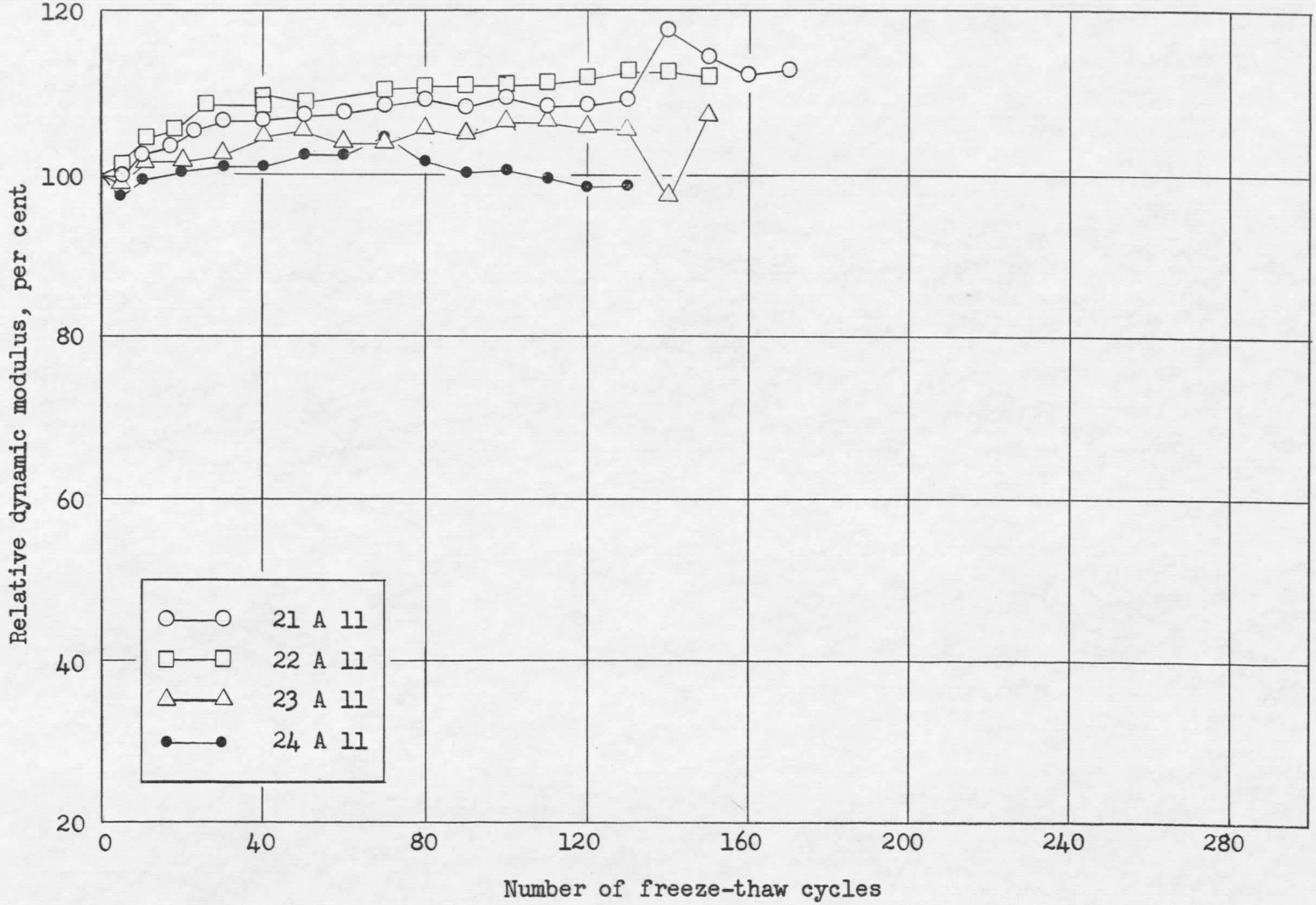


Fig. 52. Relative dynamic moduli of elasticity versus number of freeze-thaw cycles for 500 psi., steam cured, $CaCl_2$ solution ponded slabs.

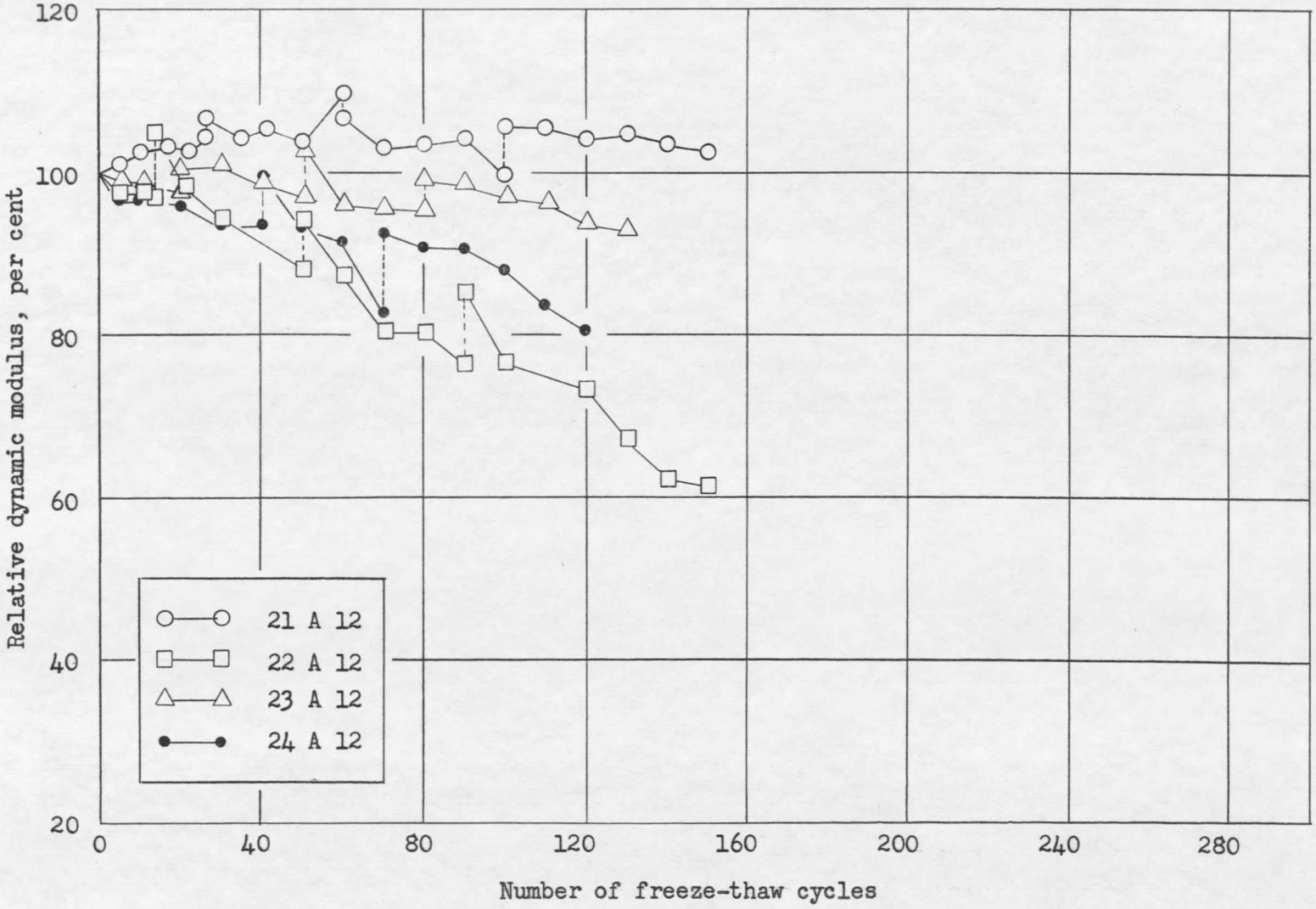


Fig. 53. Relative dynamic moduli of elasticity versus number of freeze-thaw cycles for 1200 psi., normally cured, water ponded slabs.

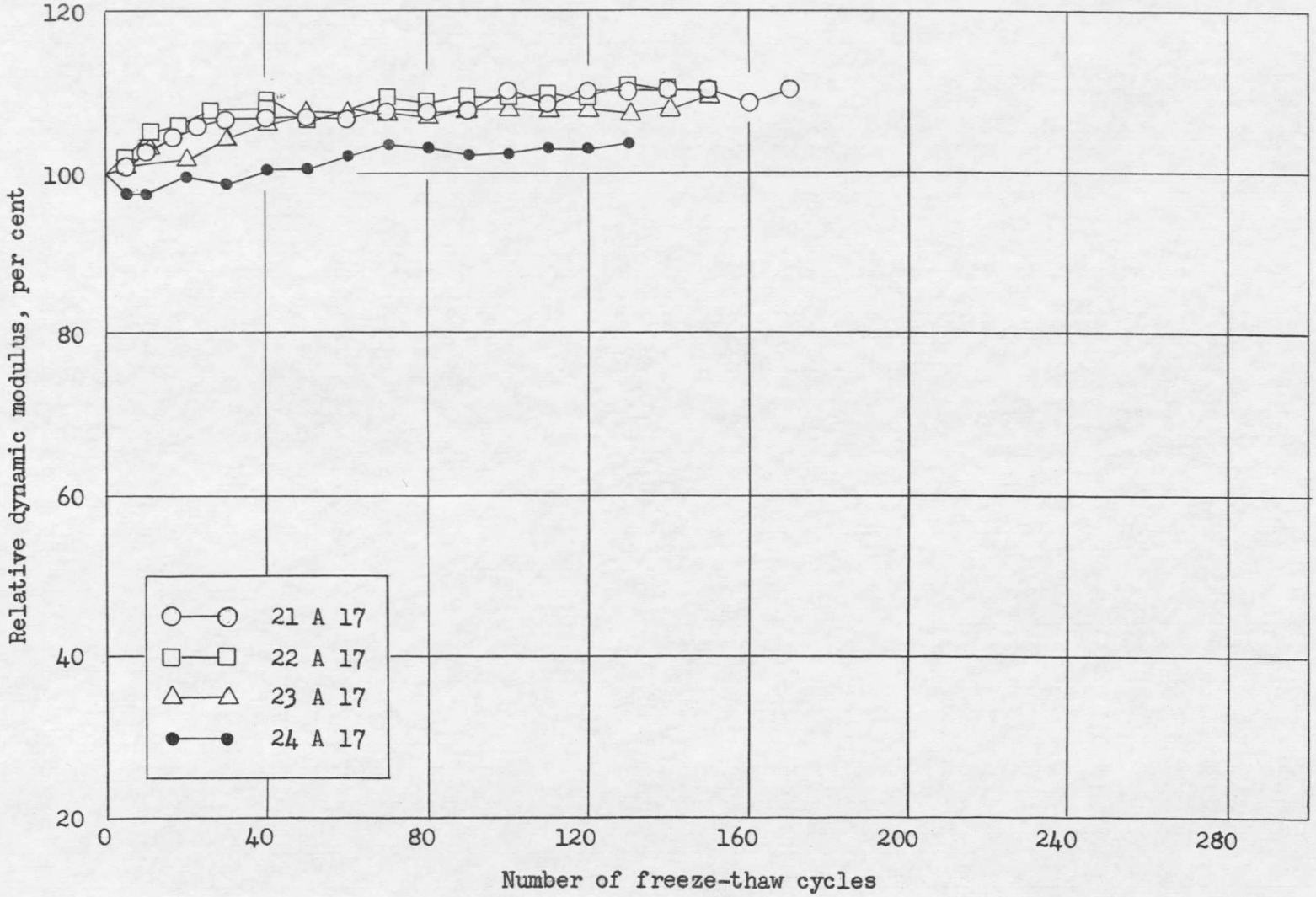


Fig. 54. Relative dynamic moduli of elasticity versus number of freeze-thaw cycles for 1200 psi., normally cured, $CaCl_2$ solution ponded slabs.

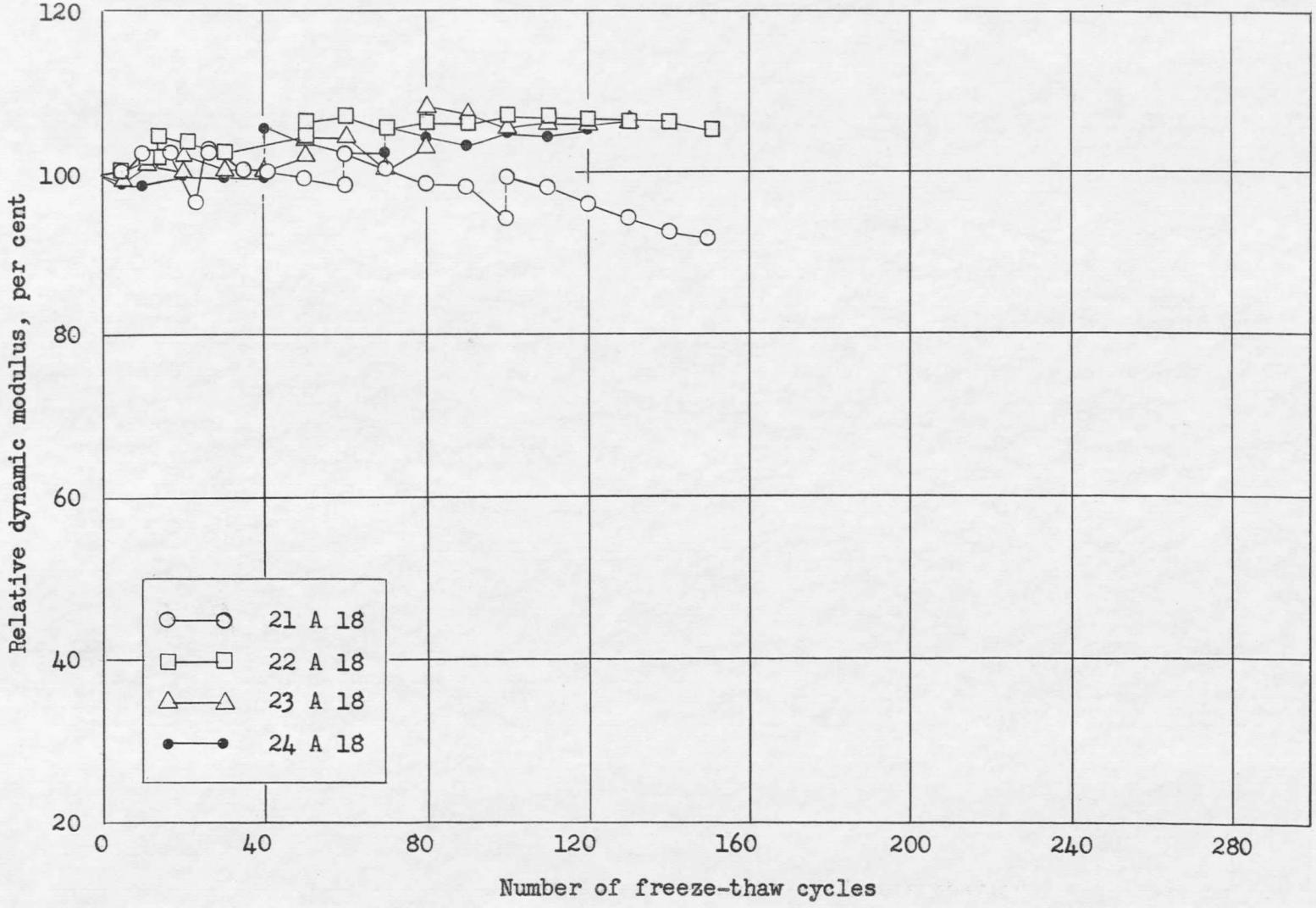


Fig. 55. Relative dynamic moduli of elasticity versus number of freeze-thaw cycles for 1200 psi., steam cured, water ponded slabs.

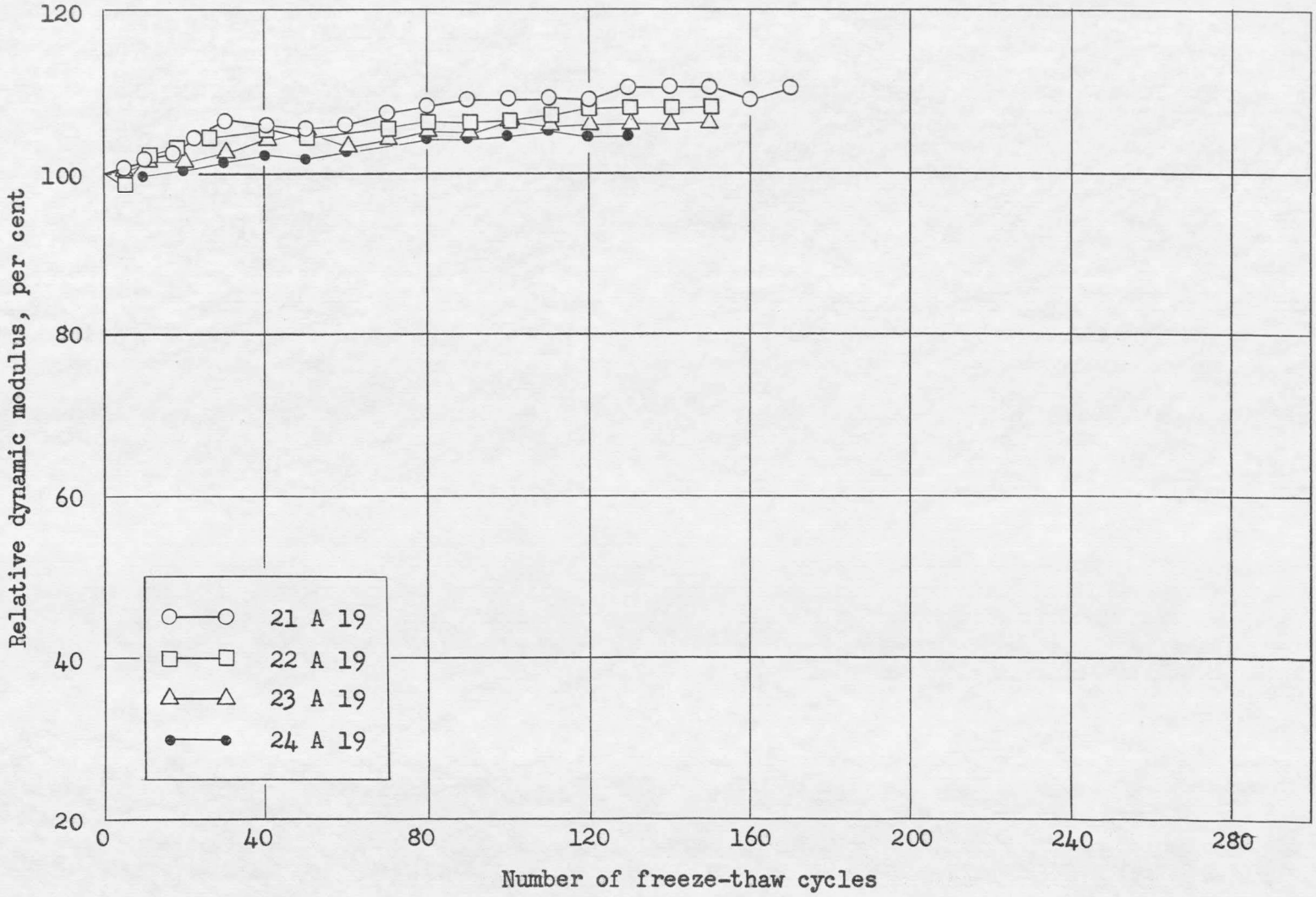


Fig. 56. Relative dynamic moduli of elasticity versus number of freeze-thaw cycles for 1200 psi., steam cured, $CaCl_2$ solution ponded slabs.

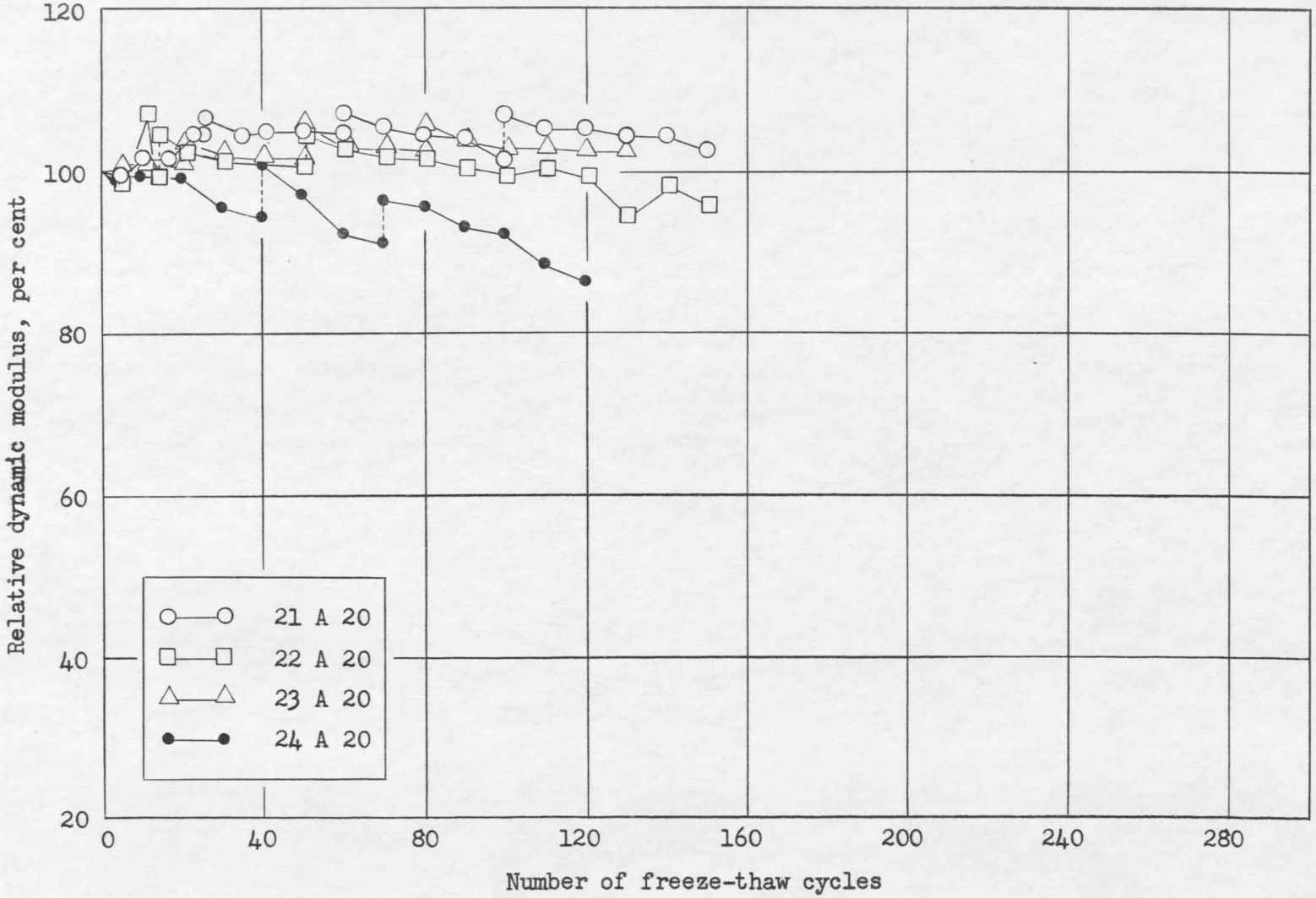


Fig. 57. Adjusted weight changes versus number of freeze-thaw cycles for non-stressed, normally cured, water ponded slabs.

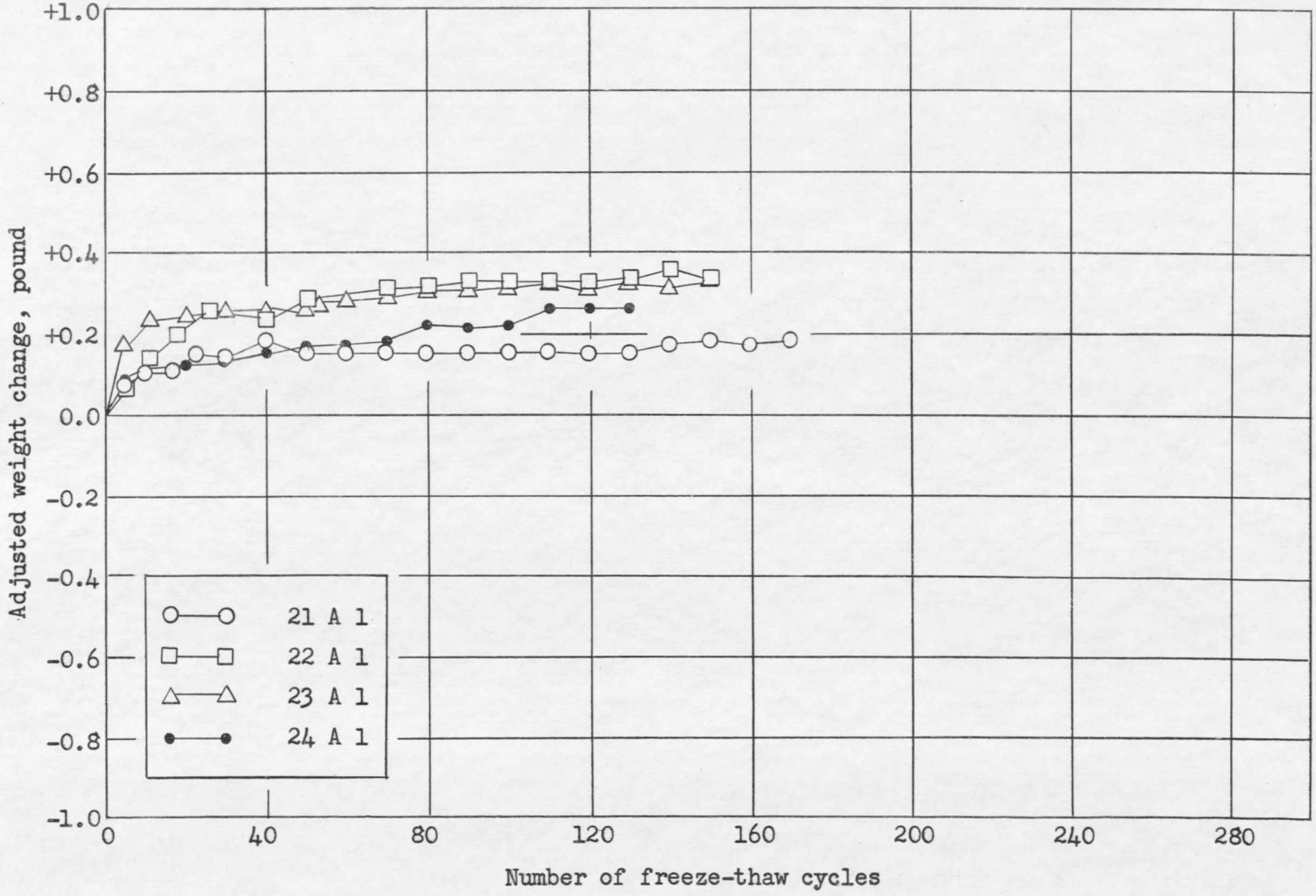


Fig. 58. Adjusted weight changes versus number of freeze-thaw cycles for non-stressed, normally cured, $CaCl_2$ solution ponded slabs.

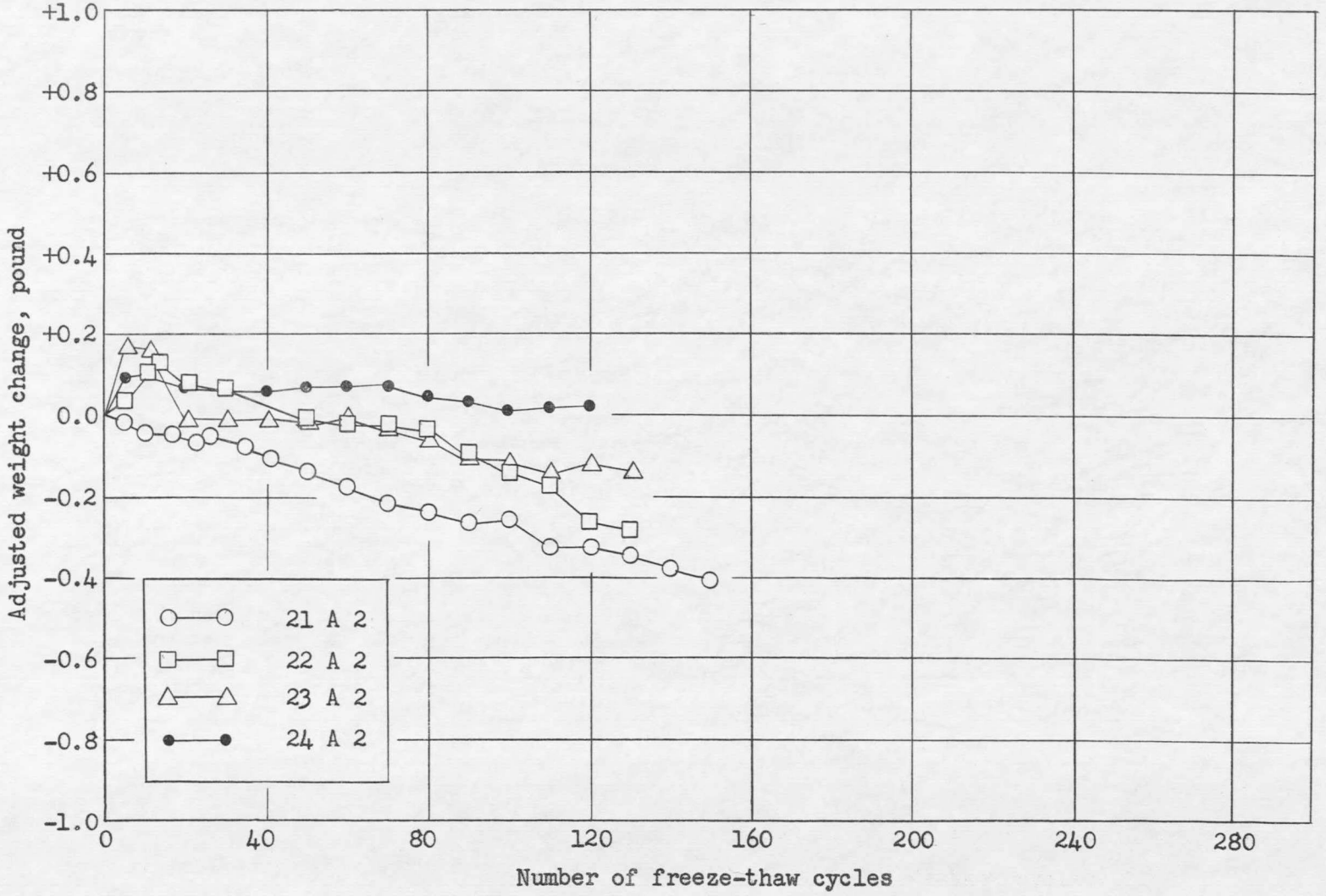


Fig. 59. Adjusted weight changes versus number of freeze-thaw cycles for non-stressed, steam cured, water ponded slabs.

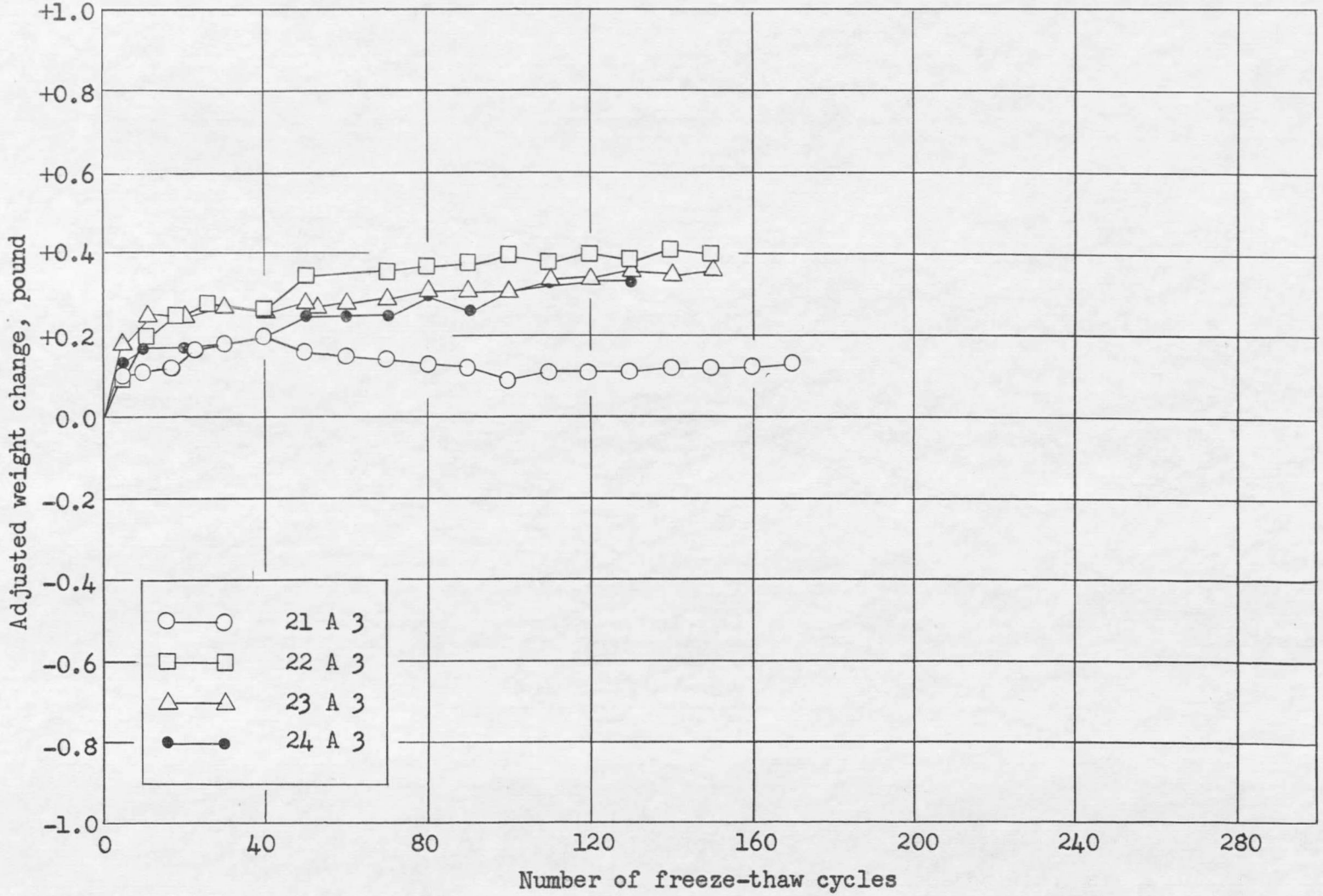


Fig. 60. Adjusted weight changes versus number of freeze-thaw cycles for non-stressed, steam cured, $CaCl_2$ solution ponded slabs.

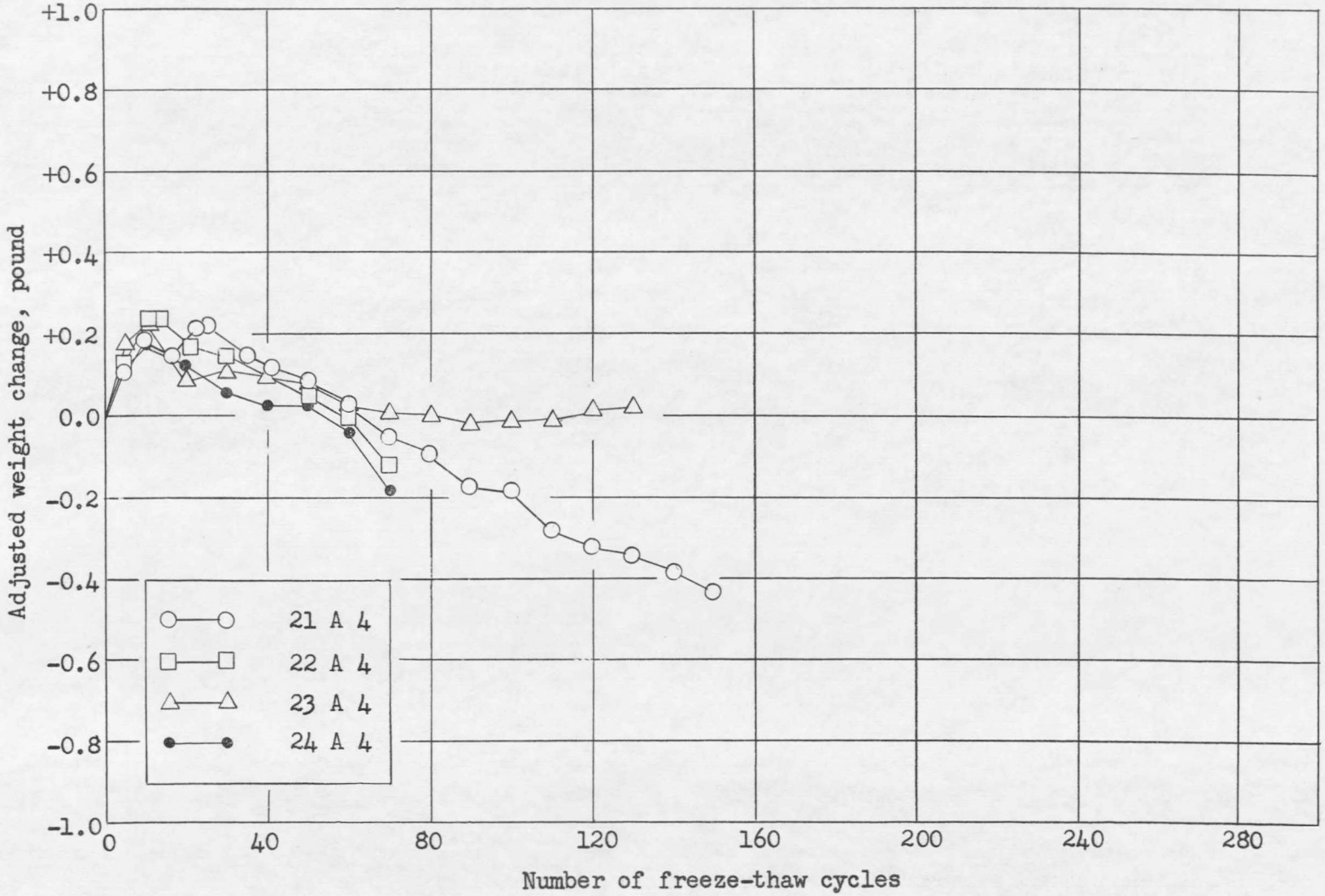


Fig. 61. Adjusted weight changes versus number of freeze-thaw cycles for 500 psi., normally cured, water ponded slabs.

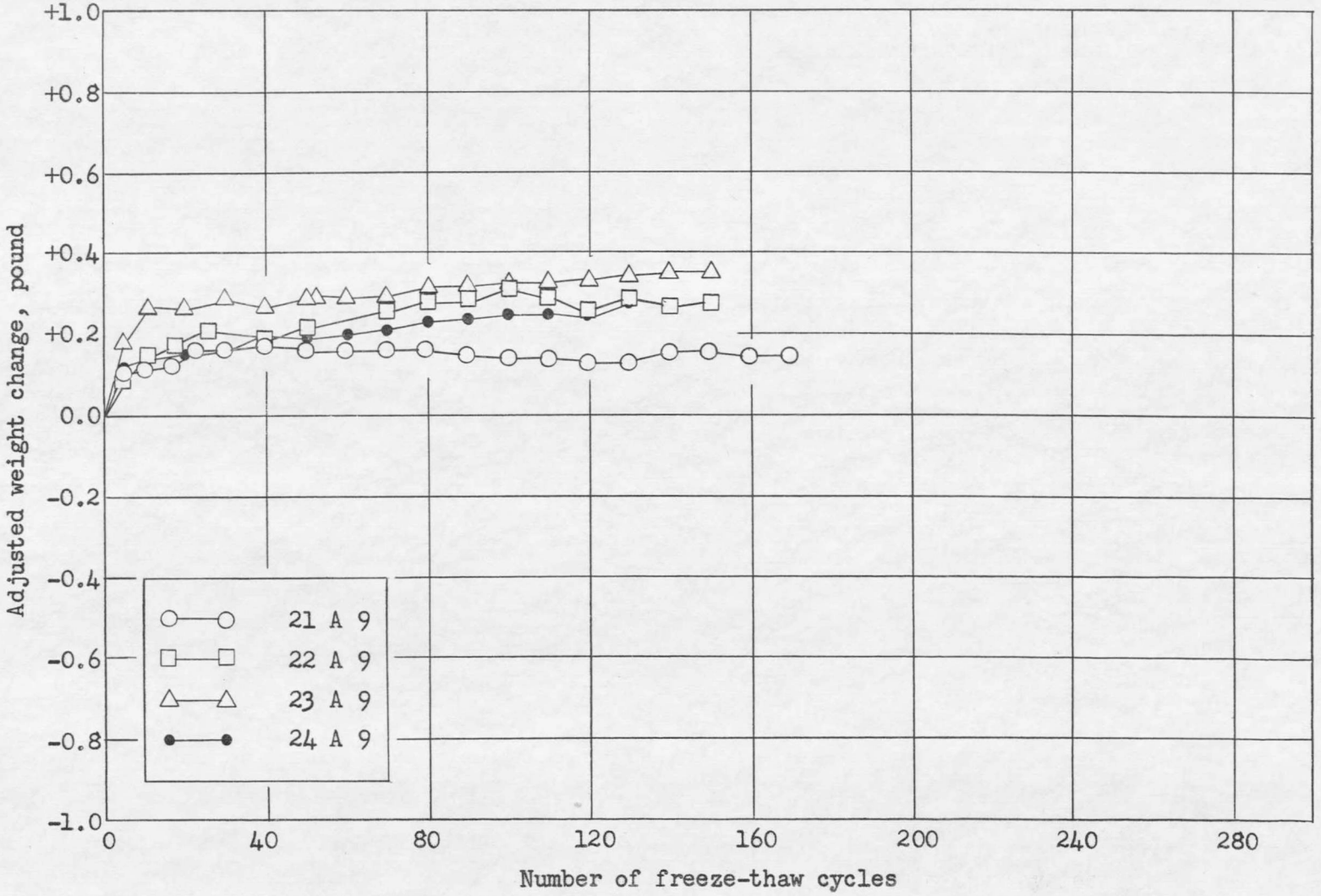


Fig. 62. Adjusted weight changes versus number of freeze-thaw cycles for 500 psi., normally cured, $CaCl_2$ solution ponded slabs.

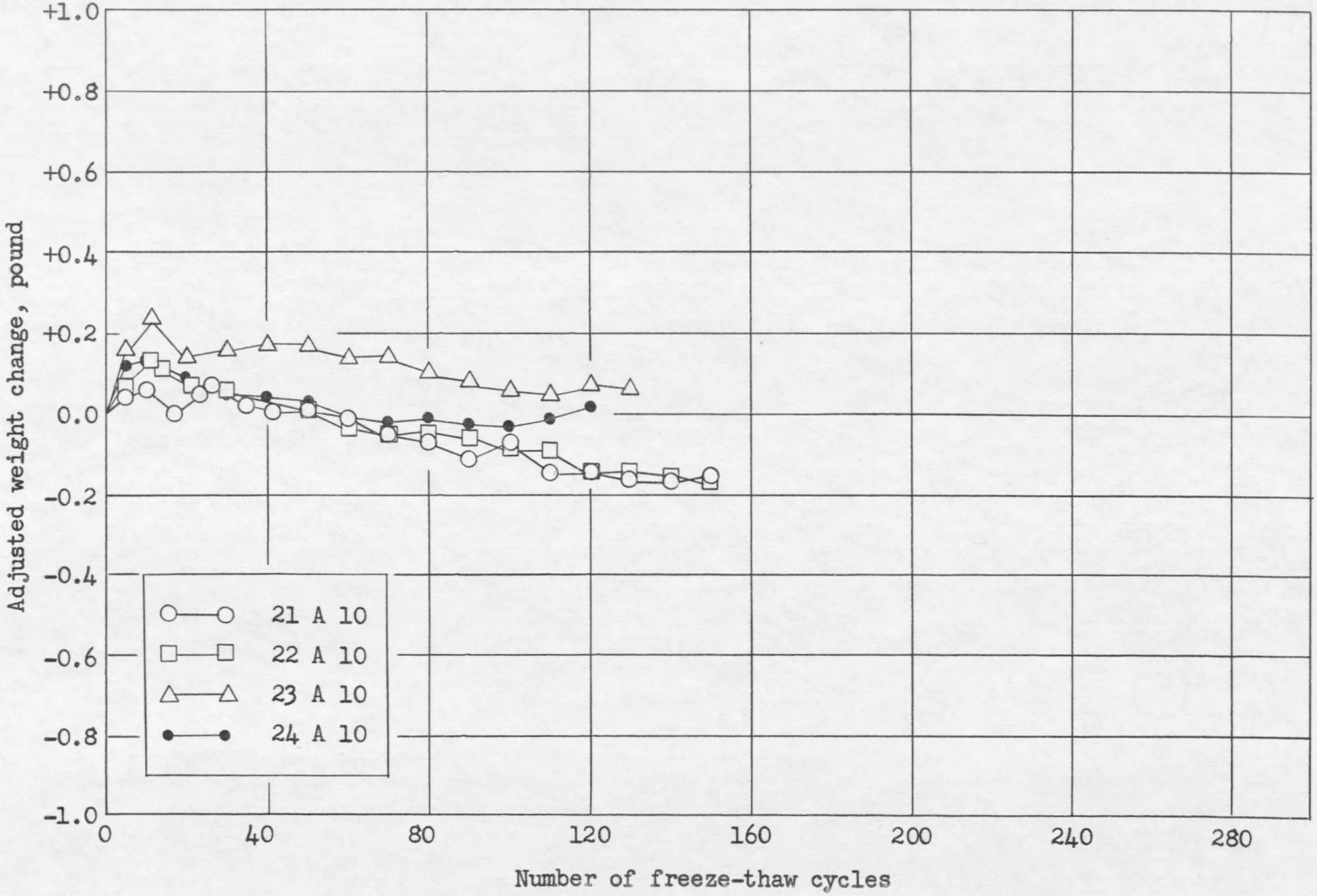


Fig. 63. Adjusted weight changes versus number of freeze-thaw cycles for 500 psi., steam cured, water ponded slabs.

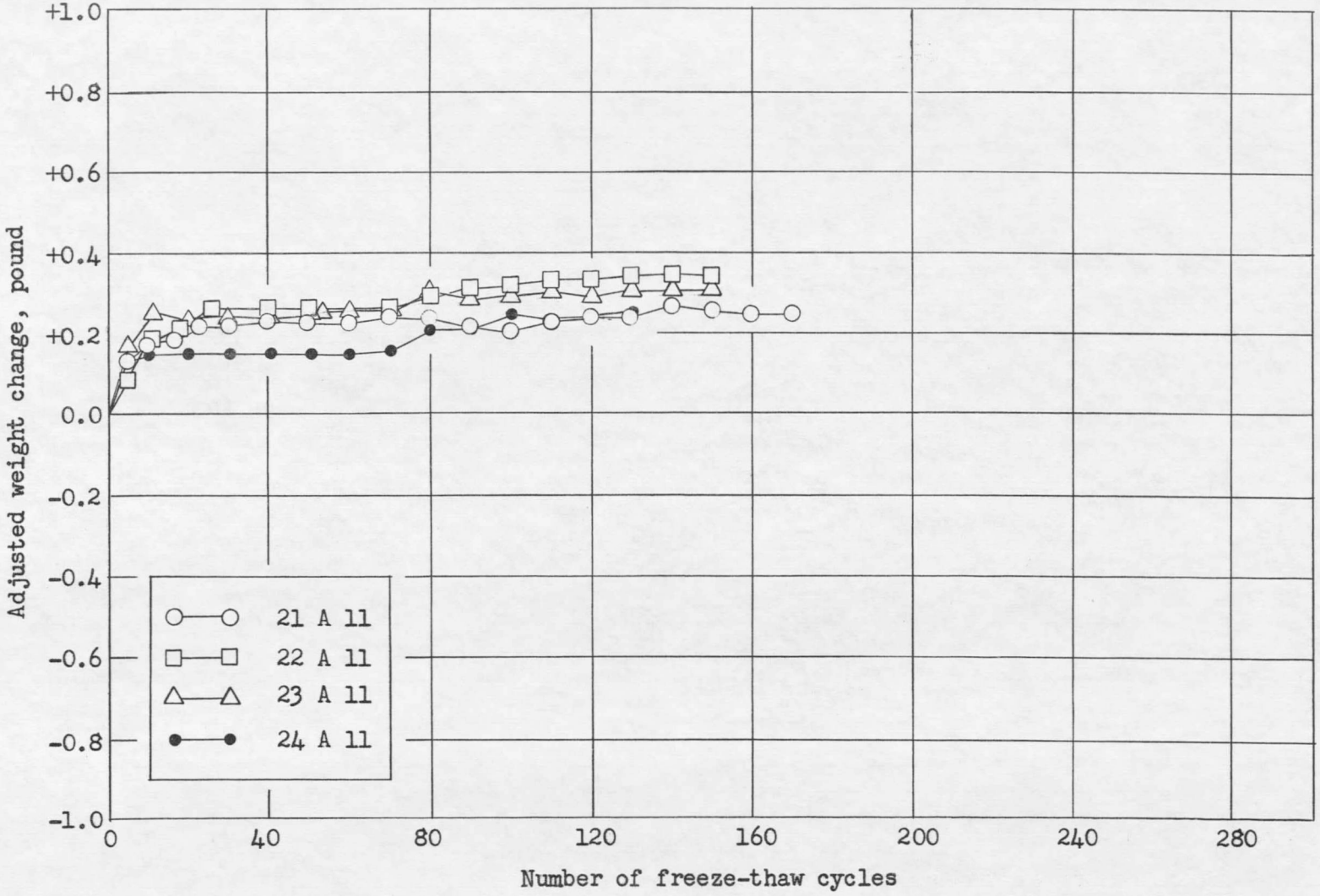


Fig. 64. Adjusted weight changes versus number of freeze-thaw cycles for 500 psi., steam cured, $CaCl_2$ solution ponded slabs.

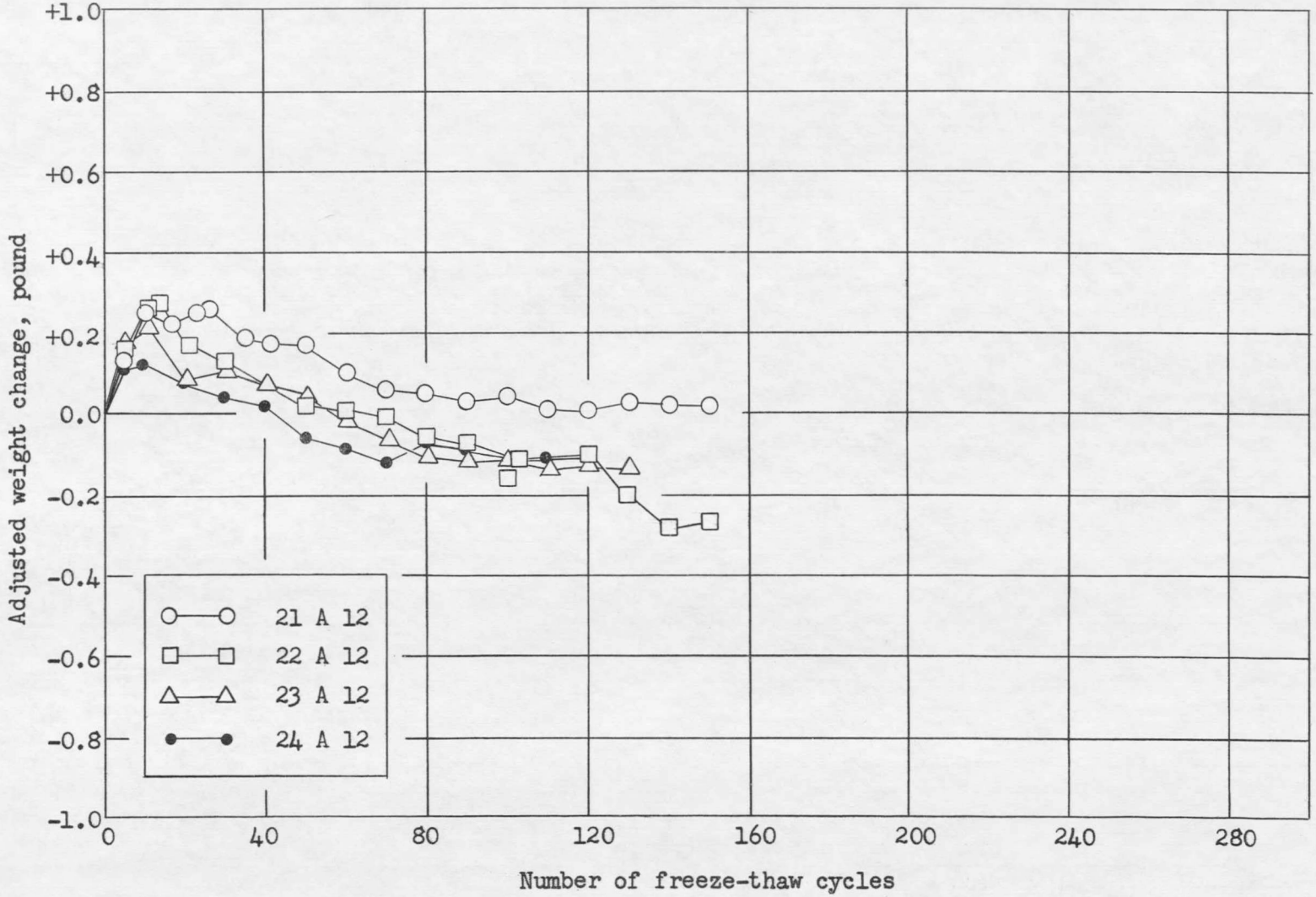


Fig. 65. Adjusted weight changes versus number of freeze-thaw cycles for 1200 psi., normally cured, water ponded slabs.

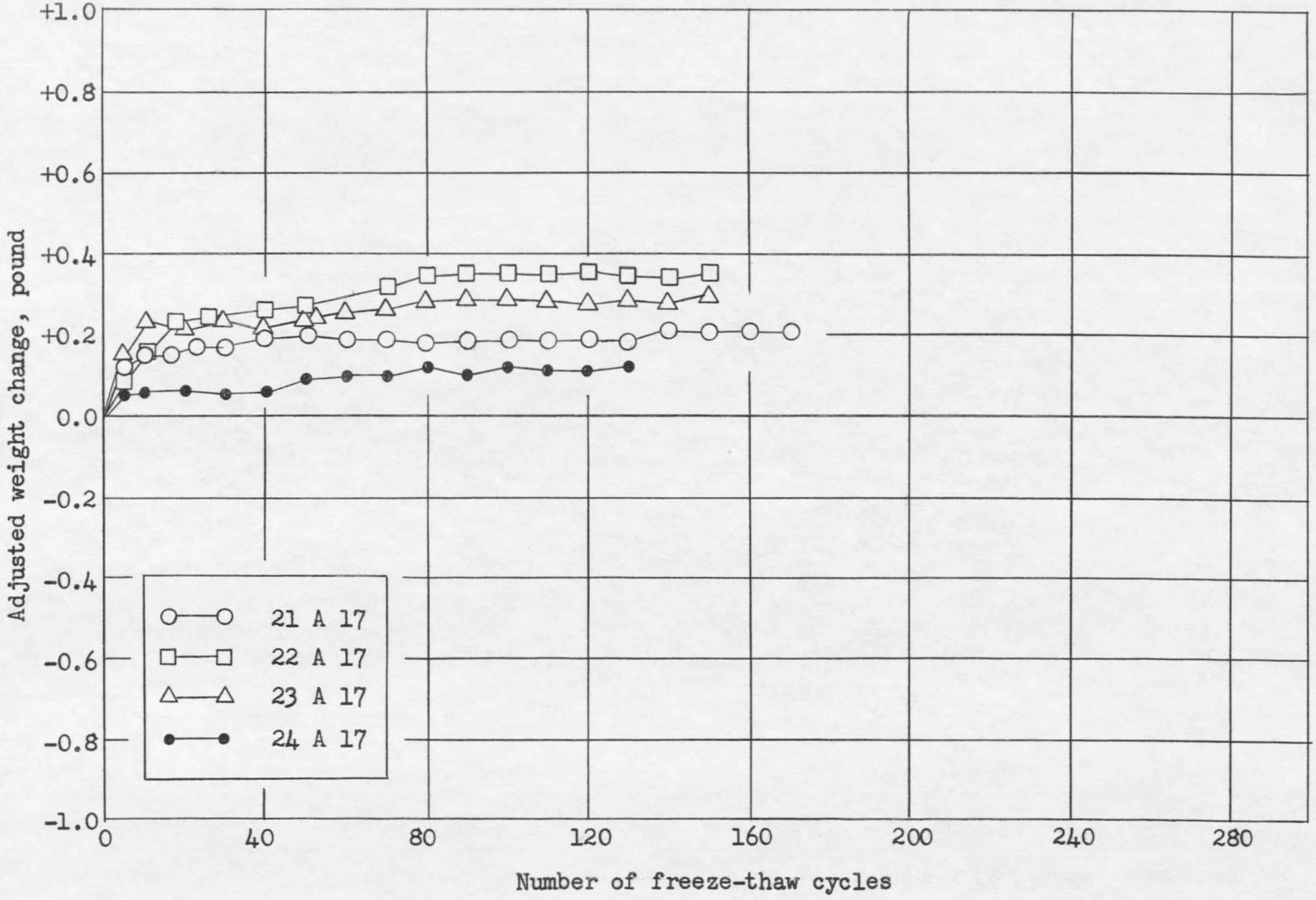


Fig. 66. Adjusted weight changes versus number of freeze-thaw cycles for 1200 psi., normally cured, $CaCl_2$ solution ponded slabs.

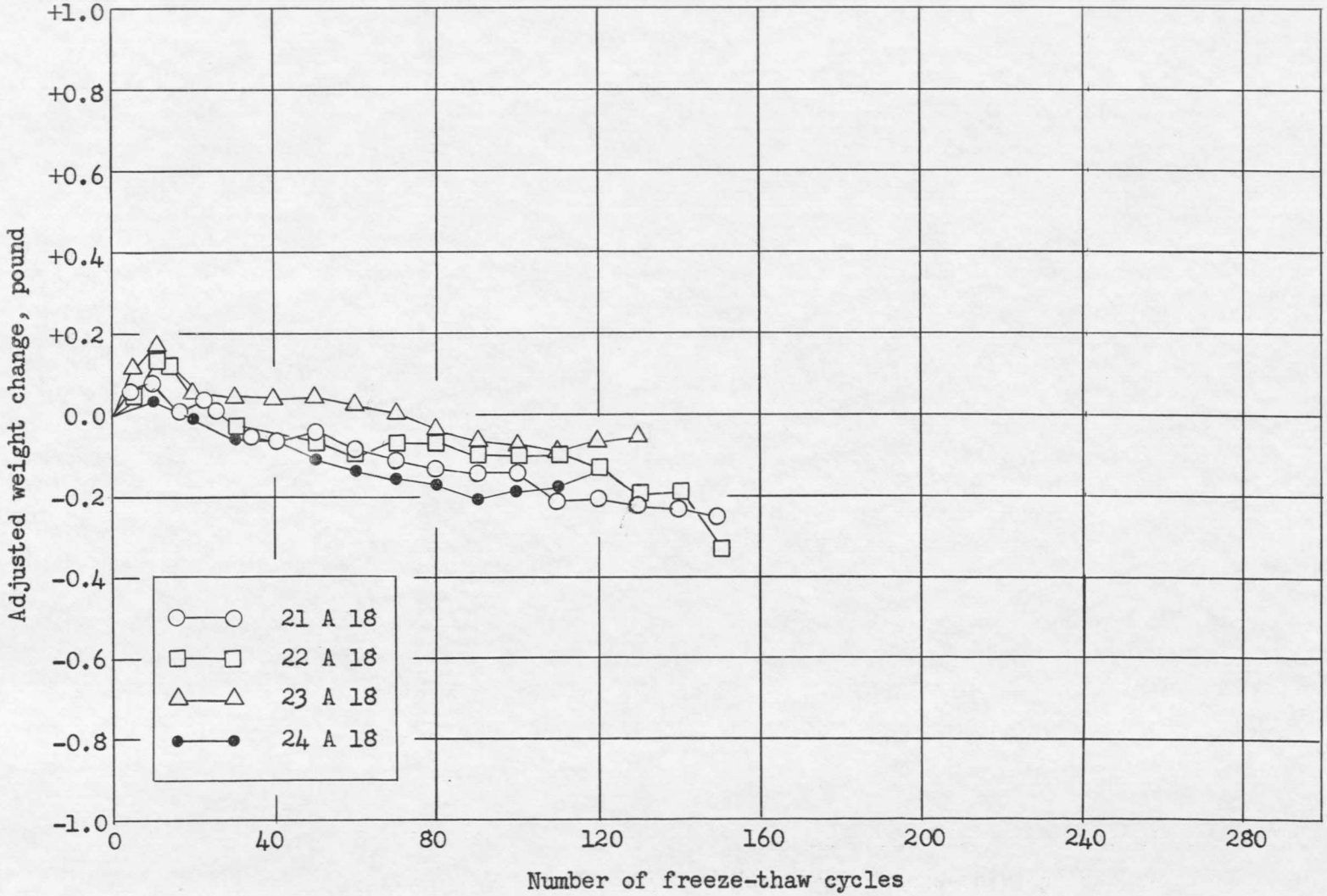


Fig. 67. Adjusted weight changes versus number of freeze-thaw cycles for 1200 psi., steam cured, water ponded slabs

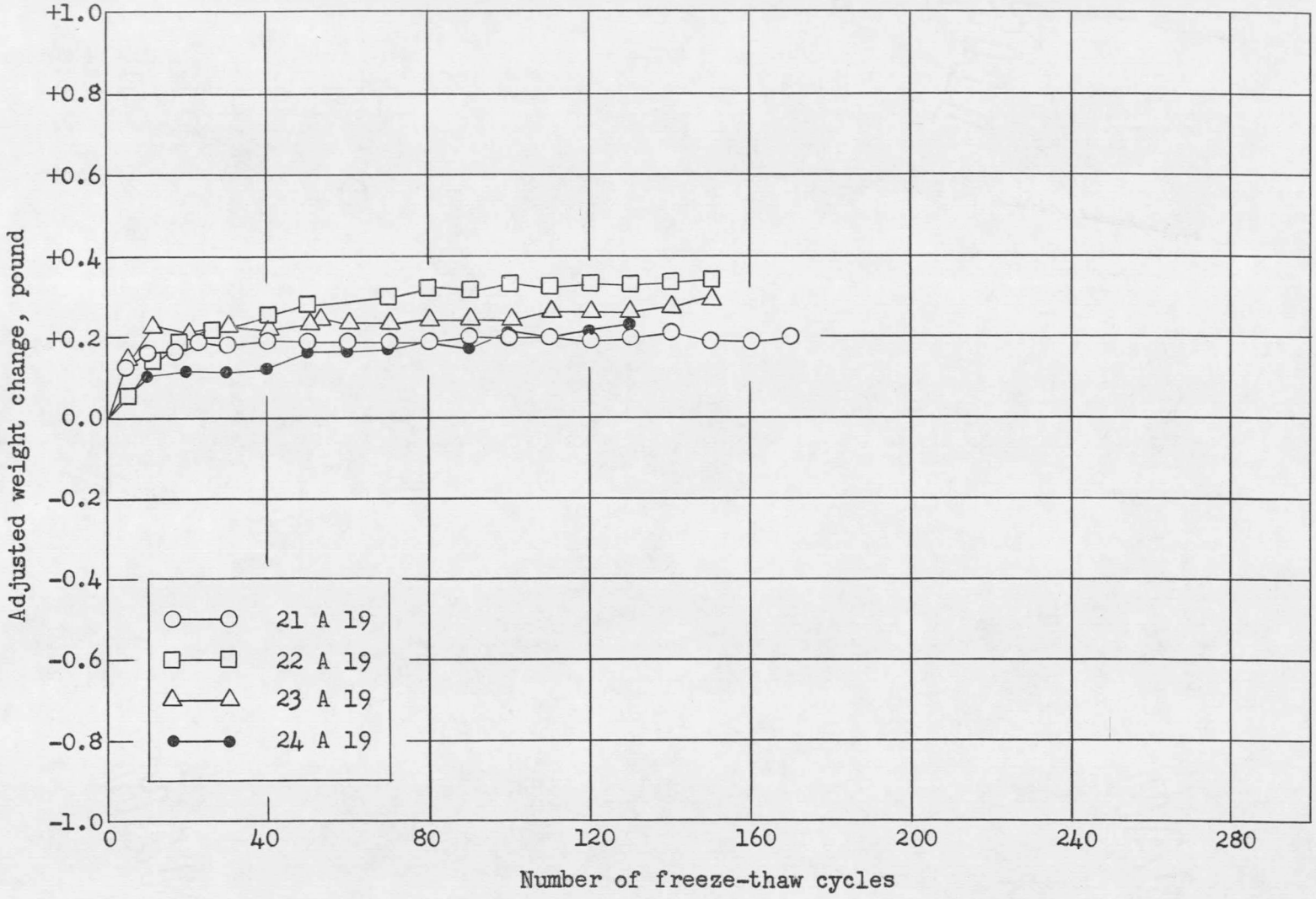


Fig. 68. Adjusted weight changes versus number of freeze-thaw cycles for 1200 psi., steam cured, $CaCl_2$ solution ponded slabs.

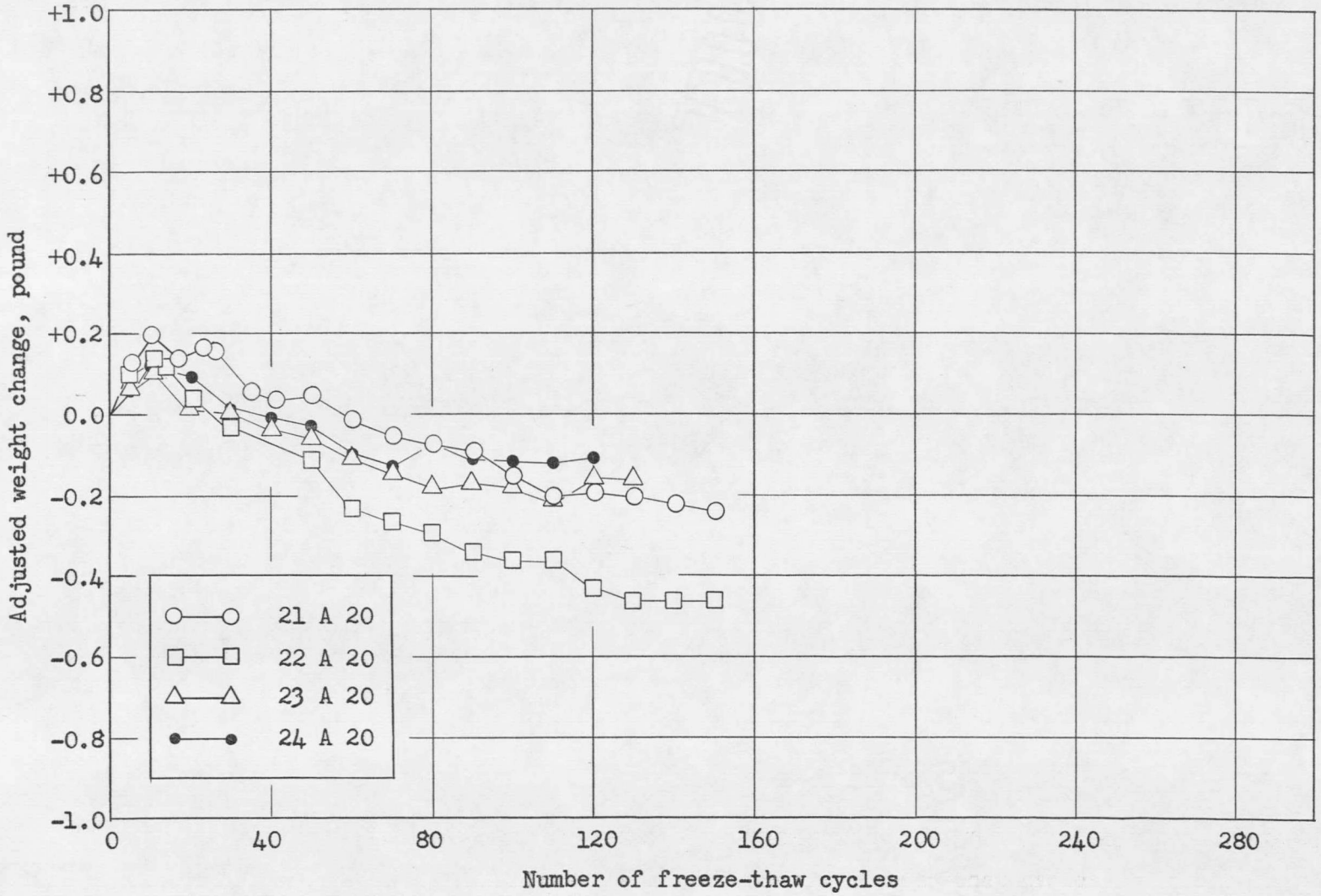


Fig. 69. Length changes versus number of freeze-thaw cycles for non-stressed, normally cured, water ponded slabs.

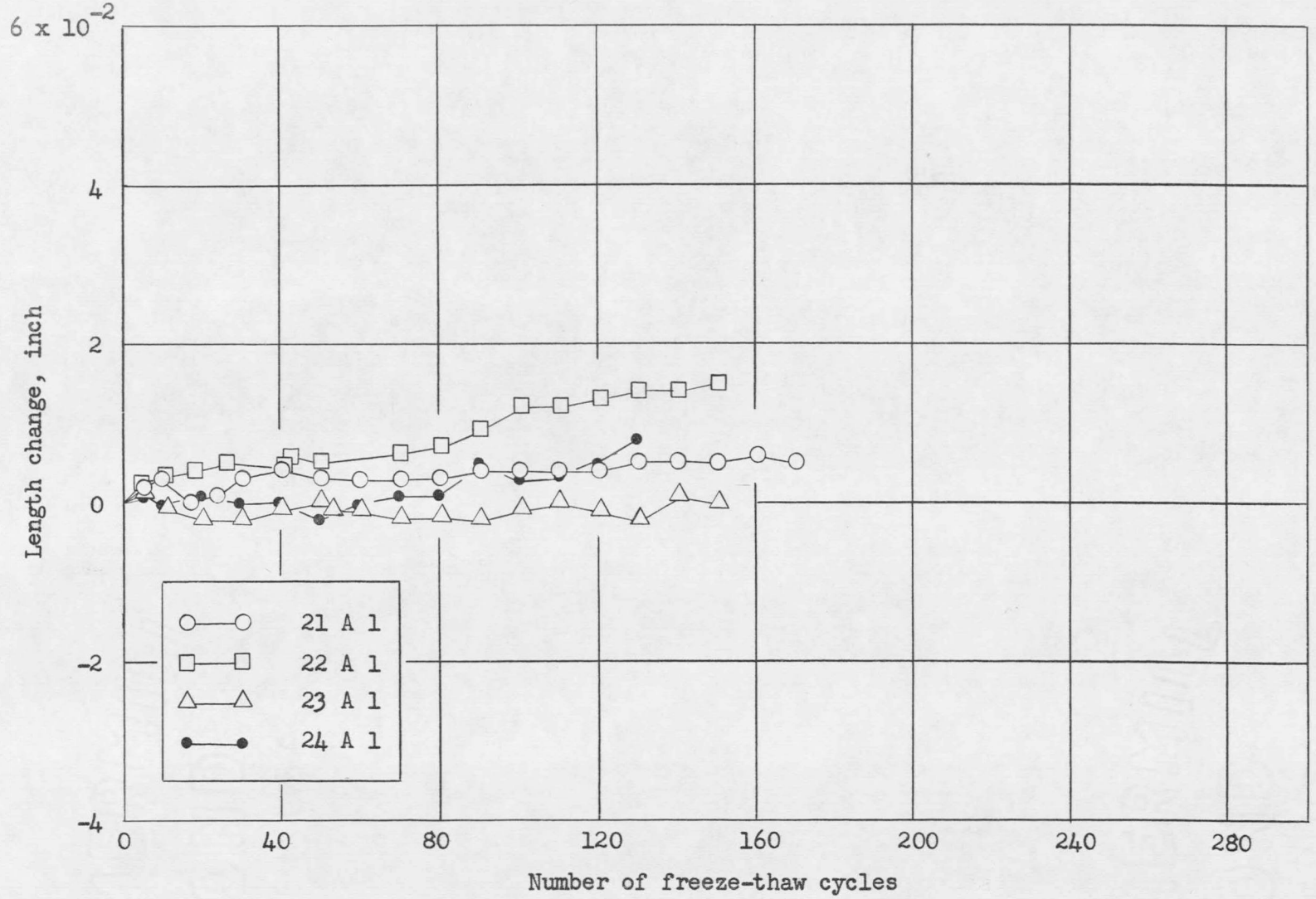


Fig. 70. Length changes versus number of freeze-thaw cycles for non-stressed, normally cured, $CaCl_2$ solution ponded slabs.

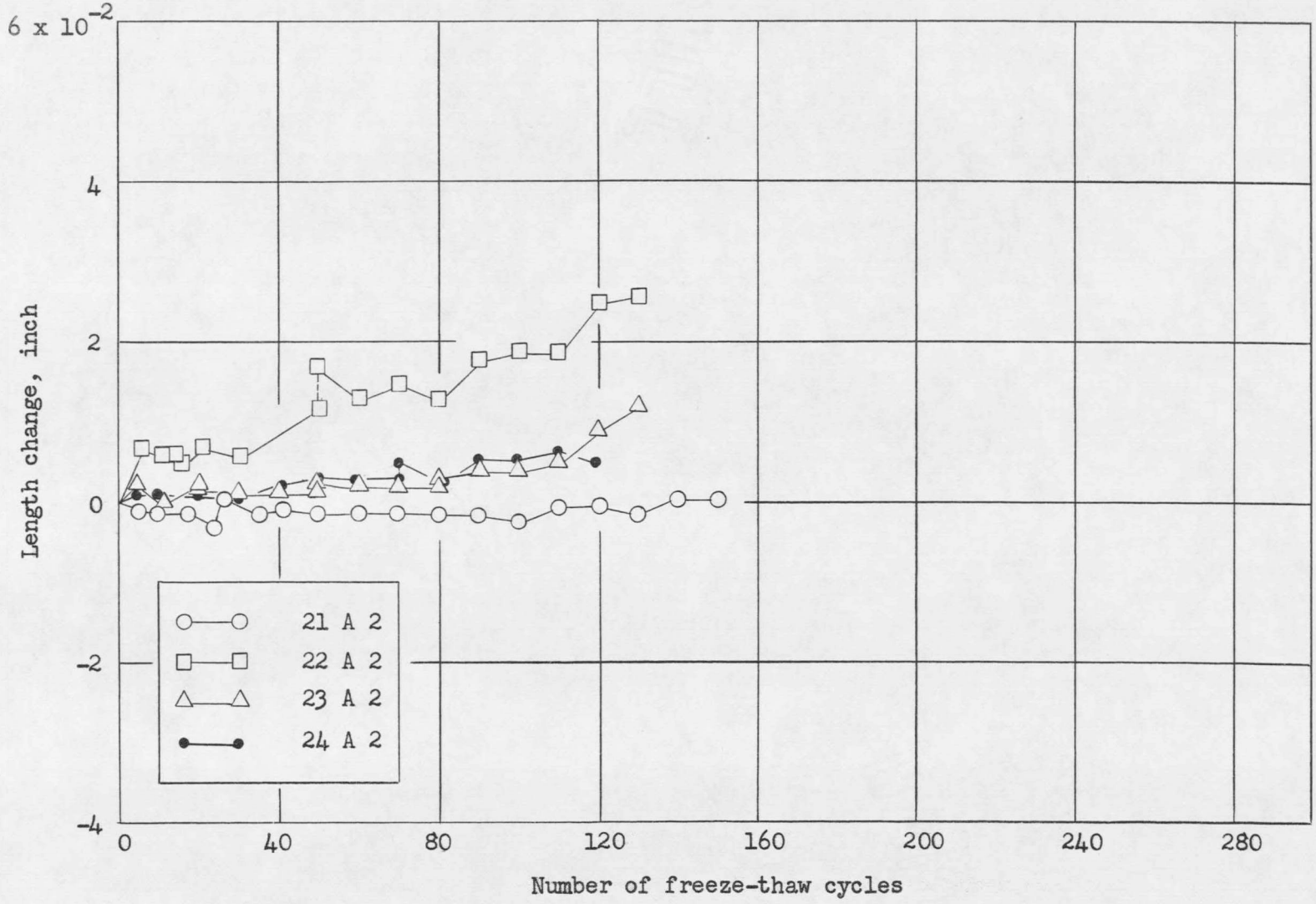


Fig. 71. Length changes versus number of freeze-thaw cycles for non-stressed, steam cured, water ponded slabs.

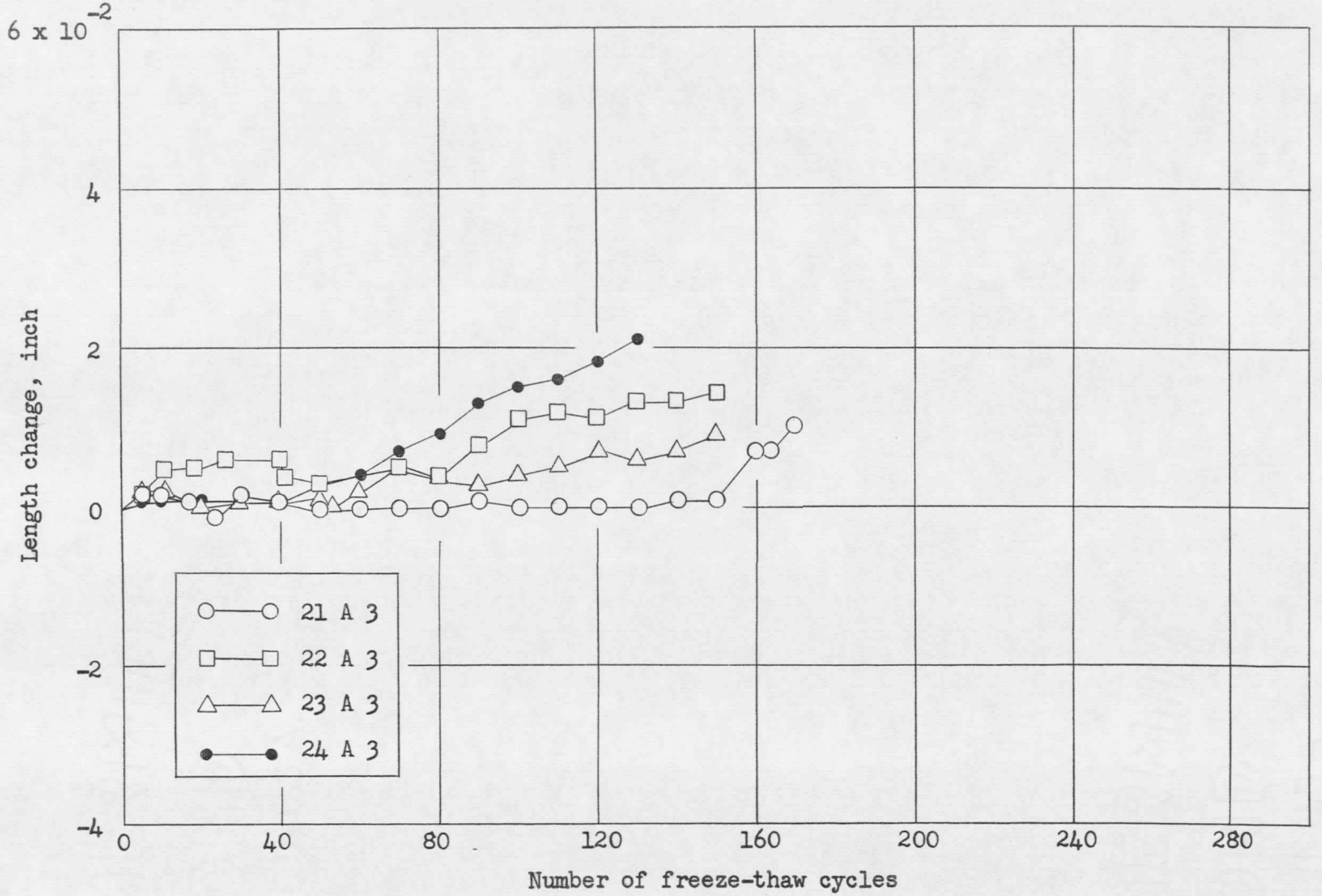


Fig. 72. Length changes versus number of freeze-thaw cycles for non-stressed, steam cured, $CaCl_2$ solution ponded slabs.

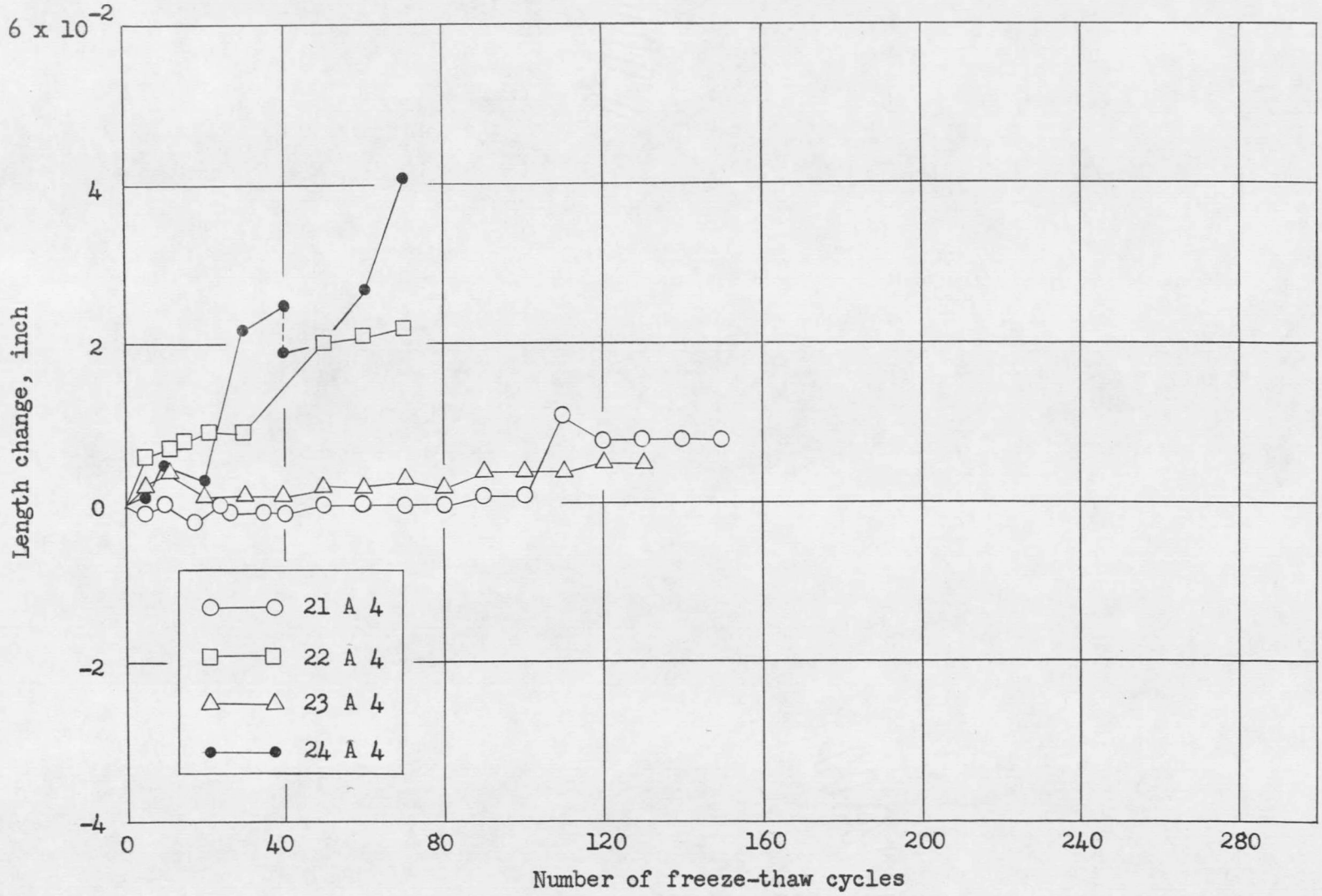


Fig. 73. Length changes versus number of freeze-thaw cycles for 500 psi., normally cured, water ponded slabs.

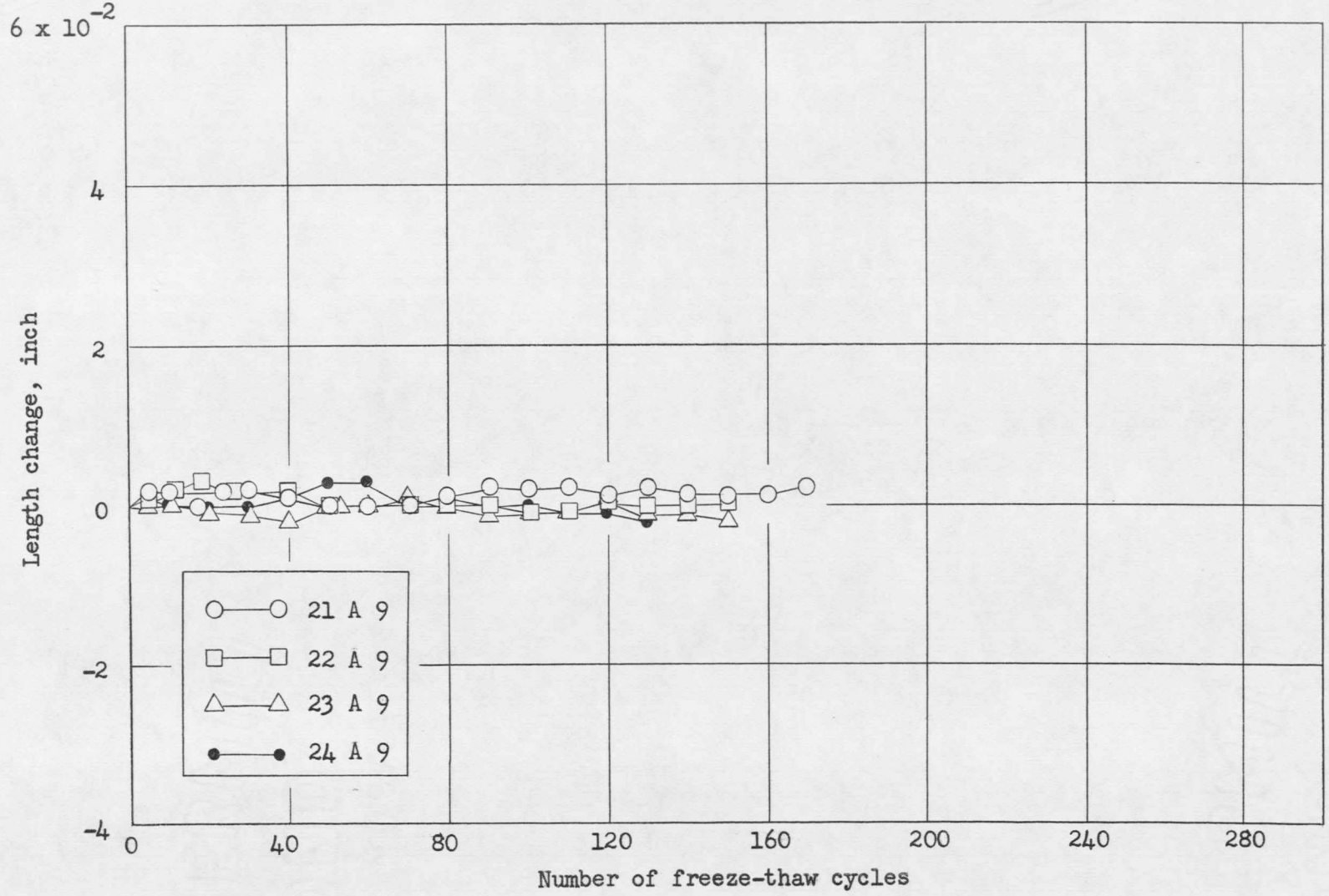


Fig. 74. Length changes versus number of freeze-thaw cycles for 500 psi., normally cured, $CaCl_2$ solution ponded slabs.

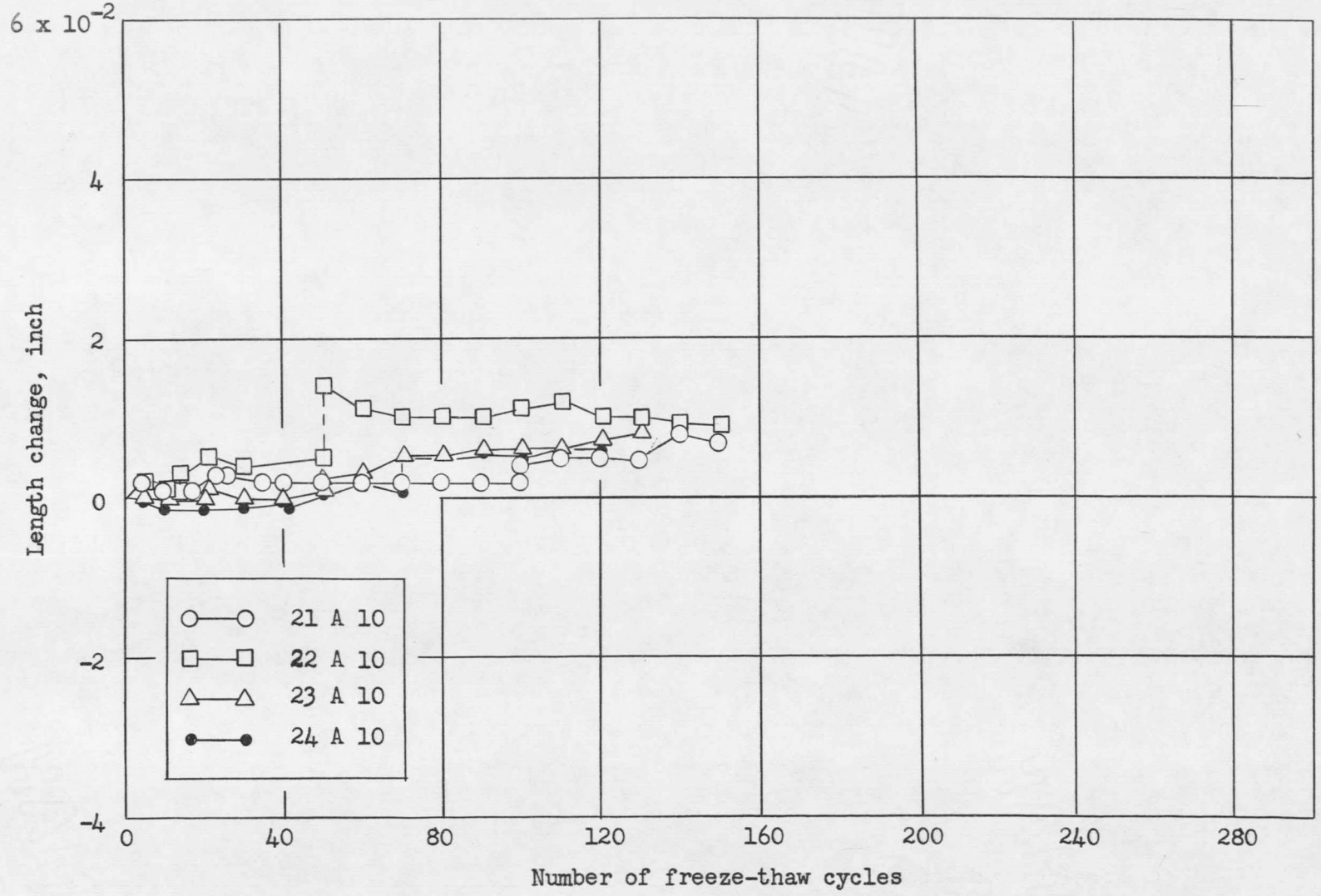


Fig. 75. Length changes versus number of freeze-thaw cycles for 500 psi., steam cured, water ponded slabs.

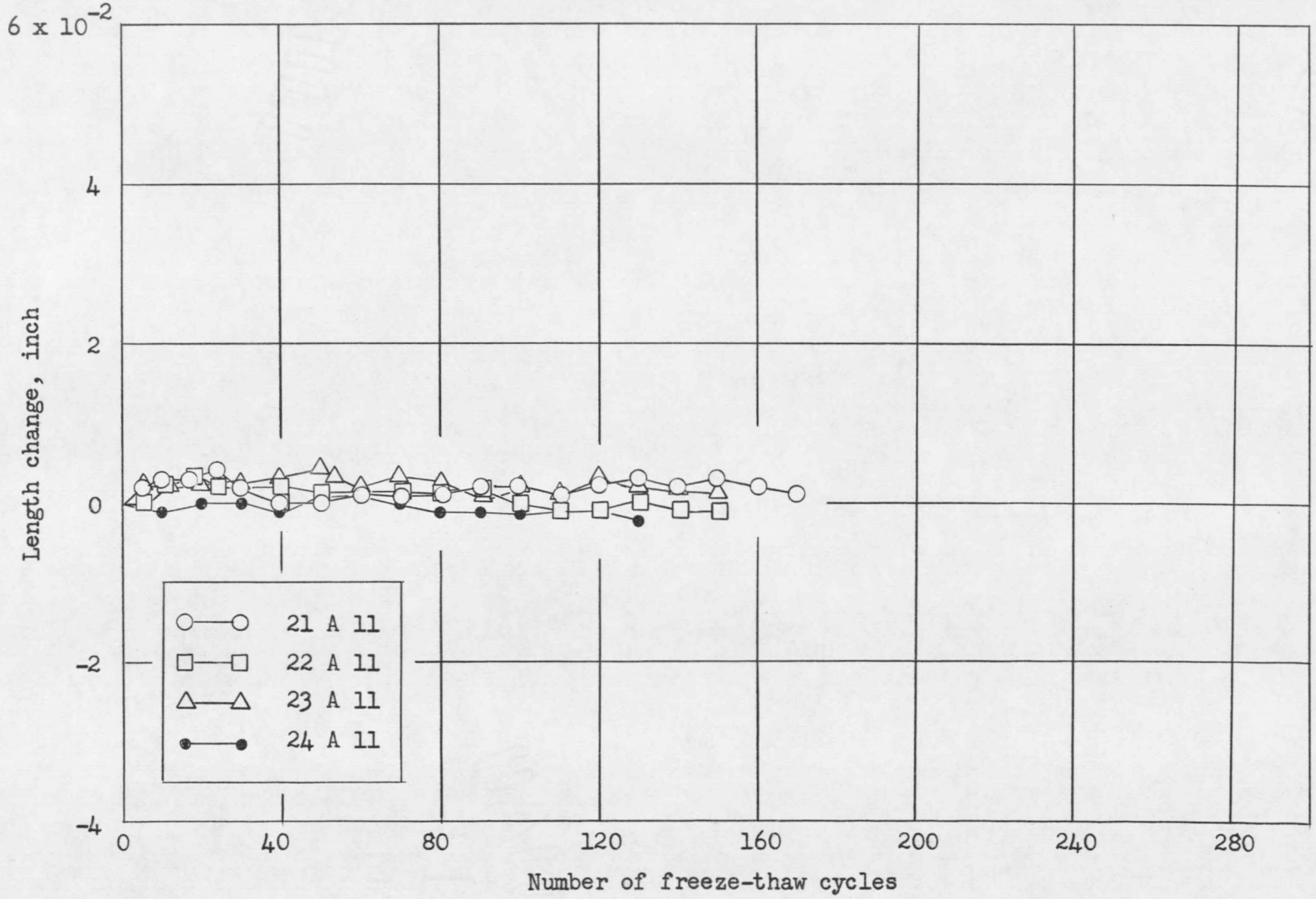


Fig. 76. Length changes versus number of freeze-thaw cycles for 500 psi., steam cured, $CaCl_2$ solution ponded slabs.

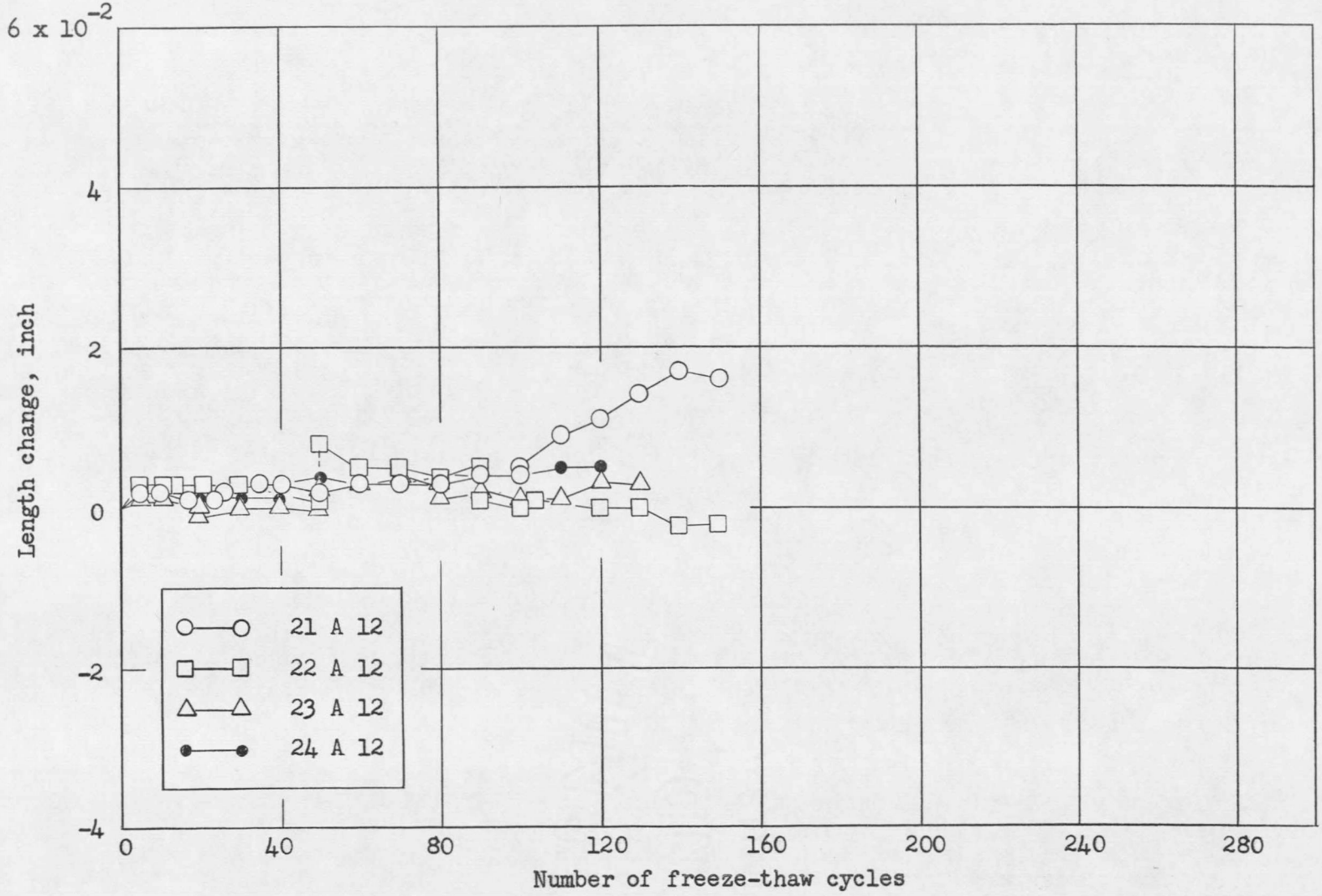


Fig. 77. Length changes versus number of freeze-thaw cycles for 1200 psi., normally cured, water ponded slabs.

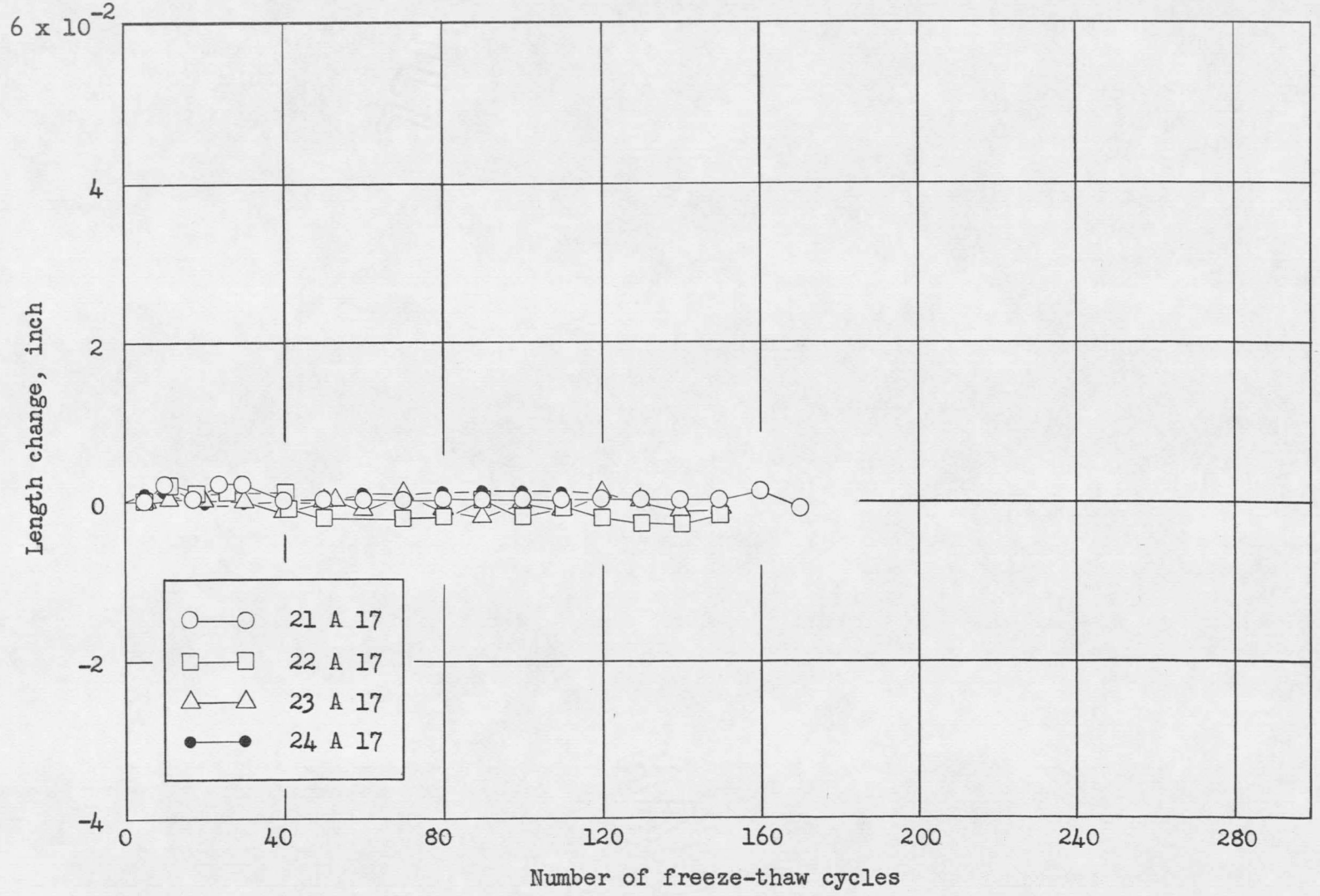


Fig. 78. Length changes versus number of freeze-thaw cycles for 1200 psi., normally cured, $CaCl_2$ solution ponded slabs.

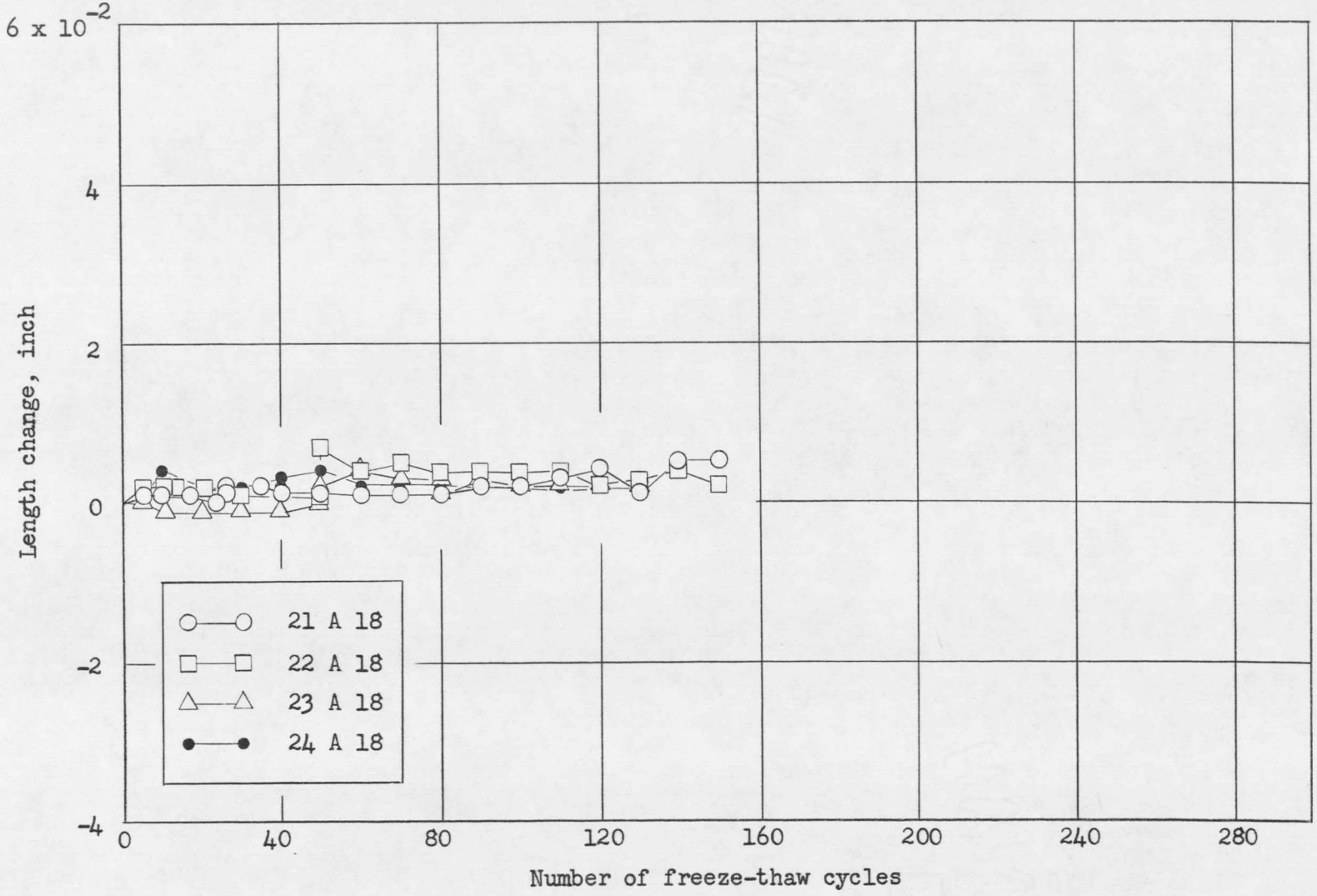


Fig. 79. Length changes versus number of freeze-thaw cycles for 1200 psi., steam cured, water ponded slabs.

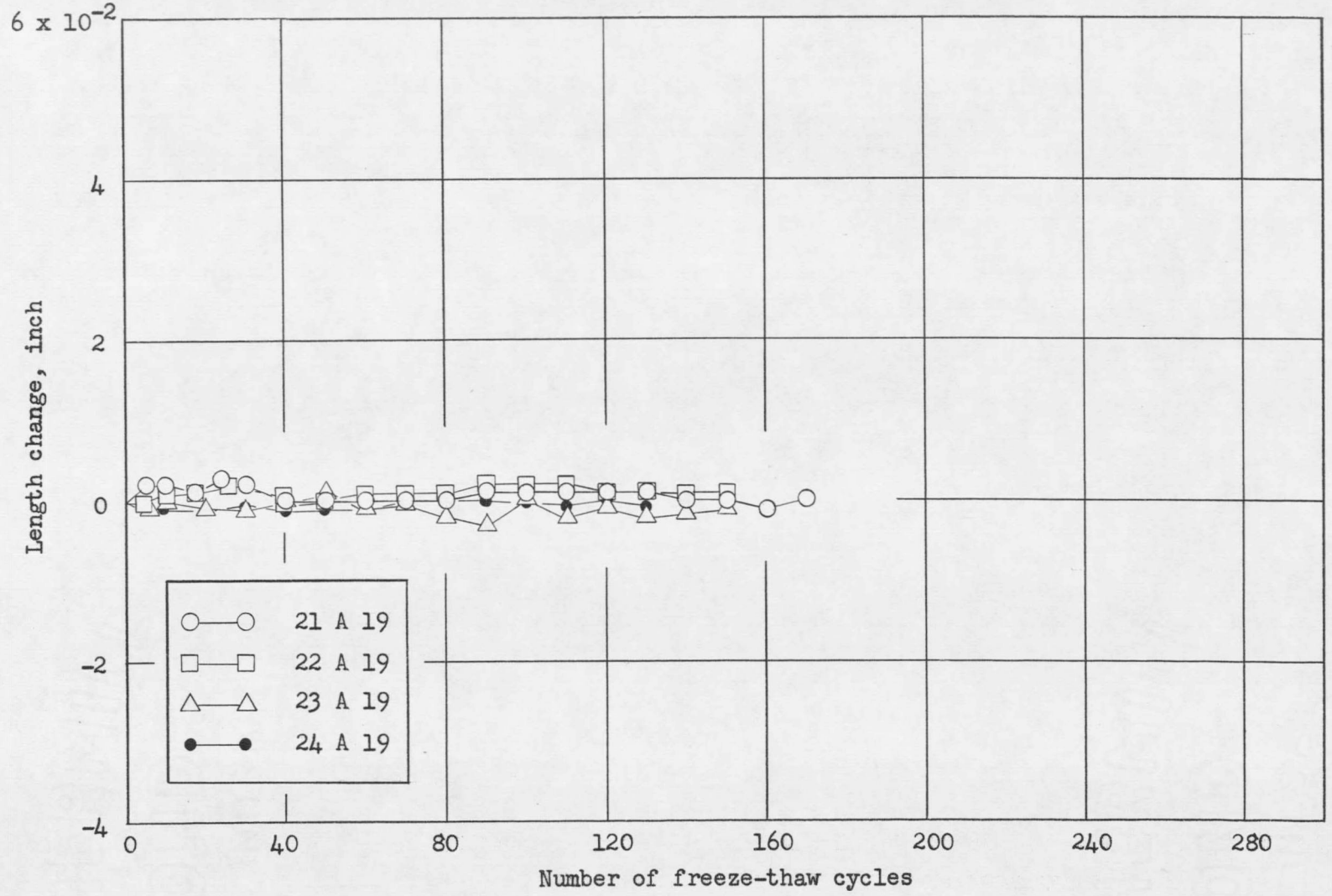


Fig. 80. Length changes versus number of freeze-thaw cycles for 1200 psi., steam cured, $CaCl_2$ solution ponded slabs.

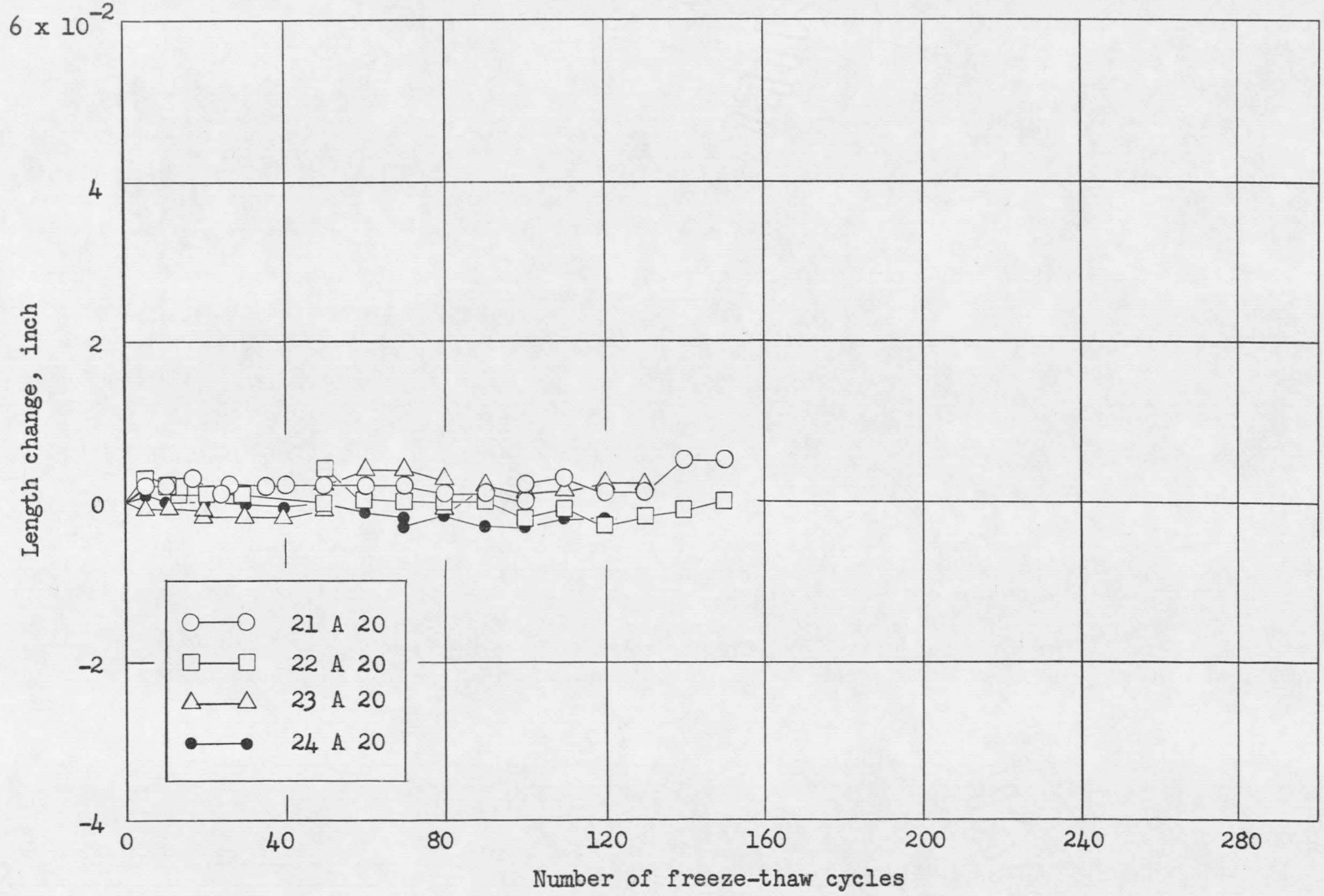


Fig. 81. Scaling weight losses versus number of freeze-thaw cycles for non-stressed, normally cured, $CaCl_2$ solution ponded slabs.

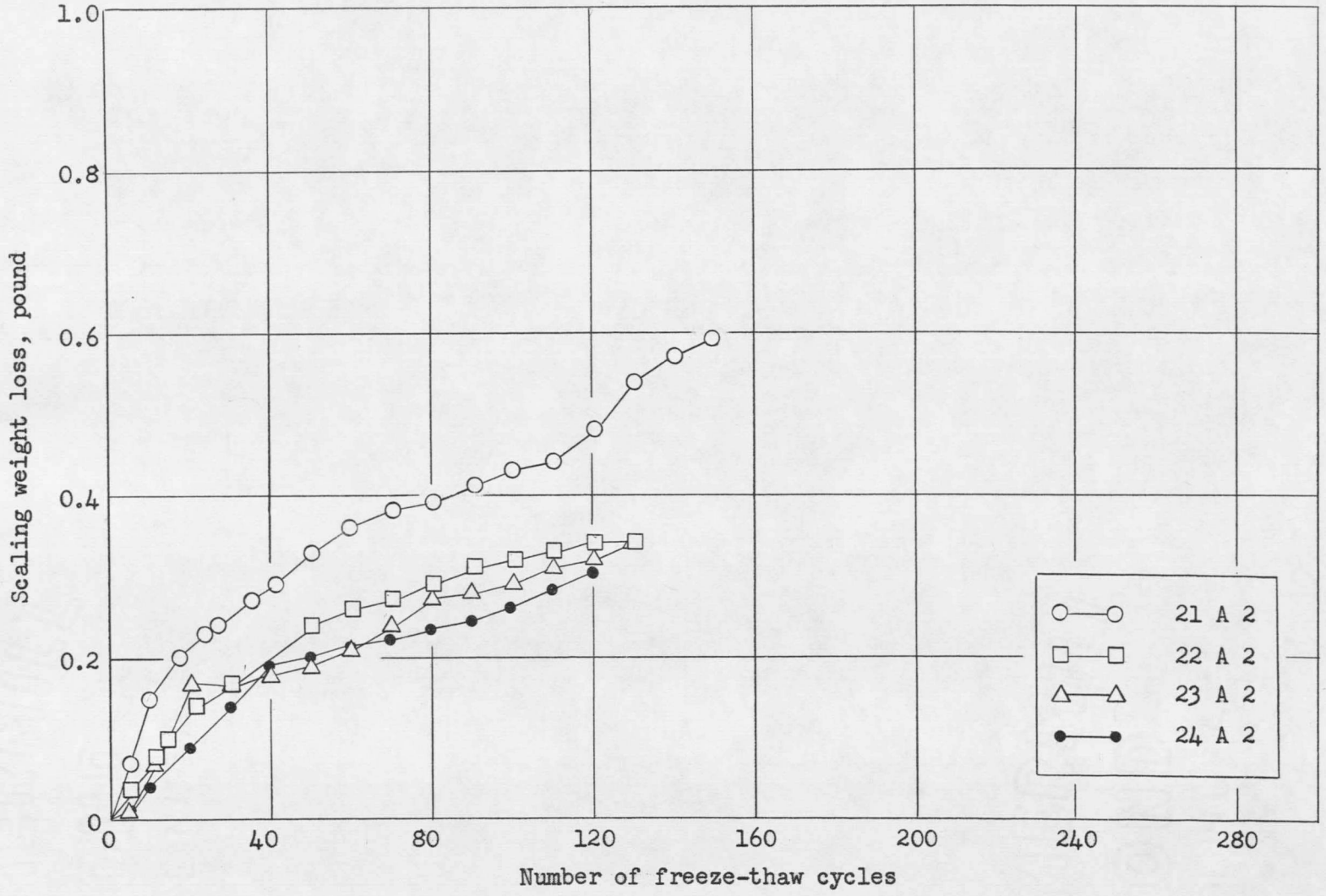


Fig. 82. Scaling weight losses versus number of freeze-thaw cycles for non-stressed, steam cured, $CaCl_2$ solution ponded slabs.

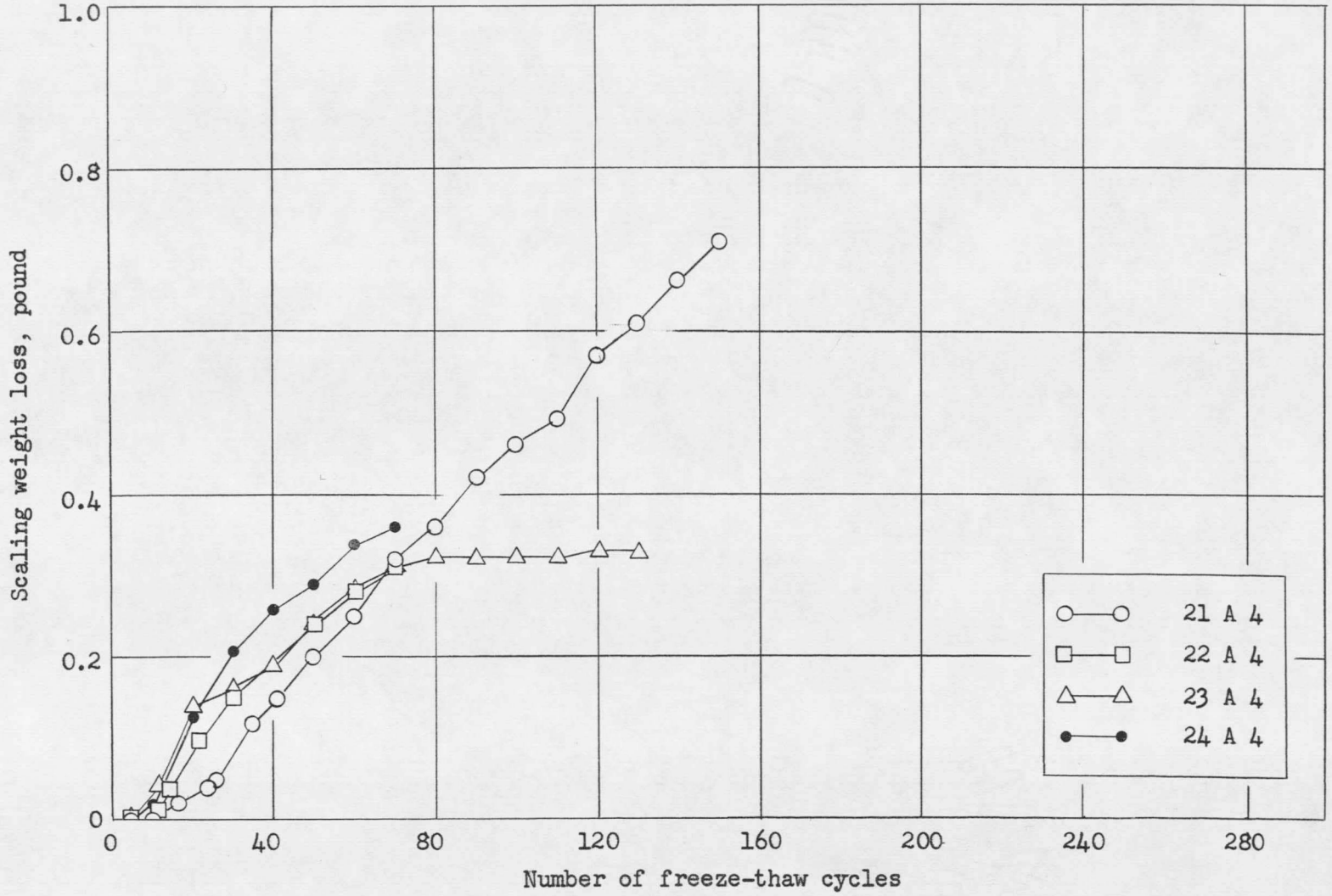


Fig. 83. Scaling weight losses versus number of freeze-thaw cycles for 500 psi., normally cured, $CaCl_2$ solution ponded slabs.

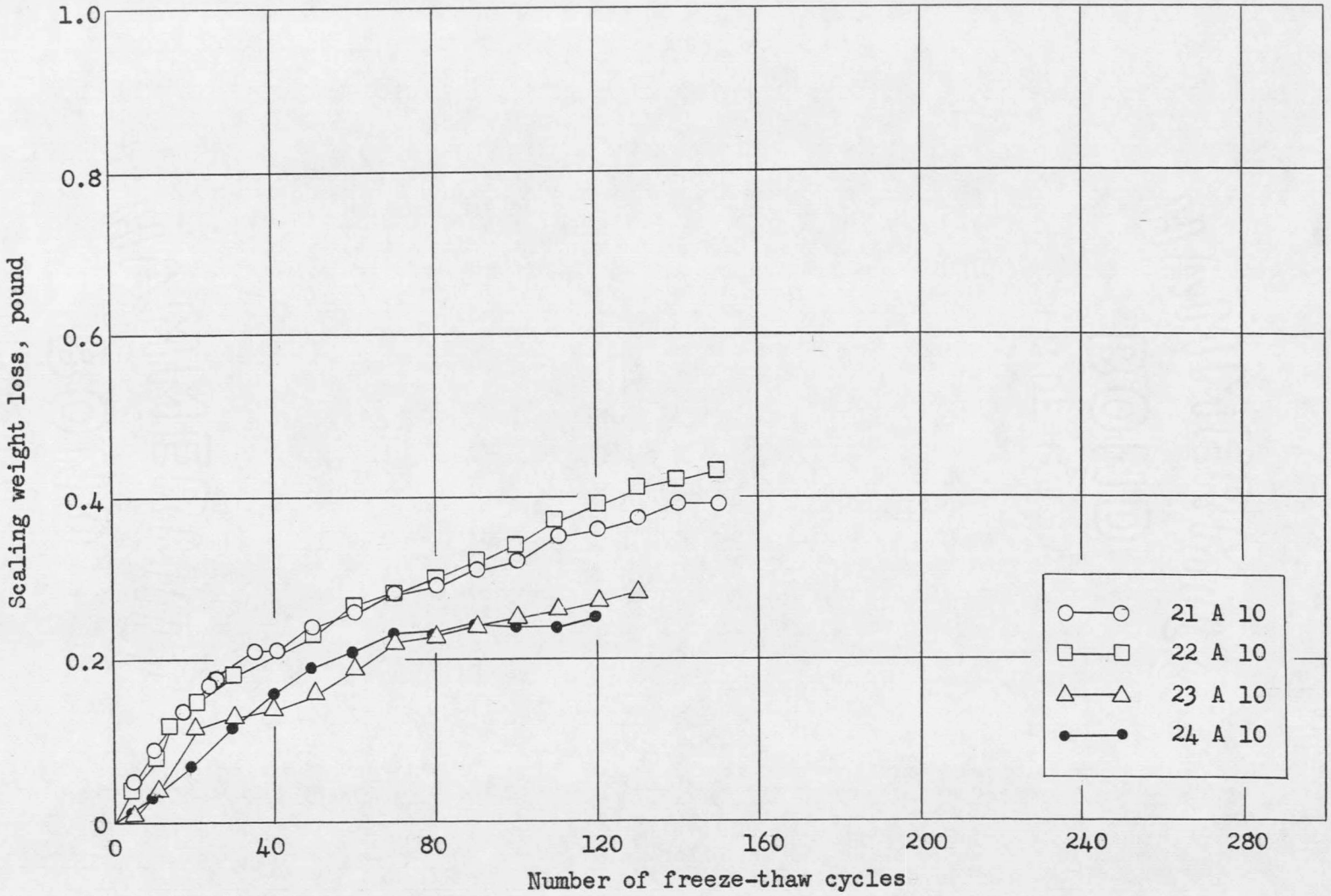


Fig. 84. Scaling weight losses versus number of freeze-thaw cycles for 500 psi., steam cured, $CaCl_2$ solution ponded slabs.

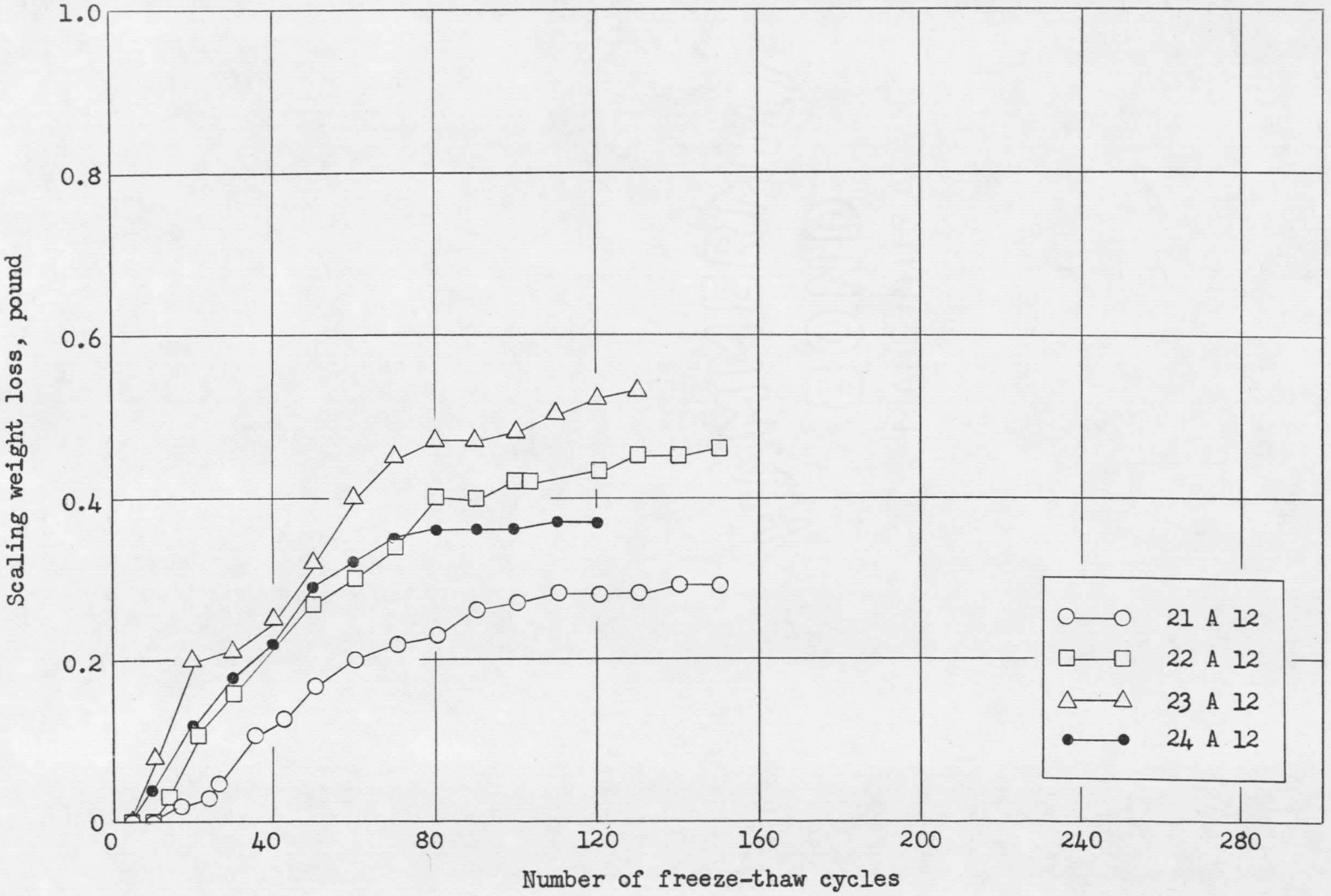


Fig. 85. Scaling weight losses versus number of freeze-thaw cycles for 1200 psi., normally cured, $CaCl_2$ solution ponded slabs.

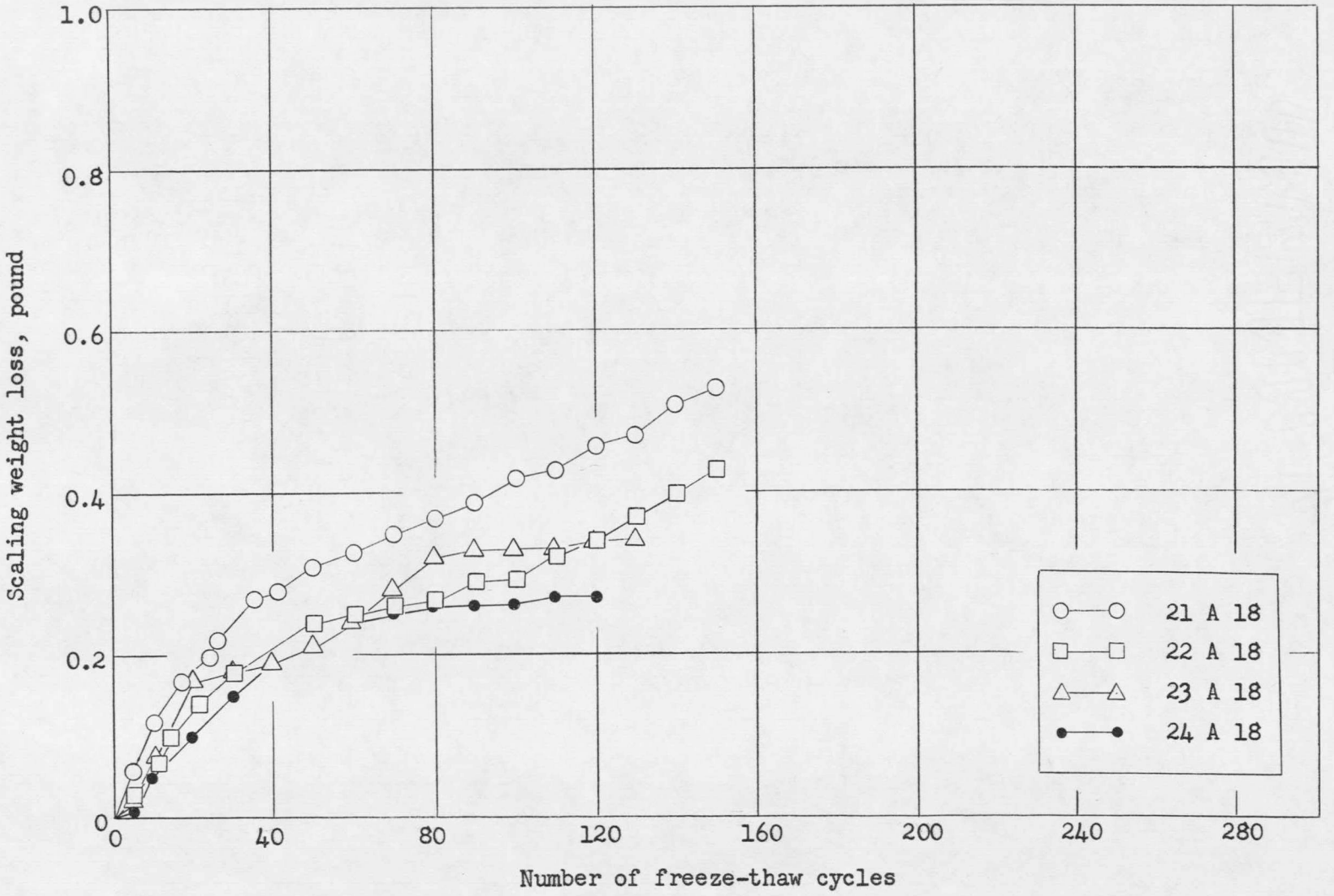
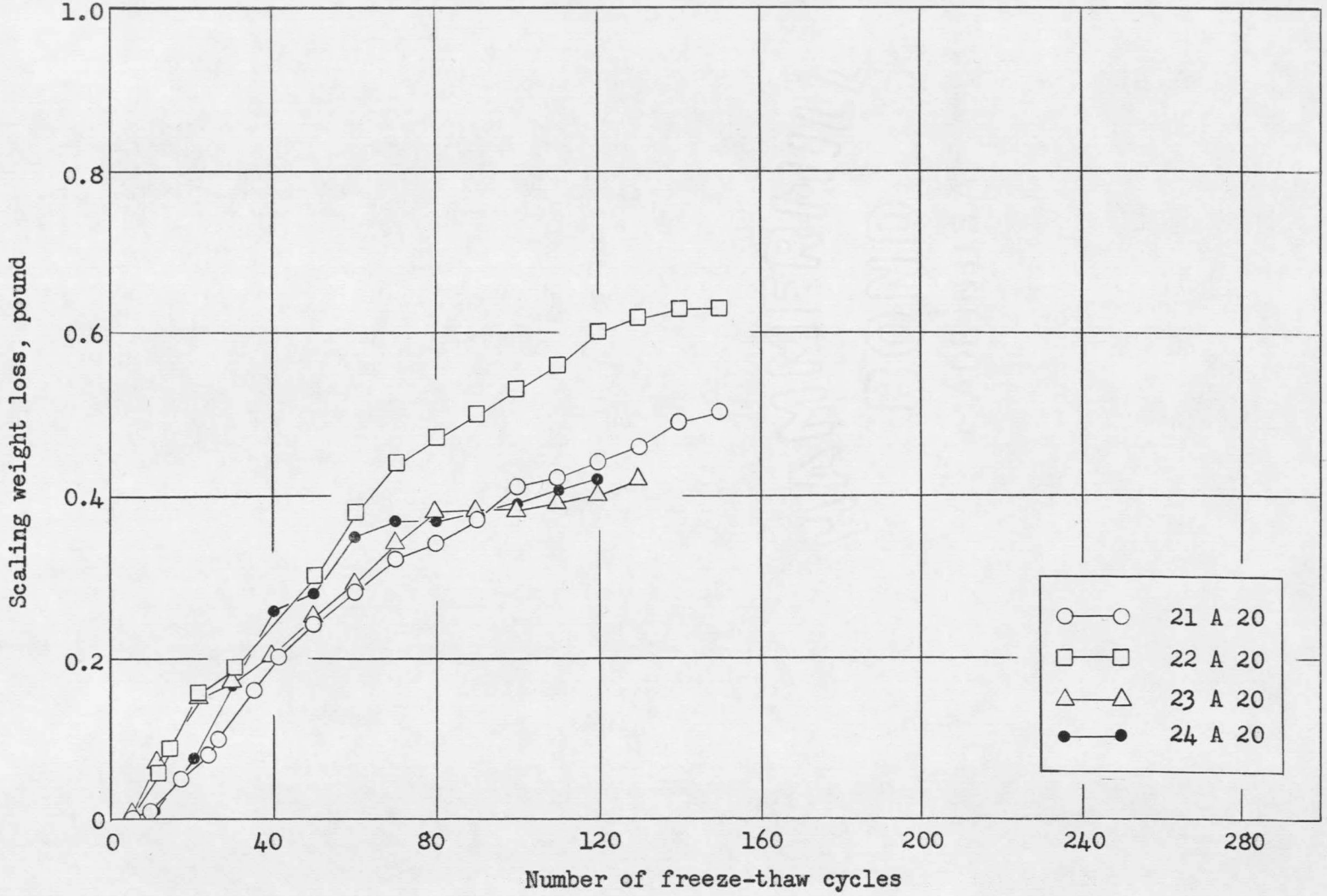


Fig. 86. Scaling weight losses versus number of freeze-thaw cycles for 1200 psi., steam cured, $CaCl_2$ solution ponded slabs.



APPENDIX F

PERMEABILITY STUDY DATA

Fig. 87. Net absorptions versus number of days for non-stressed, normally cured slabs under two-foot head of water.

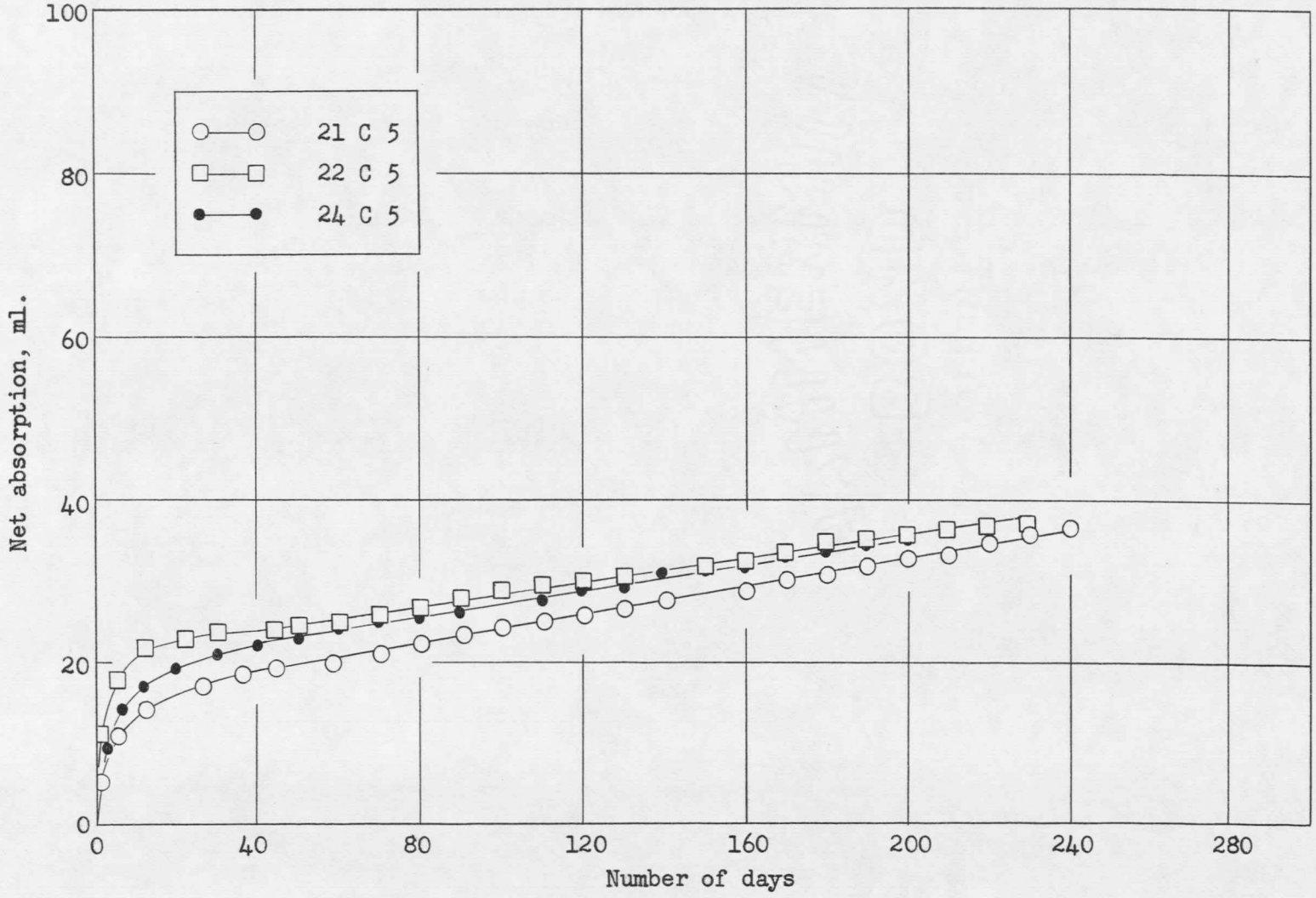


Fig. 88. Net absorptions versus number of days for non-stressed, normally cured slabs under two-foot head of $CaCl_2$ solution.

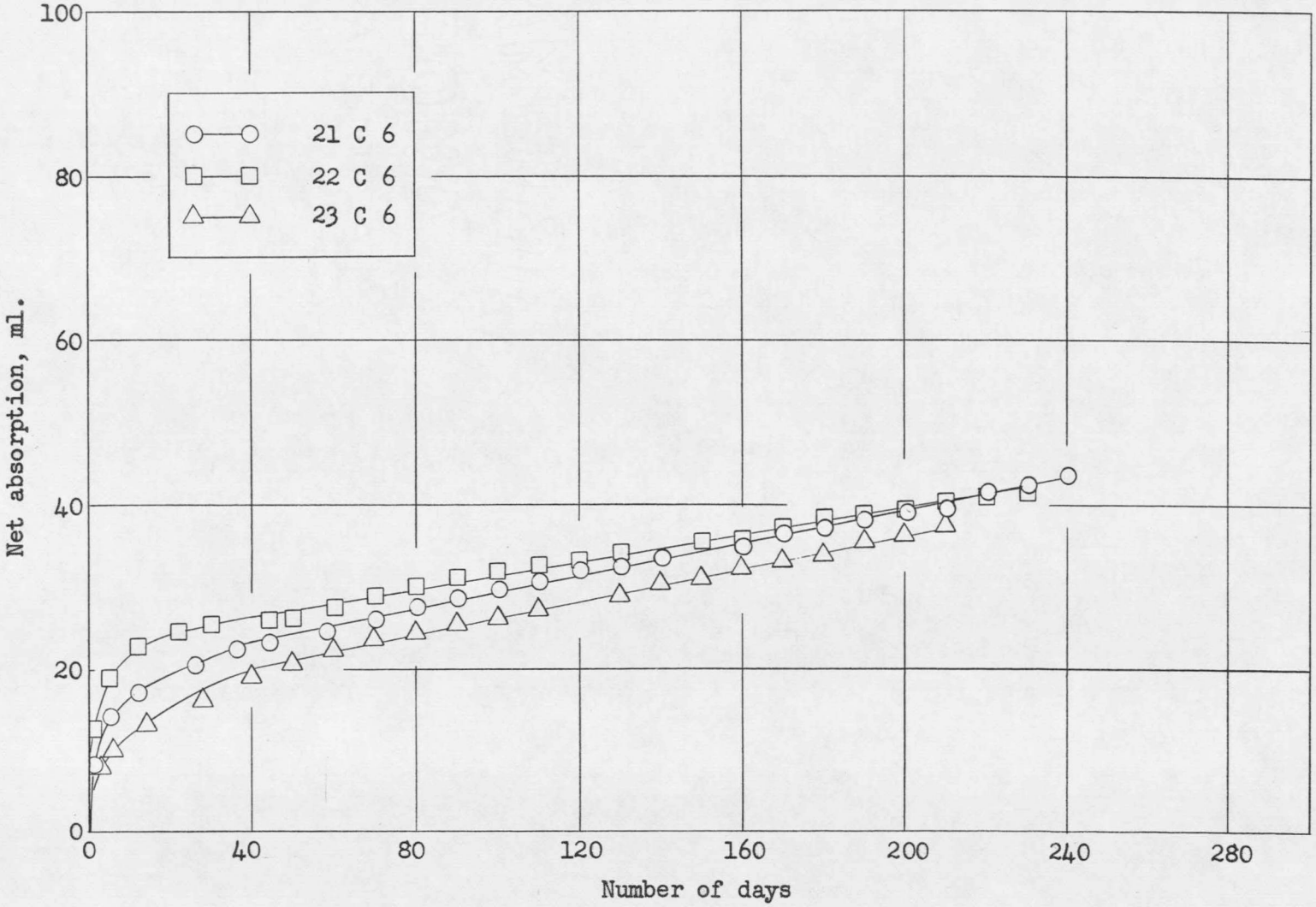


Fig. 89. Net absorptions versus number of days for non-stressed, steam cured slabs under two-foot head of water.

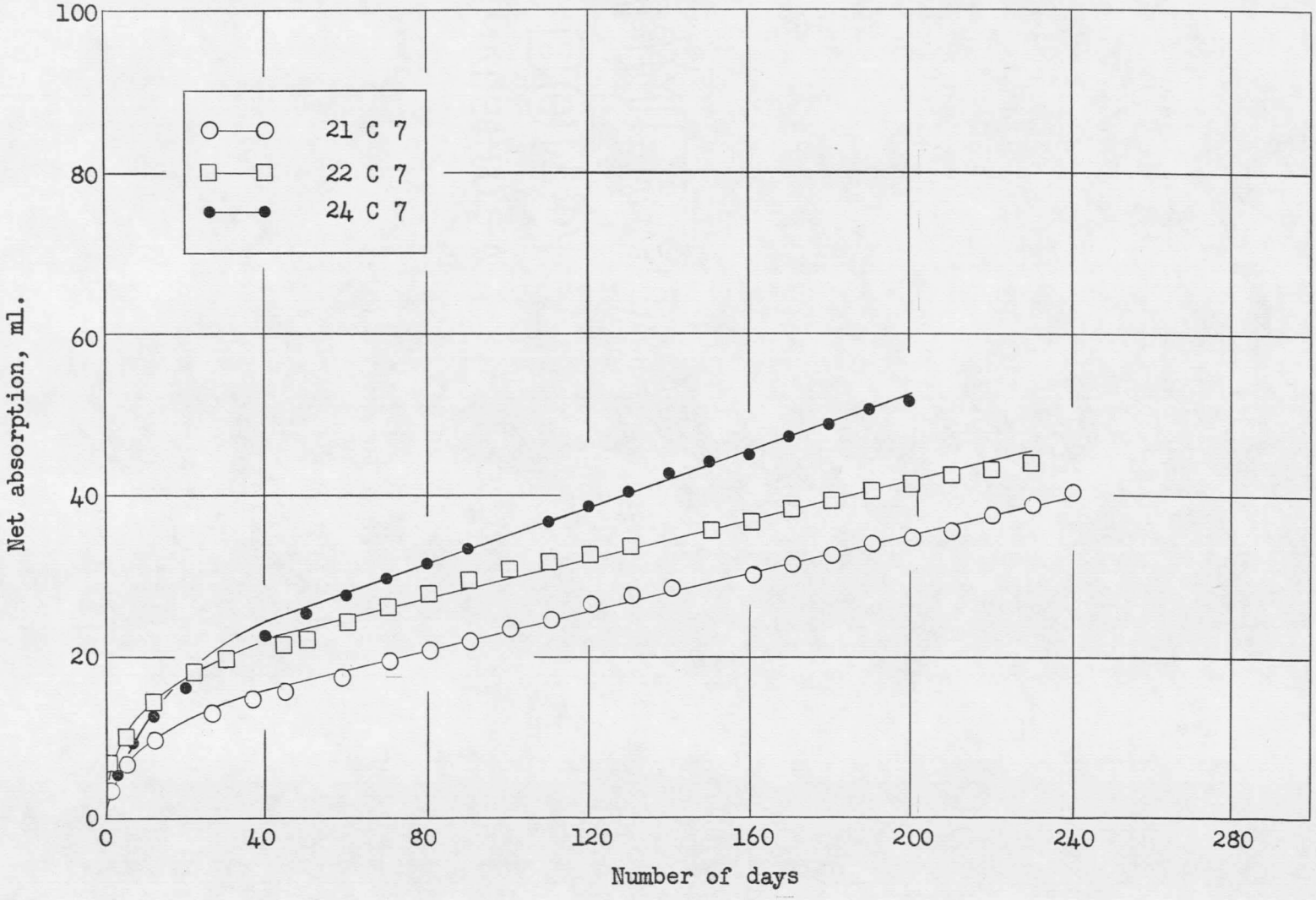


Fig. 90. Net absorptions versus number of days for non-stressed, steam cured slabs under two-foot head of $CaCl_2$ solution.

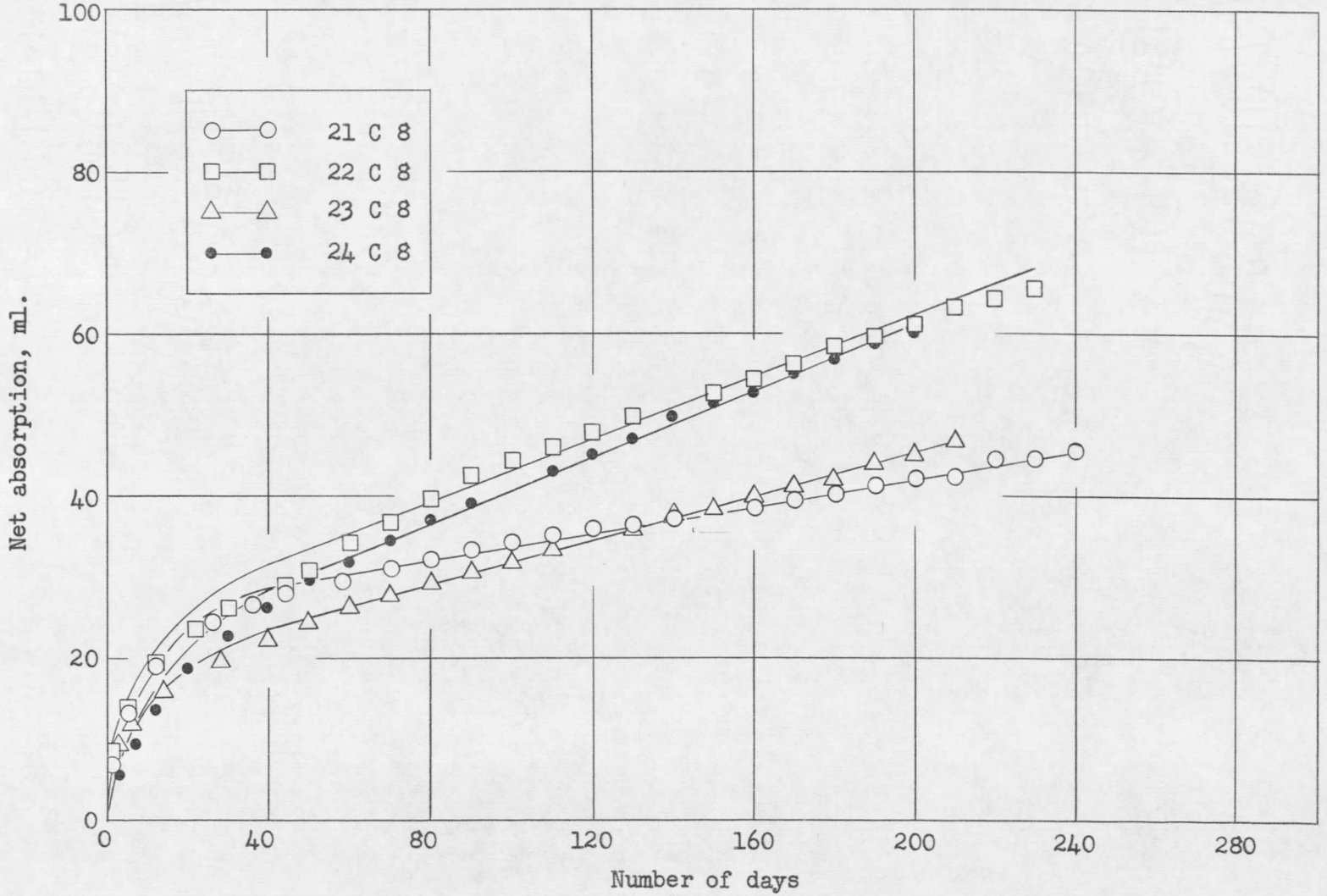


Fig. 91. Net absorptions versus number of days for 500 psi., normally cured slabs under two-foot head of water.

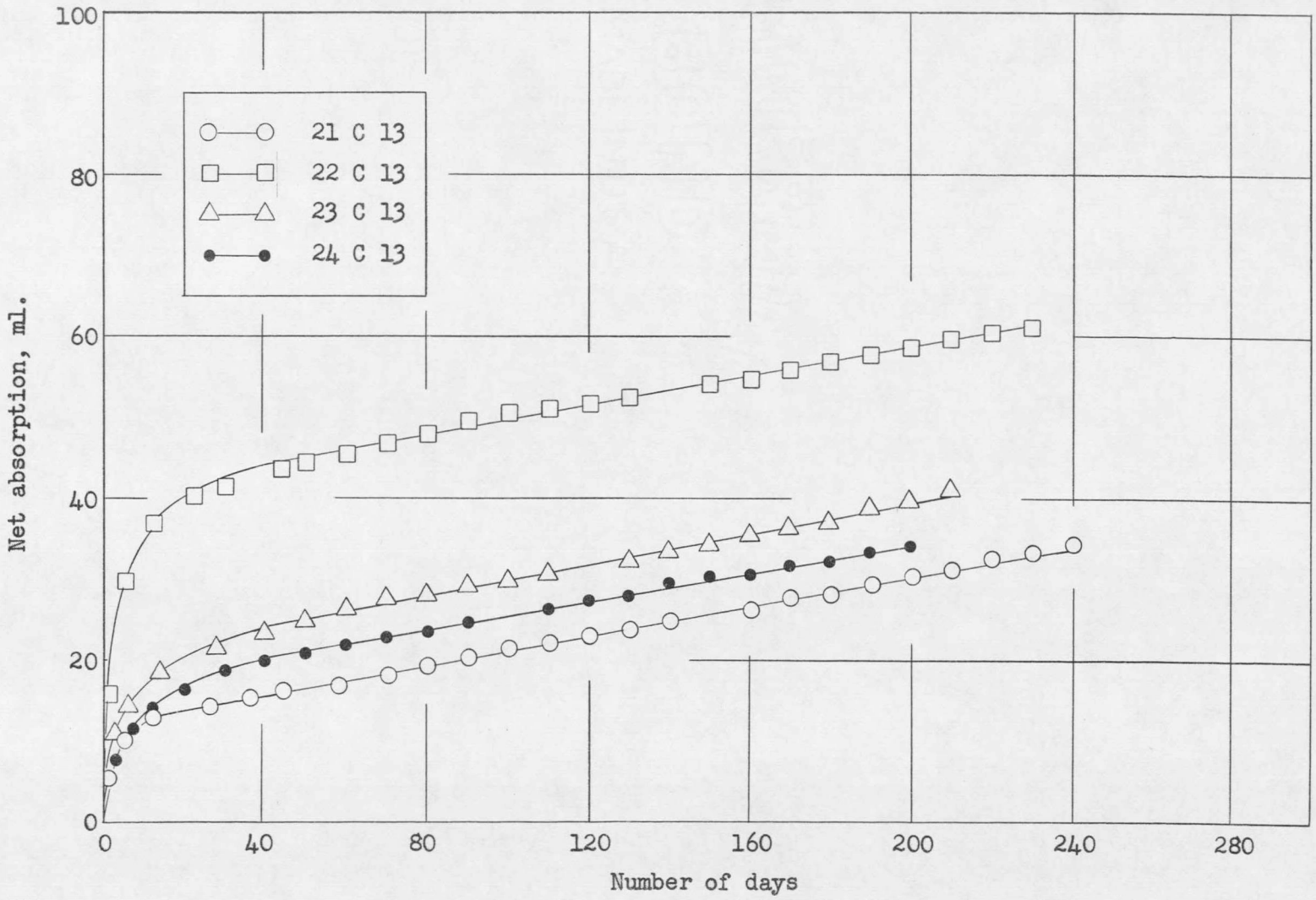


Fig. 92. Net absorptions versus number of days for 500 psi., normally cured slabs under two-foot head of $CaCl_2$ solution.

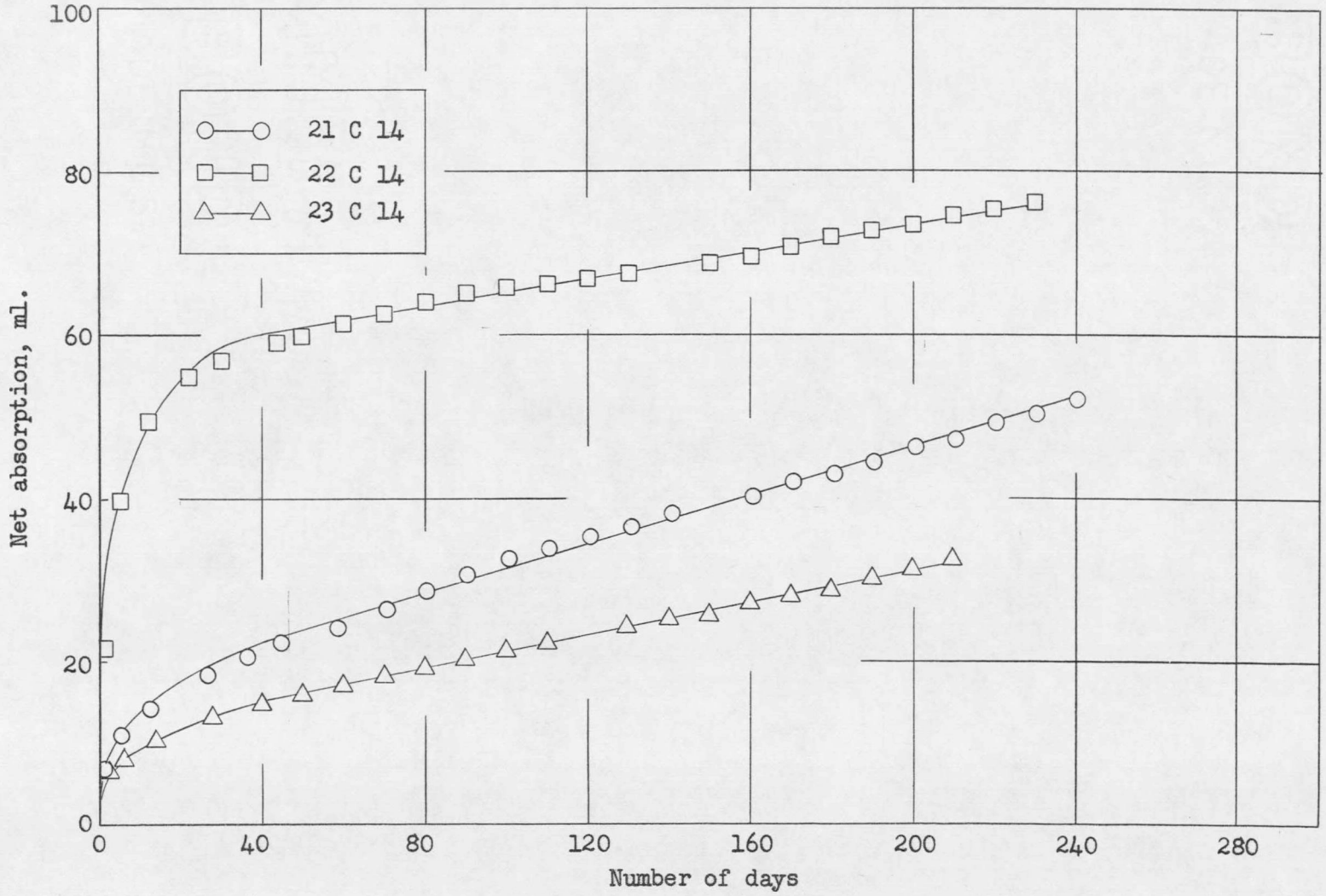


Fig. 93. Net absorptions versus number of days for 500 psi., steam cured slabs under two-foot head of water.

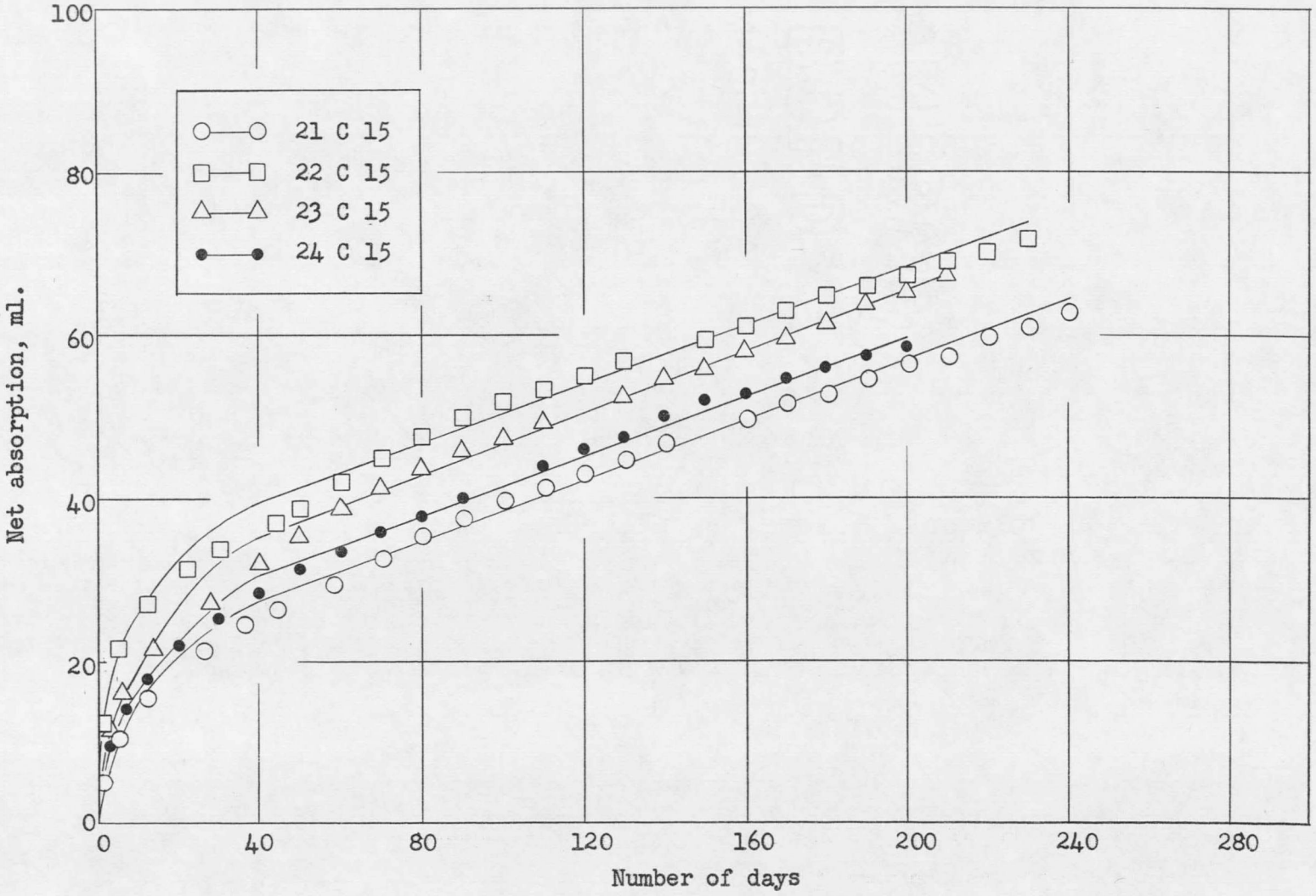


Fig. 94. Net absorptions versus number of days for 500 psi., steam cured slabs under two-foot head of $CaCl_2$ solution.

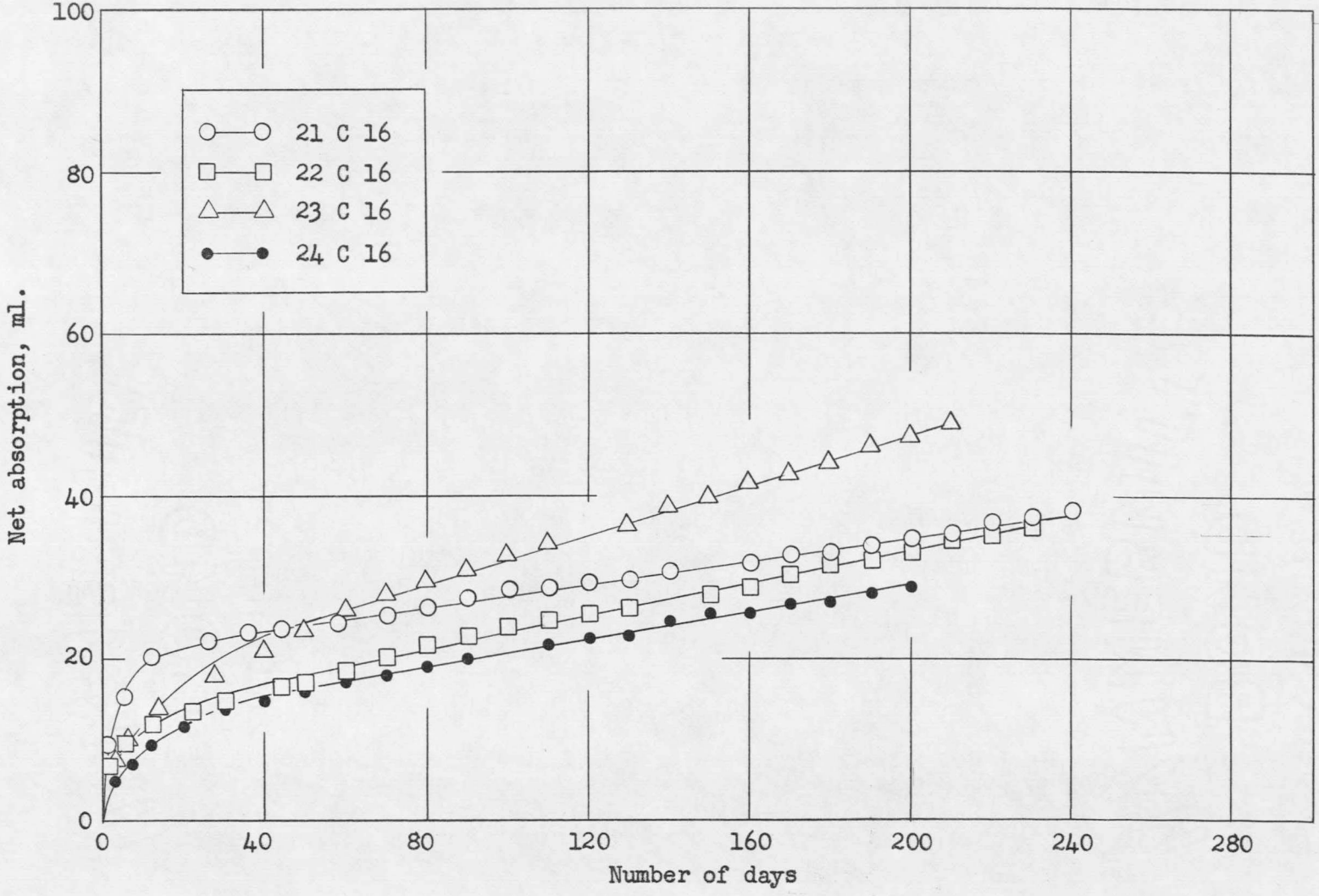


Fig. 95. Net absorptions versus number of days for 1200 psi., normally cured slabs under two-foot head of water.

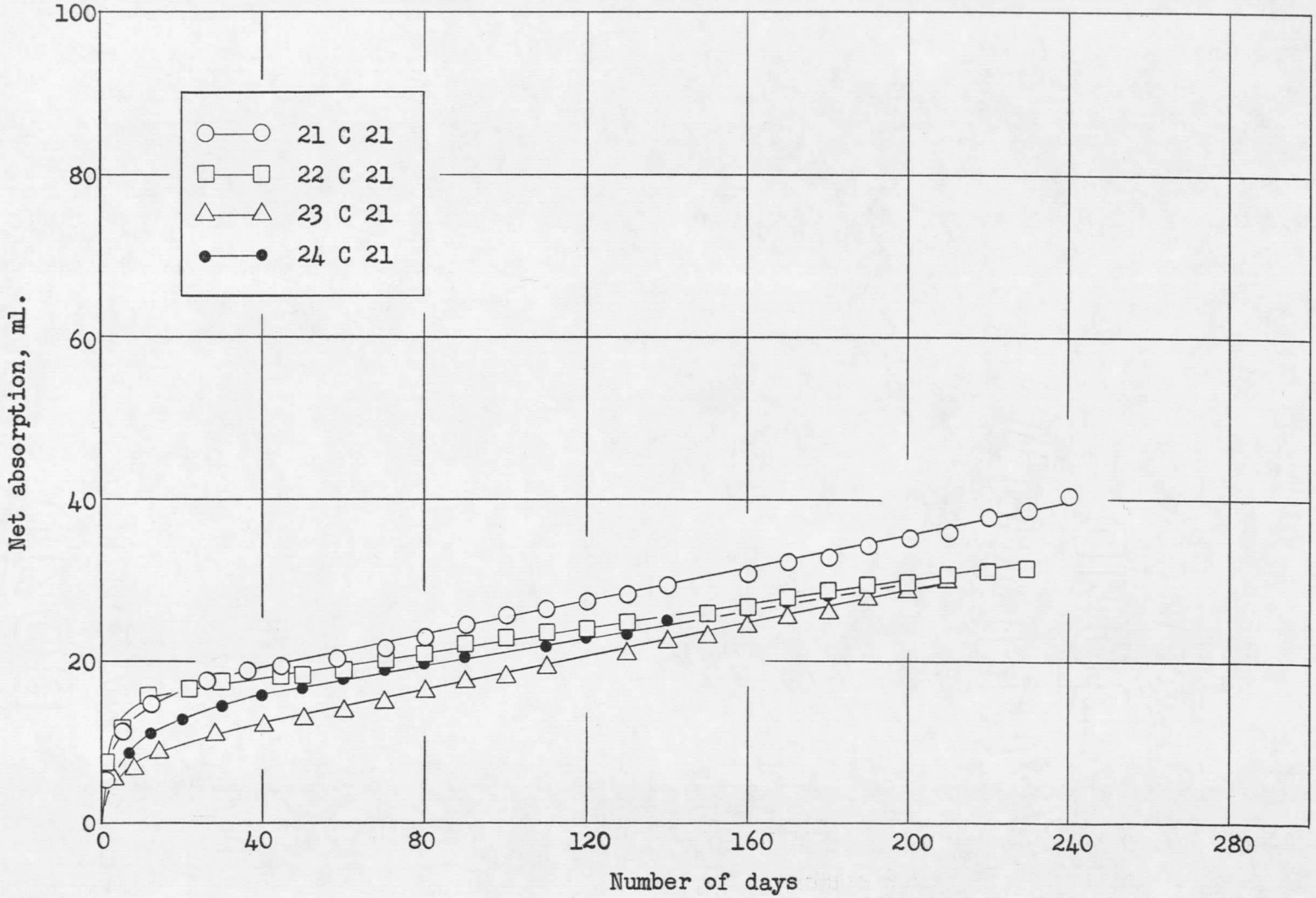


Fig. 96. Net absorptions versus number of days for 1200 psi., normally cured slabs under two-foot head of $CaCl_2$ solution.

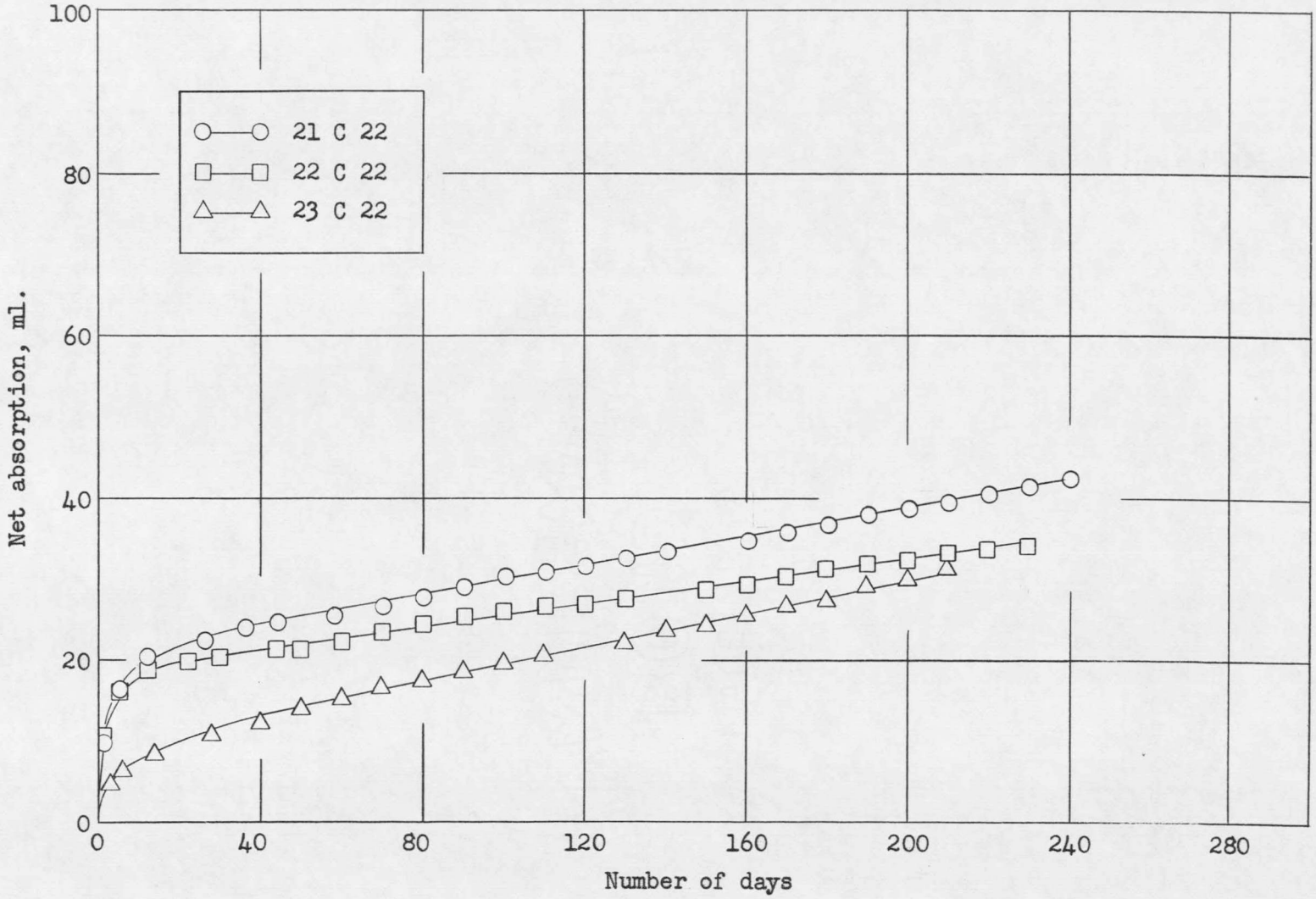


Fig. 97. Net absorptions versus number of days for 1200 psi., steam cured slabs under two-foot head of water.

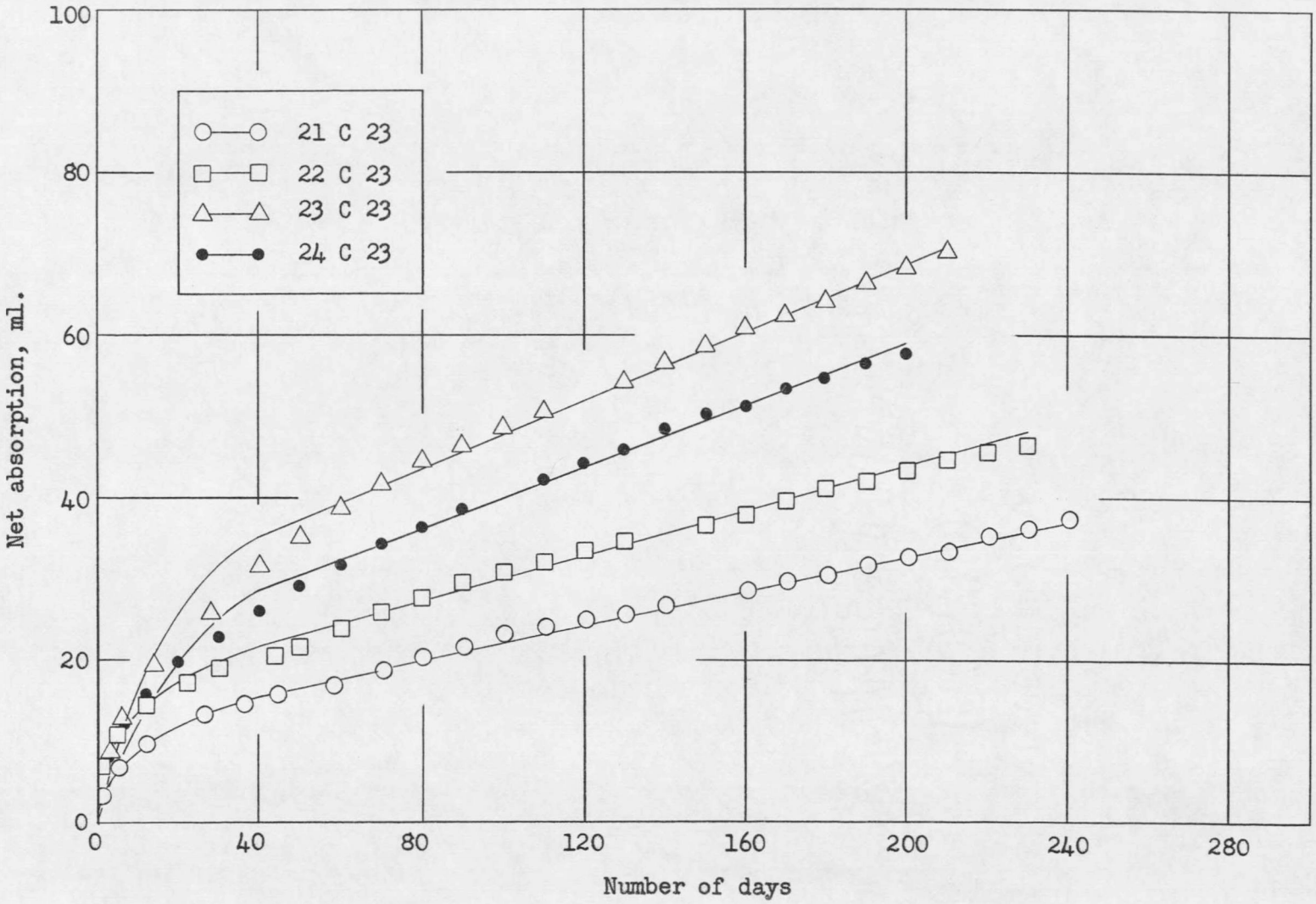
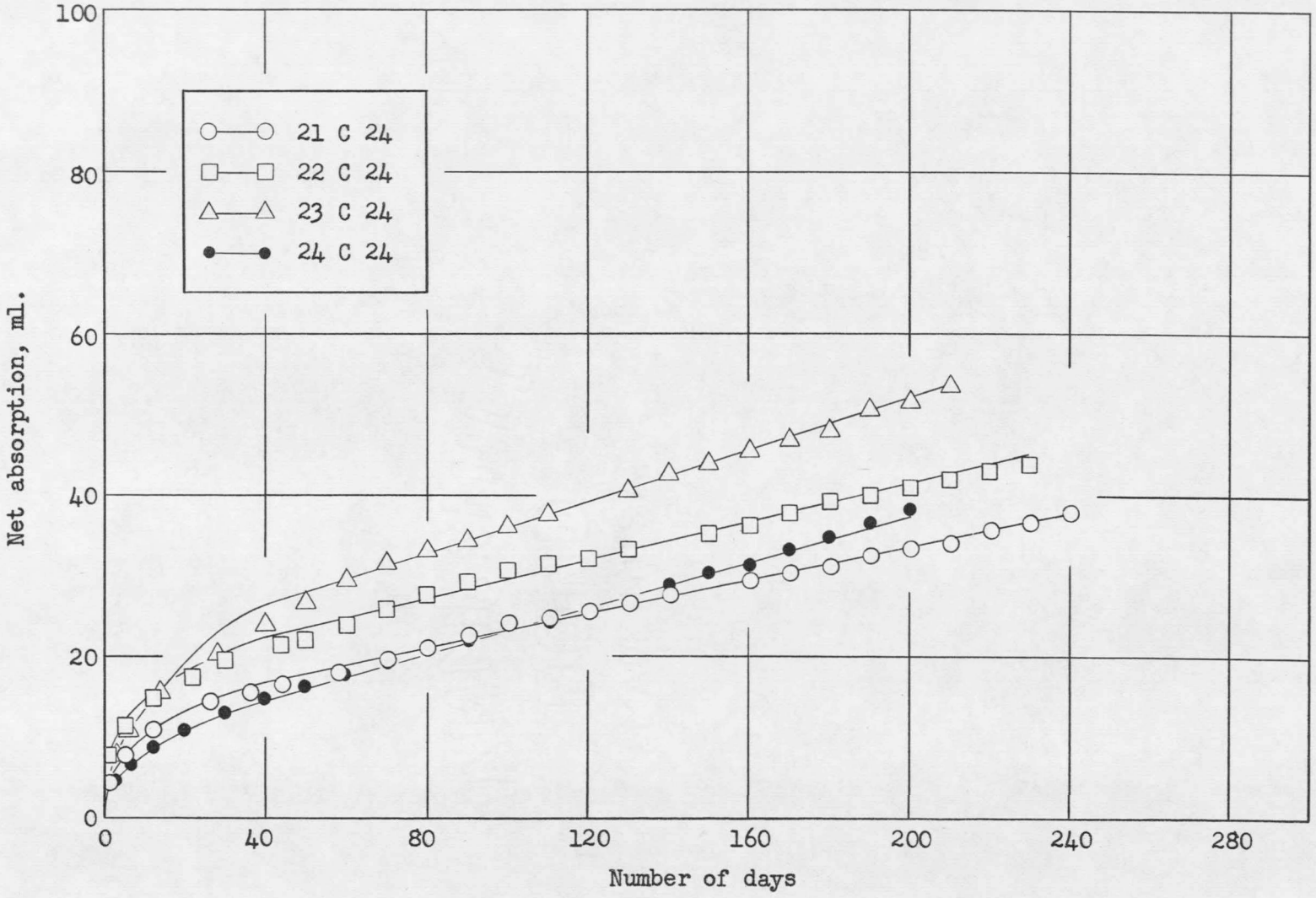


Fig. 98. Net absorptions versus number of days for 1200 psi., steam cured slabs under two-foot head of $CaCl_2$ solution.



LITERATURE CITED

1. Blanks, Robert F. and Kennedy, Henry L., The Technology of Cement and Concrete, John Wiley and Sons, Inc., New York, 1955.

2. Troxell, George E. and Davis, Harmer E., Composition and Properties of Concrete, McGraw-Hill Book Co. Inc., New York, 1956.

3. Powers, T. C., "Some Physical Aspects of the Hydration of Portland Cement," Journal of the Research and Development Laboratories, Portland Cement Association, Vol. 3, No. 1, January, 1961.

4. Brunauer, Stephen and Copeland, L. E., "The Chemistry of Concrete," Scientific American, April, 1964.

5. Neville, A. M., Properties of Concrete, John Wiley and Sons, Inc., New York, 1963.

6. Powers, T. C., "The Physical Structure and Engineering Properties of Concrete," Research Department Bulletin 90, Research and Development Laboratories of the Portland Cement Association, July, 1958.

7. Grudemo, Ake, "The Microstructure of Hardened Cement Paste," Proceedings of the Fourth International Symposium on the Chemistry of Cement, U. S. Department of Commerce, National Bureau of Standards, Monograph 43, Vol. II, 1962.

8. Brunauer, Stephen, and Greenberg, S. A., "The Hydration of Tricalcium Silicate and β-Dicalcium Silicate at Room Temperature," Proceedings of the Fourth International Symposium on the Chemistry of Cement, U. S. Department of Commerce, National Bureau of Standards, Monograph 43, Vol. I, 1962.

9. Copeland, L. E. and Schulz, Edith G., "Electron Optical Investigation of the Hydration Products of Calcium Silicates and Portland Cement," Journal of the Research and Development Laboratories, Portland Cement Association, Vol. 4, No. 1, January, 1962.

10. Powers, T. C., Copeland, L. E., and Mann, H. M., "Capillary Continuity or Discontinuity in Cement Pastes," Journal of the Research and Development Laboratories, Portland Cement Association, Vol. 1, No. 2, May, 1959.

11. Verbeck, G. J., "Hardened Concrete -- Pore Structure," Research and Development Laboratories of the Portland Cement Association, Research Department Bulletin 73, August, 1956.

12. Powers, T. C., "Structure and Physical Properties of Hardened Portland Cement Paste," Journal of the American Ceramic Society, 41, pp. 1-6, January, 1958, as cited by Neville, loc. cit.

13. Committee 201 of the American Concrete Institute, "Durability of Concrete in Service," Journal of the American Concrete Institute, Proceedings Vol. 59, No. 12, December, 1962.

14. Lea, F. M., The Chemistry of Cement and Concrete, Edward Arnold (Publishers) Ltd., London, 1956.

15. Verbeck, George and Landgren, Robert, "Influence of Physical Characteristics of Aggregates on Frost Resistance of Concrete," Research and Development Laboratories of the Portland Cement Association, Research Department Bulletin 126, 1960.

16. Powers, T. C., "What Resulted From Basic Research Studies, Influence of Cement Characteristics on the Frost Resistance of Concrete," pp. 28-43, (Chicago, Portland Cement Association, November, 1951), as cited by Neville, loc. cit.

17. Powers, T. C., Resistance to Weathering-Freezing and Thawing," American Society for Testing and Materials, Special Technical Publication No. 169, pp. 182-187, 1956, as cited by Neville, loc. cit.

18. Nerenst, Poul, "Frost Action in Concrete," Proceedings of the Fourth International Symposium on the Chemistry of Cement, U. S. Department of Commerce, National Bureau of Standards, Monograph 43, Vol. II, 1962.

19. Hansen, W. C., "Crystal Growth as a Source of Expansion in Portland-Cement Concrete," American Society for Testing and Materials, Preprint 84, 1963.

20. Moskvin, V. M., "Corrosion in Hydrotechnic Structures," Corrosion of Concrete and Its Prevention, Published for National Science Foundation, Washington, D. C., and Department of the Interior, U. S. A., by the Israel Program for Scientific Translations (translated from Russian conference held in 1953).

21. Higginson, Elmo C., "Effect of Steam Curing on the Important Properties of Concrete," Journal of the American Concrete Institute, Proceedings Vol. 58, No. 3, September, 1961.

22. Rieb, Stanley Lee, "Preparation and Durability Testing of Pre-tensioned Prestressed Concrete," Journal of the Prestressed Concrete Institute, Vol. 4, No. 3, December, 1959.

23. Neville, A. M., Discussion of Paper by O. Ishai: "Influence of Sand Concentration on Deformation of Mortar Beams Under Low Stresses," Journal of the American Concrete Institute, Proceedings Vol. 59, No. 6, Part 2, June, 1962.

24. Glucklich, Joseph and Ishai, Ori, "Creep Mechanism in Cement Mortar," Journal of the American Concrete Institute, Proceedings Vol. 59, No. 7, July, 1962.

25. Lacy, Robert R., "Effect of Steam Time on Creep of Prestressed Concrete," M. S. Thesis, Montana State College, Department of Civil Engineering and Engineering Mechanics, June, 1965.

26. Gutzwiller, M. J. and Musleh, F. E., "Freezing and Thawing Effects on Prestressed Concrete," Proceedings of the American Society of Civil Engineers, Journal of the Structural Division, Vol. 86, No. ST10, October, 1960.

27. Lin, T. Y., Design of Prestressed Concrete Structures, John Wiley and Sons, Inc., New York, 1955.

28. "Design and Control of Concrete Mixtures," Portland Cement Association, Tenth Edition.

29. Newlon, Howard H., Jr., "A Field Investigation of the AE-55 Air Indicator," Highway Research Board Bulletin 305, National Academy of Sciences, National Research Council Publication 934, Washington, D. C., 1961.

30. Hussell, D. J. T., "Freeze-Thaw and Scaling Tests on Silicone-Treated Concrete," Highway Research Record 18, National Academy of Sciences, National Research Council Publication 1115, 1963.

31. Steel, Robert G. D. and Torrie, James H., Principles and Procedures of Statistics, McGraw-Hill Book Company, Inc., New York, 1960.

32. Hanson, Norman W., "Load Cells for Structural Testing," Journal of the Research and Development Laboratories, Portland Cement Association, Vol. 1, No. 1, January, 1959.

33. Bousso, Edwin and Ishai, Ori, "Technique for Measuring Tension in Short Prestressed Wires," Materials Research and Standards, A. S. T. M., Vol. 4, No. 12, December, 1964.

34. Klieger, Paul, "Some Aspects of Durability and Volume Change of Concrete for Prestressing," Research Department Bulletin 118, Research and Development Laboratories of the Portland Cement Association, November, 1960.

35. Grieb, W. E., Werner, G., and Woolf, D. O., "Resistance of Concrete Surfaces to Scaling by De-Icing Agents," Highway Research Board Bulletin 323, National Academy of Sciences, National Research Council Publication 1002, Washington, D. C., 1962.

36. Carlson, B. C., Curtis, D. F., and Hedlund, R. C., "Development of a Concrete Admixture to Improve Freeze-Thaw Durability," Highway Research Record 62, National Academy of Sciences, National Research Council Publication 1246, Washington, D. C., 1964.

MONTANA STATE UNIVERSITY LIBRARIES
3 1762 10013827 8

N378
G588
cop. 2
Gonsior, M. J.
The effect of prestress on concrete durability

NAME AND ADDRESS

3-4-67 [illegible]

N378
G588
Cop. 2